The Central Karakorum National Park Glacier Inventory

Editors
Claudio Smiraglia and **Guglielmina Adele Diolaiuti**

Editorial board
Antonella Senese, Davide Fugazza, Carlo D'Agata, Davide Maragno, Umberto Minora, Andrea Soncini, Roberto Sergio Azzoni, Riaz Ul-Hassan, Elisa Vuillermoz, Mohammed Asif Khan, Adnan Shafiq Rana, Ghulam Rasul

CKNP

UNIVERSITÀ DEGLI STUDI DI MILANO

Pakistan Meteorological Department

EvK2CNR

Ambasciata d'Italia Islamabad

AGENZIA ITALIANA PER LA COOPERAZIONE ALLO SVILUPPO

CENTRAL KARAKORUM NATIONAL PARK
CKNP

The Central Karakorum National Park
Glacier Inventory

Project Managers:
Claudio Smiraglia and Guglielmina Adele Diolaiuti
Università degli Studi di Milano
Dipartimento di Scienze della Terra "Ardito Desio", Milan
Italy

Editorial board:
Antonella Senese, Davide Fugazza, Carlo D'Agata, Davide Maragno, Umberto Minora, Andrea Soncini, Roberto Sergio Azzoni, Riaz Ul-Hassan, Elisa Vuillermoz, Mohammed Asif Khan, Adnan Shafiq Rana, and **Ghulam Rasul**

Main text by:
Claudio Smiraglia, Antonella Senese, Guglielmina Adele Diolaiuti

Image analysis and map editing by:
Carlo D'Agata, Davide Maragno, Davide Fugazza, Umberto Minora and **Andrea Soncini**

Data validation and processing by:
Antonella Senese, Davide Fugazza and **Andrea Soncini**

Photographs kindly given by:
Efrem Ferrari
Ev-K2-CNR Pakistan
Claudia Mihalcea
Università degli Studi di Milano
Marco Belò
Trimble Inc.
Christoph Mayer
Bavarian Academy of Sciences and Humanities
Astrid Lambrecht
Bavarian Academy of Sciences and Humanities
Paolo Petrignani
MONCLER - Keep K2 Clean
Ev-K2-CNR Archive

Map production:
Università degli Studi di Milano
Dipartimento di Scienze della Terra "A. Desio"
Photo-Geology and Remote Sensing Lab
Map base: Landsat TM 2001, Landsat ETM+ 2009, Landsat TM and ETM+ 2010, Landsat TM 2011

Graphic design:
Marketing Group Milano

With the formal partnership of:
Dipartimento Scienze della Terra "Ardito Desio"
Università degli Studi di Milano
Ev-K2-CNR Pakistan
Pakistan Meteorological Department
Karakoram International University
Secretary Forest, Wildlife and Environment Gilgit Baltistan
CKNP Directorate
Agenzia Italiana per la Cooperazione allo Sviluppo

For bibliographic and reference purposes, this publication should be referred to as:
SMIRAGLIA C. & DIOLAIUTI G. (Editors) (2016)
The Central Karakorum National Park Glacier Inventory.
Ev-K2-CNR - Pakistan Ed., Islamabad, 400 pp.

This study was carried out thanks to the support of the Government of Gilgit Baltistan, in the framework of the SEED (Social Economic Environment Development in the Central Karakorum National Park) Project, funded by the Governments of Pakistan and Italy within the Pakistan-Italian Debt Swap Agreement (PIDSA).
The authors wanted to acknowledge Luca Listo (SEED Project Director), Agostino Da Polenza (Ev-K2-CNR), Stefania Mondini (Ev-K2-CNR), Ashiq Ahmad Khan (Ev-K2-CNR) and all the SEED - PMU and Ev-K2-CNR Pakistan Staff for the fundamental support to this initiative.

Ev-K2-CNR - Pakistan
Italian K2 Museum Skardu Gilgit Baltistan
Liaison Office: House 3-A, Street 55,F-7/4 Islamabad
riaz.hassan@evk2cnr.org

ISBN 978-969-23176-0-3

Table of Contents

Preface

Guglielmina Adele Diolaiuti, Università degli Studi di Milano, and Elisa Vuillermoz, Ev-K2-CNR - Pakistan

The Central Karakorum National Park Glacier Inventory is a project realized by Ev-K2-CNR Pakistan, "Ardito Desio" Earth Sciences Department of the Università degli Studi di Milano, Italy, and the Pakistan Meteorological Department. The project has been developed within the framework of the Project 'Social Economic Environment Development (SEED) in the Central Karakorum National Park (CKNP) Gilgit Baltistan Region' Phase II, funded by the Government of Italy and the Government of Pakistan in the framework of the Pakistan-Italian Debt for development Swap Agreement (PIDSA). The main aim of the Project has been to promote an integrative development of the CKNP region through supporting the implementation and management of the CKNP, improving local wellbeing and livelihood options, through achieving poverty alleviation, community development, livelihood improvement and conservation through an integration of intrinsic scientific ecosystem management oriented research, indigenous practices for natural resource management and ecotourism principles to support the development and implementation of the CKNP.
This important publication consolidates the long term scientific cooperation between Italy and Pakistan, started in early '900 with the explorations of Duca degli Abruzzi, Filippo de Filippi and Ardito Desio, then pursued by Claudio Smiraglia (professor of physical geography at the Università degli Studi di Milano) and Agostino Da Polenza (President of the Ev-K2-CNR) who have led and managed several scientific expeditions over the last two decades. This book is a fundamental achievement, providing an updated picture of the status of Pakistan-Karakorum glaciers, based on a standardized analysis of recent satellite images.
Considering that 70% of Pakistan fresh-water resources come from glacier melting, this comprehensive dataset represents key baseline information for scientific community and policy makers in the field of climate change, water resources assessment and sustainable management.
The work we performed to develop this book aimed at providing the most correct, updated and complete information needed to manage in the best way the glacierized areas of CKNP and in particular to answer the following crucial questions: How many are the actual glaciers of CKNP? What is the CKNP present glacier cover? How strong and fast has been the impact of climate change on the cold and frozen water resource of the CKNP?
Elements and data to answer the above listed questions can come only from a large scale analysis based on the most recent remote sensing and GIS techniques. Our workflow was based on the main outlines and recommendations provided by the World Glacier Monitoring Service (WGMS) to permit Worldwide comparisons. The analysis needs to be supported by the people who best know the glacierized lands of CKNP: the scientists from Italy and from Pakistan who have been studying Karakorum glaciers since the last decades with passion and motivation, the CKNP managers, and policy makers who have been managing this peculiar mountain territory and their fresh water resource. Only the competence and the knowledge of all these people can produce a reliable, robust and complete picture of the actual CKNP glaciation. All the work we perfomed was aimed at this product and is here summerized.
Last but not least we also reported a chapter devoted to describe glacial lakes in the CKNP area since these ephemeral water bodies can develop into actual glacial risk conditions, which makes it important to list them and to survey them over time. The occurrence of glacial lakes in the CKNP and their coordinates were derived from a general Glacial lakes inventory developed by PARC (Pakistan Agricultural research Council) and PMD (Pakistan Meteorological Department) for the whole HKH area; we extracted data describing lakes in the CKNP and compiled a detailed glacial lake inventory for the park. Moreover, among all the listed CKNP glacial lakes two were identified as potentially dangerous glacial lakes (PDGLs) and these were better contextualized with respect to the park extent and features.
This last part of the book, developed under strong cooperation with the PMD, better underlines that glaciers are not only a valuable water resource but they are also peculiar features triggering risk and dangerous events and thus they require updated inventories, continuous analysis and surveying over time. In this framework, this work can be a fundamental tool not only for the knowledge of the park resource but also to develop early strategies of risk mitigation and disaster management. The work is not limited to this hard-book but it is also represented by a digital database and by several digital thematic maps designed to be available to and usable by park managers, policy makers and park inhabitants and thus susceptible to periodically updating. Only a long and continuous monitoring program of the park glaciers and glacier-derived resources will support a sustainable and safe utilization of this unique and wonderful protected area.

Ghulam Rasul, Director General, Pakistan Meteorological Department

The Himalaya, Hindu Kush and Karakorum mountains ranges join each other in the extreme north of Pakistan, hosting more than 7.000 glaciers which feed the Indus River System together with the summer monsoon. Substantial amount of solid precipitation occurs in the form of snow at high altitudes while liquid precipitation as rain falls at the lower latitudes during winter. Global change has visible impacts on this part of the cryosphere which is known as the Third Pole together with Tibet Plateau and plays very important role in the global climate system dynamics. As a result, not only the rapid evolution of glaciers is witnessed but it has also been increasing the number and extent of the glacial lakes. GLOF (Glacial Lake Outburst Flood) hazard is becoming more frequent and intense in northern Pakistan. In this regard, the availability of an updated information on the CKNP Glaciers is a fundamental starting point to pursue glacier monitoring and related risk management.
For these reasons, the Pakistan Meteorological Department is now fully engaged in studying the impact of climate change on the frozen water resources and the related risk of hazards such as GLOF, avalanches and land slides/slips. Due to lack of data collection network, several claims based on perception and speculation prevailed which were not drawn from the scientific evidence. Thanks to the cooperation of the Italian researchers of Ev-K2-CNR and the University of Milan to improve the capacity of local scientists in this field through collaboration in glacier monitoring and research. PMD and Ev-K2-CNR have organized several joint campaigns in the Baltoro Region to measure glacier parameters and to run the Automatic Weather Stations installed in Askole, Urdukas and Concordia over a decade. Through this partnership it has been thus possible to contribute to the knowledge on climate of Pakistan mountain regions and glacier dynamics of HKKH region which was the least monitored and explored. The new inventory of CKNP Glaciers is another important step of this fruitful cooperation.
Government of Pakistan is now fully engaged in pursuing environmental and climate change policy, both at National level through the implementation of the Climate Change Policy in letter and spirit and the launching of initiatives such as the Green Climate Program, and at international level, through the ratification of the Paris Declaration, defined after the 2015 UNFCCC-COP21. Being among the least emitters of Green House Gases, Pakistan has already taken numerous initiatives toward green climate such as Green Pakistan, Billion Trees, Mass Transit Systems and harnessing of renewable energy resources. To pursue these objectives, reliable and comprehensive scientific information would be required to support this process, and this publication is surely one important pillar in this framework. PMD is going to improve its climate monitoring network through installation of more automatic weather stations and establishment of the community based GLOF early warning systems at 36 most vulnerable locations. Additional data resource of this region will help to better understand the glacio-hydro-dynamics for future policy formulation.

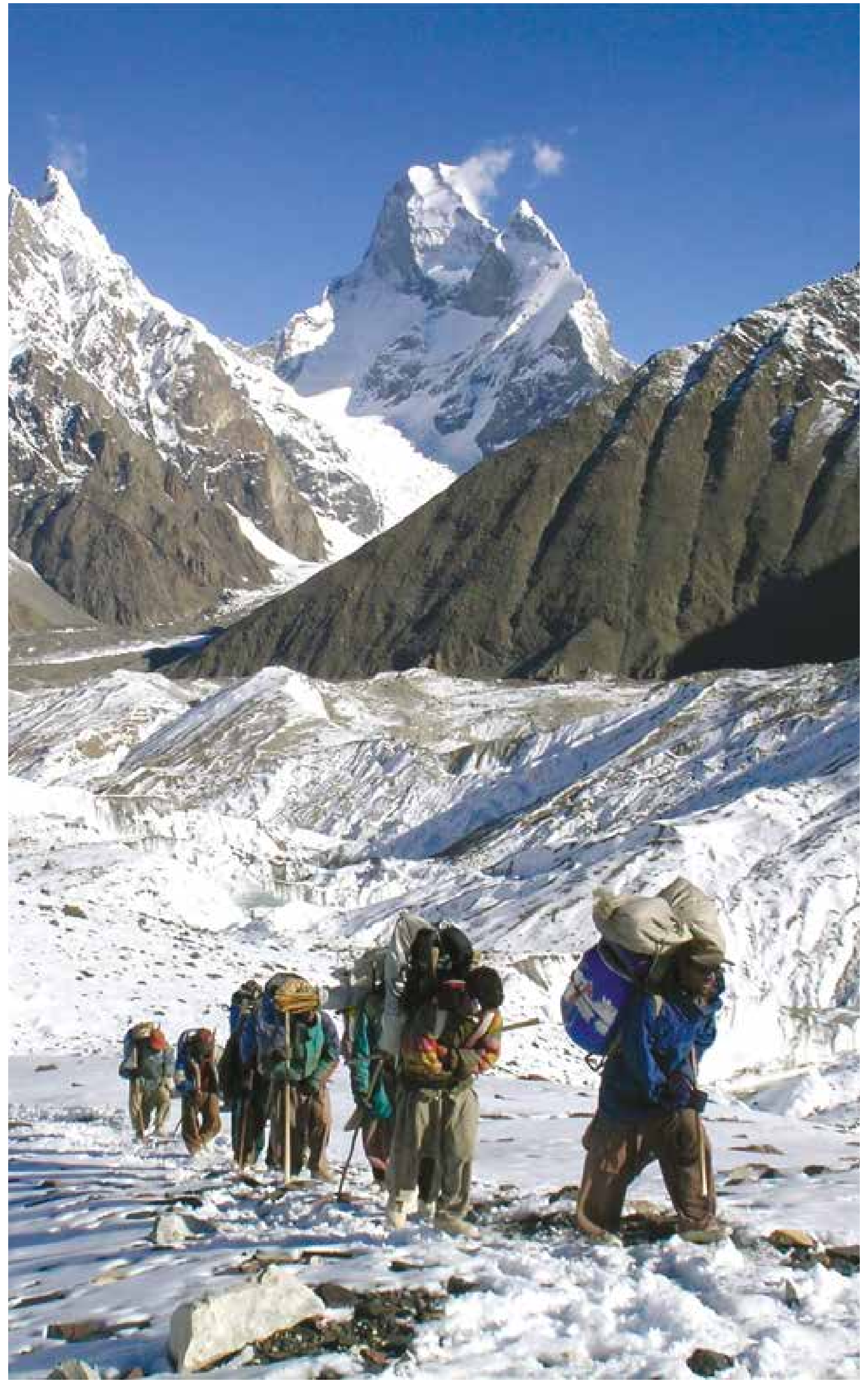

Introduction and Methods

Rationale

Glaciers are sensitive climate indicators because they adjust their size in response to changes in climate (e.g. temperature and precipitation). Understanding the impact of changing climate conditions on glaciers is a prerequisite to study mountain hydrology, to analyze natural hazard frequency, and to forecast sea level rise. The largest glacierized region outside the Arctic and the Antarctic is High Mountain Asia (HMA), the so called "The Third Pole", which covers an area of 118200 km^2 (Gardner et al., 2013), stretches for more than 2000 kilometers in length from West to East, and hosts about 40000 km^2 of ice bodies (glaciers, glacierets and perennial ice surfaces). Changes in glacier extent and volume in this region are spatially heterogeneous and poorly known (Bolch et al., 2012). Indeed, recent studies revealed that most of the northwestern Himalaya have experienced less glacier shrinkage than the eastern parts of the same mountain range (Bhambri and Bolch, 2009; Cogley, 2011; Bolch et al., 2012; Kääb et al., 2012). In the western and central Karakorum region, glaciers showed long-term irregular behavior with frequent advances, and possible slight mass gain in the last decade (Copland et al., 2011; Hewitt, 2011; Bolch et al., 2012; Gardelle et al., 2012, 2013; Kääb et al., 2012; Minora et al., 2013, 2016; Soncini et al., 2015). Recent studies of Gardelle et al. (2012, 2013) demonstrate how, in contrast to widespread global glacier retreat, glaciers in the Karakorum region as a whole have exhibited a general mass-balance stability (the so called 'Karakorum anomaly'; Hewitt, 2005, 2011). Advances of individual glaciers have also been reported in the Shyok Valley (Eastern Karakorum) during the last decade (Raina and Srivastva, 2008). The Eastern part of this region is under the influence of the Indian monsoon, which brings precipitation during summer, while the Western one (which includes the Karakorum range) receives most of the annual precipitation during winter and spring, as it is influenced primarily by the westerlies originating predominantly from Mediterranean and Caspian Sea regions (Fowler and Archer, 2006; Bookhagen and Burbank, 2010). This East-West variability in the predominant wind system leads to differences in glacier accumulation and might be one reason for the large spread in detected glacier changes within the region (Bolch et al., 2012; Kääb et al., 2012).

In this context, the individual advances and mass gain episodes could be attributed to surging (Diolaiuti et al., 2003; Barrand and Murray, 2006; Hewitt, 2007; Belò et al., 2008; Copland et al., 2011; Quincey et al., 2011), increased solid precipitation in the accumulation areas and summer cloudiness (Fowler and Archer, 2006; Bocchiola and Diolaiuti, 2013; Hewitt, 2014; Minora et al., 2016), and a simultaneous trend toward higher winter temperatures and lower summer temperatures (Fowler and Archer, 2006; Mayer et al., 2010; Shekhar et al., 2010). Such a combination, associated with the role of the elevation and elevation range of the glaciers across the Karakorum, may have caused the expansion of large, flat glaciers and probably reduced meltwater production. In an otherwise extreme continental, arid region, the glaciers comprise large stores of freshwater (Hewitt, 2014), thus contributing significantly to the stream-flow, especially during the dry season (Konovalov, 1997; Hagg and Braun, 2005).

Likely, more than 50% of the water in the Indus River originating from the Karakorum comes from snow and glacier melt. Therefore, the Karakorum glaciers are a strategic resource for Pakistan, providing fresh water for civil use, hydropower production and mainly farming (Bocchiola and Diolaiuti, 2013). With a growing population and intensifying agriculture, a secure water supply becomes more important, and the contribution from snow and ice melt is a crucial issue (Mayer et al., 2010; Minora et al., 2015, 2016).

The glacierized Karakorum is therefore a key area for studying the effects of ongoing climate change on present and future meltwater discharge and for understanding the role of the cryosphere in influencing the regional hydrology and water resources.

In order to better describe this fresh-water resource, the glacier inventory of the Central Karakorum National Park (CKNP, an extensive protected area of about 10000 km^2, in the Northern Pakistan in the main glaciated region of the Central Karakorum) was developed. It describes glacier census and features for 2001 and 2010. The CKNP Inventory describes more than 600 glaciers listing their: location, type, size, and surface conditions (i.e. debris occurrence and extent, if any). The reported data mainly derive from remote-sensing investigations, nevertheless we also reported information from modelling approaches: mean glacier ice thickness, glacier volume, supraglacial debris thickness and melt rates. All these elaborations were also carried out by early career researchers supported by DARAS (Department of Regional Affairs, Autonomies and Sport) of the Presidency of the Council of Ministers of the Italian Government through the GlacioVAR project. Although other glacier inventories covering the Karakorum region are available (Randolph Glacier Inventory, see Arendt et al., 2014; ICIMOD glacier inventory, see Bajracharya and Shrestha, 2011; GAMDAM glacier inventory, see Nuimura et al., 2015), our work focuses on the specific area of the CKNP only, providing a high-resolution and very detailed inventory.

We analyzed the CKNP glaciers firstly considering the Park as a whole and secondly focusing our study at the catchment scale. In fact, in the Park five main catchments are found (i.e. Hunza, Shigar, Shyok, Upper Indus and Gilgit) thus suggesting to describe glaciers and ice-derived fresh-water at this more detailed scale.

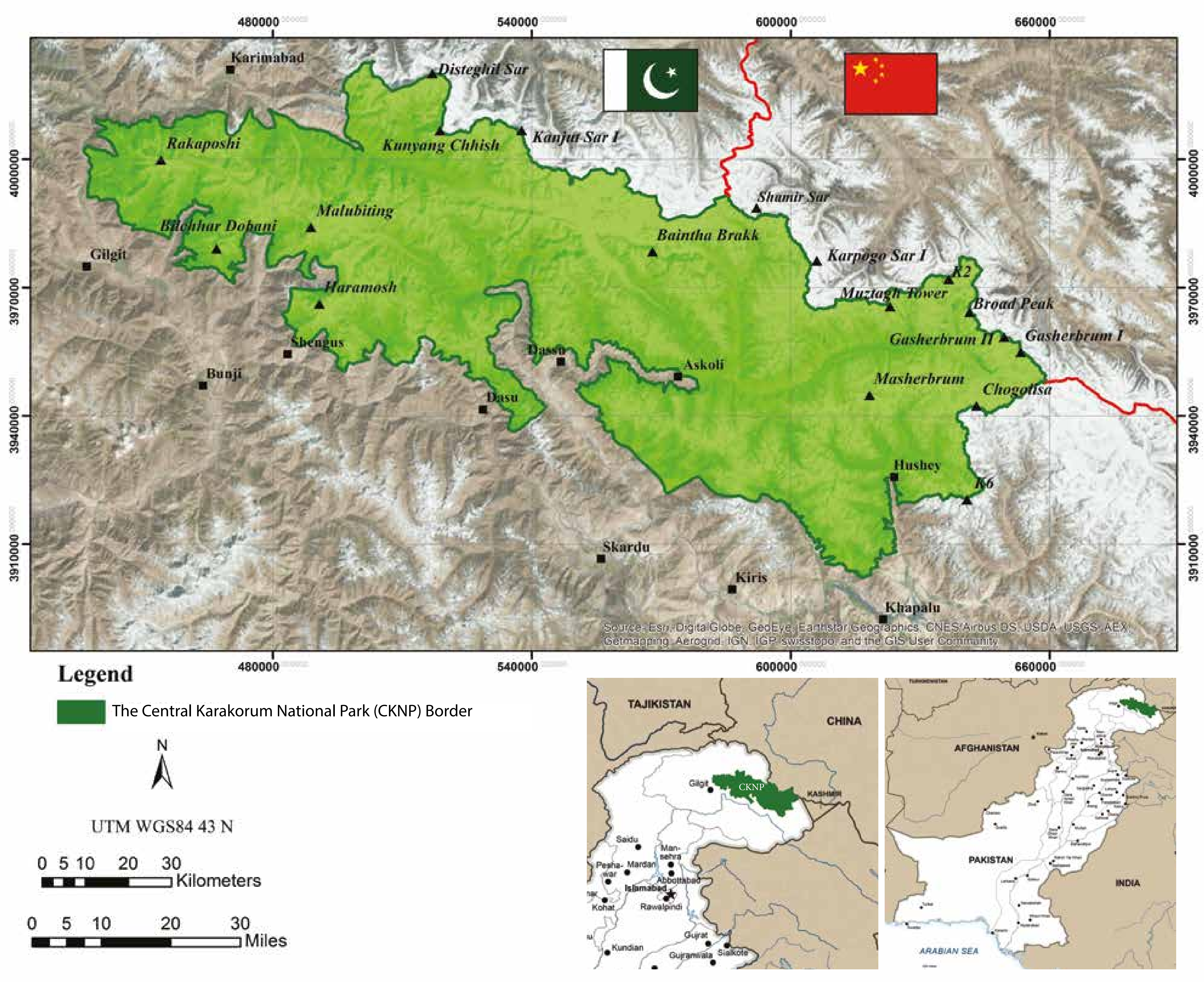

Data and methods

Observed data

For the compilation of the CKNP glacier inventory, we followed the recommendations by Paul et al. (2009), and we considered parameters such as identification code, coordinates, dates of acquisition of the image related to each glacier outline, area, length, minimum, maximum and mean elevation, and slope.
To detect glaciers, mark their boundaries and calculate their area, remote-sensing investigations were applied. More precisely, Level 1T Landsat Thematic Mapper (TM) and Enhanced TM Plus (ETM+) scenes of 2001 and 2010 were processed and analyzed (Tab. 1). In this way, the glacier changes during the first decade in the new millennium were investigated.

Before proceeding to the digitization of glacier outlines, we first increased the color contrast between the glacier bodies and the surrounding pixels by combining the near infrared and the visible bands of the TM sensor (RGB = 543). So doing, we produced false color composite (FCC) images against which we manually digitized each glacier outline separately. The minimum mapped area was 0.01 km^2 as recommended by Paul et al. (2009). The debris-free and debris-covered parts of the glaciers were not distinguished in this step. They were split afterwards by identifying the debris pixels within the glacier outlines with a supervised classification.
It is worth noting that the interpretation of the glacier perimeter under debris is not straightforward (Paul et al., 2009; Collier et al., 2015), and thus the change analysis may be problematic too. To this end, we cross-checked the position of the actual glacier border under debris with the Landsat images and the high-resolution images from Google Earth©. Another crucial aspect in glacier delineation is the location of terminus position. Indeed, it can differ by several

Table 1. Landsat imagery used for the analysis. Star symbol (*) indicates the reference images used for glacier delineation, the other ones were used to cross-check the results. We produced false color images via a band combination 543, PAN-sharpened to 15 m resolution employing the Panchromatic band of Landsat 7 (band 8).

Date	Scene identification No.	Resolution [m]	Sensor	SCAN line error	Cloud cover over glaciers [%]
21/07/2001	LE71480352001202SGS00*	15	ETM+	No	0.0
30/09/2001	LE71490352001273EDC01*	15	ETM+	No	0.0
23/07/2010	LT51480352010235KHC00*	30	TM	No	0.0
17/10/2010	LT51490352010290KHC00*	30	TM	No	0.0
18/10/2010	LE71480352010291SGS00	15	ETM+	Yes	0.0
12/08/2009	LE71480352009224SGS00	15	ETM+	Yes	0.0
22/08/2010	LE71490352010234EDC00	15	ETM+	Yes	0.1
20/09/2009	LE71490352009263SGS00	15	ETM+	No	0.0

ETM+: Enhanced Themaic Mapper Plus; TM: Thematic Mapper.

hundred meters if glacier outlines were digitized by different analysts (Paul et al., 2013). In this work, the glacier outlines for the two reference years were drawn by the same analyst, so the change analysis should be reliable. Finally, the definition of the upper glacier boundaries is also a problematic aspect. In general, steep headwalls were excluded from the mapping, similar to that by Nuimura et al. (2015). The reason is that snow can not accumulate easily on very steep surfaces (> 40°; Nuimura et al., 2015). Moreover, avalanche-fed glaciers prevail in the Karakorum, and many lack an accumulation zone as normally understood (Hewitt, 2011). We used the contour lines derived from the Shuttle Radar Topography Mission 3 DEM (SRTM3, CGIAR-CSI, 2012), to detect the steep slopes in the accumulation areas close to the glacier limits and exclude them from the inventory when there were rock-exposed walls covered by thin snow layers or spotty snow patches. However, this criterion might have excluded steep areas in the accumulation zone where snow is present throughout the year, and thus the actual final glacier area might be biased by this exclusion.
Afterwards, we used a Geographic Information System (GIS) to extract topographic parameters based on the glacier outlines and the DEM. The maximum length of each glacier was derived by manually depicting a line from the highest to the lowest altitude within each glacier outline, and passing through the main flow line (according to the contour lines). The mean slope was then calculated for each glacier from elevation range and length data.
Eventually, we identified surging glaciers according to both the magnitude of their termini advance (Cuffey and Paterson, 2010), the presence of looped moraines indicating possible past surge events (Copland et al., 2003), and by comparison against the available literature (Copland et al., 2011; Hewitt, 2007; Quincey et al. 2001; Rankl et al., 2014).

In addition to the above listed geometry parameters, the CKNP glacier inventory also reported the occurrence of supraglacial debris and the extent, if any, as supraglacial debris mantle influences the glacier system in a not negligible way (Collier et al., 2015). The most important and well-known effect is on glacier ablation and then on the production of meltwater. A valuable example of debris cover effect on ablation is found on actual debris-covered glaciers (see Kirkbride, 2011). In fact, there are many studies dealing with supraglacial debris role in driving magnitude and rate of buried ice ablation depending on its depth (Ostrem, 1959; Nakawo and Young, 1981; Nakawo and Rana, 1999; Tangborn and Rana, 2000; Sakai et al., 2000; Deline, 2005; Nicholson and Benn, 2006; Mihalcea et al., 2006; Minora et al., 2015).
First, the classifier was trained to recognize the supraglacial-debris by choosing appropriate Region of Interests (ROIs). Therefore, to map the supraglacial debris coverage for the years 2001 and 2010 a supervised maximum likelihood (SML) classification on the Landsat false-color composite (FCC, bands 543) images was applied. This approach involved training the classification algorithm with a number of sites where the classification output (i.e. presence or absence of debris on the glacier surface) was known (Brown et al., 1998). Accordingly the classifier was trained to recognize the supraglacial-debris by choosing appropriate Region of Interests (ROIs). The SML algorithm assumes that values in each spectral band from Landsat TM are normally distributed and calculates the probability that a given image pixel is debris-covered or debris-free based on the values of all spectral bands. Each pixel is finally classified as debris-covered or debris-free according to the class that has the highest probability (Richards, 1999). In particular, we used band combination 543 (as red, green, blue) of Landsat TM scenes to draw 20 regions of interest (ROIs) and trained the classifier to recognize the supraglacial debris. ROIs are sample areas that we know were covered by supraglacial debris in 2001 and 2010. After training, the classifier was run on all the glacierized areas of the CKNP, assuming a probability threshold of 90% to separate debris-covered from debris-free pixels (i.e. a pixel was classified as 'supraglacial debris-covered' when the probability of a pixel belonging to this class was >0.9). The remaining pixels within glacierized areas were considered debris-free areas. So doing we obtained the supraglacial debris maps for both years. Finally, we produced the shadow maps with the same procedure to search for the locations where the glacier area was shaded. In this way we were able to identify the areas of possible debris cover excluded by the classification and add them manually to the final map after cross-checking the actual presence of debris with different sources (other Landsat images, Google Earth©).

When dealing with the production of glacier inventories through satellite images, inaccuracies may occur due to classification errors. These depend upon the image resolution and the meteorological and environmental conditions at the time of acquisition, namely cloud- and snow-cover, presence of shadows and debris, hampering ice detection. In developing the CKNP inventory we took into consideration the impacts of different sources of error:

i) ***Geo-referencing error.*** The geo-referencing accuracy is optimized by the United States Geological Survey (USGS) by means of a correction process based both upon ground control points (GCPs, taken from the 2005 Global Land Survey) and the SRTM DEM (Landsat7 Handbook, 2013). The SRTM DEM is thought to have good accuracy (Falorni et al., 2005). The true geolocation is not too critical for our analysis because our Landsat data are processed in the same way by the USGS.

ii) ***Linear resolution error (LRE)***: Image resolution influences the accuracy of glacier mapping. Following Vögtle and Schilling (1999) and Citterio et al. (2007), the final planimetric precision value was assessed considering the uncertainty due to the sources (satellite images). The area precision for each glacier was evaluated by buffering the glacier perimeter, considering the area uncertainty. According to O'Gorman (1996), the LRE should be half the resolution of the image pixel, i.e. in our case 7.5 m for the 2001 scenes (because the scenes were PAN-sharpened), and 15 m for the 2010 scenes. This error may be too low for debris pixels, because glacier limits are more difficult to distinguish when ice is covered by debris (Paul et al., 2009). Therefore, we set the error for debris pixels to be three times that of clean ice. The precision of the whole CKNP glacier coverage was estimated as the root squared sum (RSS) of the buffer areas for 2001 and 2010:

$$AE_{yr}=\sqrt{\sum_{i=1}^{N}(p_i * LRE_{yr})^2} \qquad (1$$

where AE_{yr} is the Areal Error of year 2001 or 2010, p_i is the i^{th} glacier perimeter, LRE_{yr} is the LRE of year 2001 or 2010, and N is the total number of glaciers in the inventory.
Finally, the total error in area change ($AE_{\text{area change 2001-2010}}$) was then calculated as the RSS of the areal errors evaluated for the 2001 and 2010 (AE_{2001} and AE_{2010}):

$$AE_{\text{area change 2001-2010}} = \sqrt{AE_{2001}^2+AE_{2010}^2} \qquad (2$$

iii) ***Error depending on specific scene conditions:*** Seasonal snow, cloud cover, presence of shadows and debris can introduce errors in glacier area determination. The scenes were selected to display minimum snow and cloud over the glaciers. In case these features were still present, and to deal with the interpretation of invisible glacier boundaries in cast shadows and the actual perimeter under debris, we used images from different sources (i.e. Landsat and Google Earth©) and dates, which enabled us to cross-check the actual glacier limits and to minimize any possible interpretation error.

iv) ***Error depending on operator's misinterpretation***: Because glacier outlines are mapped manually, errors may occur due to the operator's misinterpretation of the image pixels. Nevertheless, although several semi-automated techniques for mapping debris-covered glaciers have been proposed (Paul et al., 2004; Shukla et al., 2010, amongst others), they all require more complex processing, an accurate DEM and final manual editing (Paul et al., 2013). We therefore preferred the manual approach, trying to reduce any possible misinterpretation error through the choice of an expert eye for the digitization, and a second-round check on the final mapping.

Derived data

For assessing the total fresh-water resource nested by CKNP glaciers, an indirect approach was applied. According to the method introduced by Haeberli and Hoelzle (1995), ice thickness and volume data were estimated from an indirect approach which considers glacier geometry data recorded in the inventory (2001 data base). The method was widely applied (e.g. Baumann and Winkler, 2010) and it gave good results in analyzing glaciers from New Zealand Alps and Norway thus suggesting a wide applicability. Moreover, Hoelzle et al. (2003) applied such method to estimate changes and evolution of glaciers worldwide thus supporting the use of this parameterization for CKNP glaciers (for a discussion of different methods, see Frey et al., 2014). The geometry data needed in the Haeberli and Hoelzle (1995) analytical approach are: the glacier altitudinal range (i.e. ΔH, the difference between glacier maximum and minimum elevation), the glacier maximum length (measured along the main flow line) and the area.
Average ice depth along the central flow line was estimated from average surface slope (derived from the ratio of altitude range and glacier maximum length) and a mean basal shear stress along the central flow line ($\tau_f = f\rho g h_f \sin\alpha$, with f = shape factor chosen 0.8 for simplicity in all cases, ρ = ice density, g= acceleration due to gravity, α = average surface slope), whereby τ_f depends in a nonlinear way on the altitudinal range as a function of mass turnover (cf. Driedger and Kenrad, 1986; Haeberli, 1985; Haeberli and Hoelzle, 1995; Hoelzle et al., 2003). The specific formulas we applied are reported in the Table 2. Therefore, the required input data were glacier length, area and elevation range from 2001 CKNP Glacier Inventory.
In 1954 Ardito Desio promoted an expedition to the Baltoro Glagier with the aim of acquiring important geological and glaciological information. In particular, gravimetric surveys were carried out in order to assess the glacier depth (Marussi, 1964).

Name	Term	Calculation	Unit
Surface area	F	-	m^2
Lenght	L_0	-	m
Minimum altitude	H_{min}	-	m a.s.l.
Maximum altitude	H_{max}	-	m a.s.l.
Lenght change	δL	$L_{0,old} - L_{0,new}$	m
Mean altitude	H_{mean}	$(H_{max} + H_{min})/2$	m a.s.l.
Range	ΔH	$H_{max} - H_{min}$	m
Lenght of the central flowline in ablation area	L_a	$0.5 * L_0$ if $L_0 \leq 2$ km; $0.75 * L_0$ if $L_0 > 2$ km	m
Average surface slope	α	$\arctan(\Delta H/L_0)$	rad
Average surface slope in ablòation area	α_a	arctan[(Hmean - Hmin)/ La]	rad
Mean basal shear-stress	τ	$0.005 + 1.598 * \Delta H - 0.435 * (\Delta H)^2$ if $\Delta H \leq 1.6$; 1.5 if $\Delta H > 1.6$	bar
Average ice thickness at central flowline	h_f	$\tau / (f * \rho * g * \sin\alpha)$	m
Average ice thickness at central flowline in ablation area	$h_{f,a}$	$\tau / (f * \rho * g * \sin\alpha_a)$	m
Average ice thickness over whole glacier	h_F	$(\pi/4) * h_f$	m
Total glacier volume	V	$F * h_F$	m^3
Maximum ice thickness	h_{max}	$2.5 * h_{f,a}$	m

Table 2: Applied parametrization (see also Haeberli and Hoelzle, 1995; Hoelzle et al., 2003)

As mentioned above, supraglacial debris influences the glacier system modulating the production of freshwater. In fact, the supraglacial debris cover whenever thicker than a "critical thickness" (sensu Mattson et al., 1993) reduces magnitude and rates of buried ice melt with respect to the values affecting bare ice at the same elevation. The critical thickness value has to be locally evaluated and it resulted mainly depending on rock lithology and grain size and on the geographical glacier setting (Mihalcea et al., 2006; Mihalcea et al., 2008a, b; Diolaiuti et al., 2009). Therefore, in addition to the map describing the occurrence of supraglacial debris, which highlights the separation of the debris-free and debris-covered zones of each glacier, a map of the thickness of supraglacial debris over the whole glacierized area of the CKNP was developed. We used the method developed by Mihalcea et al. (2008b) for Miage Glacier (Mont Blanc massif, Italy), and already applied to Baltoro Glacier by Mihalcea et al. (2008a). This method is based on the relationship between surface temperature and supraglacial debris thickness (Taschner and Ranzi, 2002). The input data are: i) debris thickness measured in the field on some selected representative debris-covered glacier areas (i.e. along Baltoro Glacier during an expedition in July–August 2011), and ii) satellite-derived surface temperatures at the same sites (the selected images were taken during the same period as the field measurements). The empirical relationship between these data is a valuable tool for estimating debris thickness over unmeasured glacier zones (Mihalcea et al., 2008a,b). This approach was initially developed on ASTER (Advanced Spaceborne Thermal Emission and Reflection Radiometer) temperature data and applied to Baltoro Glacier by Mihalcea et al. (2008a). Unfortunately, the ASTER images were not available for the whole CKNP area on the same date. We therefore modified the approach of Mihalcea et al. (2008a,b) to use Landsat TM images covering the entire CKNP area (full details in Minora et al., 2015).
To evaluate the suitability for debris assessment of Landsat TM images instead of ASTER ones, firstly we processed the Landsat image of the debris-covered portion of the Baltoro Glacier acquired on 14 August 2004, 5:18 GMT (10:18 h local time), only 28 minutes before the acquisition of the ASTER image analyzed by Mihalcea et al. (2008a), and then we compared the results.
To assess surface temperature from Landsat images ($T_{S\text{-}Landsat}$, in Kelvin degrees), Landsat TM band 6 (i.e. thermal wavelength) Digital Numbers were first converted to Radiance values ($R_{Landsat}$, in W m^{-2} sr^{-1} µm^{-1}) (Coll et al., 2010), and then $T_{S\text{-}Landsat}$ was calculated applying the inverted Planck function:

$$T_{S\text{-}Landsat} = \frac{K_2}{1n\left(\frac{K_1 \cdot \varepsilon}{R_{Landsat}}+1\right)} \qquad (3$$

where K_1 and K_2 are constant values (607.76 W m^{-2} sr^{-1} µm^{-1} and 1260.56 K, respectively, NASA, 2011), and ε is the sky emissivity including atmospheric scatter (set to 0.95, Barsi et al, 2003; 2005). The temperatures estimated using the two different images showed a good correlation (R^2= 0.91; mean, maximum and minimum temperature differences 2.1 K, 14.5 K, 0.0 K, respectively) thus supporting the use of Landsat data to describe supraglacial thermal conditions. Secondly, we used the same field data of debris thickness gathered in 2004 and used by Mihalcea et al. (2008a) to assess the best empirical function linking Landsat 2004 thermal data and debris thickness. The best fitting function (R^2 = 0.99) is:

$$DT=\exp(0.17 \cdot T_{S\text{-}Landsat}-51.18) \qquad (4$$

where DT is debris thickness (in m) and $T_{S\text{-}Landsat}$ is the Landsat-derived surface temperature. This equation is similar to that found by Mihalcea et al. (2008a) and describes the non-linear relation between debris thickness and surface temperature. Moreover, we compared DT values obtained applying the equation reported in Mihalcea et al. (2008a) to 2004 ASTER data against the ones derived from equation 5 on 2004 Landsat data on the Baltoro Glacier area. The results (see Minora et al., 2015) show a good correlation between the two datasets ($R^2 = 0.85$) and suggest a similar performance of the two models. Hence, these preliminary tests support the suitability of Landsat-derived surface temperatures to describe supraglacial debris thickness. We therefore used the debris thickness dataset collected in the field on the surface of the Baltoro Glacier during an expedition in July-August 2011 (a total of 57 samples ranging from a few centimeters to 2 m at the tongue). Regarding the Landsat surface temperatures, a single image covering the whole CKNP was not available; therefore, we used two images acquired on 10th August 2011 5:18 GTM and on 17th August 2011 5:24 GMT (Table 3).

Table 3: Source, acquisition date and code scene of each satellite image used for the assessment of debris thickness distribution. Site displayed by each image is also reported.

Source	Acquisition date	Code scene	Site
Landsat	10th August 2011	LT51480352011222KHC00	East part of the CKNP mosaic
Landsat	17th August 2011	LT51490352011229KHC00	West part of the CKNP mosaic
Landsat	14th August 2004	LE71480352004227PFS01	Baltoro Glacier, used in this study for comparison with Mihalcea et al. (2008a)
Aster	14th August 2004	AST_08_00308142004054614	Baltoro Glacier, analyzed by Mihalcea et al. (2008a)

The images selected were particularly useful for our analyses because they were taken during the same period as the field measurements, and they partly overlap; they both cover part of the Baltoro Glacier tongue (where field DT data were sampled). These data allowed us to assess two empirical equations linking debris thickness measured in the field to surface temperatures derived from Landsat images. The best fitting equation ($R^2 = 0.75$) obtained from the image taken on 10th August 2011 (which covers the whole Baltoro Glacier area) was:

$$DT=exp(0.16\cdot T_{S\text{-}Landsat}-49.22) \qquad (5$$

while the one ($R^2 = 0.91$) from the image acquired on 17th August 2011 (covering part of the Baltoro Glacier tongue) was:

$$DT=exp(0.20\cdot T_{S\text{-}Landsat}-59.97) \qquad (6$$

Then we applied equation 5 to thermal data derived from the Landsat image acquired on 10th August 2011, and equation 6 to thermal data derived from the Landsat image acquired on 17th August 2011. For the area covered by both overlapping images, results from equation 5 applied to the 10th August image were preferred because the Baltoro Glacier was only partially covered by the 17th August image, while it was completely covered by the 10th August image. Thus, the use of results from the 10th August image provided consistent estimates of the supraglacial debris thicknesses over the whole ablation area of the Baltoro Glacier.

Once glacier area and supraglacial debris occurrence and thickness were defined, we assessed the magnitude and rate of ice ablation and evaluated the derived meltwater amount. Unlike glacier volume, that represents the total water resource nested by CKNP glaciers, the meltwater is the actual contribution to the stream-flow and then the important current water supply for civil use, hydropower production and farming. For estimating this daily water amount, we applied two distributed melt models (full details in Minora et al., 2015) to describe ablation in debris-covered and debris-free conditions (Pellicciotti et al., 2005; Mihalcea et al., 2008a).
To model the ice melting amount in the whole CKNP glacier ablation area, we considered the following input data: i) the glacier boundaries, ii) a digital elevation model (DEM) describing the CKNP area (derived from the Shuttle Radar Topography Mission, SRTM3), iii) the supraglacial debris cover map, iv) meteorological input data (daily mean air temperature and daily mean incoming solar radiation measured by the permanent automatic weather station installed at Askole), and v) the supraglacial debris thicknesses, daily surface debris temperatures (computed from daily incoming solar radiation and debris thickness) and debris effective thermal resistance (evaluated from debris thickness).

As described above, a significant portion of the glaciers in the CKNP is covered by a supraglacial debris layer, modulating the magnitude and rate of ice ablation (Nakawo and Young, 1981; Nakawo and Takahashi, 1982; Nicholson and Benn, 2006; Mihalcea et al., 2008a, b; Reid and Brock, 2010). This debris layer must therefore be accurately considered in distributed modeling of ice melt. Mihalcea et al. (2008a) modeled debris-covered ice ablation over the whole Baltoro Glacier ablation area by applying a distributed approach, based on computation of the conductive heat flux through the debris layer and requiring information on debris thickness distribution. This approach has also been used by Zhang et al. (2011) who applied it on Hailuogou Glacier, southeastern Tibetan Plateau, and more recently by Fujita and Sakai (2014) on the Tsho Rolpa glacial lake-Trambau Glacier basin in the Nepal Himalaya. Fyffe et al. (2014) developed a melt model, which calculates sub-debris melt rates using an existing debris energy-balance model (DEB-Model introduced by Reid and Brock, 2010) and melt rates for clean ice, snow and partially debris-covered ice using standard energy-balance equations. This latter approach is more exhaustive (but also more complex) than that of Mihalcea et al. (2008a), though its application to a whole glacierized watershed or an entire glacier region is not simple, and requires input data featuring high spatial and temporal resolution, not always available in remote high-elevation glacier zones. Therefore, the results reported in this contribution were obtained for the entire CKNP debris-covered ice zone by applying the model developed by Mihalcea et al. (2008a).
More precisely, the amount of ice melt under a debris cover ($M_{DC\text{-}point}$ in m w.e.) depending on the energy available at the debris-ice interface was estimated as:

$$M_{DC\text{-}point}=\frac{G_{point}\cdot\Delta t}{\rho_i\cdot L_m} \qquad (7$$

where G_{point} corresponds to the conductive heat flux (in W m^{-2}), Δt the time-step, ρ_i the ice density (917 kg m^{-3}) and L_m is the latent heat of melting (3.34 x 10^5 J kg^{-1}). According to Mihalcea et al. (2008a), G_{point} can be estimated assuming a linear temperature gradient from the top of the debris layer to the ice surface for mean daily conditions (Nakawo and Young, 1981; Nakawo and Takahashi, 1982; Mihalcea et al., 2008a):

$$G_{point}=\frac{T_{s\text{-}point}-T_i}{DR_{point}} \qquad (8$$

where T_i is the ice temperature (set to the melting point, 0°C; i.e. we neglected refreezing phenomena, which generally do not occur during the main ablation season, Mihalcea et al. 2006, 2008a) and DR_{point} is the effective thermal resistance of the debris layer (m^2 °C W^{-1}).
To derive DR_{point} over the whole debris-covered glacier area, an empirical relationship was applied (Mihalcea et al., 2008a):

$$DR_{point}=19.841\ DT_{point}+1.0262 \qquad (9$$

DR_{point} can be assumed constant over an ablation season as it mainly depends on debris thickness, which is generally considered stable over short periods (1-2 months, Fyffe et al., 2014).
To model the daily mean debris surface temperature at each pixel ($T_{S\text{-}point}$), we considered both daily incoming solar radiation ($SW_{in\text{-}point}$) and debris thickness (DT_{point}), because higher radiation and thicker debris lead to higher surface temperatures (Mihalcea et al., 2006; 2008a,b; Mayer et al., 2010). $T_{S\text{-}point}$ was estimated according to the following empirical function:

$$T_{S\text{-}point}=13.1667\cdot DT_{point}+0.0352\cdot SW_{in\text{-}point} \qquad (10$$

with a root mean square error of 2.1°C. This relation was based on field data of debris thickness and surface temperature sampled on the Baltoro Glacier during the summer of 2011 and incoming solar radiation estimated in the same grid points. Finally, the daily ablation ($M_{DC\text{-}point}$, value in m w.e.) at each pixel of the CKNP debris-covered glacier area was modeled as:

$$M_{DC\text{-}point} = \frac{T_{s\text{-}point}}{DR_{point}} \frac{1}{L_m \cdot \rho_w} \Delta t \qquad (11$$

where Δt is the number of seconds in a day (8.64 x 10^4).

The ice melt over debris-free areas was evaluated by applying an enhanced T-index approach (following Pellicciotti et al., 2005), which also considers solar energy inputs in driving ice melt in addition to air temperature.
The daily ice melt at each pixel with debris-free ice ($M_{DF\text{-}point}$) was estimated by applying an enhanced T-index model (Pellicciotti et al., 2005):

$$M_{DF\text{-}point} = \begin{cases} TMF \cdot T_{a\text{-}point} + RMF \cdot (1-\alpha) \cdot SW_{in\text{-}point} & T_a > 0°C \\ 0 & T_a \leq 0°C \end{cases} \qquad (12$$

where $T_{a\text{-}point}$ is the daily mean air temperature (°C), α is the surface albedo, $SW_{in\text{-}point}$ is the daily mean incoming solar radiation (W m^{-2}), and TMF (32.43 x 10^{-4} m d^{-1} °C^{-1}) and RMF (0.79 x 10^{-4} m d^{-1} W^{-1} m^2) are the temperature and radiative melting factors, respectively. These melting factors are assessed from ablation measured at some selected sites on the Baltoro Glacier (from 3939 m to 5200 m a.s.l.) from 23 July to 7 August 2011. Melting factors estimated from field data are taken as constant in time and space (Hock, 1999). Albedo was estimated by analyzing incoming and outgoing solar radiation data recorded during 2012 by a net radiometer (CNR1, Kipp&Zonen) installed at the Concordia supraglacial AWS.
Both melt models (i.e. one for debris-covered and one for debris-free areas) were calibrated using field data gathered during an expedition on Baltoro Glacier performed during summer 2011.

Skardu where CKNP Headquarter is located. In the photo is also visible the confluence between the Indus and the Shigar Rivers which are mainly fed by glacier meltwater.

Results

1. Observed data

1.1 Glacier area

In the CKNP there are 608 glaciers (among which some of the largest Karakorum glaciers: Baltoro, Biafo, and Hispar). Glaciers span a broad range of sizes, types (i.e. mountain glaciers, glacierets, hanging glaciers, compound-basin valley glaciers), and surface conditions (i.e. debris-free and debris-covered ice).
Their total area in 2001 was 3681.8 ± 27.7 km², ~35% of the CKNP area. This area represents ~24% of the glacier surface of the entire Karakorum Range within Pakistan (total area from Bajracharya and Shrestha, 2011). The biggest ice body is Baltoro Glacier with an area of 604.2 km², while the mean glacier size results 6.1 km². In Figure 1 it is shown the frequency distribution of glaciers sorted according to size classes (following Bhambri et al., 2011). Only 11 glaciers fall within the largest size-class (> 50 km²), but they cover more than half of the glacierized surface of the CKNP (Fig. 2). Glaciers in the smallest classes (< 1 km²) account for ca. 61% of the census (Fig. 1), while covering only 3.8% of the total glacier area (Fig. 2). Glacier minimum elevation (i.e. ~ glacier terminus elevation) ranges between 4000 and 5000 m a.s.l. on average (Fig. 3), with few larger glaciers reaching farther down (between 3000 and 3500 m a.s.l., Fig. 4). Smaller glaciers (< 1 km²) show higher termini location, similarly to what is observed in other glaciated regions, including e.g. the Alaska Brooks Range (Manley, 2005), the Swiss glaciers (Kääb et al., 2002), the Cordillera Blanca (Racoviteanu et al., 2008), and the Italian Alps (Diolaiuti et al., 2012). Finally, more than the 60% of glaciers features a length of 1-5 km (Fig. 5).

All glaciers

Debris-covered glaciers

Debris-free glaciers

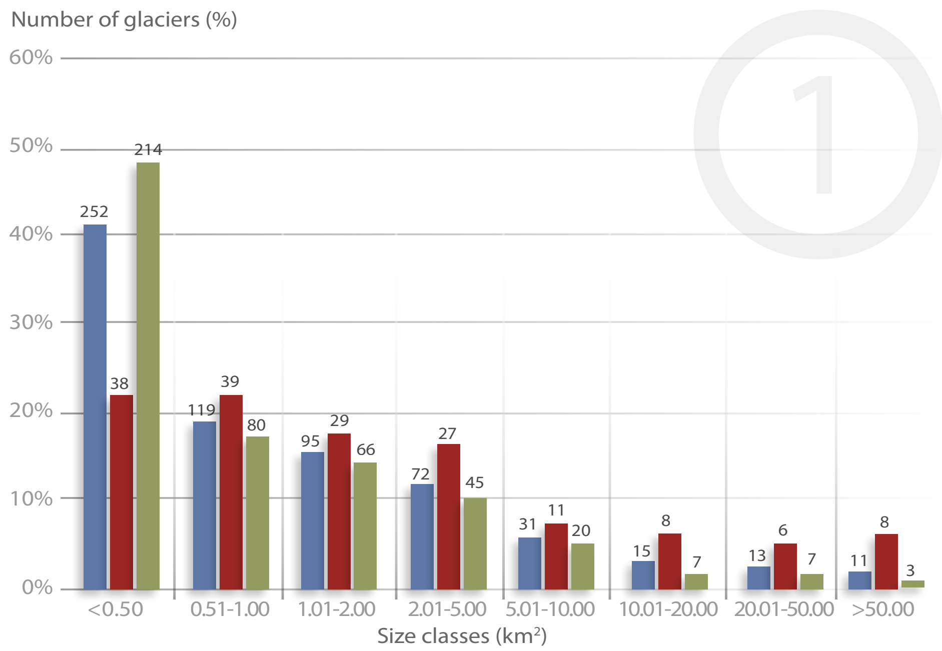

Fig. 1: Glacier distribution (percentage values, %, evaluated with respect to the total glacier number). Data are sorted according to 2001 glacier size class and surface conditions are reported as well. The labels show the number of glaciers of each size class.

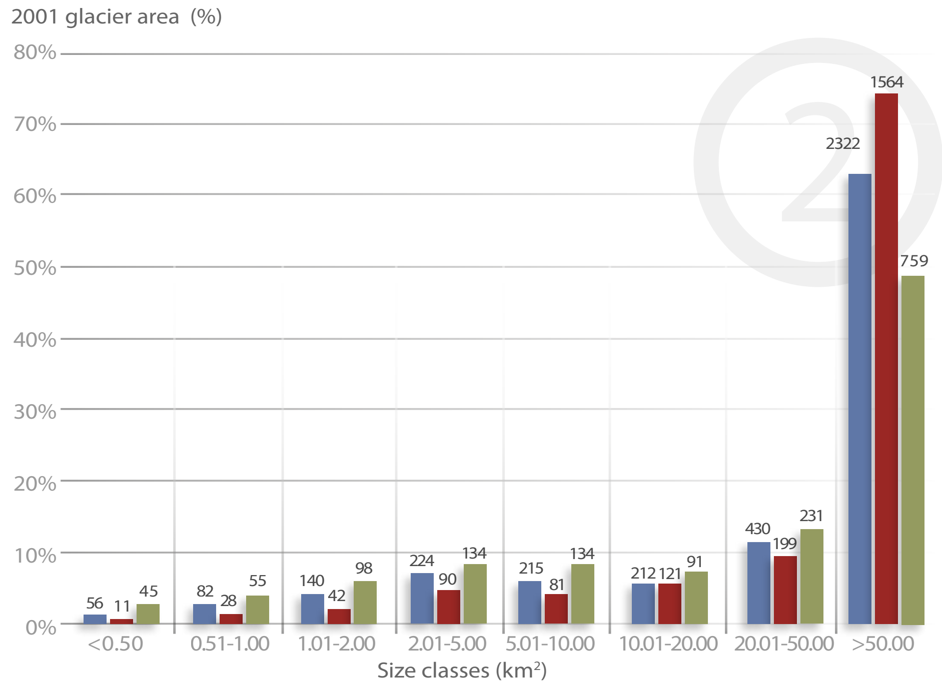

Fig. 2: Glacier distribution (percentage values, %, evaluated with respect to the total glacier area). Data are sorted according to 2001 glacier size class and surface conditions are reported as well. The labels show the total glacier area (km²) of each size class.

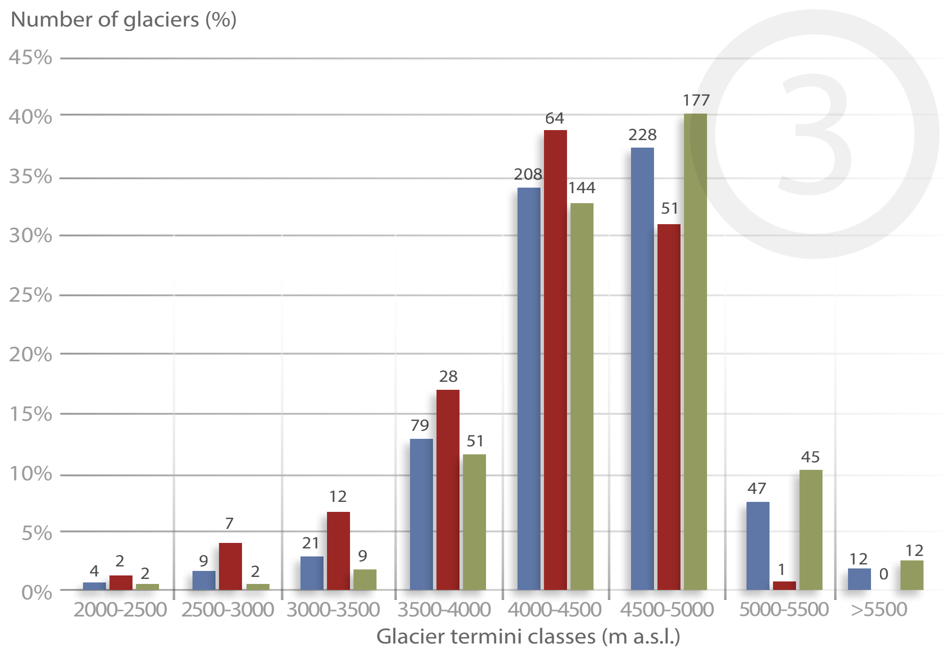

Fig. 3: Glacier termini distribution (percentage values, %, evaluated with respect to the total glacier number). Data are sorted according to glacier termini elevation based on the 2001 inventory data, surface conditions are reported as well. The labels show the number of glaciers of each size class.

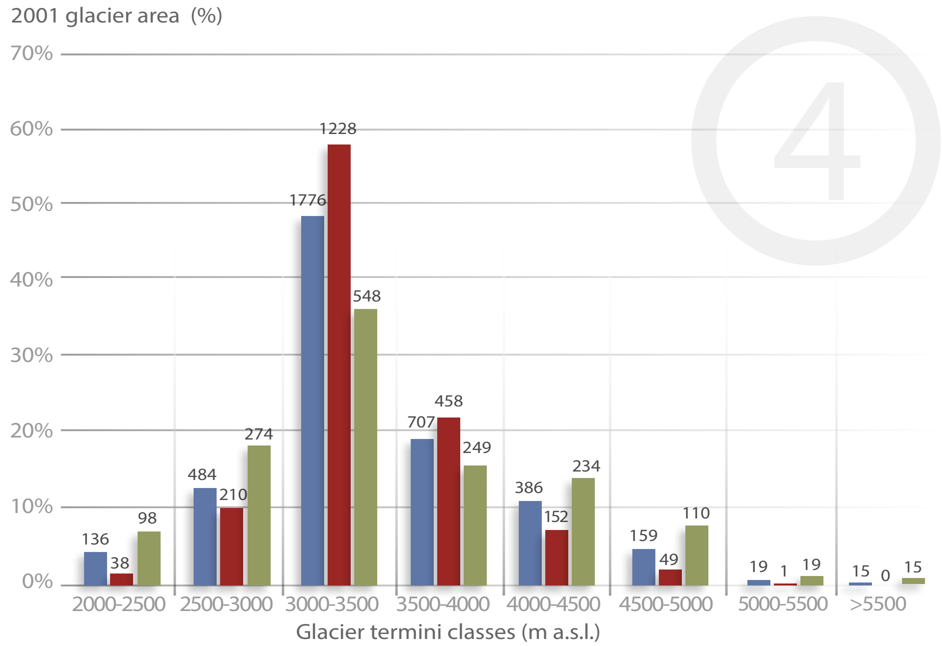

Fig. 4: Glacier termini distribution (percentage values, %, evaluated with respect to the total glacier area). Data are sorted according to glacier termini elevation based on the 2001 inventory data, surface conditions are reported as well. The labels show the total glacier area (km²) of each termini elevation class.

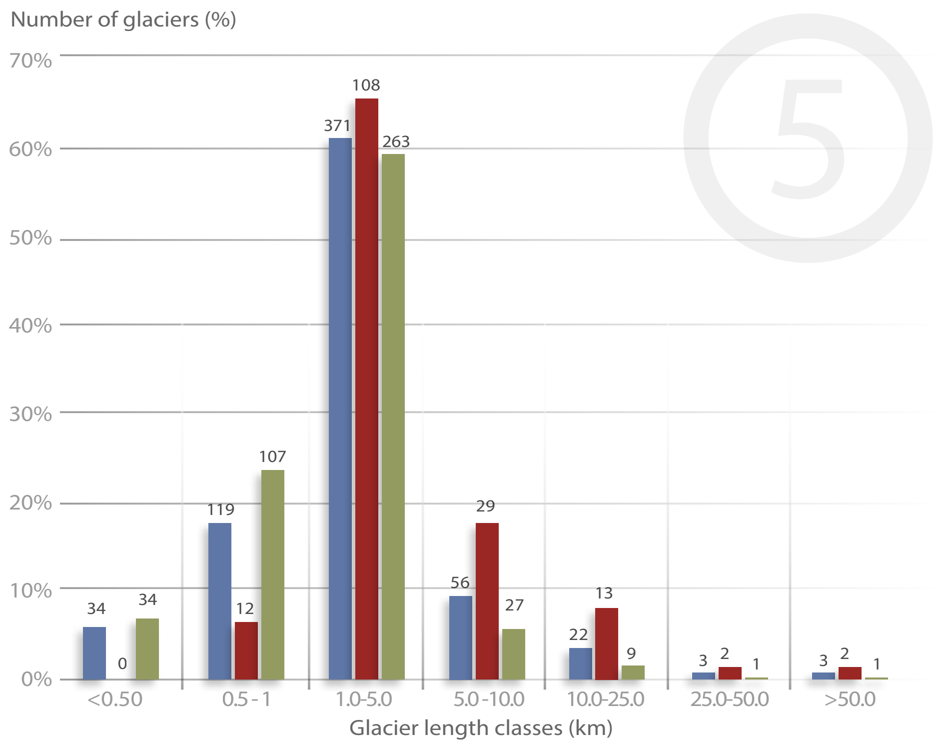

Fig. 5: Glacier length distribution (percentage values, %, evaluated with respect to the total glacier number). Data are sorted according to glacier length class for 2001, surface conditions are reported as well. The labels show the number of glaciers of each length class.

From the glacier hypsography (Fig. 6), we observe that glaciers range in elevation from 2250 to 7900 m a.s.l. Small glaciers with areas smaller than 1 km² are restricted to elevations above 3500 m a.s.l. Their elevation range is not very high, but some of them are even found up to 7000 m a.s.l. (Fig. 7). Most of the large and prominent glaciers instead originate above 7000 m a.s.l., and have a wide elevation range. Further, the minimum elevation reached by some of these large glaciers is much lower than in the Greater Himalaya of India and Nepal (Hewitt, 2005). We found a significant correlation (ρ = 0.5) of area vs altitudinal range (i.e. difference between maximum and minimum elevation). Glaciers with smaller vertical extent (i.e. maximum elevation close to the average) feature smaller areas. This is because they have small mass exchanges and therefore they cannot produce long tongues. Also, they can only survive in elevation where accumulation is secured.
In the available literature (Mayer et al., 2006; Mihalcea et al., 2008; Bocchiola et al., 2011; Soncini et al., 2015), the Equilibrium Line Altitude (ELA, the altitude of the theoretical line dividing the accumulation basin from the ablation zone,

on this line accumulation equals ablation and the yearly net mass balance is zero, see Cuffey and Paterson, 2010) for CKNP glaciers is placed between 5200-5300 m a.s.l. According to Braithwaite and Raper (2009), the ELA can be estimated from the median glacier elevation with an error of ±82 m. The median glacier elevation derived from our inventory is 4869 m a.s.l. Rather than an indication of negative mass budgets, this discrepancy with the literature value is more likely due to i) the exclusion of the steep headwalls from the upper glacier limits in our inventory (which entails a lower value of median elevation), and ii) the fact that many glaciers are significantly nourished by avalanches and hence have small accumulation regions. As a suitable approximation, the actual ELA of the CKNP glaciers could be placed between 5000 and 5200 m a.s.l. (Fig. 6).

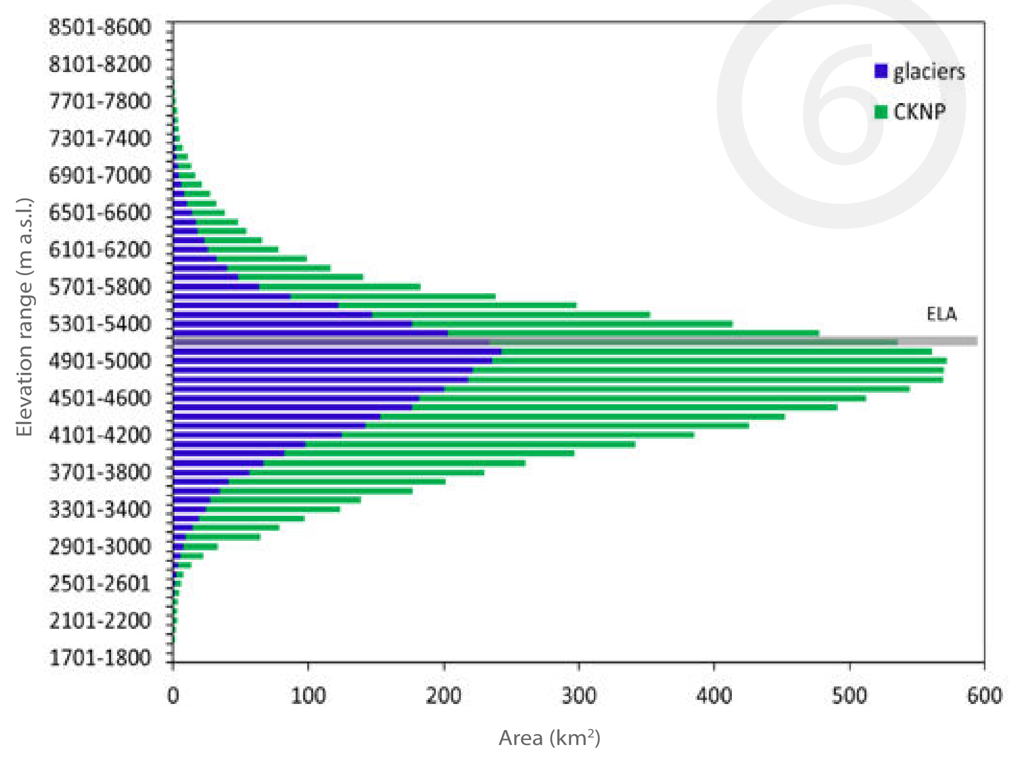

Fig. 6: Hypsography of glacier area distribution by 100 m elevation bins (based on 2001 glacier mask). Elevation data are based on the SRTM DEM of 2000. The grey bar represents approximate placement of ELA (Equilibrium Line Altitude).

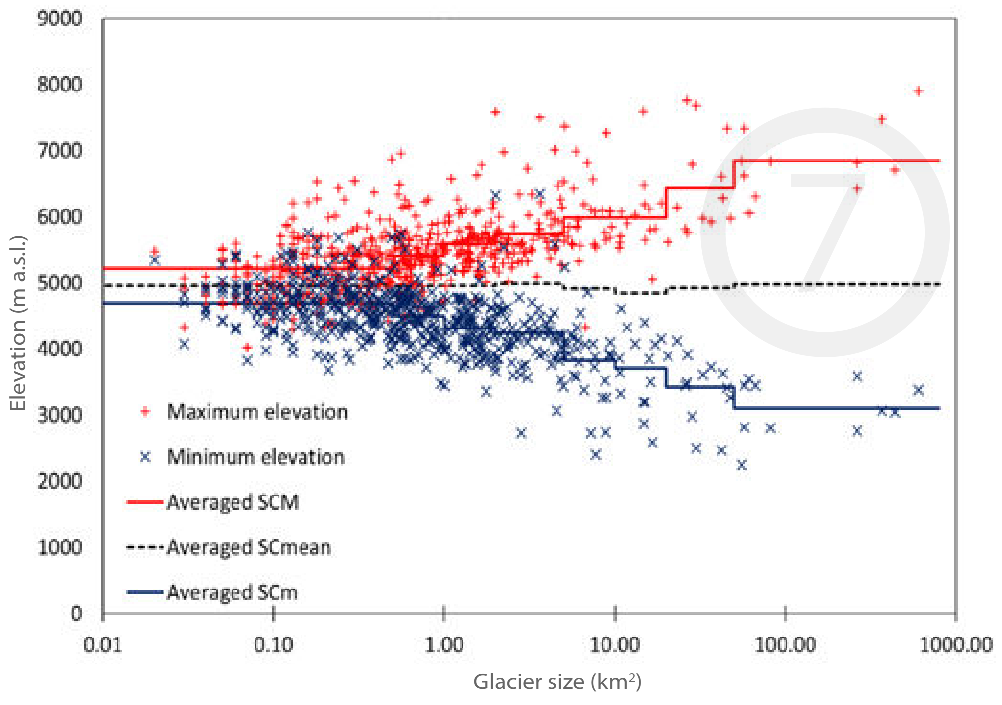

Fig. 7: Minimum and maximum elevation versus area size (2001). Values for discrete Size Classes (SC) are also given (m: minimum, M: Maximum). Notice the logarithmic scale for glacier size.

In 2010 glacier area of CKNP is 3682.1 ± 61.0 km², slightly more than 2001. Figure 8 shows glacier area from 2001 and 2010, and it highlights some important changes between the two years.

The analysis of the area changes during 2001–2010 reveals a general stability, evidence of the peculiar behavior of glaciers in the Karakoram in contrast to a worldwide shrinkage of most mountain glaciers outside the Polar Regions (Vaughan et al., 2013). The total area change is +0.3 ± 67.0 km²; 116 glaciers compared to the entire sample of 609 glaciers changed their area (namely the 19% of all the glaciers). Glaciers increasing their areas since 2001 account for an area gain of +7.7 ± 40.1 km², while the loss is -7.4 ± 53.0 km².

The Baltoro Glacier is found to be the glacier with the largest loss (-2.1 km²: from 604.2 km² in 2001 to 602.1 km² in 2010). On the other hand, a quite large debris-free glacier (i.e. Shingchukpi Glacier) experienced the maximum area gain (+1.7 km²: from 11.8 km² in 2001 to 13.5 km² in 2010).

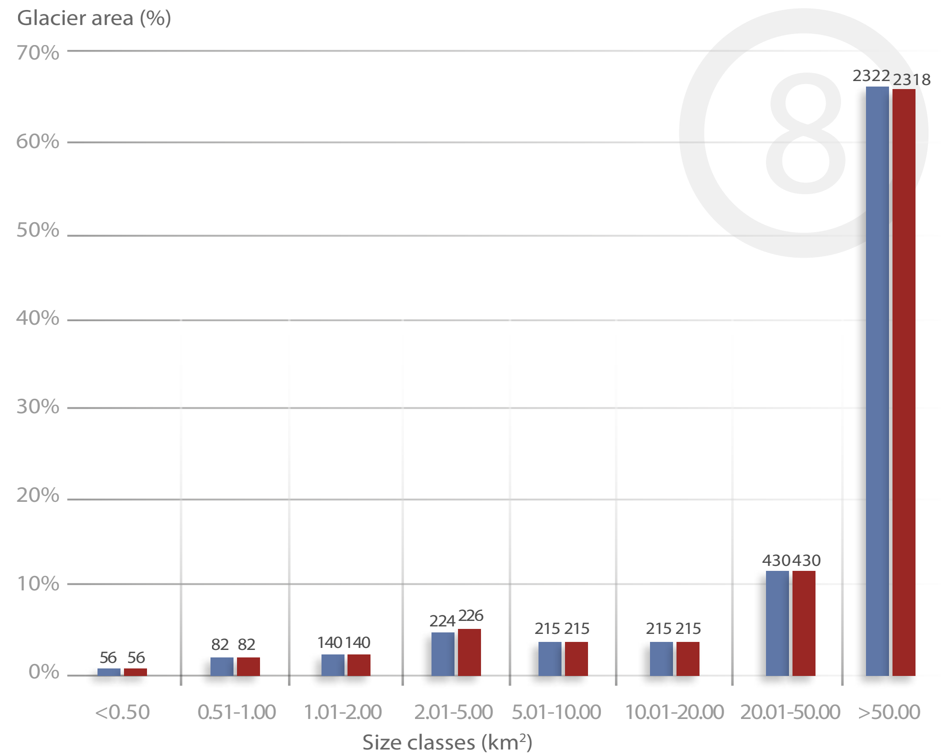

Fig. 8: Glacier coverage in 2001 and 2010 reported as percentage (%) calculated with respect to the total values (i.e. total area coverage in 2001 and 2010, respectively) sorted according to 2001 size class. The labels show the total glacier area (km²) of each size class.

In spite of the overall stable situation, some glaciers showed considerable changes. Some of these are surge-type glaciers (Table 1). In fact, the Karakorum is known to host several surge-type glaciers: this type of ice bodies displays cyclically short-term active phases involving rapid mass transfer from high to low elevations, and long-term quiescent phases of low mass fluxes. The most prominent surge example is the Shingchukpi Glacier with the largest surge advance (ca. 2220 m) (Fig. 9a). It is now in touch with the Panmah Glacier. Examples of important advances are also given by other tributaries of the Panmah Glacier (Maedan Glacier that collided with Chiring Glacier, Fig. 9b), which have experienced surges in 2001 and 2005 (Hewitt, 2007; Paul, 2015), now protruding far onto the main trunk of the Panmah Glacier. The overall contribution of the advancing surge-type glaciers to the CKNP area gain is 2.6 km², about 33% of the total area gain in 2010 with respect to 2001. The net area gain of 2.6 km² was evaluated without considering glacier tributaries; for these latter the area increase is already accounted for in the extent of the main glaciers. Neglecting the surge-type advances, the remaining glacier surface is still more or less stable, even if slightly negative.

Despite the relatively large length and area changes, and the high flow velocities during the active phase of a surge (up to 5 km yr^{-1} for the Khurdopin Glacier in the 1970s according to Quincey and Luckman, 2014), it is difficult to connect such advances to changes in mass balance. Previous works on surging glaciers in the Karakorum have suggested that climatically induced changes in glacier thermal conditions may be linked to observed exceptional surging (Hewitt, 2005), while others indicate that a change in subglacial drainage is the dominant control (Mayer et al., 2011). Quincey et al. (2011) speculated that recent surges in the Karakorum might be controlled by thermal rather than hydrological conditions, coinciding with high-altitude warming from long-term precipitation and accumulation patterns. Nevertheless, there is consensus that surge events are increasing in the Karakorum, and this is likely to reflect somehow recent changes in precipitation and temperature in the region (Hewitt, 2007; Copland et al., 2011). Recently, Herreid et al. (2015), found no significant difference in the Hunza basin between surging and non-surging glaciers in terms of total glacier area in a period of 37 years on a sample of 93 glaciers. However, according to the present knowledge, surge-type glaciers might obscure the actual glacier response to climate change in this region (in particular because their return periods are poorly constrained, Quincey and Luckman, 2014) and should therefore be discussed separately.

Glacier ID	Name	Latitude(°)	Longitude(°)	Advance (m)	Area gain (km²)	DC/DF
367	Feriole Glacier	35.86	76.00	1800	0.8	DF
368	Shingchukpi Glacier	35.90	76.02	2220	1.7	DF
357*	Maedan Glacier	35.93	76.03	900	0.8	/
357*	Drenmang Glacier	35.97	76.02	800	1.2	/
112	Unnamed	36.12	75.23	310	0.1	DC
111**	Kunyang Glacier	36.14	75.11	600	2.4	/

** glacier code refers to Panmah Glacier, whose these glaciers are tributaries.*

*** glacier code refers to Hispar Glacier, whose this glacier is tributary.*

Table 1: List of advancing surging glaciers in the CKNP from 2001 to 2010. DC means debris-covered glaciers, DF refers to debris-free glaciers.

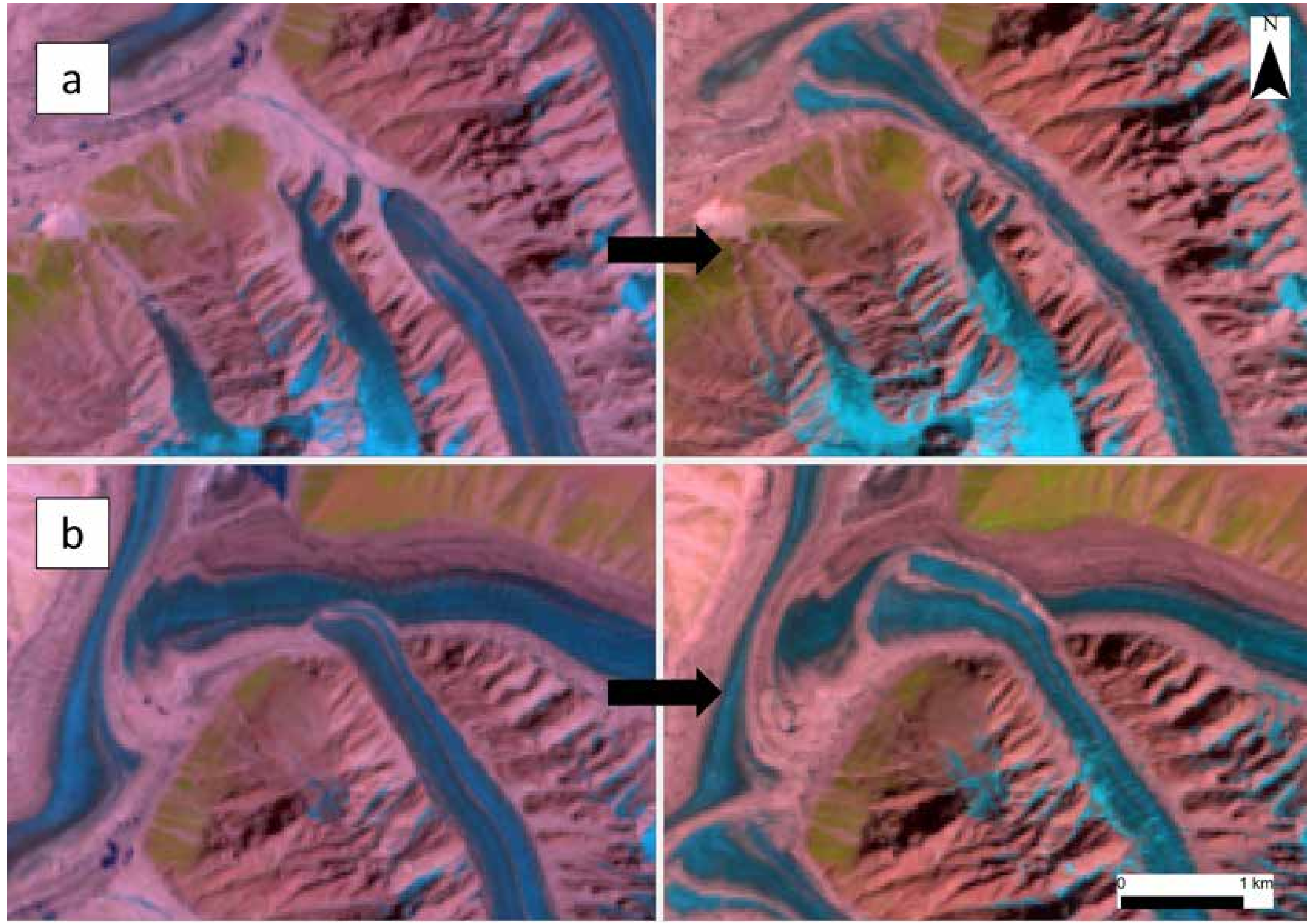

Fig. 9: Comparison of Shingchukpi Glacier's (a) and Maedan Glacier's (b) positions in 2001 (left) and 2010 (right) from Landsat TM imagery.

1.2 Supraglacial debris occurrence

A supervised classification applied to the Landsat images allowed the spatial analysis of the supraglacial debris (Fig. 10), which can be brought by landslides from the steep rock-walls surrounding the glaciers, rock falls and debris-laden snow avalanches. The supraglacial debris coverage was found to be equal to 765.5 ± 25.7 km² in 2001 and 919.1 ± 58.6 km² in 2010, i.e. about 21% of the total ice covered area. According to our calculation, the debris cover increased by 153.6 ± 64.0 km². Despite the error affecting our results and mainly due to the resolution of the analyzed satellite imageries, the debris enlargement can be clearly observed on selected glaciers, as for the Chogo Lungma Glacier (Fig. 11).

In general, the 27.3% of the CKNP glaciers was found to be debris-covered. Therefore, if CKNP glaciers are divided into debris-free and debris-covered

Supraglacial debris on the Hinarche Glacier (Bargot valley, Gilgit Basin).

types, we can immediately recognize two patterns. On the one hand, debris-covered glaciers are mostly larger (Baltoro and Hispar Glaciers belong to this group, see also Fig. 1) and they reach the lowest elevations (even below 3000 m a.s.l., see Fig. 3). In fact, the supraglacial-debris covers 20 to 27% of glaciers in the size classes larger than 2 km^2, with maximum in size class from 20 to 50 km^2 (Fig. 2). Moreover, they are covered by debris almost entirely up to about 4000 m a.s.l.: the maximum supraglacial-debris cover is found at 4300 m a.s.l. (see also Fig. 6). On the other hand, debris-free glaciers are in general smaller (see also Fig. 1), and their termini are found higher up on average (4500 m a.s.l., almost 700 m above the mean termini of debris-covered glaciers) (Figs. 3 and 12).

Supraglacial debris and dirty ice cones at the surface of the Hinarche Glacier (Bagrot valley, Gilgit Basin).

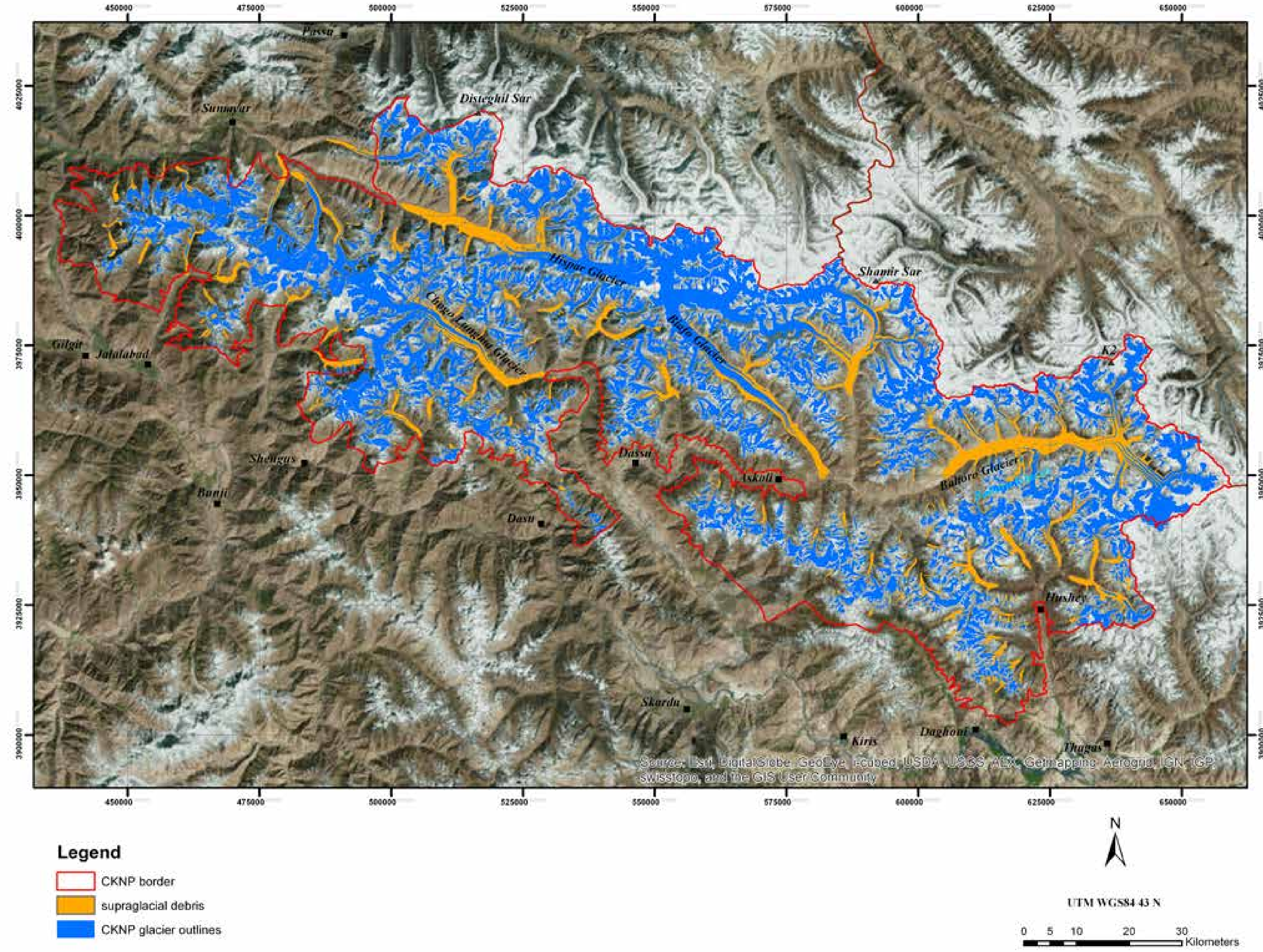

Fig. 10: Map describing the supraglacial debris coverage of CKNP glaciers in 2001.
The map was obtained by applying a supervised classification to Landsat imageries.

Finally, we observe that area changes of debris-free and debris-covered glaciers are similar but opposite, being the first positive and the second negative. Nevertheless, these variations (mainly due to the different elevation range featured by the two glacier types) represent less than 1% of the glacier area of both categories.
From our analysis, the presence of glaciers below 4000 m a.s.l. seems to be linked to the presence of a supraglacial debris cover. Debris can have two opposite effects on the ice. If it is thick enough (more than a "critical" thickness, to be derived from field observations, Mattson et al., 1993), it decreases ice melt rates by reducing the heat flux from the top of the debris layer to the debris-ice interface. According to Juen et al. (2014) a debris layer thicker than 0.1 m is able to diminish ablation efficiently, while Mihalcea et al. (2006) reported a critical debris thickness of around 0.05 m on the Baltoro Glacier. The debris thickness over most of the glacier termini in this region

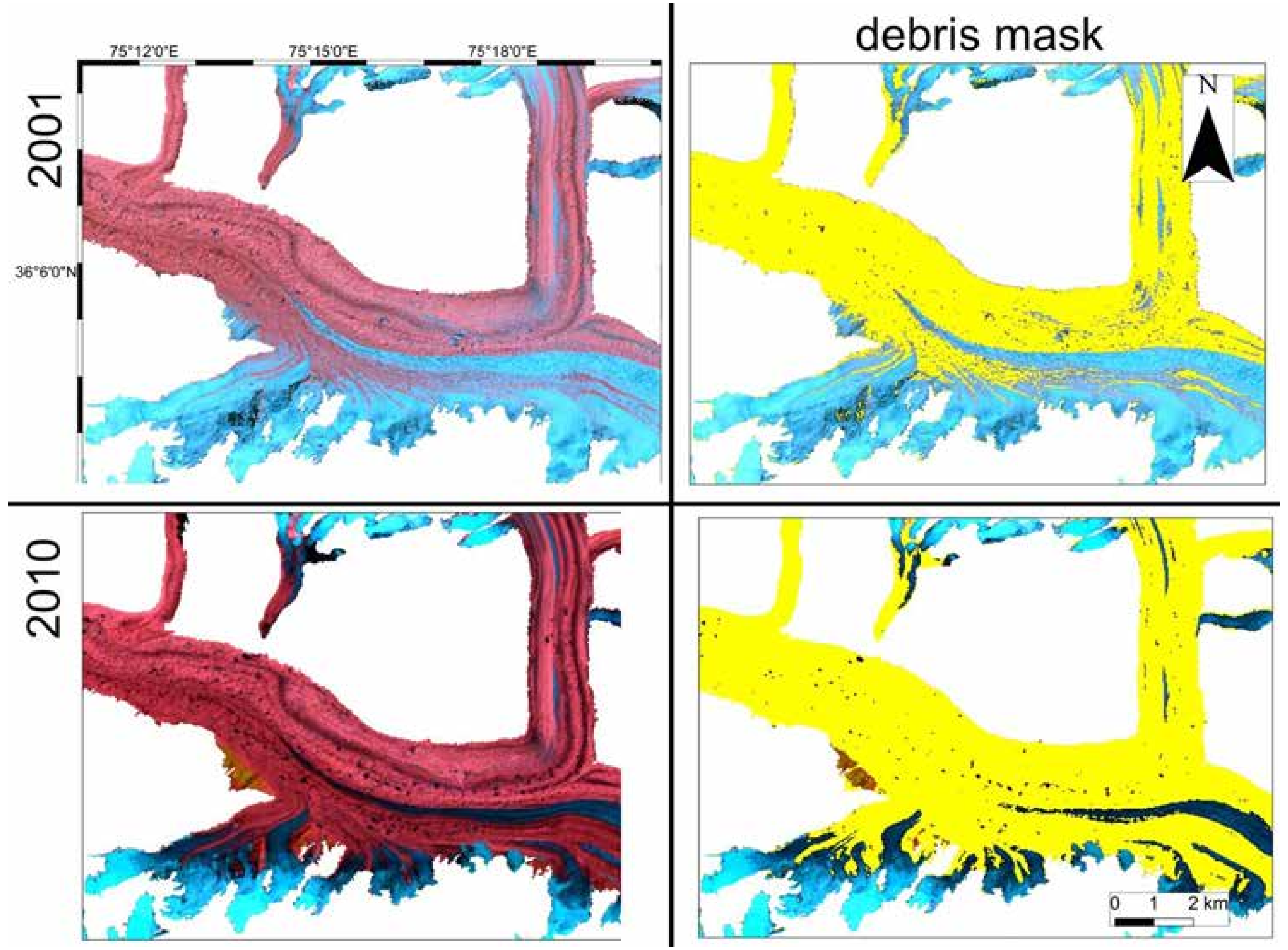

Fig. 11: Supraglacial debris coverage for 2001 (upper figures) and 2010 (lower figures) for a portion of the Chogo Lungma Glacier. False Color Composite (FCC) images (on the left, these were derived from combining the near infrared and the visible bands of the TM sensor, RGB=543, with the aim of increasing the color contrast between the glacier bodies and the surrounding pixels) and debris coverage mask (in yellow, on the right) are shown.

was previously found to be very high (often > 1 m, Mayer et al., 2006; Copland et al., 2009), and therefore able to reduce ice melt and preserve glaciers at such low altitudes where temperatures are generally higher. On the other hand, exposed ice cliffs and meltwater ponds, the presence of which is usually related to debris occurrence (Benn et al., 2012), can enhance ice ablation. Sakai et al. (2002) have shown that ice cliffs on glaciers in Nepal could make a large net contribution to total ablation of debris-covered glaciers, although covering a small percentage of the total glacier area. Juen et al. (2014) stated, however, that melt on ice cliffs plays a significant role for ice ablation, but not as high as concluded by Sakai et al. (1998). Reid and Brock (2014) concluded that ice cliffs (even the smallest ones) account for ~7.4% of the total ablation on the Miage Glacier, the largest debris covered glaciers of the Italian Alps. The effect of ice cliffs at a local scale can be clearly seen in patterns of glacier elevation change from DEM (Digital Elevation Model) differencing (Bolch et al., 2011). However, Gardelle et al. (2012) found no significant differences in surface elevation change between debris-free and debris-covered glaciers in the Karakoram over the last decade, indicating that the Karakorum Anomaly likely is mainly controlled by other factors than debris cover.

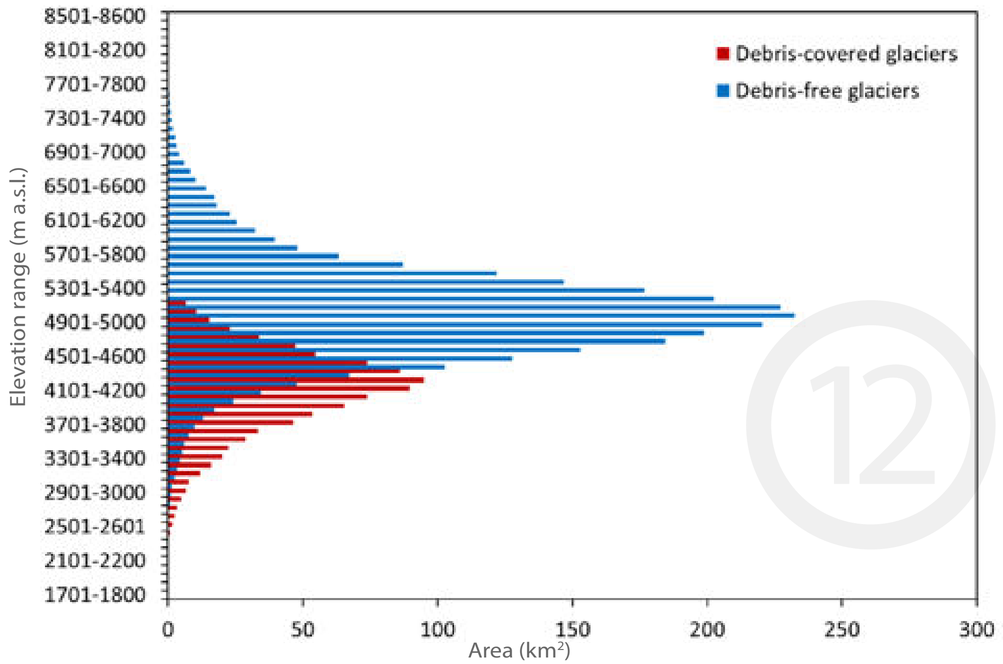

Fig. 12: Debris-free and debris-covered glacier areas distribution per 100 m altitude bins.

	All glaciers	Debris-covered glaciers	Debris-free glaciers
Glacier number	609	166	443
Glacier number (%)	100%	27%	73%
2001 Area (km^2)	3682.06 ± 27.7	2135.09 ± 24.8	1546.97 ± 13.4
2010 Area (km^2)	3682.38 ± 61.0	2132.45 ± 53.3	1549.93 ± 42.2
ΔA2001-2010 (km^2)	+0.3	-2.6	+3.0
ΔA2001-2010 (%)	+0.01%	-0.12%	+0.19%

Table 2: Glacier area changes during 2001–2010.
Data are also divided into debris-covered and debris-free glaciers .

Debris-free and debris-covered areas at the surface of the Hinarche Glacier (Bagrot valley, Gilgit Basin).

2. Derived data

2.1. Glacier thickness and volume

The ice thickness data (Fig. 13) were estimated from a physically based approach, which considers glacier geometry data recorded in the inventory (2001 data base). The mean ice thickness over the whole glacier was found ranging from more than 200 m (totally 2 glaciers: 285 and 213 m at Biafo and Baltoro Glaciers, respectively) to 5 m (only one glacier), with an average value of 32 m. Very small glaciers (i.e. with a surface area smaller than 0.1 km^2) result characterized by lower thickness values. Debris-covered glaciers feature a mean ice thickness of 41 m (ranging from 9 to 213 m), higher than the one found for debris-free glaciers (equal to 29 m, ranging from 5 to 285 m). The maximum ice thickness value was found at the Biafo Glacier (1362 m) and deep ice thicknesses were also found at the Baltoro (1016 m), Braldu (984 m) and Hispar (906 m) Glaciers. Generally higher ice thickness were found over the ablation area compared to accumulation zones (mean value of 53 m, ranging from 6 to 545 m).

The unique possible comparison is with Baltoro data which were acquired in 1954 during the well known expedition led by A. Desio. In that occasion gravimetric surveys gave a maximum glacier depth of about 900 m (Marussi, 1964) thus suggesting that our computations are in the reliable.

For assessing the total fresh-water resource nested by CKNP glaciers, an indirect approach based on glacier area and thickness data was applied. A total ice volume of 532.37 km^3 was found, divided in 308.30 km^3 regarding debris-covered glaciers and 224.07 km^3 for debris-free ones. Considering the total value, the mean ice thickness is about 145 m. On the one hand, Baltoro Glacier is characterized by the maximum volume value (128.79 km^3). This is the largest glacier (with an area of 604 km^2), even if Biafo Glacier has the highest mean ice thickness (area of 438 km^2, the second largest glacier). On the other hand, more than half of all CKNP glaciers (68.5%) contains a volume of water lower than 0.05 km^3 (Fig. 14), contributing only for the 0.98% over the total volume (Fig. 15). In particular, ice bodies such as glacierets (with an area of about 0.02 km^2) feature the minimum volume equal to 0.0001 km^3 (Fig. 16).

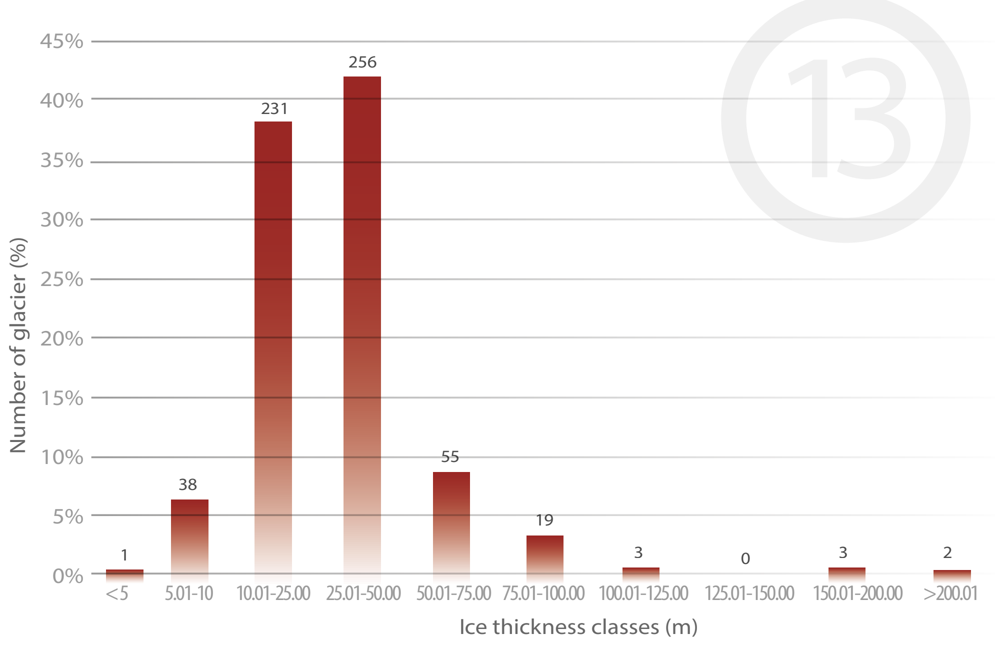

Fig. 13: Glacier thickness distribution. Data are sorted according to mean ice thickness class for 2001. The labels show the number of glaciers of each thickness class.

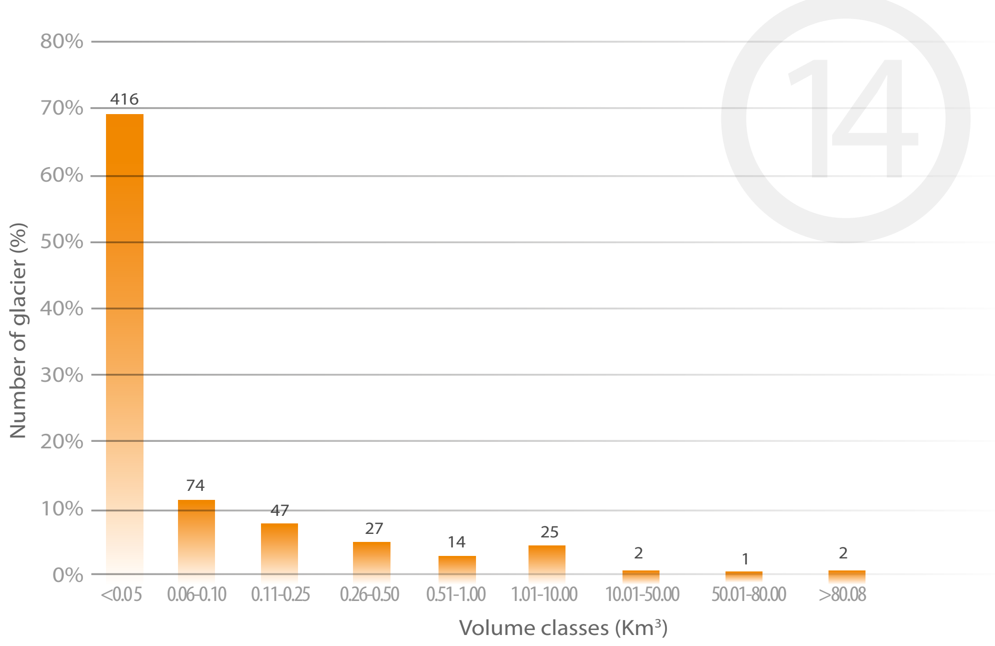

Fig. 14: Glacier volume distribution. Data are sorted according to 2001 glacier volume class. The labels show the number of glaciers of each volume class.

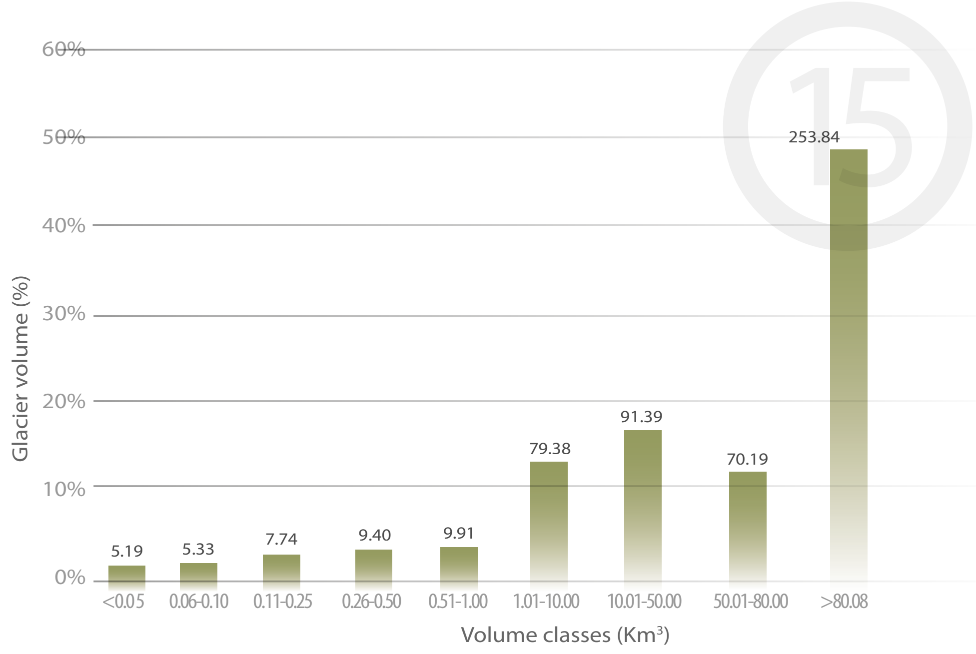

Fig. 15: Glacier volume distribution. Data are sorted according to 2001 glacier volume class. The labels show the glacier volume (km³) of each volume class.

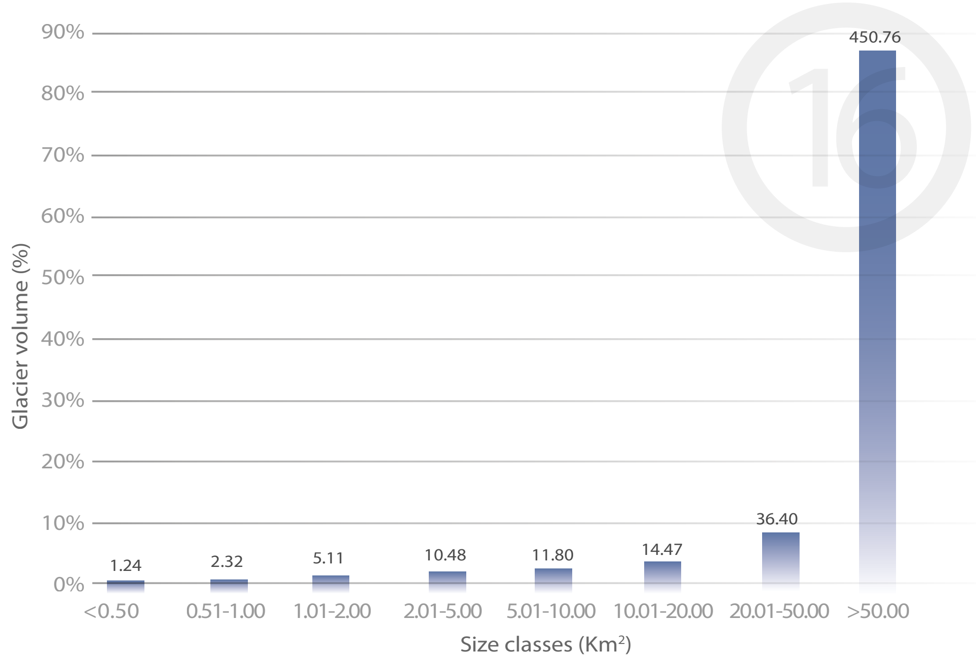

Fig. 16: Glacier volume distribution. Data are sorted accord ing to 2001 glacier size class. The labels show the glacier volume (km³) of each size class.

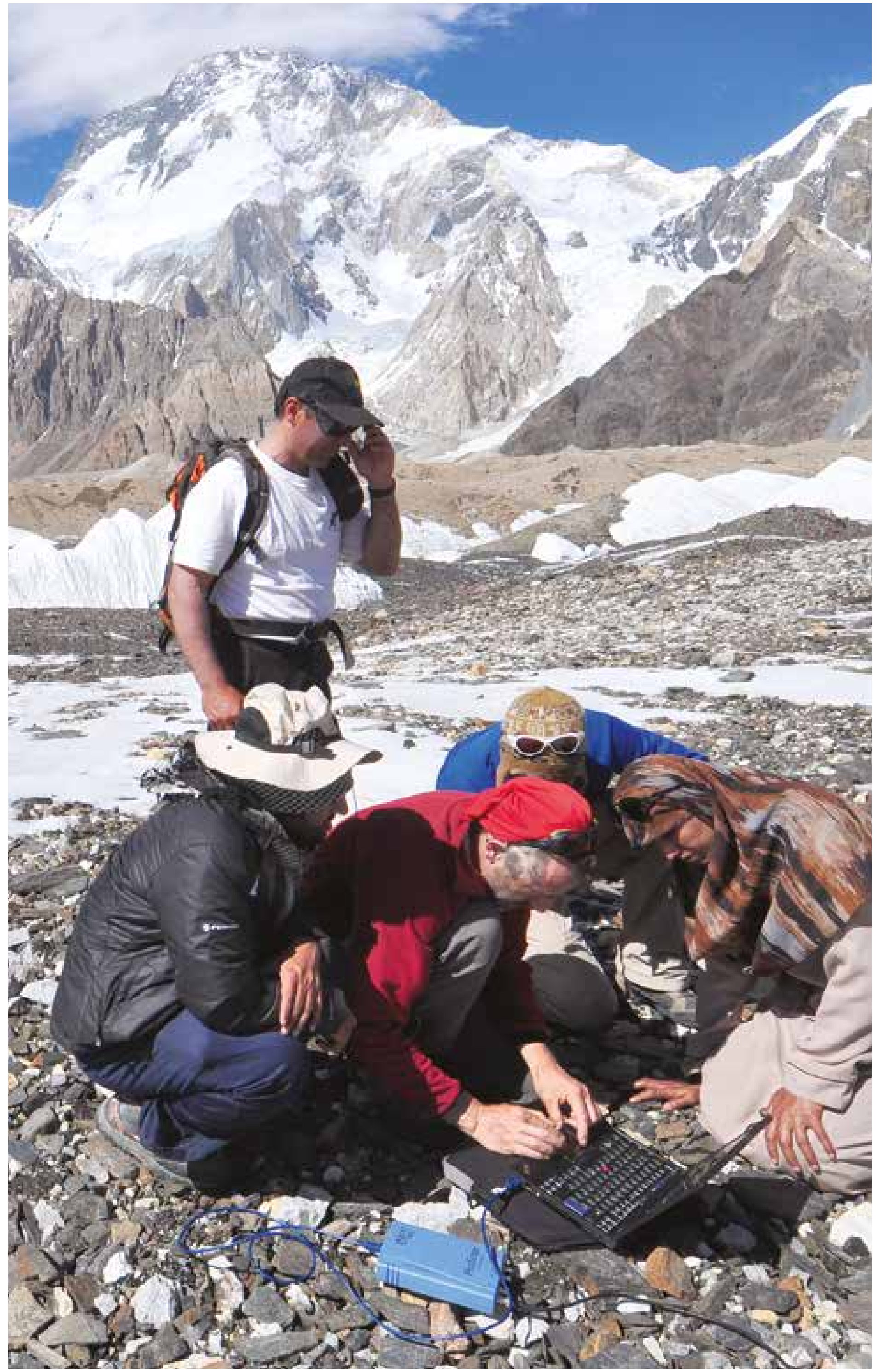

Radar measurements at the Baltoro Glacier (Shigar Basin) to evaluate ice thickness.

2.2. Supraglacial debris thickness

To derive a map of the thickness of supraglacial debris over the whole glacierized area of the CKNP (Fig. 17), a method based on the relationship between surface temperature and supraglacial debris thickness was applied (see Mihalcea et al., 2008a; 2008b).

The input data are debris thickness measured in the field on some selected representative debris-covered glacier areas (i.e. along the Baltoro Glacier) and satellite-derived surface temperatures at the same sites (see also Minora et al., 2015). The empirical relationship between these data represents a valuable tool for estimating debris thickness over unmeasured glacier zones. Supraglacial debris thickness results very high at the terminus (up to ~3 m) with a mean value of 0.22 m thus giving an overall rock debris volume of about 0.20 km³.

The supraglacial debris features different size and thickness

Measuring debris thickness during a field survey.

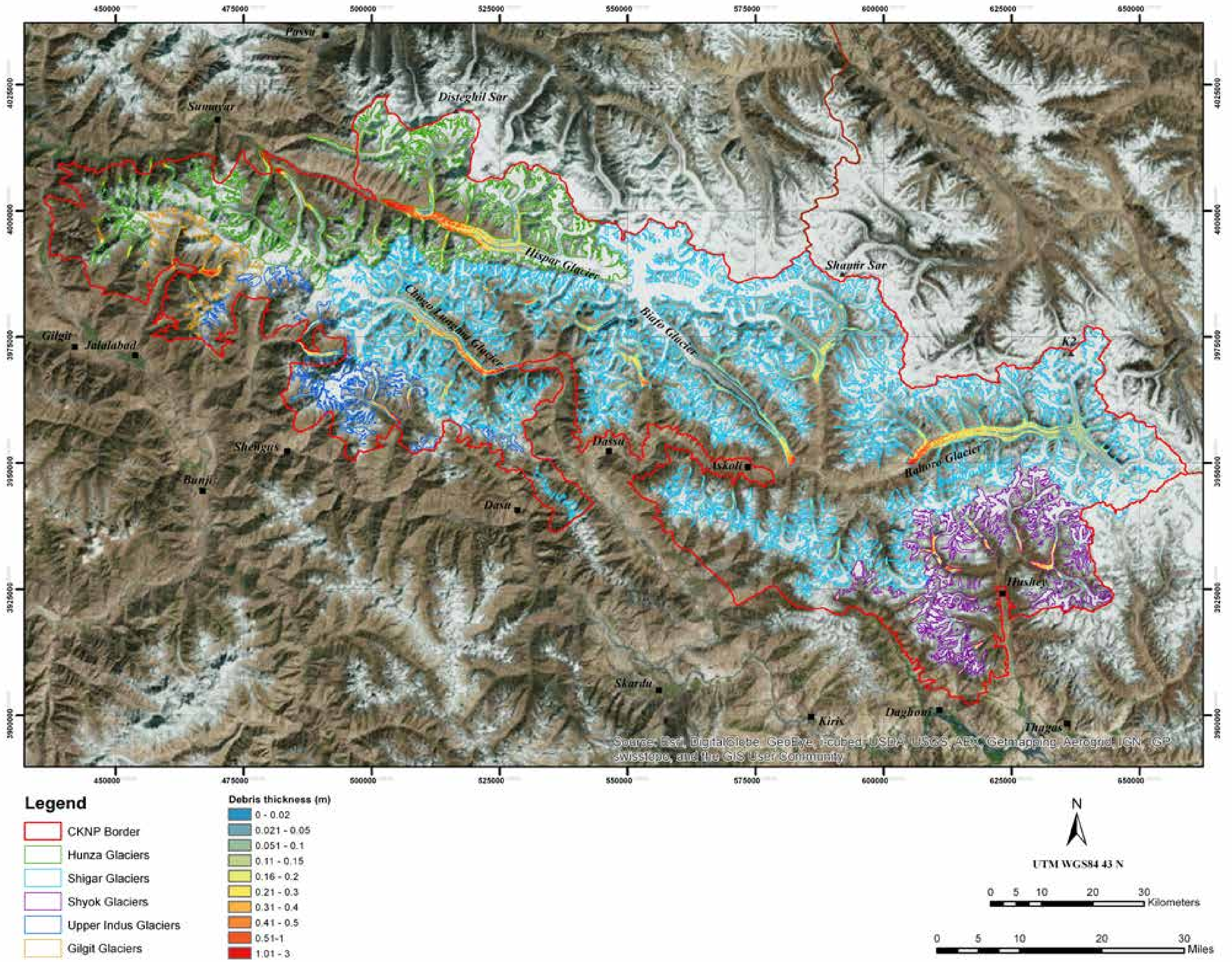

Fig. 17: Map showing the supraglacial debris thicknesses over CKNP glaciers.

The obtained supraglacial debris thickness values were cross-checked against a selection of field data, and a good fit was found (see Table 3). The main limitation comes from the fact that the supraglacial debris thicknesses derived from Landsat thermal data are average values at the pixel scale. The approach does not consider meltwater ponds, supraglacial lakes and sectors with crevasses and ice seals covering glacier areas smaller than the pixel size. Consequently, the model performs better in estimating debris layers thicker than 0.1 m (i.e. debris coverage is relatively continuous), while slight overestimation occurs for thin and sparse debris areas (< 0.1 m; Table 3).
The same limitation in supraglacial debris thickness modeling by means of remote sensing was found by Mihalcea et al. (2008a). Mapping of debris thickness is fundamental for estimating debris resistivity, and therefore debris-covered ice melt.
Other approaches have been proposed to produce debris thickness maps at higher resolution than ours (Foster et al., 2012), but they require meteorological data (including, among others, wind speed and direction and turbulent heat fluxes) on the glacier surface, as well as high-resolution DEMs (e.g. from lidar surveys), which were not available for glaciers in the CKNP area. Hence, our simple approach is suitable for investigating a wide and remote glacier area where high-resolution information is not available.

Elevation (m a.s.l.)	X	Y	DT-observed	DT-modeled	DT- residual (modeled minus observed values)
3699	606400	3952497	0.38	0.55	+0.17
3822	610488	3953487	0.32	0.43	+0.11
3923	613550	3954650	0.13	0.17	+0.04
3980	615221	3955685	0.20	0.14	-0.06
3985	616248	3955171	0.03	0.10	+0.07
3997	616148	3955855	0.15	0.41	+0.26
4008	616056	3956353	0.02	0.20	+0.18
4188	623369	3956355	0.41	0.11	-0.30
4077	618774	3955909	0.03	0.25	+0.22
4163	621318	3955889	0.11	0.00	-0.11
4178	623804	3955827	0.02	0.08	+0.06
4178	623801	3955858	0.02	0.05	+0.03
4178	623798	3955889	0.01	0.05	+0.04
4178	623808	3955914	0.04	0.05	+0.01
4178	623813	3955942	0.02	0.05	+0.03
4178	623833	3955939	0.05	0.05	+0.00
4178	623851	3955914	0.06	0.05	-0.01
4178	623807	3955982	0.01	0.05	+0.04
4178	623818	3955951	0.01	0.05	+0.04
4178	623878	3956476	0.10	0.17	+0.07
AVE					**+0.04**
RMSE					**0.13**

Table 3: Comparison between measured and modelled supraglacial debris thickness values (in m). X and Y are projected coordinates (WGS84 – UTM Zone 43N).

Concordia, the confluence between the Baltoro Glacier and the Godwing-Austen Glacier. In the background the Pyramid of Gasherbrum IV (Shigar Basin).

The Bagrot River (Gilgit Basin).

2.3. Meltwater

We developed two melt models capable to describe both debris-free and debris-covered ice ablation and we tested them in the time window 23 July–9 August 2011 (i.e. 18 days) for which were available field ablation data (see also Minora et al., 2015). The derived map with cumulated melting values is shown in Figure 18. However, the model is available to be applied on different time spans. During the 2011 ablation season, we collected 29 measurements on Baltoro Glacier (both debris-covered and debris-free conditions). We divided this dataset into two subgroups: one for calibrating our melt models and the other one for validating them. Table 4 reports the two sub-datasets used to calibrate and validate the models. The validation indexes display the performance of our models for estimating debris-free and debris-covered ice melt. In particular, we found a mean error of +0.01 m w.e. (corresponding to 2%) and a root mean square error (RMSE) equal to 0.09 m w.e. (17%).

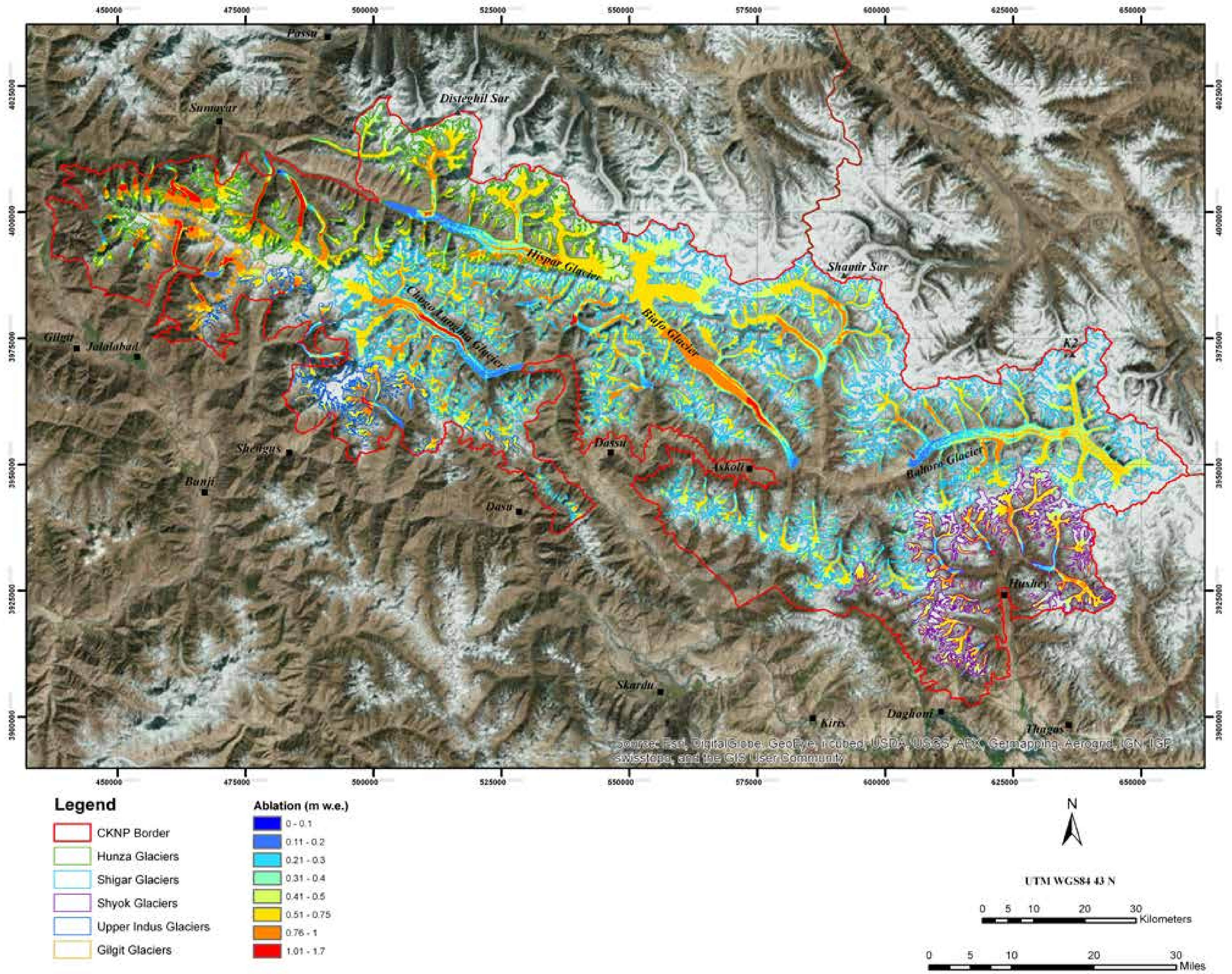

Fig. 18: Ablation map of CKNP glaciers below the equilibrium line altitude (ELA) in the period 23 July–9 August 2011.

Dataset-Debris	Elev.	X	Y	DR	M-observed	M-modeled	M-res	err
C-DC1	3699	606400	3952497	8.47	0.12	0.15	-0.04	+30%
C-DC2	3822	610488	3953487	7.28	0.14	0.18	-0.04	+26%
C-DC3	3923	613550	3954650	3.61	0.40	0.29	+0.11	-28%
C-DC4	3980	615221	3955685	6.18	0.25	0.21	+0.04	-16%
C-DF1	3939	612778	3954341	-	0.85	0.85	0.00	0%
C-DF2	4554	636142	3956930	-	0.62	0.61	+0.01	-2%
C-DF3	5200	639556	3968575	-	0.00	0.34	-0.34	0%
C-AVE							**+0.04**	**+2%**
C-RMSE							**0.14**	**25%**
V-DC1	3985	616248	3955171	1.52	0.640	0.48	+0.16	-25%
V-DC2	3997	616148	3955855	4.00	0.240	0.21	+0.03	-11%
V-DC3	4008	616056	3956353	1.42	0.590	0.51	+0.08	-13%
V-DC4	4188	623369	3956355	9.16	0.110	0.46	-0.01	+11%
V-DC5	4077	618774	3955909	1.62	0.490	0.26	+0.03	-7%
V-DC6	4163	621318	3955889	3.21	0.270	0.52	+0.01	-5%
V-DC7	4178	623804	3955827	1.42	0.460	0.59	-0.06	+12%
V-DC8	4178	623801	3955858	1.42	0.490	0.41	-0.03	+5%
V-DC9	4178	623798	3955889	1.23	0.480	0.52	-0.11	+23%
V-DC10	4178	623808	3955914	1.82	0.395	0.38	-0.02	+5%
V-DC11	4178	623813	3955942	1.42	0.490	0.35	-0.03	+5%
V-DC12	4178	623833	3955939	2.02	0.380	0.59	-0.11	-1%
V-DC13	4178	623851	3955914	2.22	0.300	0.59	-0.02	+16%
V-DC14	4178	623807	3955982	1.23	0.580	0.27	-0.03	+2%
V-DC15	4178	623818	3955951	1.23	0.475	0.49	+0.00	+24%
V-DC16	4178	623878	3956476	3.01	0.350	0.49	-0.05	-23%
V-DF1	4181	623382	3955368	-	0.470	0.21	-0.01	+4%
V-DF2	4178	623848	3955914	-	0.370	0.51	-0.12	+32%
V-DF3	4178	623830	3955979	-	0.560	0.12	+0.07	-13%
V-DF4	4178	623832	3955985	-	0.540	0.46	+0.05	-9%
V-DF5	4178	623827	3956013	-	0.640	0.26	+0.15	-24%
V-DF6	4178	623894	3956430	-	0.390	0.52	-0.10	+26%
V-AVE							**0.00**	**+2%**
V-RMSE							**0.08**	**16%**
AVE							**-0.01**	**+2%**
RMSE							**0.09**	**17%**

Table 4: Dataset used to calibrate and validate melt models. Dataset indicates whether ablation recorded at that site was used to calibrate (C) or to validate (V) the models; the site was debris-covered (DC) or debris-free (DF); Elev: elevation (m a.s.l.); X and Y: projected coordinates (WGS84 – UTM Zone 43N); DR: debris effective thermal resistance (m² °C W⁻¹); M-res: melt residuals (modeled minus observed values); err: melt residual (%). The period considered is from the end of July to mid-August.

In addition, we assessed any error due to the methodology applied for distributing the meteorological variables used as input in the melt models: air temperature (Ta), surface debris temperature (T_S) and incoming solar radiation (SWin). For this purpose, we firstly compared the modelled meteorological values with those measured by automatic weather stations at Urdukas and Concordia, finding a good agreement between two datasets. Root mean square errors (RMSEs) regarding air temperature are found equal to 1.2°C (for Urdukas) and 1.3°C (for Concordia) (Fig. 19). Modeled incoming solar radiation values resulted in a good match with the measured ones (Fig. 20), with RMSE values of 39 and 125 W m^{-2} for Urdukas and Concordia, respectively. Finally, the daily mean debris surface temperature was found featuring a RMSE of 2.1°C in comparison with field data sampled on Baltoro Glacier during summer 2011.

Then, we calculated the melt amount at selected debris-free (C-DF1, C-DF2, C-DF3) and debris-covered (C-DC1, C-DC2, C-DC3, C-DC4) ice field points varying the meteorological model inputs (Ta, T_S and SWin) by their maximum RMSE (i.e. ±1.3°C, ±2.1°C and ±125 W m^{-2}, respectively). Changing Ta and SWin, the debris-free ice melt variations range from ±10% to ±25% (at higher altitudes); debris-covered ice melt instead shows differences around ±30% when changing SWin, while variations in T_S drive a lower alteration around ±15%, not particularly influenced by elevation. Thus, the debris-covered ice melt model is more sensitive to the errors in the meteorological input data. However, debris-covered ice melt accounts for only 11% of the total melt. Moreover, these error tests were made considering the worst cases (maximum RMSE).

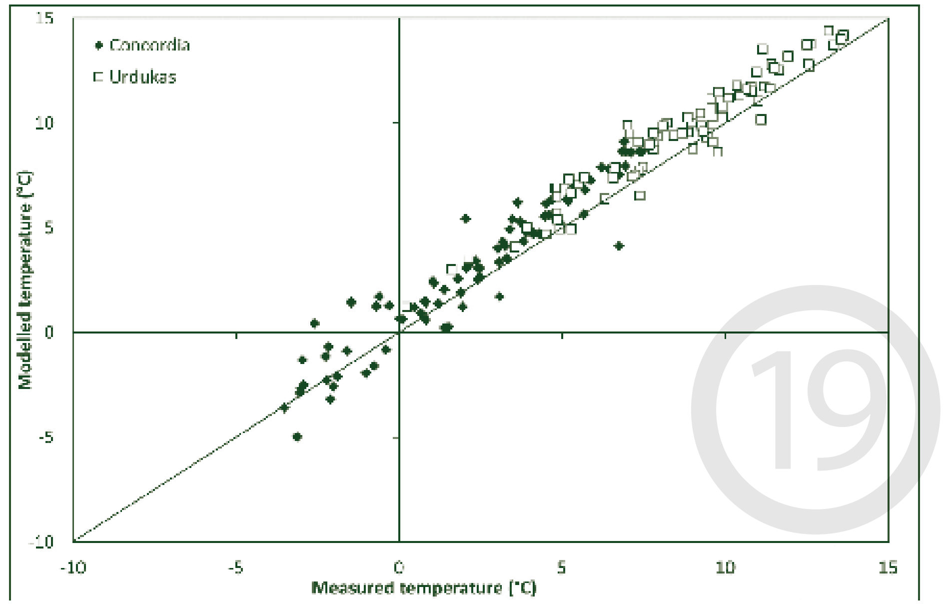

Fig. 19: Daily mean temperatures recorded by the AWS installed at Urdukas during 2011 (x-axis) vs modeled daily mean temperatures (y-axis) obtained by applying a constant local lapse rate of −0.0075°C m-1 to Askole temperatures (open box). The same analysis was performed for the Concordia dataset during 2012 (solid diamond).

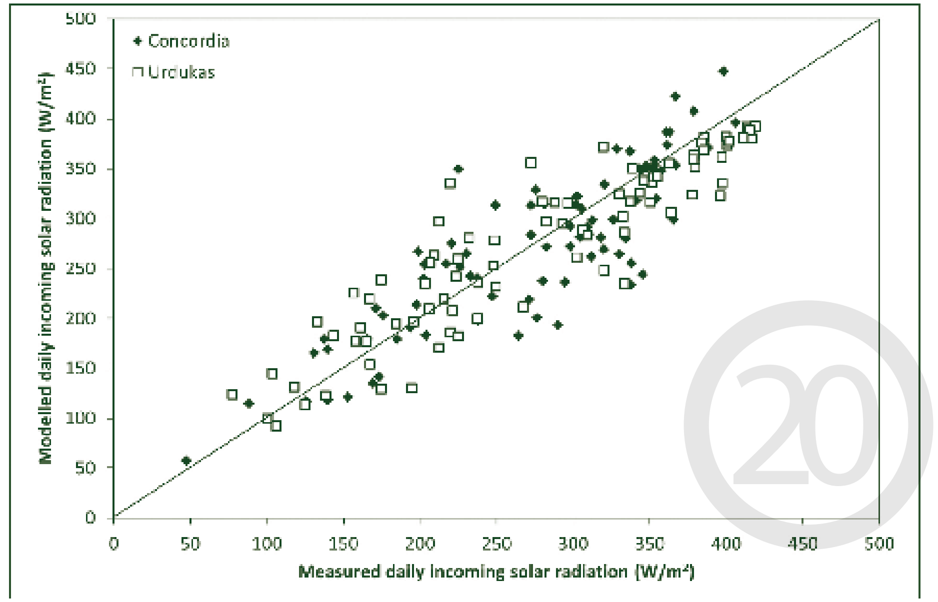

Fig. 20: Daily mean incoming solar radiation recorded by the AWSs installed at Urdukas during 2011 and at Concordia during 2012 (x-axis) vs the modeled values (y-axis) derived from Askole data

Given that the solar radiation was used to estimate debris surface temperatures, affecting in turn conductive heat fluxes, melt in debris-covered areas (M_{DC}) was largely linked to incoming solar radiation (SWin). Indeed, the minimum and maximum daily melt (0.008 and 0.023 km^3 w.e. d^{-1}, respectively) occurred during days with the lowest and highest incoming solar radiation (respectively, 112 and 371 W m^{-2}, in Askole; Fig. 21a). Conversely, melting in debris-free areas showed extreme daily values (0.026 and 0.099 km^3 w.e. d^{-1}) in days with extreme air temperatures (respectively +14.1°C and +22.1°C recorded at Askole; Fig. 21b). Overall, the greatest ablation occurred on 5 August, when incoming solar radiation was high, but not the highest, while the minima occurred on a day (29 July) with minimum air temperature.

Supraglacial ponds and rivers derived from glacier melting.

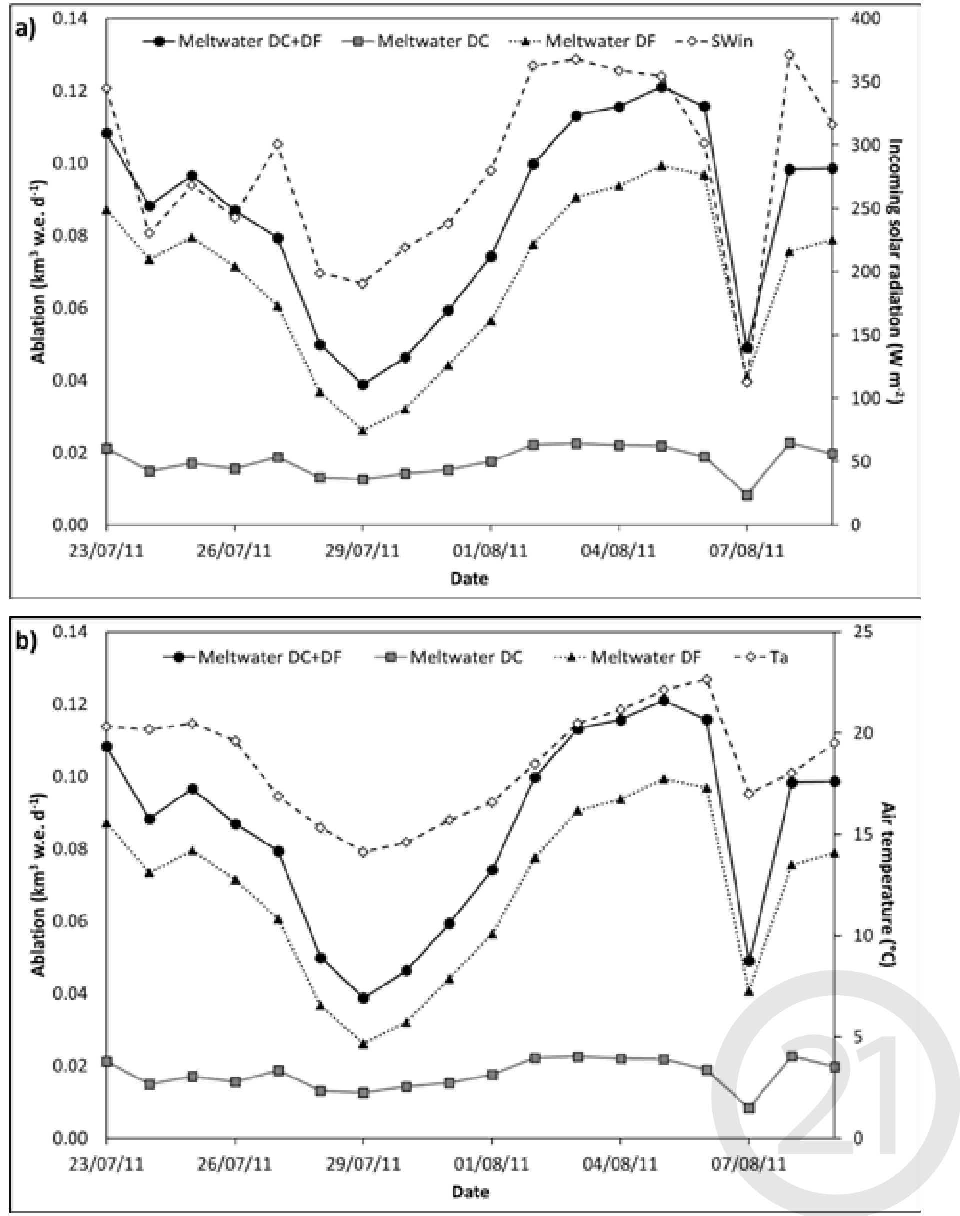

Fig. 21: Daily meltwater production from 23 July to 9 August 2011 from all the CKNP glaciers over the debris-free (DF) and debris-covered (DC) areas and the total (DC + DF). Same data are presented with (a) daily incoming solar radiation (SWin) and (b) daily mean air temperature (Ta) recorded at Askole. Date format is dd/mm/yy.

These findings indicate that i) melt from the debris-covered parts of the glaciers (M_{DC}) is mostly influenced by the incoming solar radiation, since it depends on the conductive heat flux, and ii) melt of debris-free parts of the glaciers (M_{DF}) is more sensitive to air temperature.

Over the period we considered, melting of the debris-covered parts of all the glaciers in the CKNP produced 0.319 km^3 of meltwater (total M_{DC}), with a daily average of 0.018 km^3 w.e. d^{-1}. The total meltwater from the debris-free parts (total M_{DF}) was 1.221 km^3, with an average of 0.068 km^3 d^{-1}. The total ice melt from the CKNP was thus equal to 1.540 km^3 w.e., with a daily average of 0.086 km^3 w.e. d^{-1}. This water volume equals ~11% of the reservoir capacity of the Tarbela Dam, a very large dam on the Indus River that plays a key role for irrigation, flood control and the generation of hydroelectric power for Pakistan (Thompson, 1974). Table 5 shows a summary of the model results.

	DC	DF	Total
area (km^2)	697	1929	2626
min daily M (m w.e. d^{-1})	0.012	0.014	0.012
max daily M (m w.e. d^{-1})	0.033	0.051	0.051
mean daily M (m w.e. d^{-1})	0.025	0.035	0.033
M (m w.e.)	0.458	0.633	0.586
min daily M (km^3 d^{-1})	0.008	0.026	0.008
max daily M (km^3 d^{-1})	0.023	0.099	0.099
mean daily M (km^3 d^{-1})	0.018	0.068	0.055
M (km^3)	0.319	1.221	1.540

Table 5: Modeled melt rates over debris-covered (DC) and debris-free (DF) areas, and the total ablation in the period 23 July–9 August 2011.

We performed several sensitivity tests and evaluated model responses to varying input data at field survey sites (Tables 6 and 7) as well as over the whole CKNP ablation area (Table 8). First, we considered the debris-covered areas. We varied the daily incoming solar radiation by ±10% and ±20%. Then we studied the effect of varying the debris thickness upon melt results (±10%, ±1 cm, ±5 cm and ±10 cm with respect to the actual debris thickness values). The model response at field survey points (C-DC1 to C-DC4) is shown in Table 6.

These tests suggest that changing the debris thickness or radiative input noticeably affects the debris-covered ice melt. In particular, this appears more evident in the presence of a thin debris thickness. Indeed, whenever shallow debris layers occur (see C-DC3 compared to C-DC1 in Table 6), even slight input variations entail evident changes in the underlying ice ablation, as the debris insulating effect is weaker.

	C-DC1	C-DC2	C-DC3	C-DC4
Elevation (m a.s.l.)	3699	3822	3923	3980
Debris thickness (cm)	37.5	31.5	13.0	26.0
Time frame (days)	11	12	12	13
M meas (m w.e.)	0.12	0.14	0.4	0.25
R (°C m2 W-1)	84.67	72.76	36.06	61.85
MDC mod (m w.e.)	0.15	0.18	0.29	0.21
ΔM +10% SWin (m w.e.)	0.01	0.013	0.025	0.016
ΔM -10% SWin (m w.e.)	0.01	0.013	0.025	0.016
ΔM ave % ±10% SWin	±6.7	±8.7	±16.7	±10.7
ΔM +20% SWin (m w.e.)	0.021	0.025	0.05	0.031
ΔM -20% SWin (m w.e.)	0.021	0.025	0.012	0.031
ΔM ave % ±20% SWin	±14	±16.7	±20.7	±20.7
ΔM +10% DT (m w.e.)	0.008	0.009	0.015	0.011
ΔM -10% DT (m w.e.)	0.009	0.011	0.018	0.013
ΔM ave % ±10%DT	±5.7	±6.7	±11.0	±8.0
ΔM +1cm DT (m w.e.)	0.002	0.003	0.012	0.005
ΔM -1cm DT (m w.e.)	0.002	0.003	0.013	0.005
ΔM ave % ±1 cm DT	±1.3	±2.0	±8.3	±3.3
ΔM +5cm DT (m w.e.)	0.01	0.014	0.05	0.02
ΔM -5cm DT (m w.e.)	0.013	0.019	0.088	0.028
ΔM ave % ±5 cm DT	±7.7	±11.0	±46.0	±16.0
ΔM +10cm DT (m w.e.)	0.018	0.025	0.082	0.035
ΔM -10cm DT (m w.e.)	0.029	0.044	0.283	0.069
ΔM ave % ±10 cm DT	±15.7	±23.0	±121.7	±34.7

Table 6: Sensitivity tests performed by applying different input data to the debris-covered ice melt model. We applied the model to four points where actual ablation data were collected in the field and calculated melt anomalies (ΔM) respect to M_{DC} by modifying the incoming shortwave radiation and debris thickness. The reference modeled melt is given by M_{DC} mod.

Next, we considered the debris-free areas. We varied the daily incoming solar radiation by ±10%. Then we shifted the daily air temperature by ±0.1, ±1.0 and ±2.5°C with respect to the measured values. Finally, we investigated the effect of changing the albedo values by ±10%. Table 7 shows the model responses at field survey points (C-DF1 to C-DF3).
The debris-free ice model is very sensitive to variations in air temperature and the ablation varied by ±45% with changes of ±2.5°C. Minor impacts derived from changing SWin inputs, showing a maximum variation of only 6%. This is a consequence of applying an enhanced T-index model, which indeed gives a primary role to temperature in driving ice-melt, and a complementary role to incoming solar radiation (see e.g. Pellicciotti et al., 2005). Concerning ice albedo (α), our model assumes a constant value of 0.30 for the whole area, thus probably entailing an over- or under-estimation of the actual ice melt. Common albedo values for snow and ice surfaces range from 0.20 to 0.85; the albedo therefore has a very large and important influence on the total shortwave radiation absorbed by the surface, SWin*(1-α), and hence on ablation. In the absence of direct measurements, albedo is often estimated from "typical" published values for snow or ice (Cutler and Munro, 1996): a clean ice surface generally features an albedo of 0.30-0.46, while a debris-rich ice one is characterized by an albedo of 0.06-0.30 (Cuffey and Paterson, 2010). Thus, the choice of albedo is a very critical issue in accurately estimating the ice melt. In this study, we adopted the mean value (i.e. 0.30) obtained by incoming and outgoing solar radiation data gathered by the supraglacial automatic weather station (AWS) placed at Concordia (in a debris-free area of the Baltoro Glacier). In previous studies, some authors applied similar approaches using an albedo of 0.30 (e.g. Pellicciotti et al., 2005). Oerlemans (2001) reported a mean albedo value for debris-free ice of about 0.30. So we followed these previous studies supporting the use of a constant albedo of 0.30. The sensitivity test at field survey sites showed that changing the albedo by ±10% may lead to melt change of up to ±9% on debris-free areas (Table 7).
In addition to these model sensitivity tests, we considered the whole CKNP area totally debris-free obtaining a total melt of 1.86 km^3, with an increase of 0.64 km^3 (more than twice as much) with respect to that obtained on actual debris-free areas (Table 8). This suggests that the debris layer is thick enough (more than the local critical value, Mattson et al., 1993) to constrain the ice melt rates on average. To assess the effects of albedo, we changed the albedo of debris-free areas by a factor of ±10%, finding only a moderate impact on total melt (±1.5%). Similar results were obtained by changing SWin by ±10%. Moreover, stronger impacts (±8%) are caused by changing air temperature by

	C-DF1	C-DF2	C-DF3
Elevation (m a.s.l.)	3939	4554	5200
Time frame (days)	18	18	18
M meas (m w.e.)	0.850	0.615	0.000
MDF mod (m w.e.)	0.850	0.615	0.335
ΔM -0.1°C (m w.e.)	-0.005	-0.005	-0.004
ΔM +0.1°C (m w.e.)	0.005	0.005	0.004
ΔM ave % ±0.1°C (m w.e.)	±0.6%	±0.8%	±1.2%
ΔM -1.0°C (m w.e.)	-0.052	-0.052	-0.075
ΔM +1.0°C (m w.e.)	0.052	0.052	0.066
ΔM ave % ±1.0°C (m w.e.)	±6.1%	±8.4%	±20.9%
ΔM -2.5°C (m w.e.)	-0.130	-0.130	-0.138
ΔM +2.5°C (m w.e.)	0.130	0.130	0.161
ΔM ave % ±2.5 °C (m w.e.)	±15.3%	±21.1%	±44.7%
ΔM +10% SWin (m w.e.)	0.025	0.025	0.020
ΔM -10% SWin (m w.e.)	-0.025	-0.025	-0.020
ΔM ave % ±10% SWin (m w.e.)	±2.9%	±4.1%	±6.1%
ΔM +10% albedo (m w.e.)	-0.035	-0.036	-0.029
ΔM -10% albedo (m w.e.)	0.035	0.036	0.029
ΔM ave % ±10% albedo (m w.e.)	±4.1%	±5.8%	±8.7%

Table 7: Sensitivity tests performed by applying different input data to the debris-free ice melt model. We applied the model to three points where actual ablation data were collected in the field and calculated melt anomalies (ΔM) respect to M_{DF} by varying the air temperature, the incoming shortwave radiation and the albedo. The reference modeled melt is given by M_{DF} mod.

±1.0°C. Finally, we investigated the impact of debris thickness (DT) by changing its values by ±10%, ±50%, and +100%. In spite of the small impact on the total melt amount (+6.8% with -50% of DT and -5.9% with +100% of DT), the applied changes largely affected debris-covered ice melt. As the overall mean DT we derived from Landsat image (0.22 m) is surely higher than the local critical value (around 0.05 m on the Baltoro Glacier according to Mihalcea et al., 2006), the model is more sensitive to reduction than to increases of the actual DT value. This agrees with the well-known non-linear relation between debris-covered ice melt and DT (see also Figure 7 in Mihalcea et al., 2006). Indeed, when DT was decreased by 50%, melt in debris-covered areas increased by up to +33%, while when it was doubled, melt decreased by -28.5% (see Table 8).

	DC (km^3)	DF (km^3)	DC+DF (km^3)	%ΔDC	%ΔDF	%Δtotal
M	0.319	1.221	1.540	-	-	-
M all debris-free	0.000	1.861	1.861	-	-	20.8%
M +10% albedo	0.319	1.198	1.517	-	-1.9%	-1.5%
M -10% albedo	0.319	1.244	1.563	-	1.9%	1.5%
M +10% SWin	0.347	1.274	1.622	8.8%	4.4%	5.3%
M -10% SWin	0.291	1.167	1.458	-8.8%	-4.4%	-5.3%
M +1.0°C	0.319	1.343	1.662	-	10.0%	8.0%
M -1.0°C	0.319	1.095	1.414	-	-10.3%	-8.2%
M +10% DT	0.305	1.221	1.526	-4.3%	-	-0.9%
M -10% DT	0.334	1.221	1.555	4.8%	-	1.0%
M +50% DT	0.263	1.221	1.484	-17.4%	-	-3.6%
M -50% DT	0.424	1.221	1.645	33.0%	-	6.8%
M +100% DT	0.228	1.221	1.449	-28.5%	-	-5.9%

Table 8: Sensitivity test performed by applying different input data to both the debris-free and debris-covered ice melt models. The model results without input variation are shown in line 2 (M). We considered the whole CKNP ablation area.

Bagrot valley (Gilgit Basin): terrace coultivation supported by glacier-derived waters.

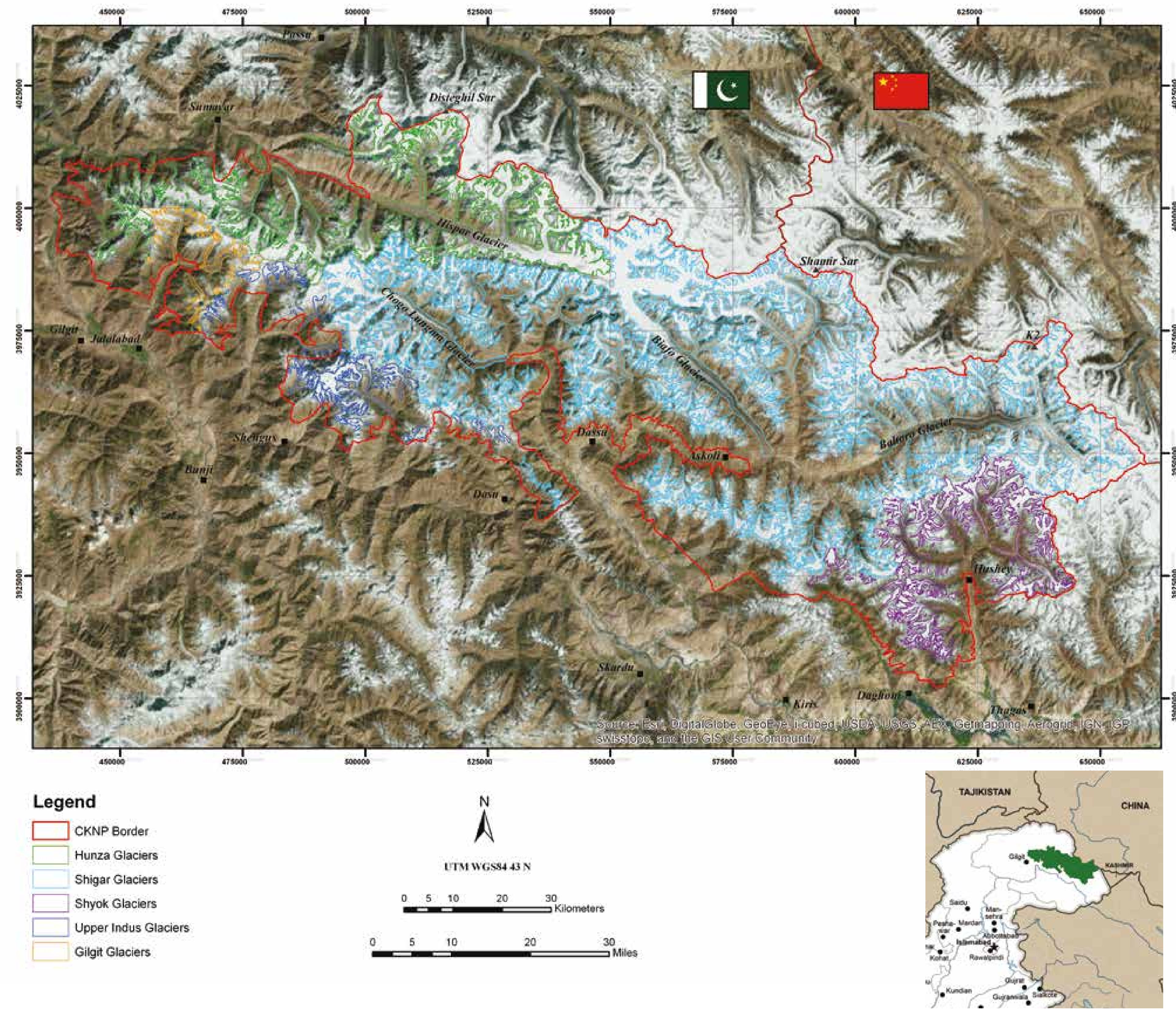
Legend
CKNP Border
Hunza Glaciers
Shigar Glaciers
Shyok Glaciers
Upper Indus Glaciers
Gilgit Glaciers
N
UTM WGS84 43 N
Kilometers
Miles
TAJIKISTAN
CHINA
KASHMIR
Gilgit
Passu
Sumayar
Disteghil Sar
Hispar Glacier
Shaanir Sar
K2
Biafo Glacier
Baltoro Glacier
Jalalabad
Askoli
Dassu
Hushey
Skardu
Kiris
Daghoni
Thagas
Bunji
Dasu

Catchments

Glaciers in the Hunza basin

Observed data

Hunza basin hosts totally 1384 glaciers (Bajracharya and Shrestha, 2011), whose 123 in the CKNP area, corresponding to ~20% of the total CKNP glacier census (Fig. A) and covering a cumulative area of 766.03 km^2 (21% of the total CKNP glacierized surface, Fig. B). Sorting glaciers according to size classes (Fig. C), the 50.4% of ice bodies in this basin is characterized by an area lower than 0.5 km^2, but altogether they represent only 1.4% of the whole Hunza glaciation (Fig. D).
Only 3 glaciers fall within the largest size-class (i.e. >50 km^2, Fig. C), however their cumulative area is ca. 66.2% of the Hunza glacierized extent (Fig. D). The mean glacier size is found to be 6.23 km^2 (Fig. E) and the widest ice body within this basin is the Hispar Glacier, featuring an area of 369.06 km^2 (Fig. F).
As regards the glacier terminus elevation (Fig. G), Hunza basins is characterized by the highest variability, and it ranges from 2250 to 6350 m a.s.l. (the minimum and maximum terminus value, respectively). However, the mean elevation of the glacier snout is found to be 4401 m a.s.l., very similar to the values of the other four basins. About the 50% of the Hunza glaciers features a length ranging between 1 and 5 km (Fig. H) and the maximum length is reached by Hispar glacier, the biggest one of this basin (i.e. 51.16 km).
By means of the supervised classification which we applied to the Landsat images, it was possible to investigate occurrence and spatial distribution of supraglacial debris and then to sort glaciers into debris-free and debris-covered types. In the Hunza basin, 26 glaciers were found to be debris-covered (Fig. I), covering 541.7 km^2 (i.e. 70.7% of Hunza glacierized area). The mean glacier terminus elevation of these glaciers (i.e. 3851 m a.s.l.) is found below the average value considering all Hunza ice bodies (4401 m a.s.l.): this lower value is probably due to the abundant presence of supraglacial debris.
In Table 1 glacier area values in 2001 and 2010 are shown sorted according to 2001 size classes. The Hunza glacierized area is characterized by a slight shrinkage from 2001 to 2010 (i.e. -0.76 km^2), with the highest retreat for the 10-20 km^2 size class and equal to -0.52 km^2. Nevertheless, the area variations during this period are found to be both positive (11 glaciers, totally +0.30 km^2) and negative (10 glaciers, totally -1.06 km^2).

Size class (km²)	2001 Area		2010 Area		Δ2001-2010	
	km²	%	km²	%	km²	%
<0.5	10.32	1.3%	10.28	1.3%	-0.04	-0.01%
0.5–1.0	12.98	1.7%	13.04	1.7%	0.06	0.01%
1.0–2.0	22.93	3.0%	22.93	3.0%	0.00	0.00%
2.0–5.0	43.21	5.6%	43.36	5.7%	0.15	0.02%
5.0–10.0	35.59	4.6%	35.61	4.7%	0.02	0.00%
10.0–20.0	45.76	6.0%	45.24	5.9%	-0.52	-0.07%
20.0–50.0	88.30	11.5%	88.14	11.5%	-0.16	-0.02%
>50.0	506.94	66.2%	506.67	66.2%	-0.27	-0.04%
Total	**766.03**	**100.0%**	**765.27**	**100.0%**	**-0.76**	**-0.10%**

Table 1: Glacier coverage in 2001 and 2010 and glacier area change in the time window 2001-2010 (km^2) sorted according to 2001 size classes, and reported also as percentage (%) calculated with respect to their total values.

Derived data

The ice thickness data were assessed applying a physically based approach (fully described in the section "Data and methods" of Introduction and Methods chapter), which considers the glacier geometry data recorded in the CKNP inventory (2001 data base). The mean ice thickness of the Hunza basin glaciers is estimated ranging from 5 m to 190 m (this latter featured by Hispar Glacier), with an average value of 28 m (Fig. L). The most part of glaciers (69.9%) features a thickness value between 10 and 50 m. Debris-covered glaciers feature a mean ice thickness of 46 m (ranging from 9 to 190 m), higher than the one found for debris-free glaciers (equal to 23 m, ranging from 5 to 97 m).
For assessing the total fresh-water resource nested by CKNP glaciers, an indirect approach based on glacier area and thickness data was applied (see section "Data and methods" of Introduction and Methods chapter). A total ice volume of 98.40 km^3 was estimated (Fig. M), 83.16 km^3 of ice is entrapped into debris-covered glaciers and 15.24 km^3 of ice into debris-free glaciers. Considering the total value (i.e. 98.40 km^3), the mean ice thickness results about 128 m. The largest part of the Hunza glaciers (73.2%) features a volume lower than 0.05 km^3 but contributing only to 0.89% of the total Hunza glacier volume, and the mean value is equal to 0.80 km^3 (Fig. N, higher than the overall CKNP condition but lower compared to Shigar basin). The Hispar Glacier is characterized by the highest volume value (i.e. 70.19 km^3).

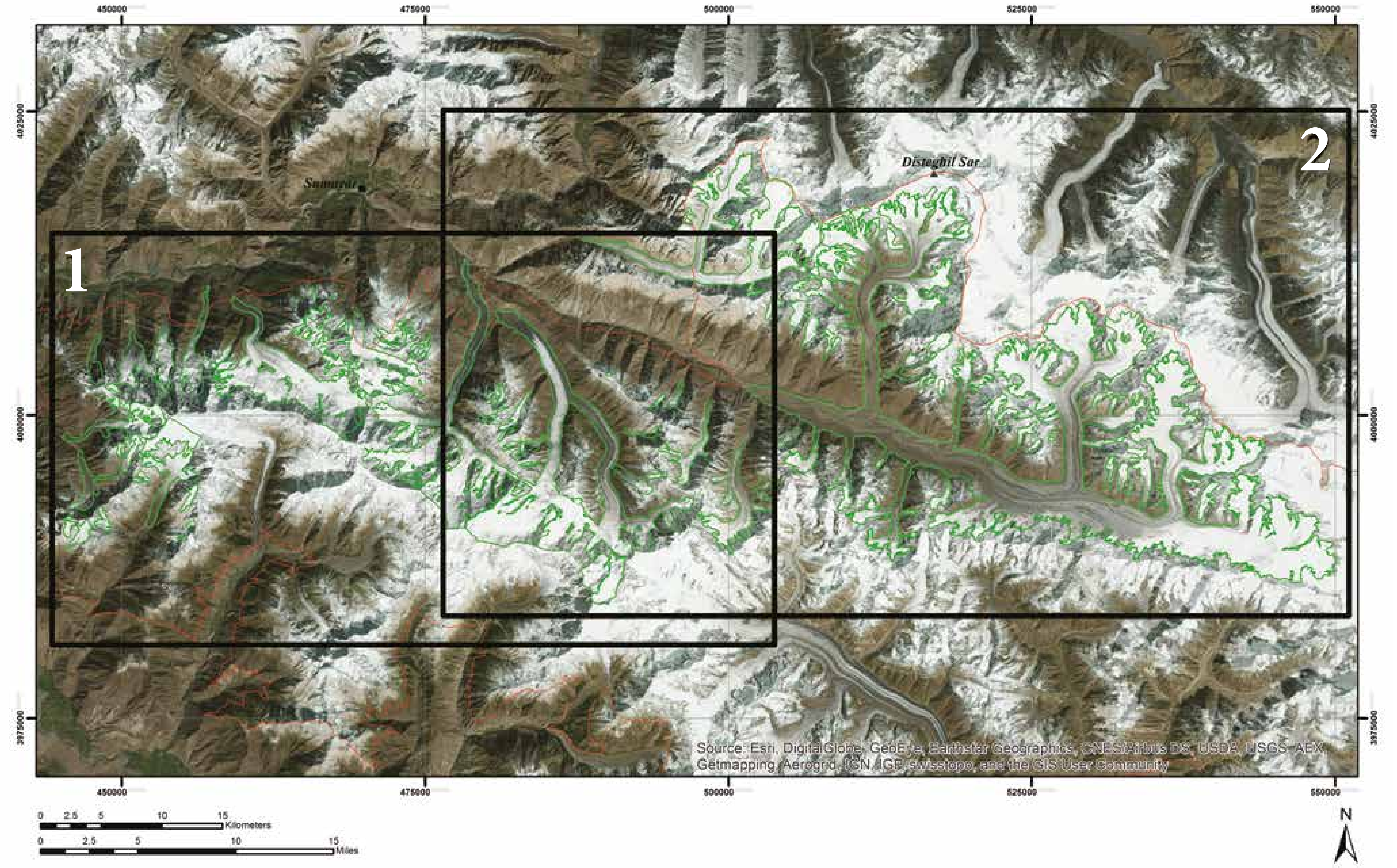

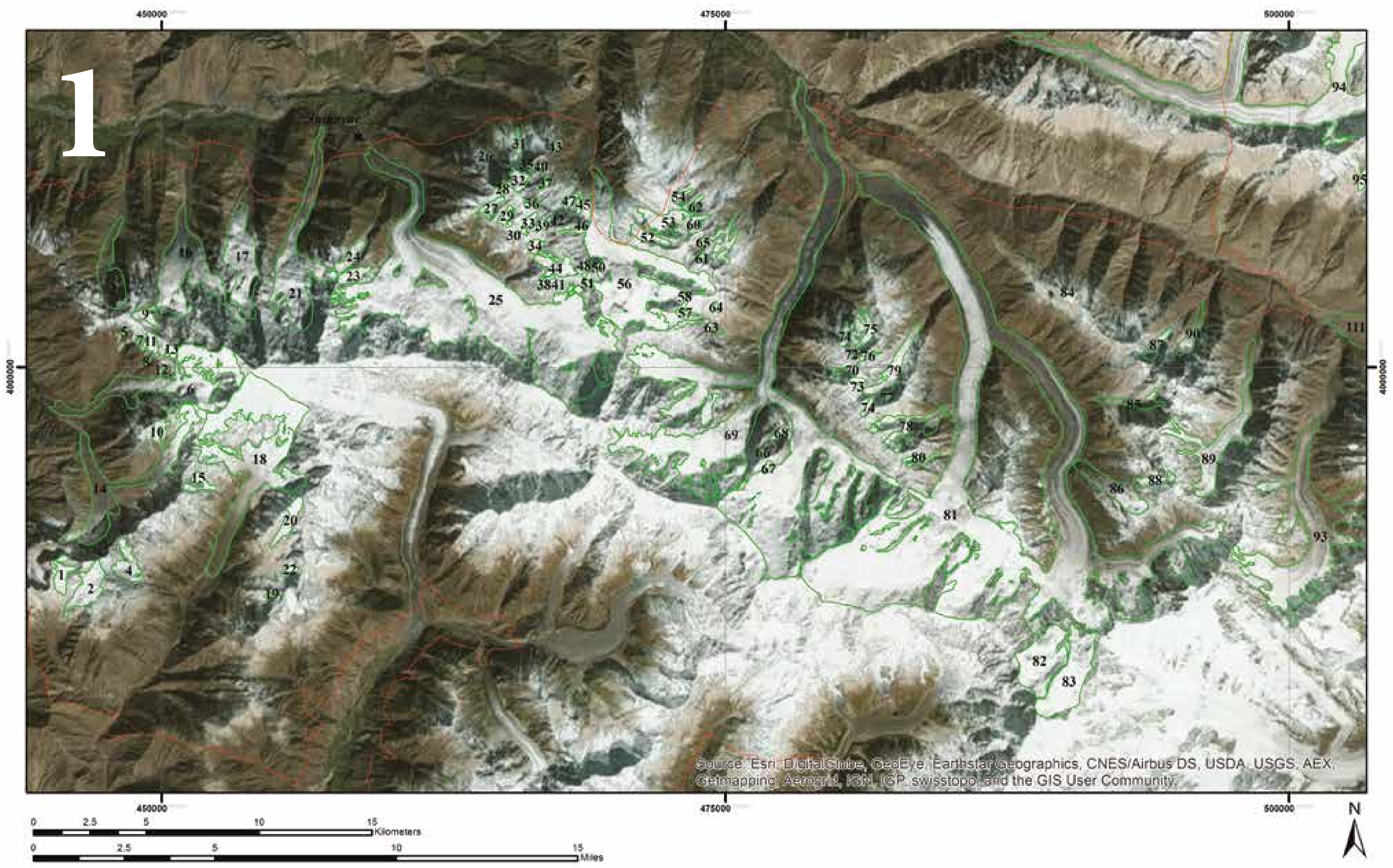
1
Source: Esri, DigitalGlobe, GeoEye, Earthstar Geographics, CNES/Airbus DS, USDA, USGS, AEX, Getmapping, Aerogrid, IGN, IGP, swisstopo, and the GIS User Community
450000
475000
500000
Kilometers
Miles
N

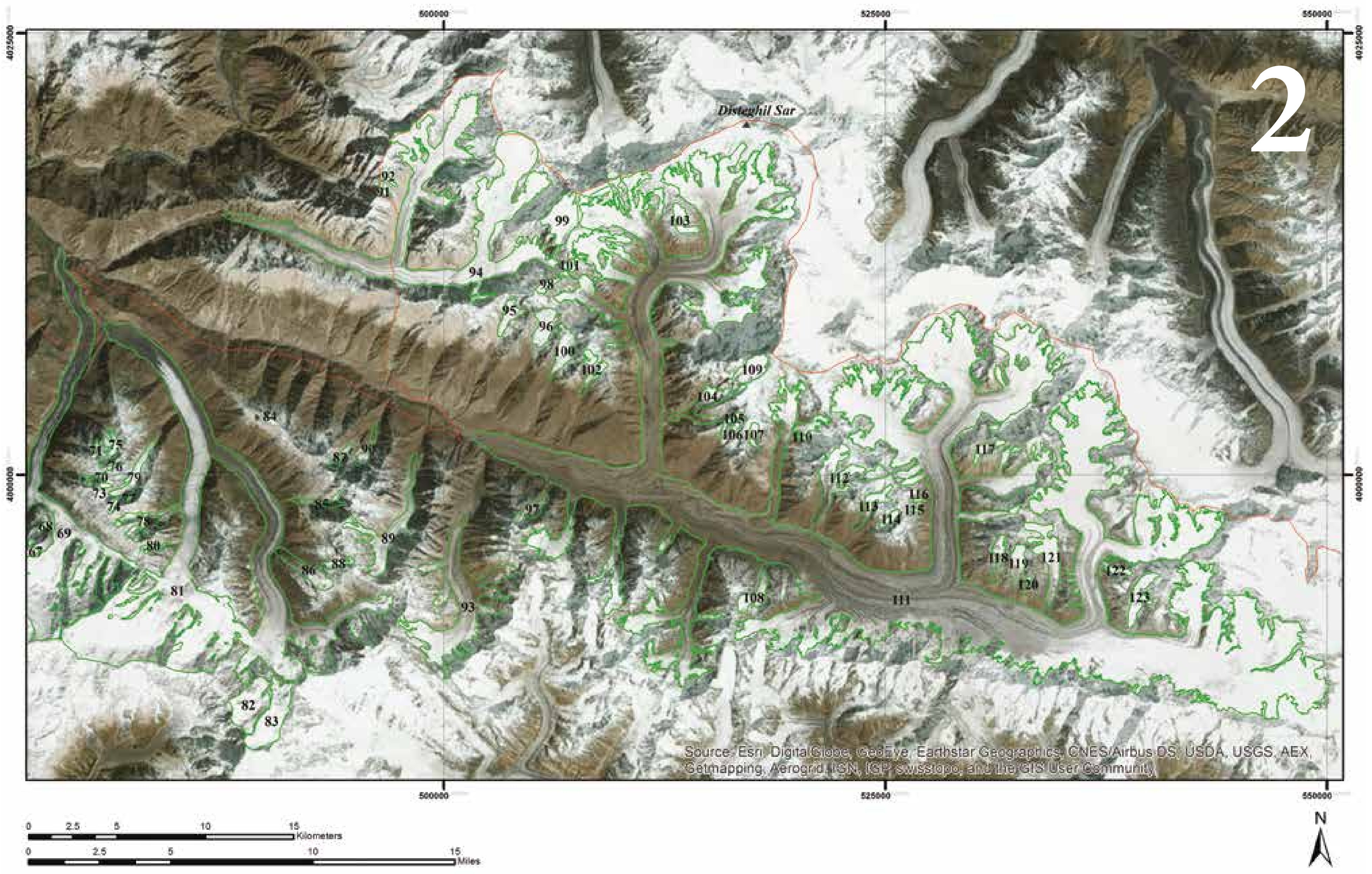
2
Disteghil Sar
Source: Esri, DigitalGlobe, GeoEye, Earthstar Geographics, CNES/Airbus DS, USDA, USGS, AEX, Getmapping, Aerogrid, IGN, IGP, swisstopo, and the GIS User Community
500000
525000
550000
Kilometers
Miles
N

A

Number of glaciers
(data of each glacier basin are reported)

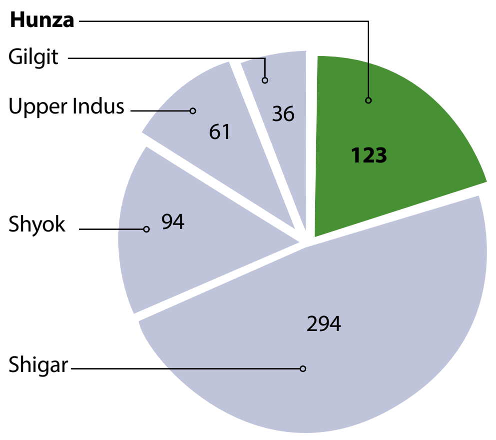

B

Glacier area
(km², the cumulative value of each glacier basin is reported)

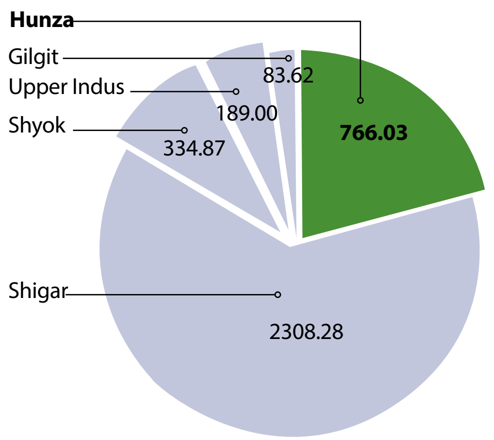

C

Glacier distribution
(data of each glacier basin are reported)

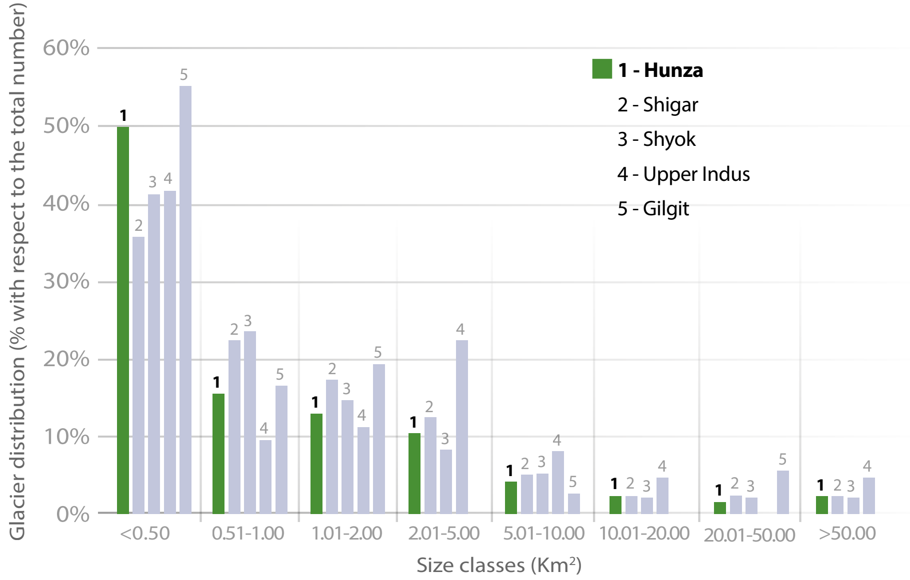

D

Glacier area distribution
(data of each glacier basin are reported)

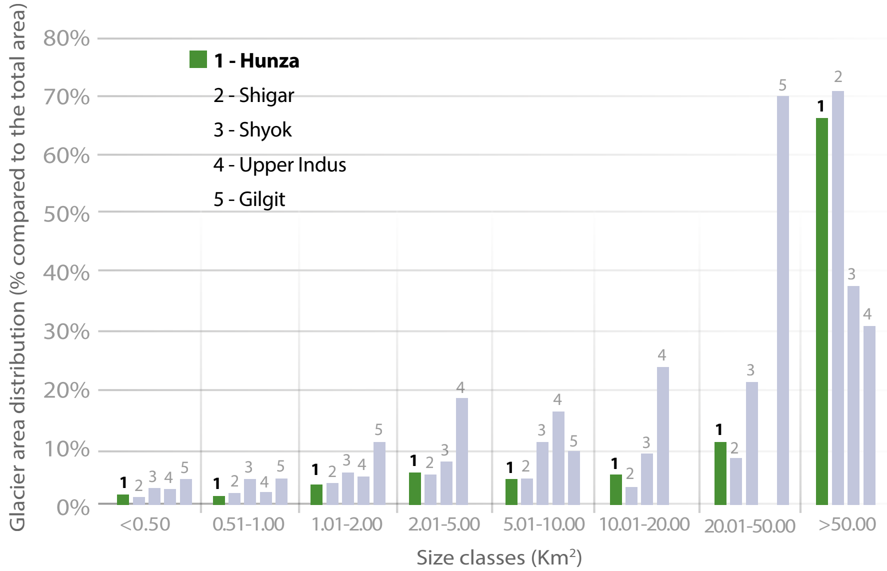

E

Area of glaciers
(mean and minimum value of each basin is reported)

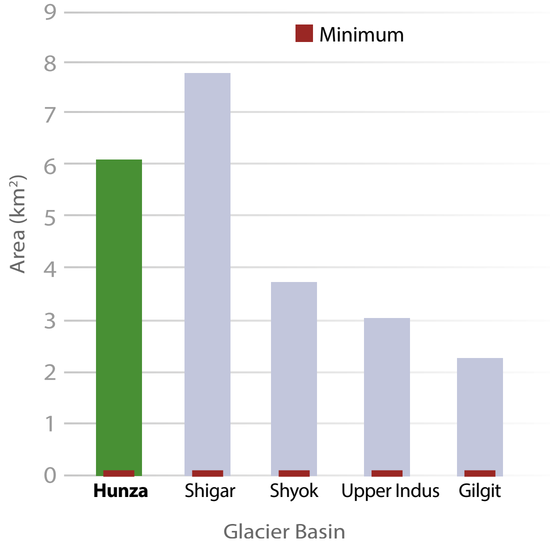

F

Area of glaciers
(the maximum value of each basin is reported)

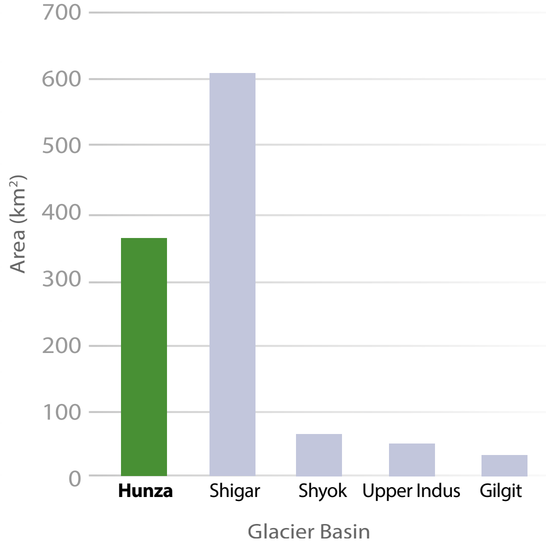

G

Glacier terminus elevation
(mean, minimum and maximum value
for each basin is reported)

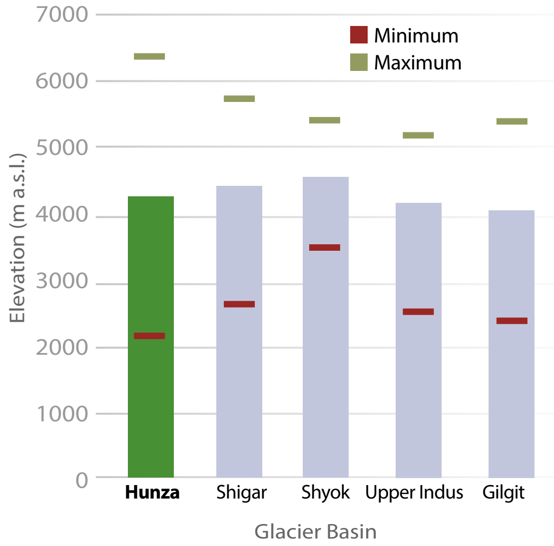

H

Glacier length
(mean, minimum and maximum value
for each basin is reported)

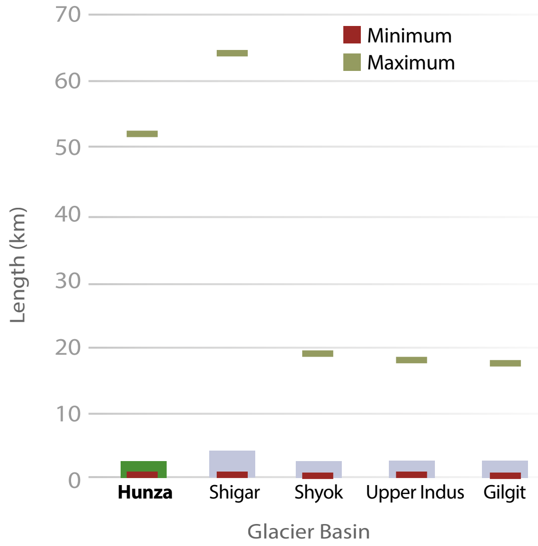

I

Distribution of debris-coverd glaciers
(data of each glacier basin are reported)

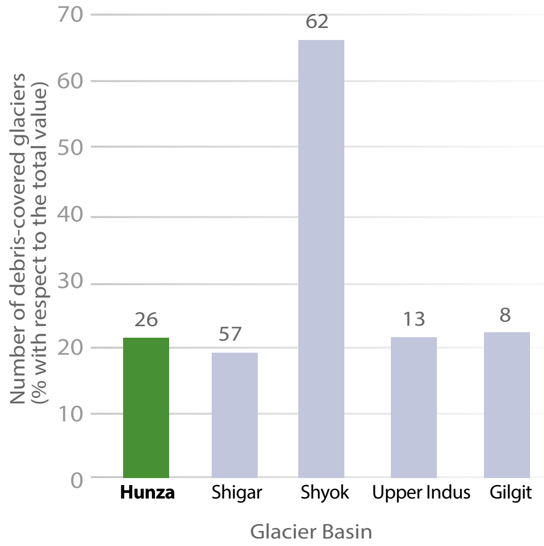

L

Glacier thickness
(mean, minimum and maximum value
for each basin is reported)

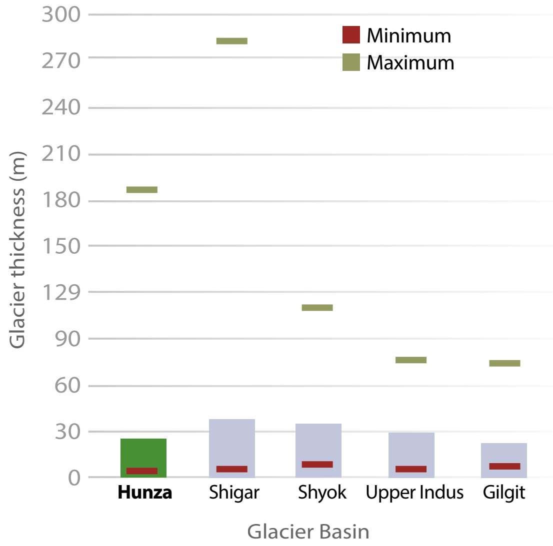

M

Glacier volume
(km³, the cumulative value of each basin is reported)

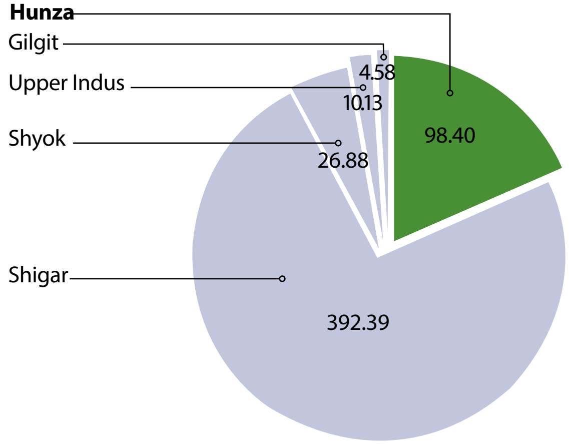

N

Glacier volume
(mean, minimum and maximum value
for each basin is reported)

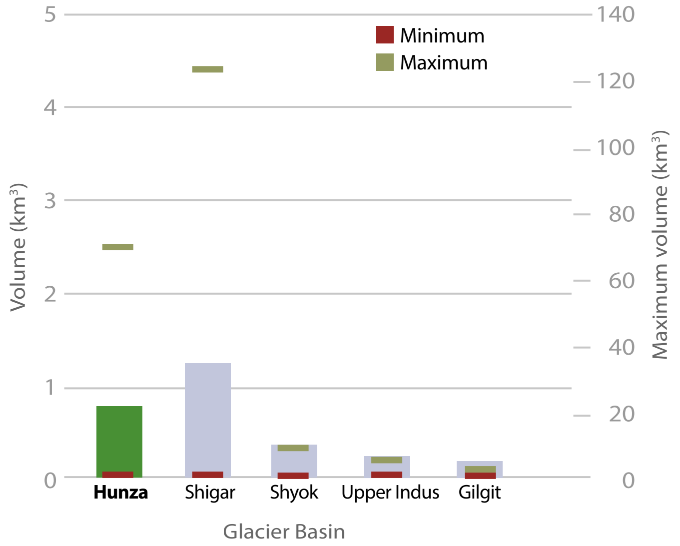


The upper sector of Hispar Glacier (Hunza Basin).


The upper sector of Hispar Glacier (Hunza Basin).

Glaciers in the Shigar basin

Observed data

The Shigar glacierized area is the widest of the CKNP basins, covering more than half of the whole glacierized surface of the park (i.e. 2308.3 km², Fig. B), and featuring the highest number of glaciers (i.e. 294 bodies, 48% of the total CKNP census, Fig. A). In addition, four of the biggest CKNP ice bodies are located into this basin: namely Baltoro Glacier (604.2 km², Fig. F), Biafo Glacier (438.1 km²), Chogo Lungma Glacier (265.0 km²) and Panmah Glacier (264.2 km²). On the one hand, as we found also for the other basins, the most part of glaciers (36.1% of all Shigar glaciers) features an area lower than 0.5 km² (Fig. C), covering only 1.1% of the whole Shigar glaciation (Fig. D). On the other hand, glaciers larger than 50 km² cover the 70.8% of the whole Shigar glaciation. Averaging all glacier areas, the mean value is the highest one compared to glaciers of the other basins and equal to 7.85 km² (Fig. E). The mean glacier terminus elevation is found to be 4443 m a.s.l. (in agreement to the other four basins), ranging from 2740 to 5760 m a.s.l. (Fig. G). As found also for the overall CKNP condition, the mean glacier length is 3.38 km (Fig. H) and the maximum length (not only for the Shigar basin but for the all CKNP glaciers) is reached by the Biafo Glacier (63.71 km).
Investigating the spatial distribution of supraglacial debris, debris-covered glaciers are 57 (corresponding to 19.4% of all Shigar ice bodies, Fig. I), covering about half of the Shigar glaciation (i.e. 41.2%, 950.7 km²). As we found also for the other basins, the abundant presence of supraglacial debris can probably explain the mean glacier terminus elevation which for the debris covered ice bodies results lower than the average value considering all Shigar ice bodies (i.e. 4332 and 4443 m a.s.l., respectively).
In Table 1, glacier area values in 2001 and 2010 are reported sorted according to 2001 size classes. Unlike Hunza basin, the Shigar glacierized area features a slight increase from 2001 to 2010 (i.e. +0.32 km²), with the highest growth for the sixth size class (i.e. 10-20 km²) and equal to +2.53 km², and the highest retreat for the biggest size class (i.e. >50 km²) and equal to -3.62 km². Totally, 37 glaciers (13% of all Shigar glaciers) were found to be characterized by a positive area variation (+5.90 km²) and 26 ice bodies (9% of all Shigar glaciers) by a negative one (-5.58 km²).

Size class (km²)	2001 Area		2010 Area		Δ2001-2010	
	km²	%	km²	%	km²	%
<0.5	26.21	1.1%	26.18	1.1%	-0.03	-0.001%
0.5–1.0	46.24	2.0%	46.29	2.0%	+0.05	+0.002%
1.0–2.0	76.69	3.3%	76.6	3.3%	-0.09	-0.004%
2.0–5.0	118.43	5.1%	119.7	5.2%	+1.27	+0.055%
5.0–10.0	106.88	4.6%	107.23	4.6%	+0.35	+0.015%
10.0–20.0	86.77	3.8%	89.3	3.9%	+2.53	+0.110%
20.0–50.0	213.89	9.3%	213.75	9.3%	-0.14	-0.006%
>50.0	1633.17	70.8%	1629.55	70.6%	-3.62	-0.157%
Total	**2308.28**	**100.0%**	**2308.60**	**100.0%**	**+0.32**	**+0.014%**

Table 1: Glacier coverage in 2001 and 2010 and glacier area change in the time window 2001-2010 (km²) sorted according to 2001 size classes, and reported also as percentage (%) calculated with respect to their total values.

Derived data

The iphysically based approach applied to the 2001 Shigar glacier geometry data permitted to estimate a mean ice thickness equal to 35 m (in agreement with the overall CKNP condition, Fig. L), ranging from a minimum value of 6 m to a maximum one of 285 m (this latter featured by the Biafo Glacier and corresponding to the highest value of all CKNP glaciers). The most part of glaciers (81.6%) is characterized by an estimated thickness value ranging between 10 and 50 m. Debris-free glaciers feature a higher variability of ice thickness (i.e. from 6 to 285 m), instead debris-covered glaciers have ice depth ranging from 11 to 213 m; however the mean value is lower: 32 m for debris-free glaciers and 45 m for debris-covered ice bodies.
The largest part of glacier-derived fresh-water resource of CKNP is nested by Shigar basin (74% and equal to 392.39 km³, Fig. M), of which 187.06 km³ of ice is entrapped into debris-covered glaciers and 205.33 km³ of ice into debris-free glaciers. Considering the total volume value (i.e. 392.39 km³), the mean ice thickness results about 170 m. As Shigar basin hosts very wide glaciers (among which Baltoro Glacier with an estimated ice volume of 128.79 km³), the mean volume is higher whenever compared to the other basins (equal to 1.33 km³, Fig. N). Nevertheless, the largest part of glaciers (65.7%) features a volume lower than 0.05 km³ as we found also for the other basins.

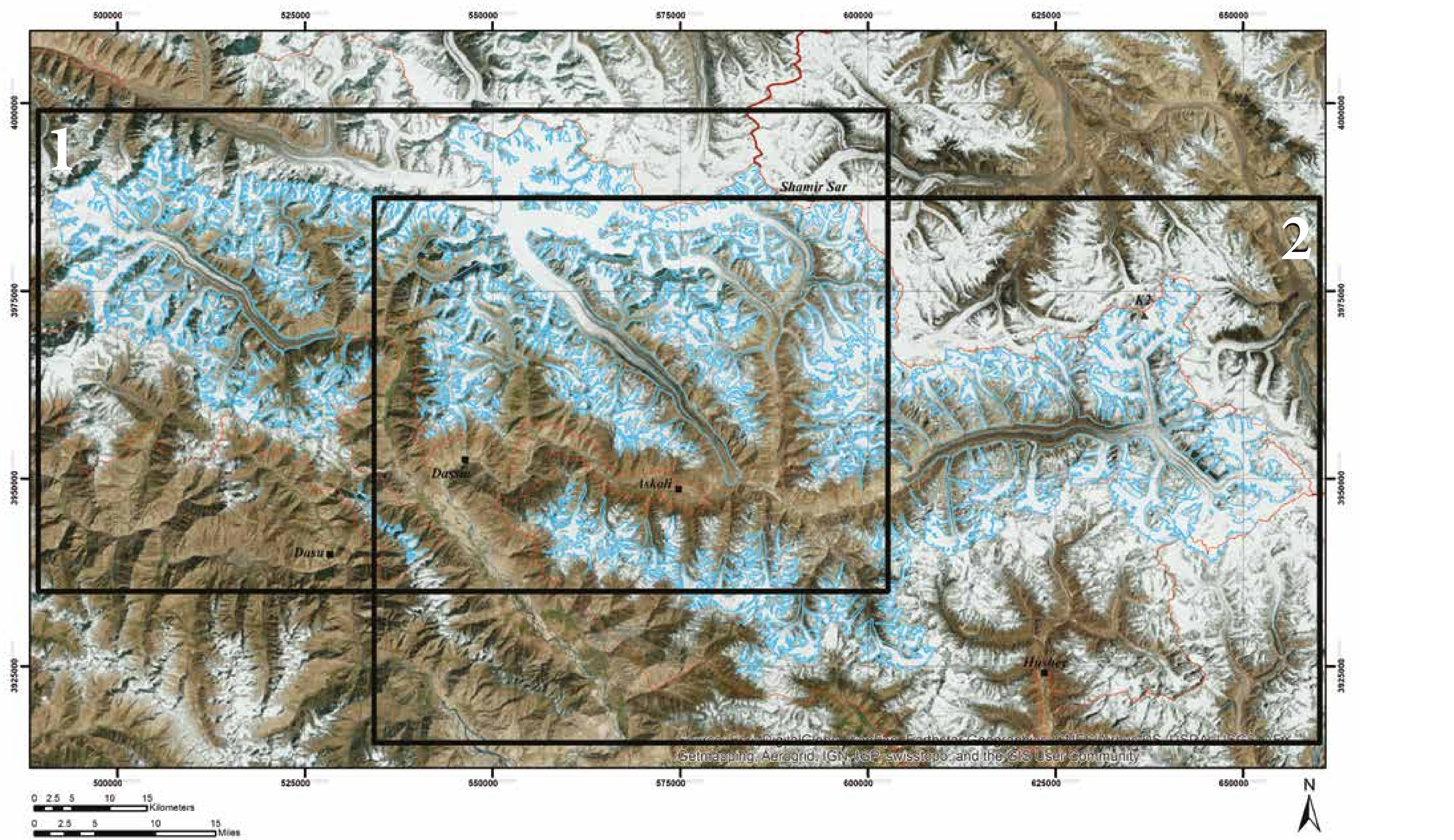

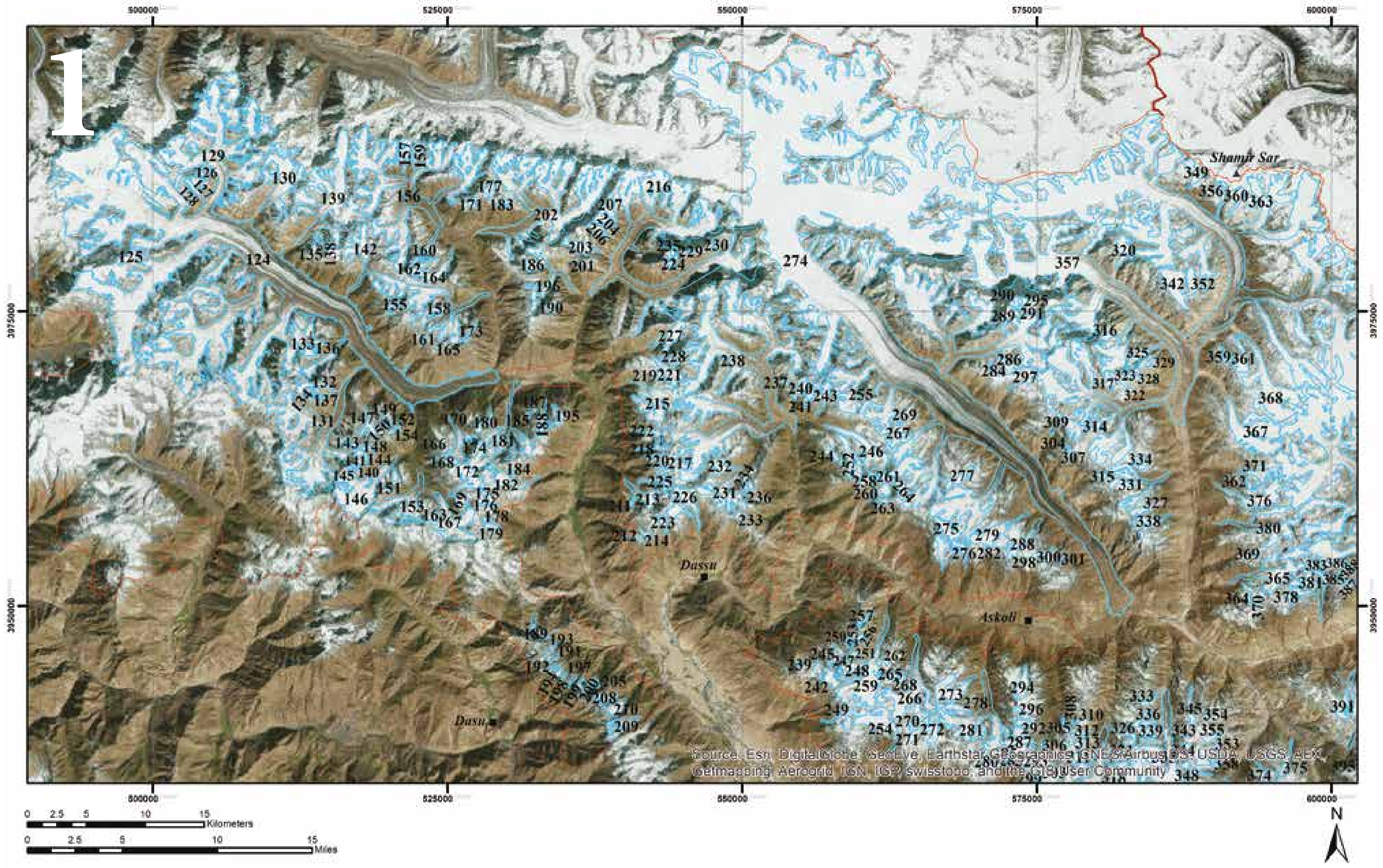
1
Dassu
Askoli
Kilometers
Miles
N

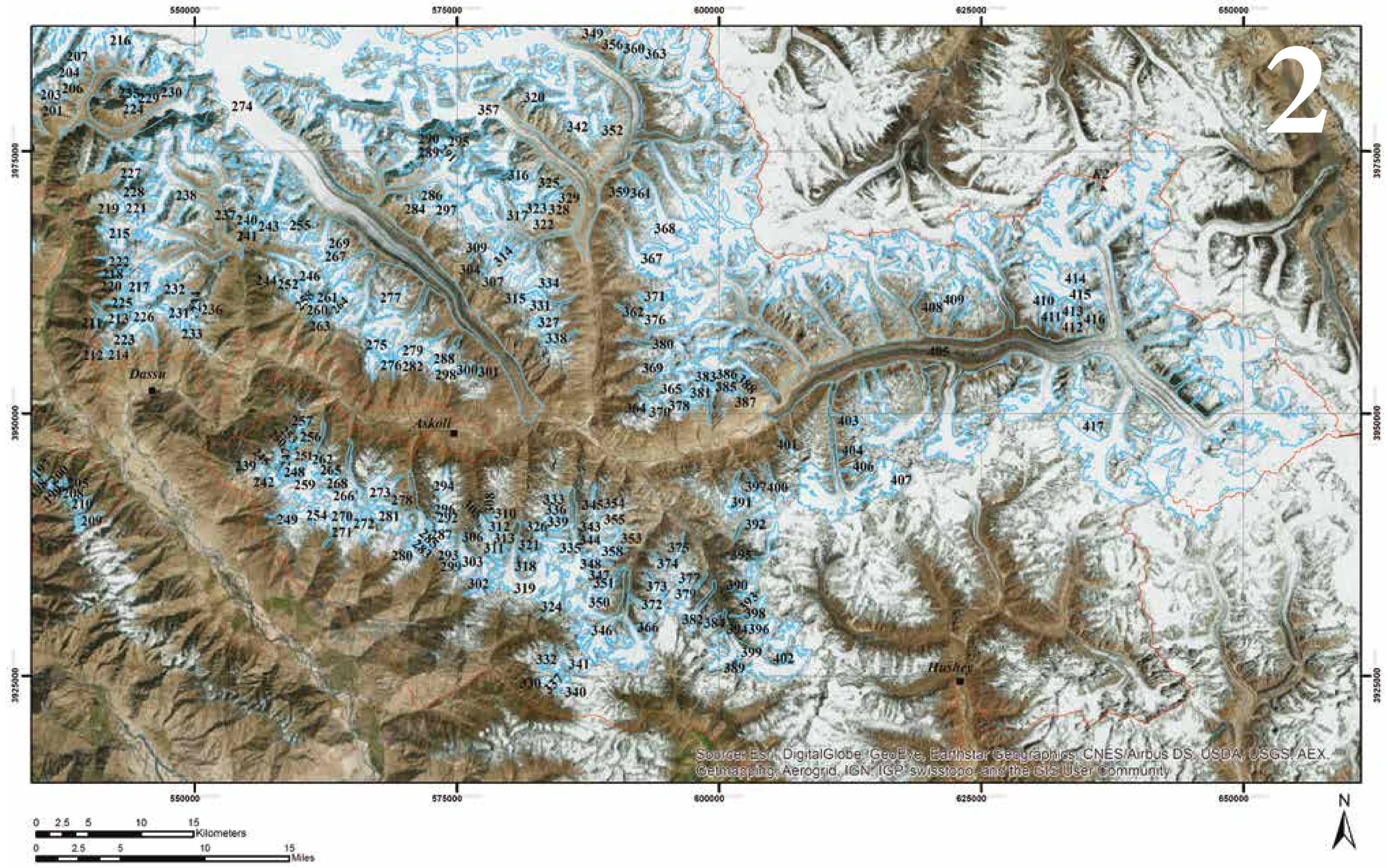
2
Dassu
Askoli
Hushey
Kilometers
Miles
N

A
Number of glaciers
(data of each glacier basin are reported)

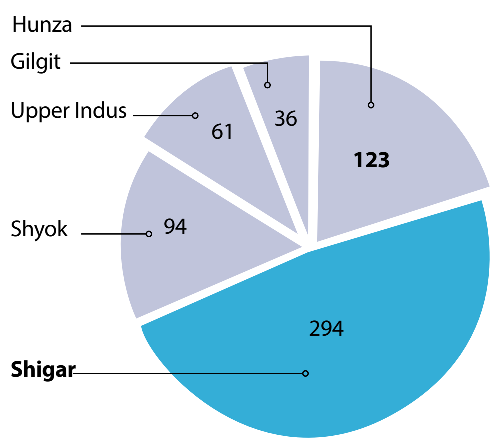

B
Glacier area
(km², the cumulative value of each glacier basin is reported)

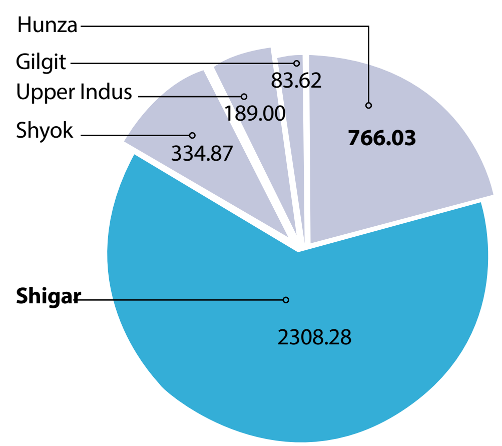

C
Glacier distribution
(data of each glacier basin are reported)

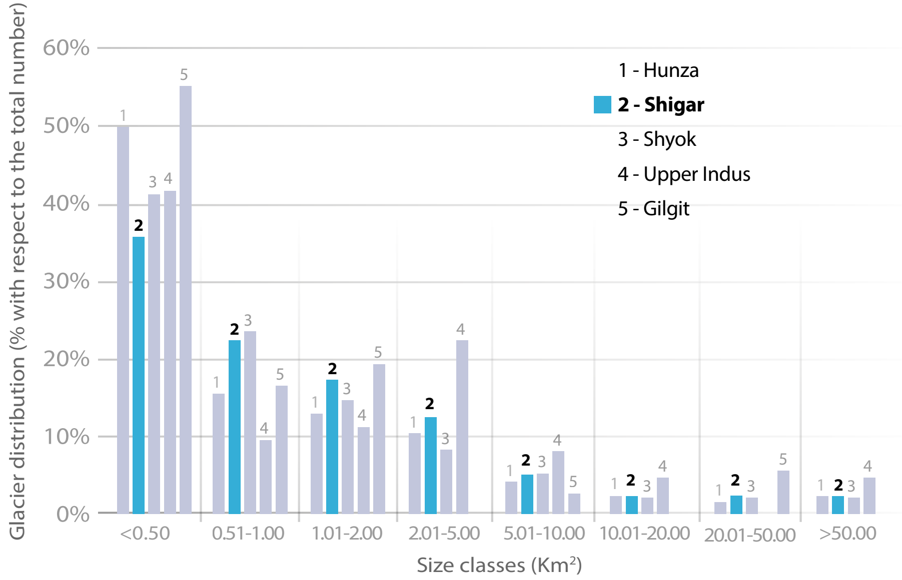

D
Glacier area distribution
(data of each glacier basin are reported)

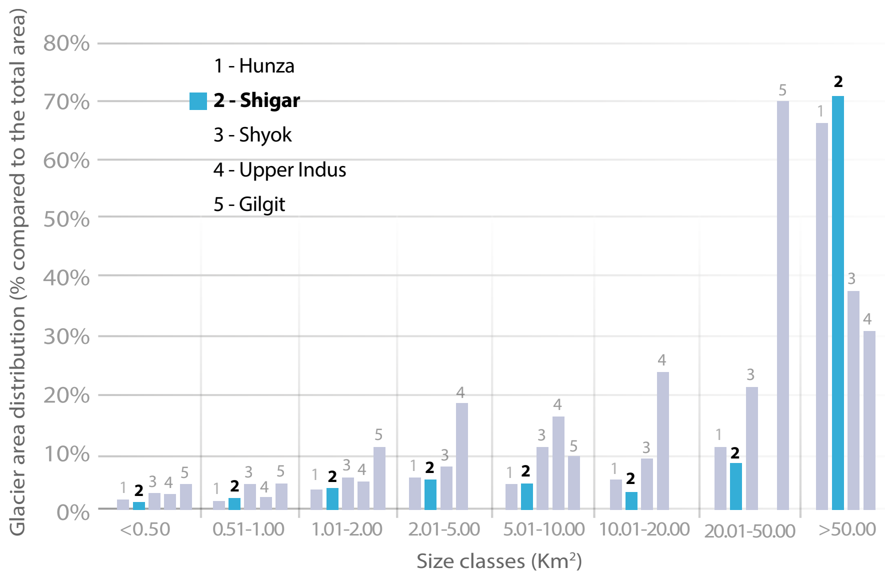

E
Area of glaciers
(mean and minimum value of each basin is reported)

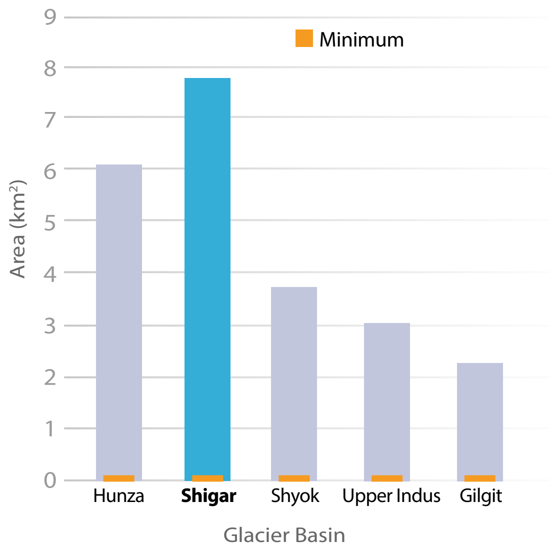

F
Area of glaciers
(the maximum value of each basin is reported)

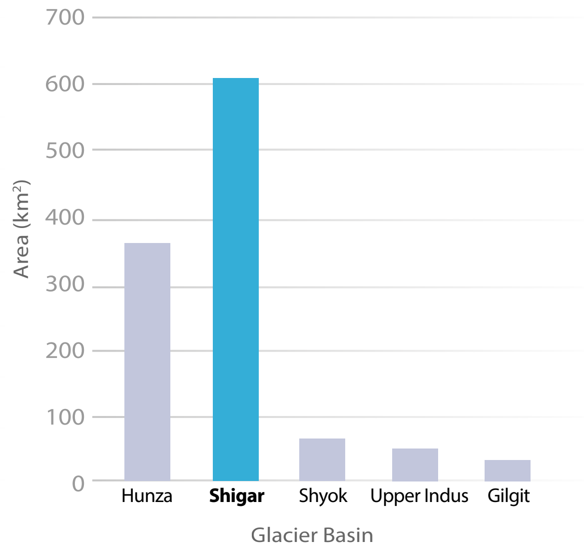

G
Glacier terminus elevation
(mean, minimum and maximum value
for each basin is reported)

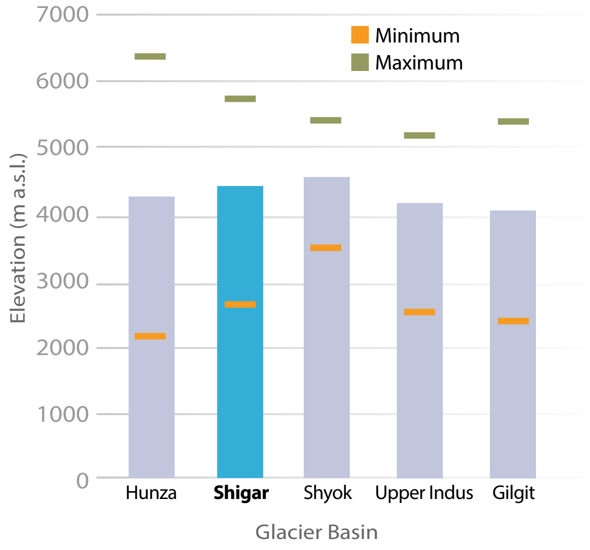

H
Glacier length
(mean, minimum and maximum value
for each basin is reported)

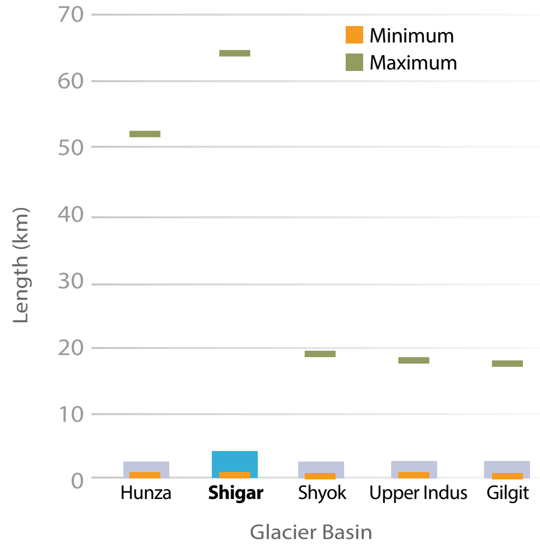

I
Distribution of debris-coverd glaciers
(data of each glacier basin are reported)

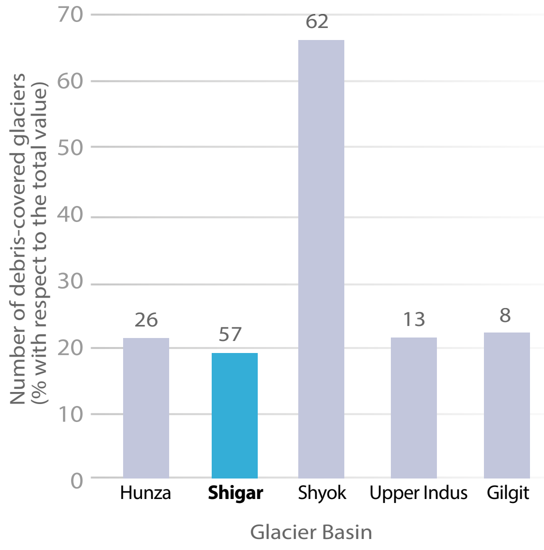

L
Glacier thickness
(mean, minimum and maximum value
for each basin is reported)

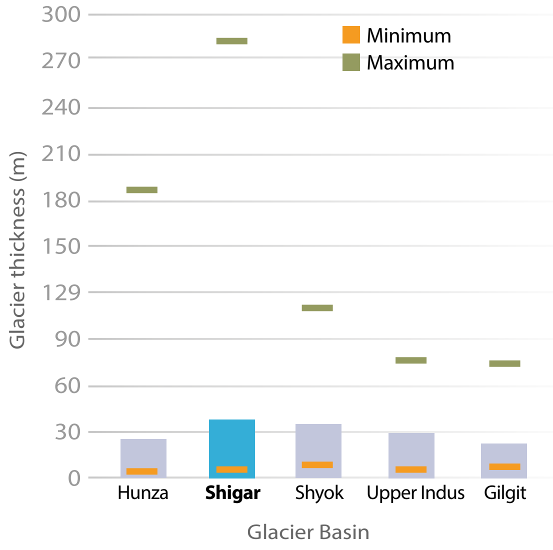

M
Glacier volume
(km³, the cumulative value of each basin is reported)

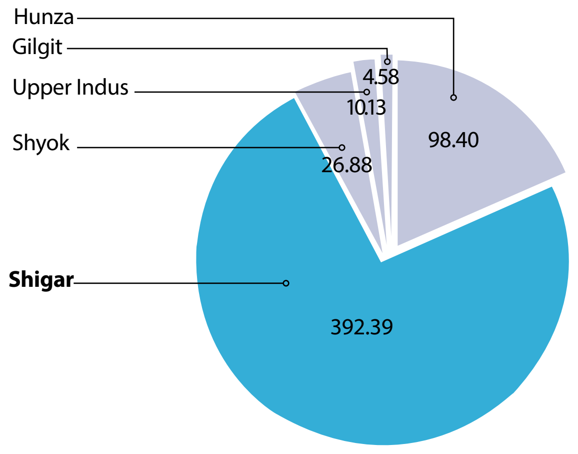

N
Glacier volume
(mean, minimum and maximum value
for each basin is reported)

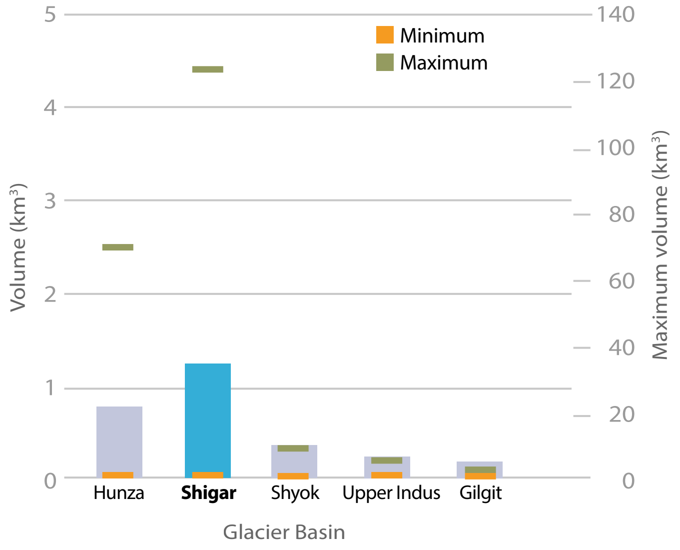

The upper sector of the Biafo Glacier (Hunza Basin).

The ablation tongue of the Biafo Glacier (Hunza Basin).

Glaciers in the Shyok basin

Observed data

Only ninety-four (94) of 3357 glaciers of the whole Shyok basin (Bajracharya and Shrestha, 2011) are included in the park area, corresponding to ~15% of the total CKNP glacier census (Fig. A) and covering a cumulative area of 334.87 km² (9% of the total CKNP glacierized surface, Fig. B). The glaciers belonging to the smallest size class (i.e. <0.5 km²) are the most abundant (41.5%, Fig. C), but altogether they cover only 3.1% of the whole Shyok glacierized area (Fig. D). The three classes of larger size (i.e. 10-20 km², 20-50 km² and >50 km²) count only 2 glaciers per class (Fig. C), even if their cumulative extent (i.e. 226.4 km², corresponding to the sum of 32.3, 69.8 and 124.3 km², respectively) is ca. 67.6% of the Shyok glacierized area (Fig. D). Whenever compared to Hunza and Shigar basins, the Shyok glaciers result smaller on average, featuring a mean area of 3.56 km² (Fig. E), and also the widest ice body is quite small (i.e. 66.50 km², Fig. F). As opposed to Hunza basin, Shyok basin is characterized by the lowest variability of glacier terminus elevation (from 3440 to 5460 m a.s.l., Fig. G). However, the mean elevation of the glacier snout is found to be 4558 m a.s.l., very similar to the overall CKNP situation. More than 50% of the Shyok glaciers features a length ranging between 1 and 5 km (Fig. H) with a maximum value of 19.13 km (lower if compared to Hunza and Shigar conditions, but similar to Upper Indus and Gilgit ones).

Depending on the occurrence of supraglacial debris mantle, glaciers were sorted into debris-free and debris-covered types. Shyok basin hosts the highest number of debris-covered glaciers (62 ice bodies, Fig. I) which cover about the whole glacierized area (313.2 km² corresponding to the 93.5% of Shyok glaciation).

Sorting 2001 and 2010 glacier areas according to 2001 size classes (Table 1), Shyok basin glaciers are found to feature a general increase (with a general value of +0.25 km²) except for the largest class (i.e. >50 km²) which accounts for a total shrinkage of -0.45 km². Totally 14 glaciers are characterized by a positive area variation and only 2 glaciers by a negative one.

Size class (km²)	2001 Area		2010 Area		Δ2001-2010	
	km²	%	km²	%	km²	%
<0.5	10.26	3.1%	10.27	3.1%	+0.01	+0.003%
0.5–1.0	14.94	4.5%	15.01	4.5%	+0.07	+0.021%
1.0–2.0	20.65	6.2%	20.7	6.2%	+0.05	+0.015%
2.0–5.0	27.22	8.1%	27.48	8.2%	+0.26	+0.078%
5.0–10.0	35.43	10.6%	35.5	10.6%	+0.07	+0.021%
10.0–20.0	32.26	9.6%	32.43	9.7%	+0.17	+0.051%
20.0–50.0	69.8	20.8%	69.87	20.8%	+0.07	+0.021%
>50.0	124.31	37.1%	123.86	37.0%	-0.45	-0.134%
Total	**334.87**	**100.0%**	**335.12**	**100.0%**	**+0.25**	**+0.075%**

Table 1: Glacier coverage in 2001 and 2010, and glacier area change in the time window 2001-2010 (km²) sorted according to 2001 size classes, and reported also as percentage (%) calculated with respect to their total values.

Derived data

The mean ice thickness data assessed from the glacier geometry data is equal to 33 m ranging from 9 m to 112 m (Fig. L). About the 50% of Shyok glaciers features a thickness value between 25 and 50 m. Debris-covered glaciers feature a mean ice thickness of 39 m (ranging from 13 to 112 m), higher than the one found considering all Shyok glaciers (i.e. 33 m) and evaluating only debris-free glaciers (equal to 21 m, ranging from 9 to 47 m).

The total ice volume (26.88 km³, Fig. M) is almost totally entrapped into debris-covered glaciers, while only the 2.7% of ice is nested into debris-free glaciers. Considering the total volume value, the mean ice thickness results about 80 m. No glacier has a volume higher than 10 km³ while about the 50% of bodies features a volume lower than 0.05 km³ (contributing only to 3.3% of the total Shyok glacier volume). This is evident if considering the mean value (equal to 0.29 km³, Fig. N) that is lower respect to Hunza and Shigar conditions.

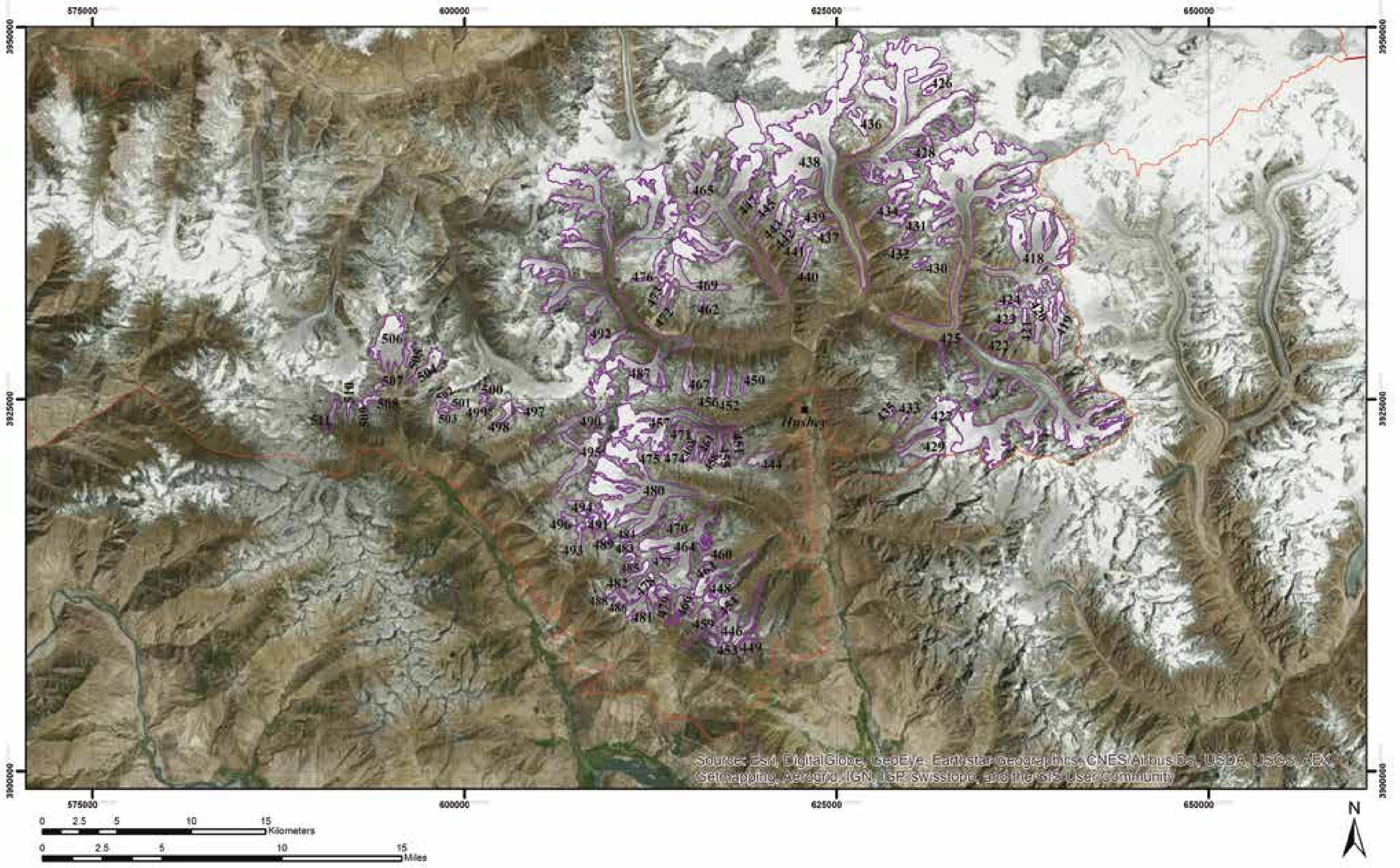

A

Number of glaciers
(data of each glacier basin are reported)

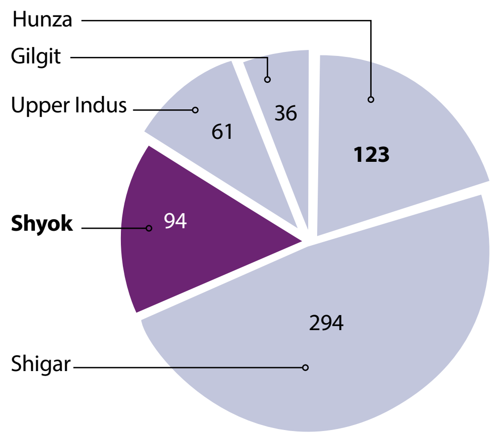

B

Glacier area
(km², the cumulative value of each glacier basin is reported)

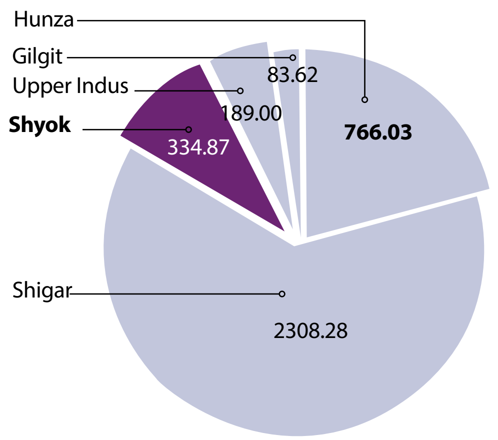

C

Glacier distribution
(data of each glacier basin are reported)

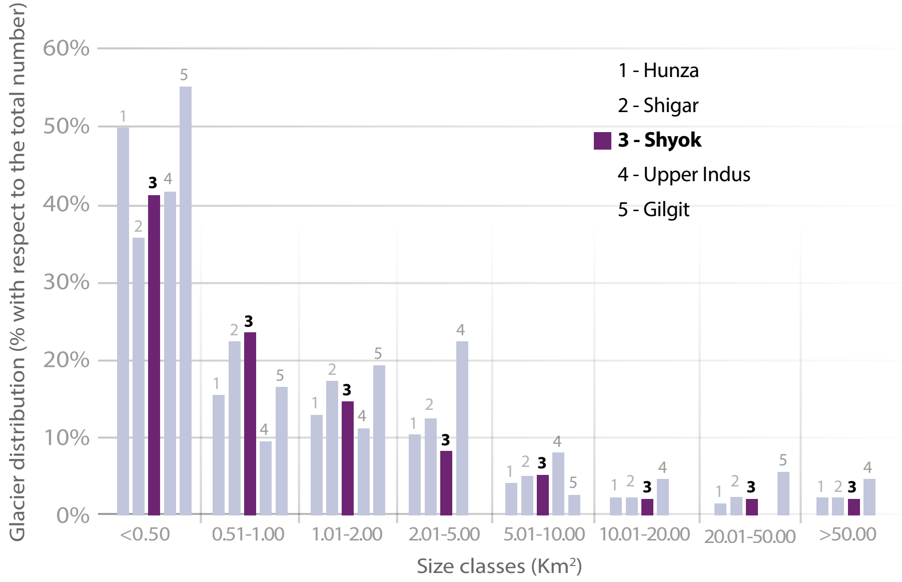

D

Glacier area distribution
(data of each glacier basin are reported)

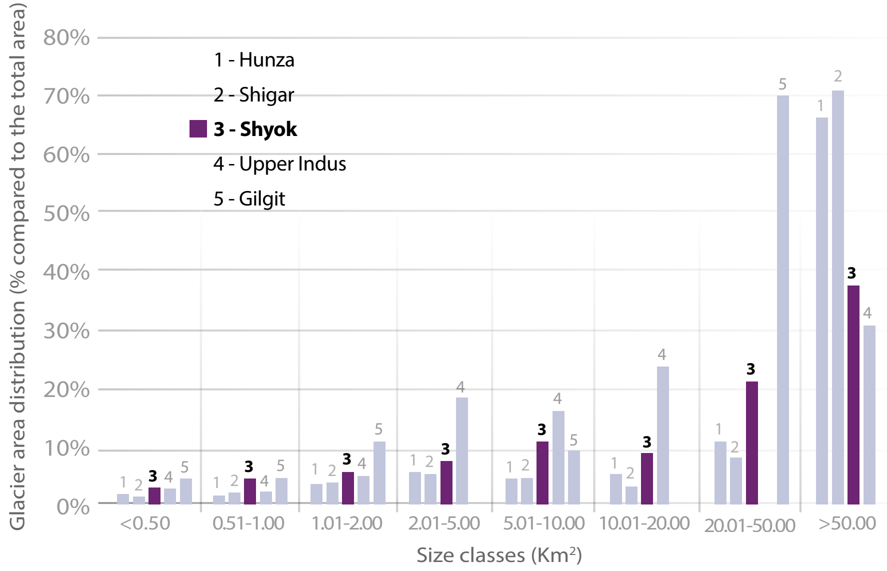

E

Area of glaciers
(mean and minimum value of each basin is reported)

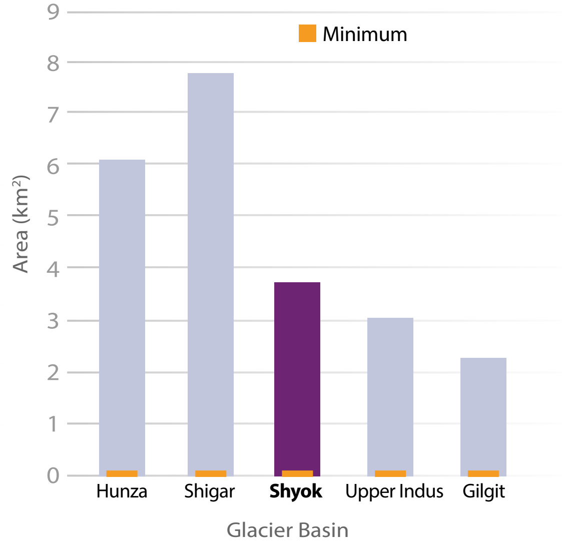

F

Area of glaciers
(the maximum value of each basin is reported)

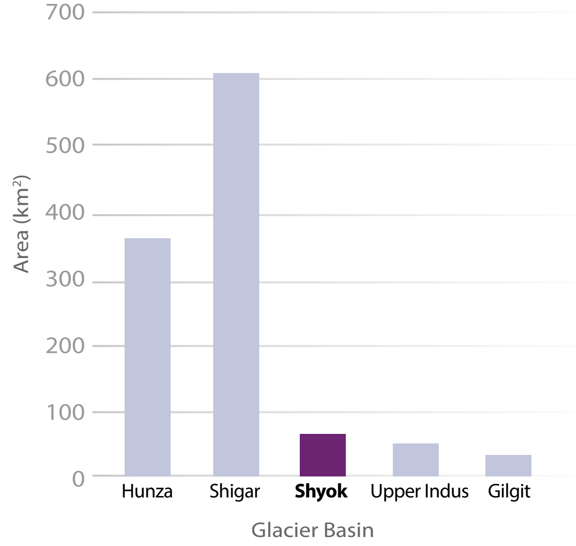

G

Glacier terminus elevation
(mean, minimum and maximum value
for each basin is reported)

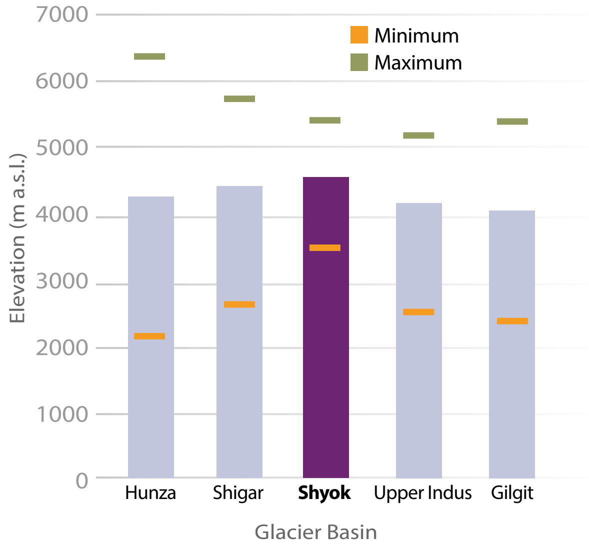

H

Glacier length
(mean, minimum and maximum value
for each basin is reported)

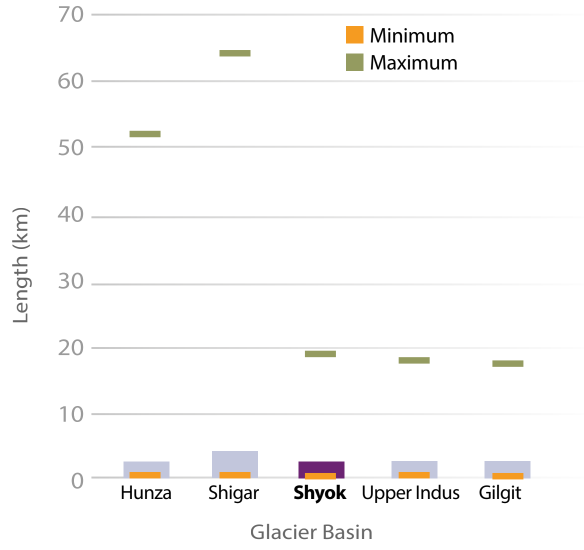

I

Distribution of debris-coverd glaciers
(data of each glacier basin are reported)

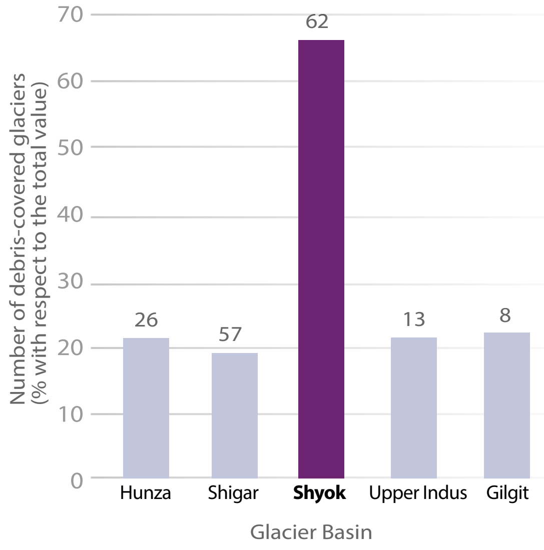

L

Glacier thickness
(mean, minimum and maximum value
for each basin is reported)

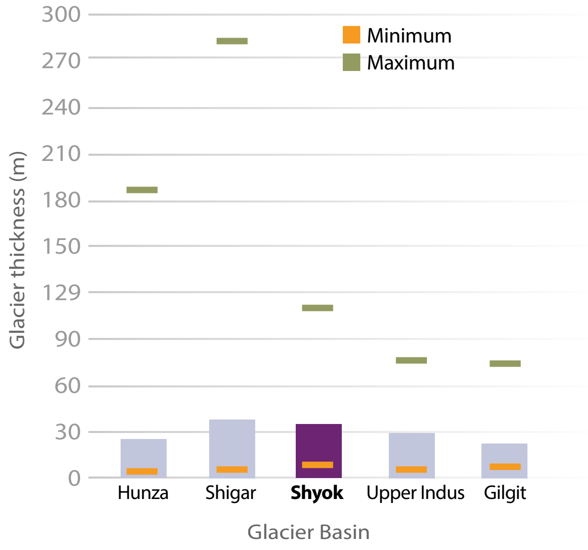

M

Glacier volume
(km³, the cumulative value of each basin is reported)

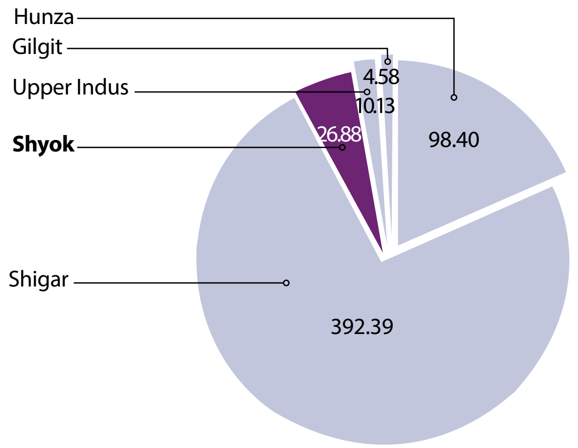

N

Glacier volume
(mean, minimum and maximum value
for each basin is reported)

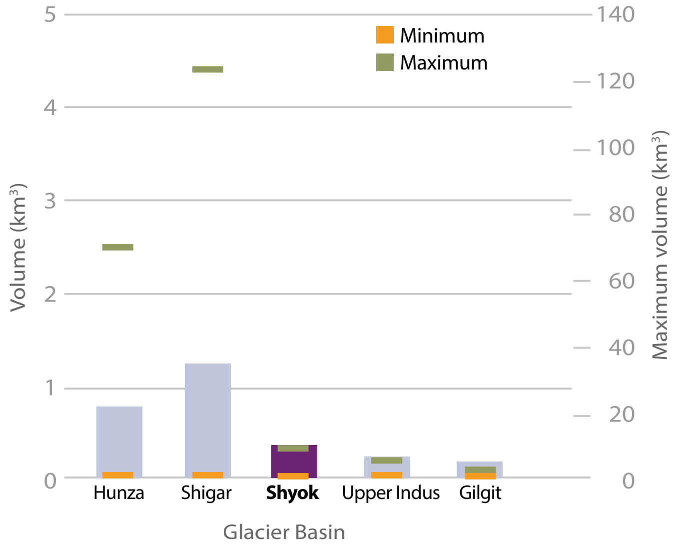

The Ghandogoro La Glacier from Ghandogoro pass (Shyok Basin).

Ghandogoro La Glacier (Shyok Basin).

Glaciers in the Upper Indus basin

Observed data

Upper Indus hosts totally 2814 glaciers (Bajracharya and Shrestha, 2011), of which 61 in the CKNP area (~10% of the total CKNP glacier census, Fig. A, and 5% of the CKNP glaciation, equal to 189.00 km^2, Fig. B). Despite of the other three already investigated basins (i.e. Hunza, Shigar and Shyok), the glacier distribution per size class in the Upper Indus basin does not feature a decreasing trend with increasing glacier area (Fig. C): a first peak corresponds to the smallest size class (i.e. <0.5 km^2) with 41.9% of glaciers, but another peak (even if of lower importance) is present at the class of 2-5 km^2 with 22.6% of glaciers. This particular trend is also evident in Fig. D where the glacier area distribution is shown. In addition to the peak in correspondence of the largest class (>50 km^2, with 30.5% of the totally Upper Indus glacierized area), other two peaks occur at 2-5 km^2 and 10-20 km^2 size classes with 18.6% and 25.2% of total area, respectively. Finally, no glaciers are included in the size class of 20-50 km^2. As we found also for the Shyok basin, the Upper Indus glaciers are smaller on average, with a mean area of 3.05 km^2 (Fig. E), if compared to Hunza and Shigar glaciers, and the widest ice body is not so large (57.72 km^2, Fig. F). The glacier terminus elevation ranges from 2590 to 5190 m a.s.l. (Fig. G), with a mean value of 4272 m a.s.l., in agreement to the other basins. About the 3/4th of the glaciers features an elevation of the snout at 4000-5000 m a.s.l. Similar to the general CKNP situation, the mean glacier length is equal to 2.89 km (ranging from 0.35 to 18.82 km, Fig. H) and the 66% of the glaciers has a length of 1-5 km.
In this basin, there are only 13 debris-covered glaciers but they represent the 21% of the total basin glacier census similar to the other basins (Fig. I, sorted in base of the supraglacial debris coverage), with a cumulative area of 125.2 km^2 (66% of the Upper Indus glaciation).
Comparing glacier area in 2001 and 2010 sorted according to 2001 size classes (Table 1), there is a more intense increase in 10-20 km^2 size class (equal to +0.68 km^2) and slight decreases in <50 km^2, 5-10 km^2 and >50km^2 size classes (-0.02, -0.01 and -0.19 km^2), thus contributing totally to an increase of +0.52 km^2. As the number of glaciers featuring a positive or negative area change is similar (8 and 6, respectively), we could conclude that the largest shrinkage is suffered by the smaller glaciers.

Size class (km^2)	2001 Area		2010 Area		Δ2001-2010	
	km^2	%	km^2	%	km^2	%
<0.5	5.45	3.0%	5.43	3.0%	-0.02	-0.011%
0.5–1.0	4.21	2.2%	4.21	2.2%	0.00	0.000%
1.0–2.0	10.27	5.4%	10.27	5.4%	0.00	0.000%
2.0–5.0	35.11	18.6%	35.17	18.5%	+0.06	+0.032%
5.0–10.0	28.64	15.1%	28.63	15.1%	-0.01	-0.005%
10.0–20.0	47.6	25.2%	48.28	25.4%	+0.68	+0.359%
20.0–50.0	0	0.0%	0	0.0%	0.00	0.000%
>50.0	57.72	30.5%	57.53	30.3%	-0.19	-0.100%
Total	**189.00**	**100.0%**	**189.52**	**100.0%**	**+0.52**	**+0.275%**

Table 1: Glacier coverage in 2001 and 2010 and glacier area change in the time window 2001-2010 (km^2) sorted according to 2001 size classes, and reported also as percentage (%) calculated with respect to their total values.

Derived data

The estimated ice thickness results in agreement with the overall CKNP data: i) mean value equal to 30 m (from 6 to 75 m, Fig. L), ii) about the 50% of glaciers with thicknesses ranging from 25 to 50 m, and iii) debris-covered glaciers feature a mean ice thickness higher than the one estimated for debris-free ice bodies (43 and 27 m, respectively).
Only the 2% of the total CKNP glacier-derived fresh-water resource is nested in the Upper Indus (10.13 km^3, Fig. M) and the 1/4th of this amount is entrapped into debris-free glaciers. Considering the total volume value, the mean ice thickness results about 54 m. The maximum volume is estimated to be 4.05 km^3 (Fig. N), and the 52% of glaciers nests a water reserve between 1 and 5 km^3.

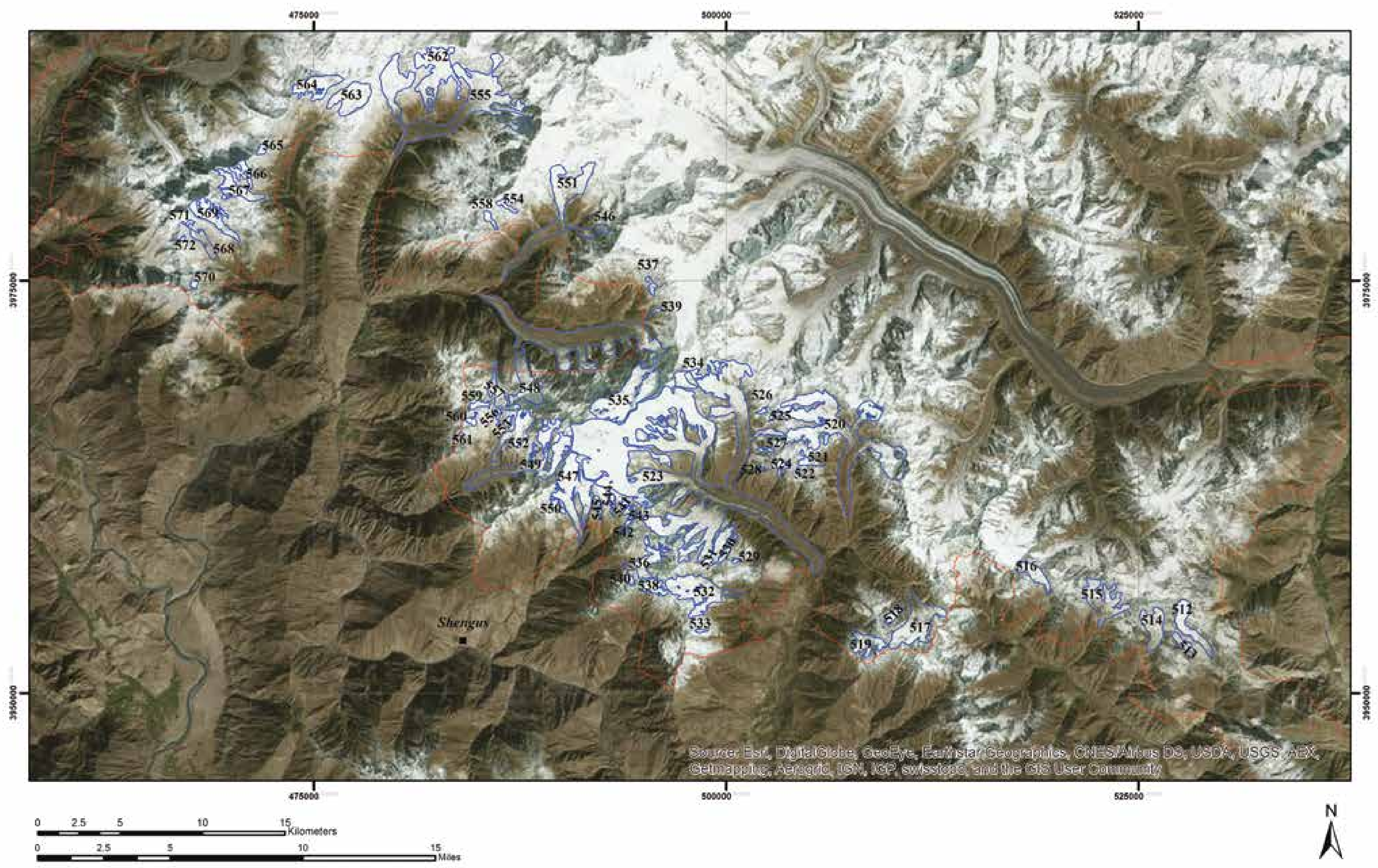

A
Number of glaciers
(data of each glacier basin are reported)

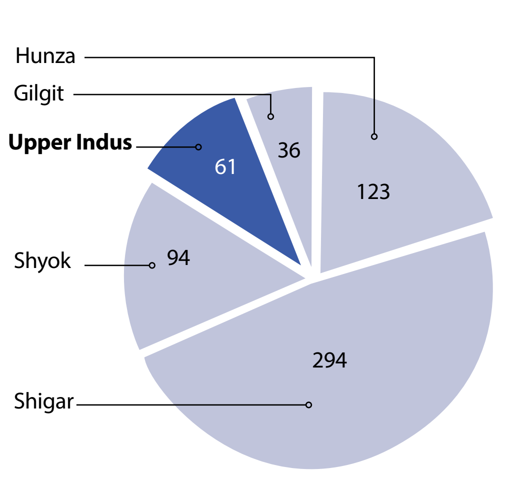

B
Glacier area
(km², the cumulative value of each glacier basin is reported)

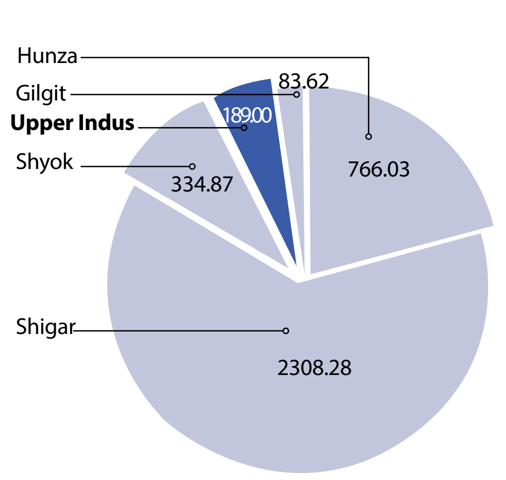

C
Glacier distribution
(data of each glacier basin are reported)

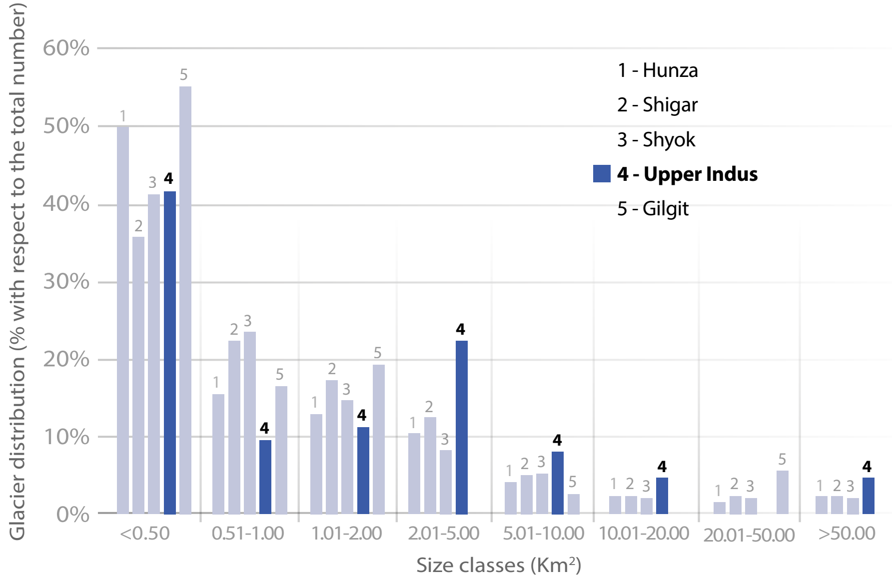

D
Glacier area distribution
(data of each glacier basin are reported)

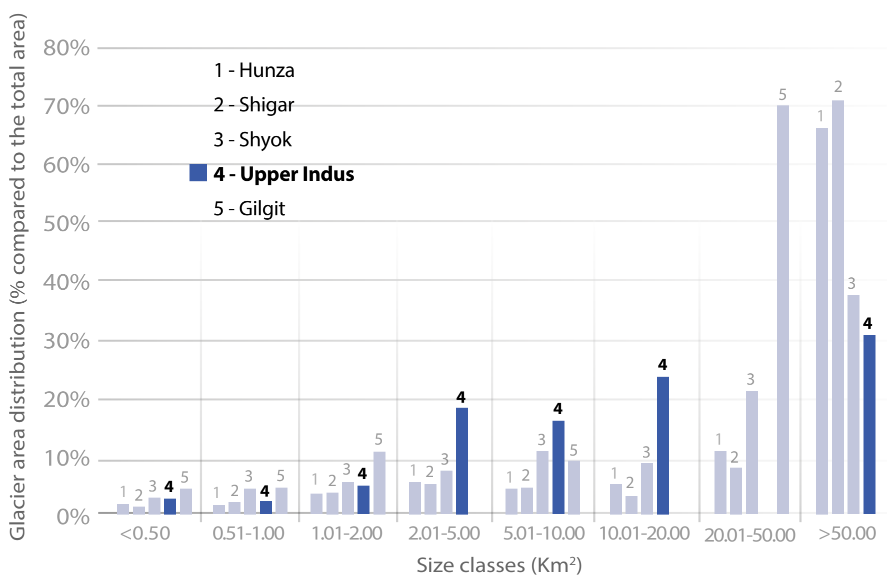

E
Area of glaciers
(mean and minimum value of each basin is reported)

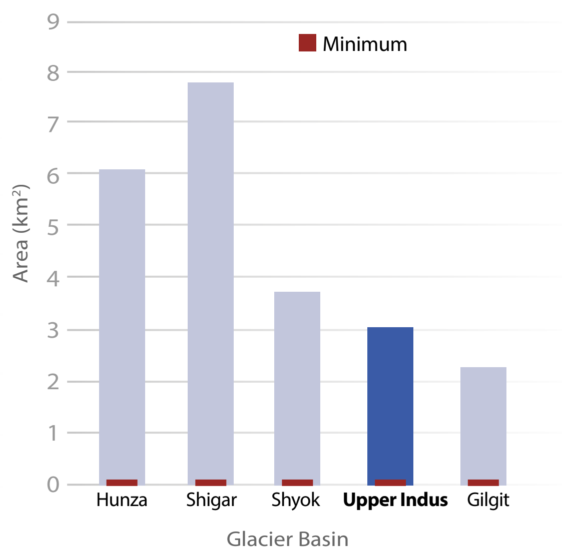

F
Area of glaciers
(the maximum value of each basin is reported)

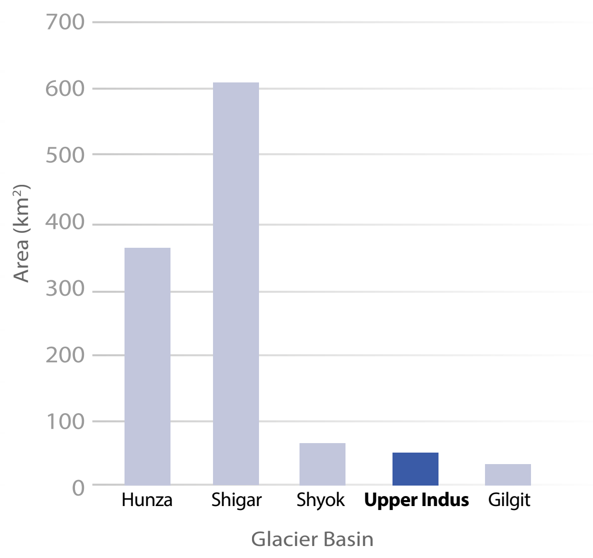

G
Glacier terminus elevation
(mean, minimum and maximum value
for each basin is reported)

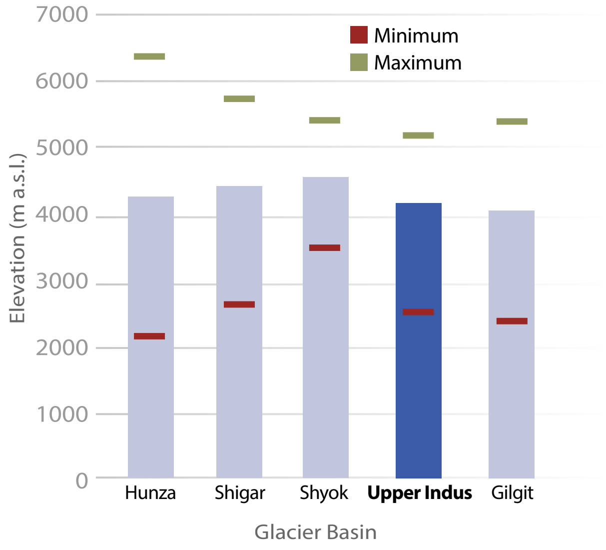

H
Glacier length
(mean, minimum and maximum value
for each basin is reported)

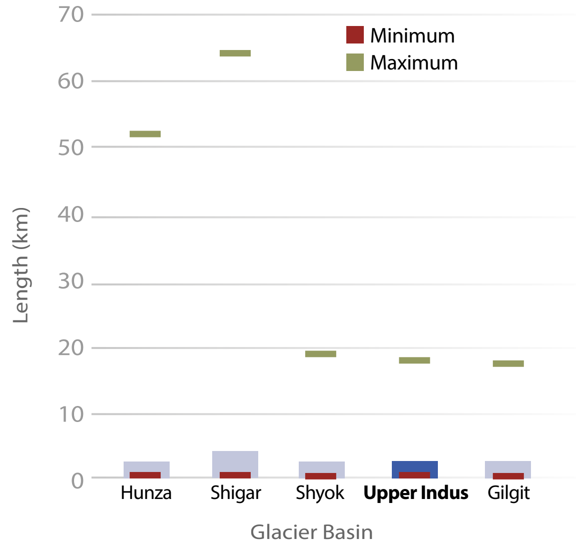

I
Distribution of debris-coverd glaciers
(data of each glacier basin are reported)

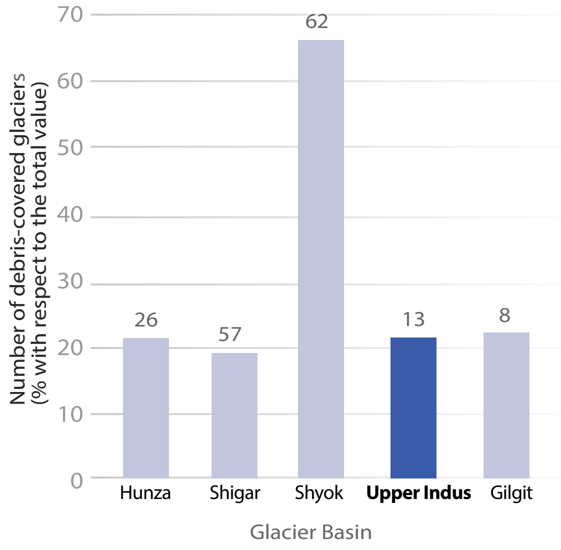

L
Glacier thickness
(mean, minimum and maximum value
for each basin is reported)

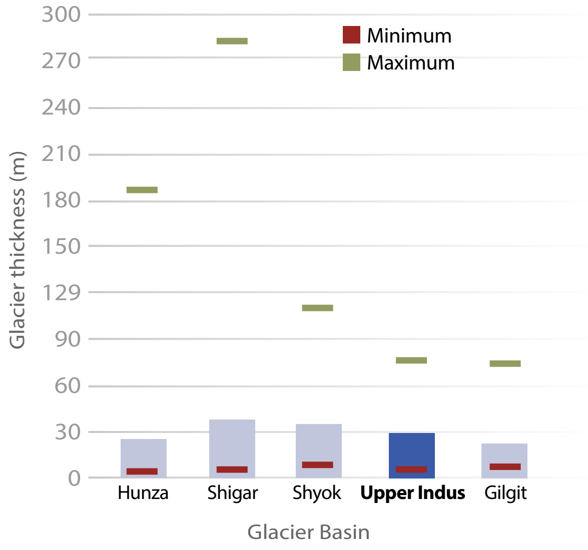

M
Glacier volume
(km³, the cumulative value of each basin is reported)

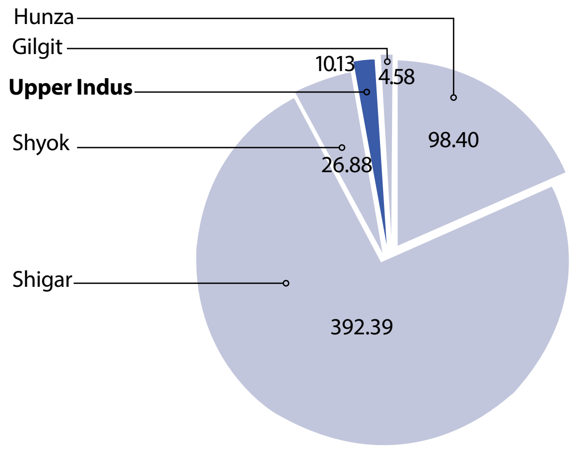

N
Glacier volume
(mean, minimum and maximum value
for each basin is reported)

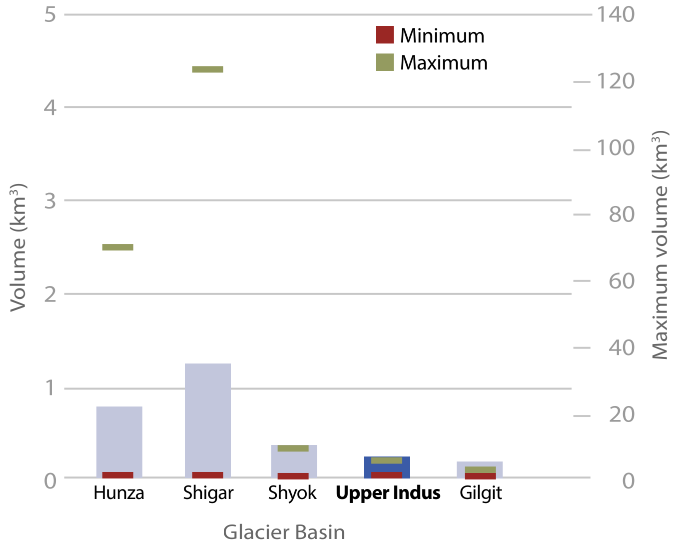

Daltsampa (near Hushe valley)

Muztagh glacier (Baltoro Side)

Glaciers in the Gilgit basin

Observed data

Gilgit basin hosts the lowest number of glaciers (36, Fig. A, corresponding to 6% of the whole CKNP glacier census) and the glacierized area is the 2% (83.62 km^2, Fig. B) of the total CKNP glaciation, thus representing the smallest one compared to the other basins. Analyzing the frequency distribution of glaciers sorted according to size classes (Fig. C), the most part of ice bodies in this basin feature an area lower than 0.5 km^2 (55.6%), but they only cover 4.3% of the whole Gilgit glaciation (Fig. D). Even if only 2 ice bodies fall within a larger size-class (i.e. 20-50 km^2, Fig. C), they cover more than 50% of the total Gilgit glacierized area (Fig. D). The biggest glacier we found is 29.95 km^2 wide (Fig. F), then the Gilgit basin is the only one without glaciers in the largest class (i.e. >50 km^2). This results in a lower average size of glaciers (equal to 2.32 km^2), which is the lowest one with respect to the other CKNP basins (Fig. E). Glacier minimum elevation (i.e. ~ glacier terminus elevation) prevails between 4000 and 4500 m a.s.l. (50% of all Gilgit glaciers), with a mean value of 4158 m a.s.l., the maximum one of 5370 m a.s.l. and the minimum one of 2500 m a.s.l. (Fig. G). Finally, the 50% of glaciers is found featuring a length ranging between 1 and 5 km, similar to the overall CKNP condition (Fig. H) but the maximum length is the lowest one with respect to the other basins.

By means of the supervised classification which we applied to the Landsat images, it was possible to investigate the spatial distribution of supraglacial debris and then to sort glaciers into debris-free and debris-covered types. In the Gilgit basin, only 8 debris-covered glaciers were found (Fig. I), but altogether they cover the 4/5th of the Gilgit glacierized area (i.e. 69.5 km^2). As we found for all the others basins, the minimum elevation of these glaciers is found at lower altitude compared to the one of debris-free glaciers.

In 2010 the glacier area of the whole Gilgit basin is 83.61 km^2, a value quite similar to the one found analyzing 2001 images. Table 1 shows glacier area values in 2001 and 2010, highlighting almost null changes in the 2001-2010 time window. The area variations of the Gilgit basin during this period suggest a general glacier stability, in agreement with the other CKNP basins and in contrast to the worldwide shrinkage of glaciers outside the Polar Regions. Only 2 glaciers in the Gilgit basin changed their area: in particular, one glacier feature a slight increase (i.e. +0.01 km^2) and the other one a small decrease (i.e. -0.02 km^2). Both these ice bodies are debris-free and belong to the size class <0.5 km^2.

Size class (km^2)	2001 Area		2010 Area		Δ2001-2010	
	km^2	%	km^2	%	km^2	%
<0.5	3.55	4.2%	3.54	4.2%	-0.01	-0.012%
0.5–1.0	3.78	4.5%	3.78	4.5%	0.00	0.000%
1.0–2.0	9.42	11.3%	9.42	11.3%	0.00	0.000%
2.0–5.0	0.00	0.0%	0.00	0.0%	/	/
5.0–10.0	8.46	10.1%	8.46	10.1%	0.00	0.000%
10.0–20.0	0.00	0.0%	0.00	0.0%	/	/
20.0–50.0	58.41	69.9%	58.41	69.9%	0.00	0.000%
>50.0	0.00	0.0%	0.00	0.0%	/	/
Total	**83.62**	**100.0%**	**83.61**	**100.0%**	**-0.01**	**-0.012%**

Table 1: Glacier coverage in 2001 and 2010 and glacier area change in the time window 2001-2010 (km^2) sorted according to 2001 size classes, and reported also as percentage (%) calculated with respect to their total values.

Derived data

The ice thickness data were estimated applying a physically based approach (fully described in the section "Data and methods" of Introduction and Methods chapter), which considers the glacier geometry data recorded in the CKNP inventory (2001 data base). The mean ice thickness of the Gilgit basin glaciers is found ranging from 6 m to 70 m, with an average value of 23 m (Fig. L). The most part of glaciers (86.1%) features a thickness value between 10 and 50 m. Debris-covered glaciers feature a mean ice thickness of 37 m (ranging from 13 to 70 m), higher than the one found for debris-free glaciers (equal to 19 m, ranging from 6 to 31 m).

For assessing the total glacier-derived fresh-water resource of the CKNP, an indirect approach based on glacier area and thickness data was applied. Due to the small size of Gilgit glaciers, only the 1% of fresh-water of the whole CKNP resource is present in this basin (for a total ice volume of 4.58 km^3, Fig. M), of which 4.23 km^3 of ice is entrapped into debris-covered glaciers and 0.35 km^3 of ice into debris-free glaciers. Considering the total volume value (i.e. 4.6 km^3), the mean ice thickness results about 55 m. The largest part of the Gilgit glaciers (88.9%) features a volume lower than 0.05 km^3 (but contributing only to 8.3% of the total Gilgit glacier volume) and the mean value is equal to 0.13 km^3 (Fig. N, lower compared to the overall CKNP condition).

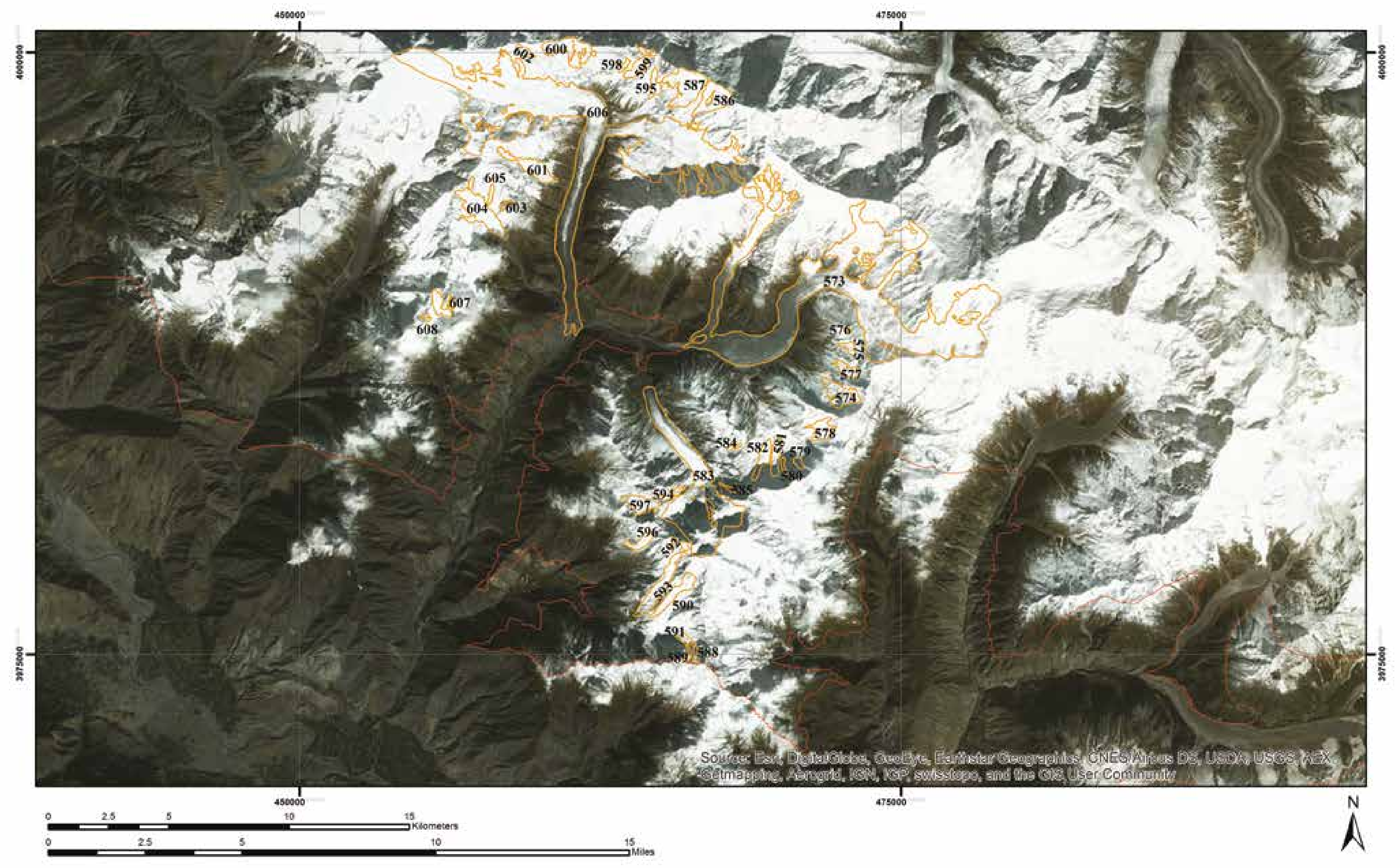

A

Number of glaciers
(data of each glacier basin are reported)

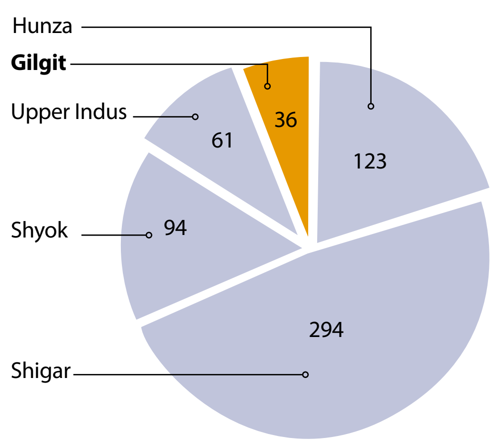

B

Glacier area
(km², the cumulative value of each glacier basin is reported)

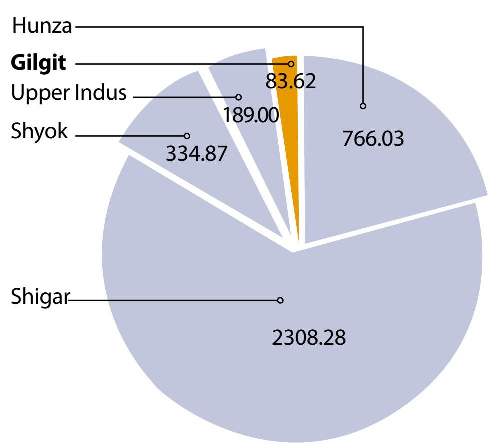

C

Glacier distribution
(data of each glacier basin are reported)

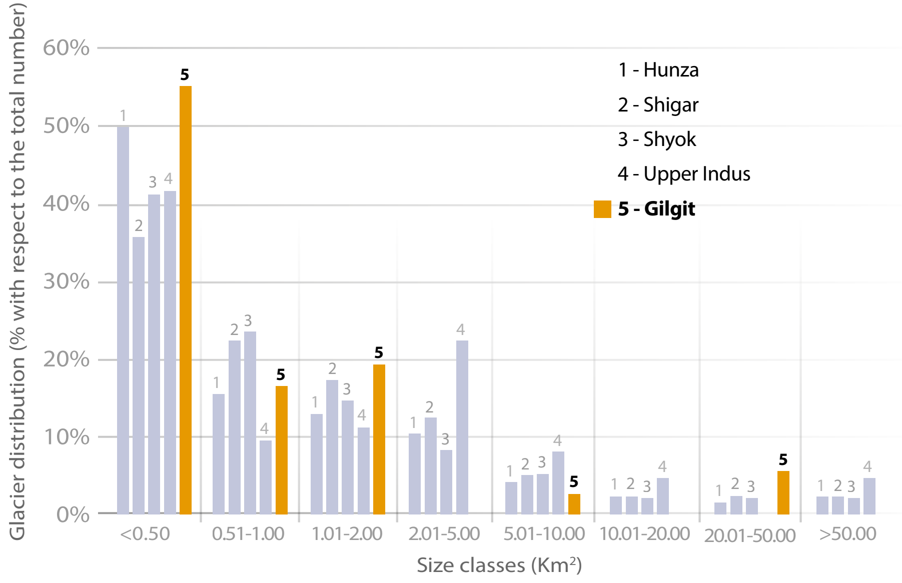

D

Glacier area distribution
(data of each glacier basin are reported)

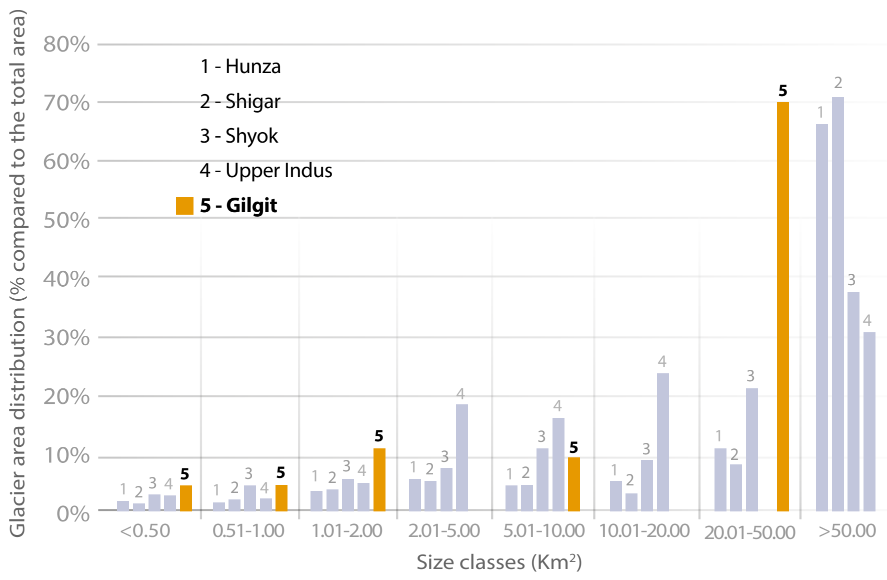

E

Area of glaciers
(mean and minimum value of each basin is reported)

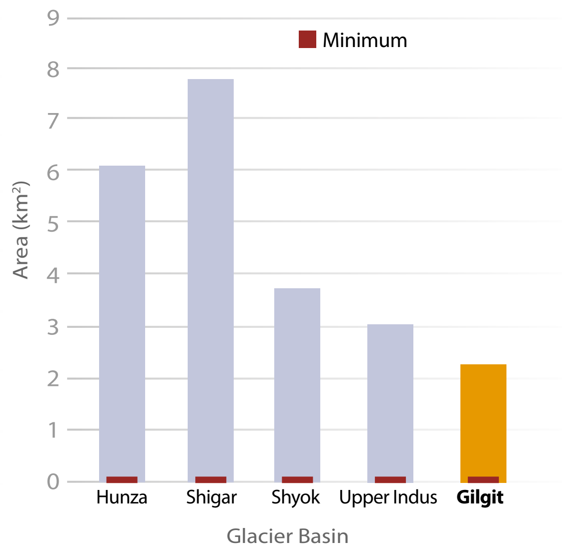

F

Area of glaciers
(the maximum value of each basin is reported)

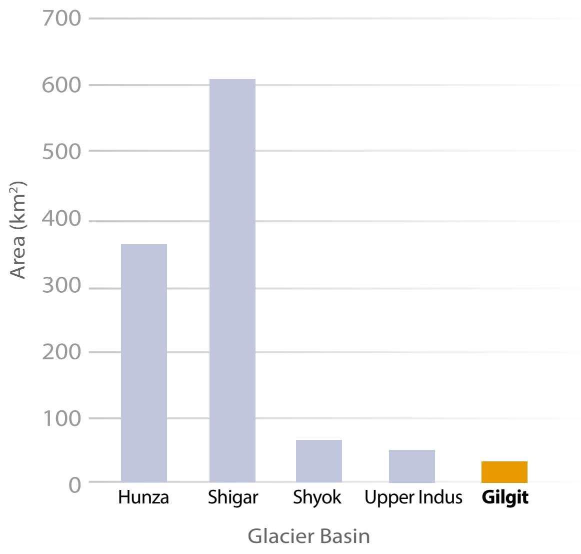

G

Glacier terminus elevation
(mean, minimum and maximum value
for each basin is reported)

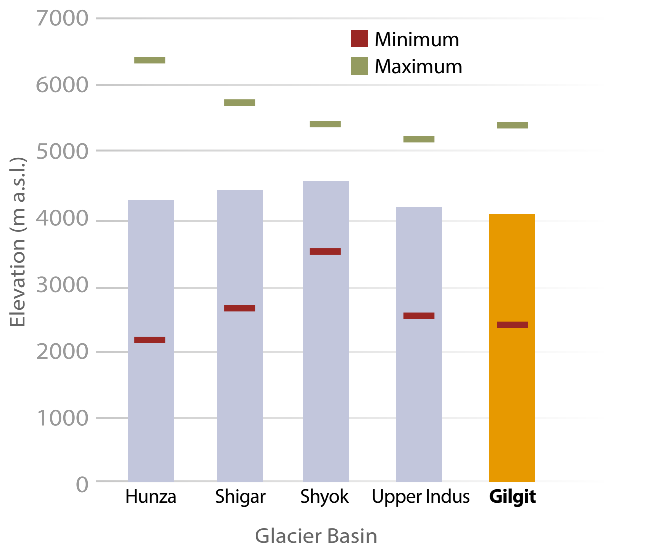

H

Glacier length
(mean, minimum and maximum value
for each basin is reported)

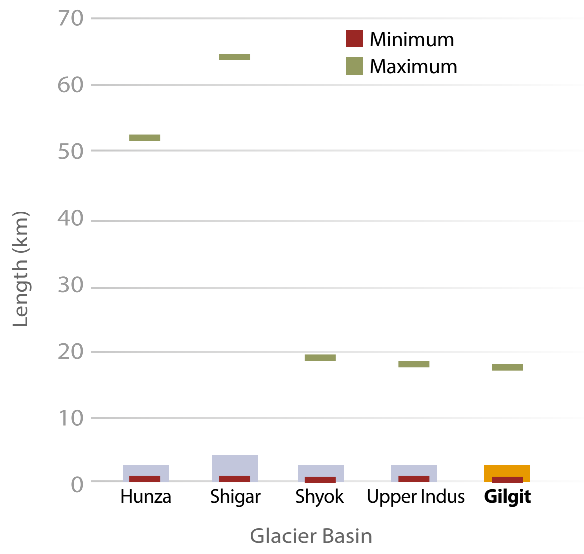

I

Distribution of debris-coverd glaciers
(data of each glacier basin are reported)

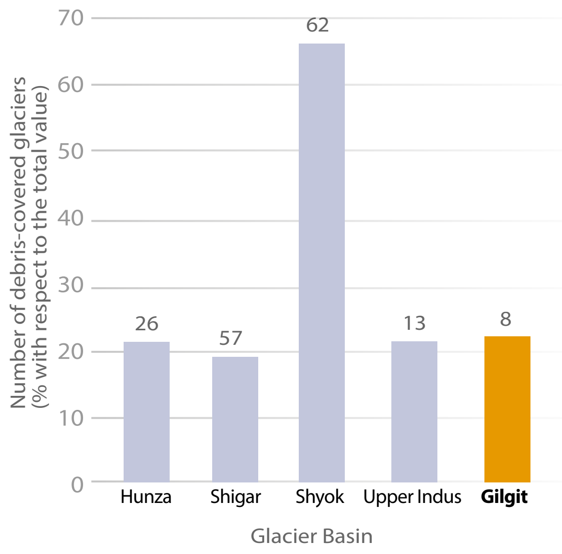

L

Glacier thickness
(mean, minimum and maximum value
for each basin is reported)

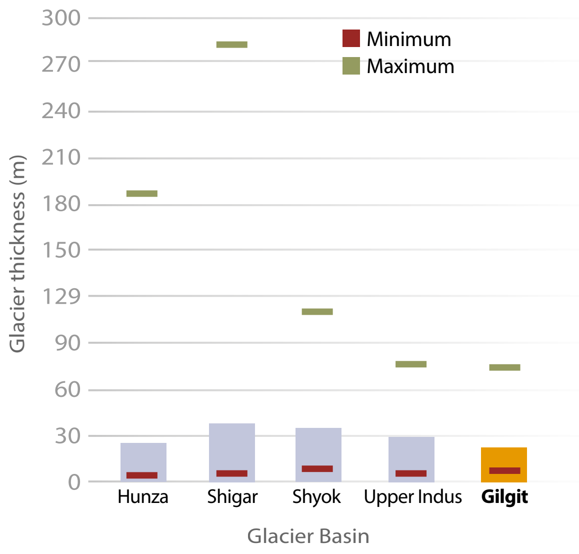

M

Glacier volume
(km³, the cumulative value of each basin is reported)

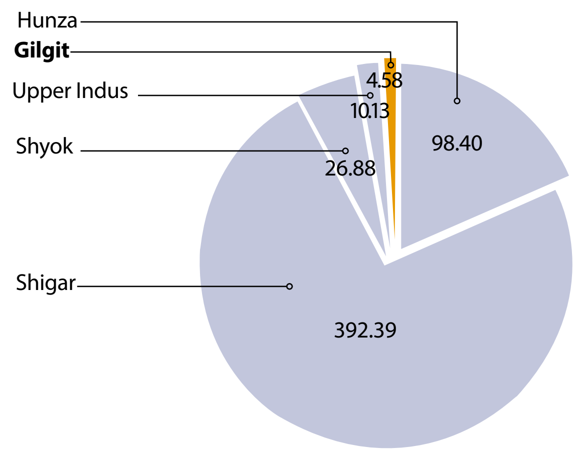

N

Glacier volume
(mean, minimum and maximum value
for each basin is reported)

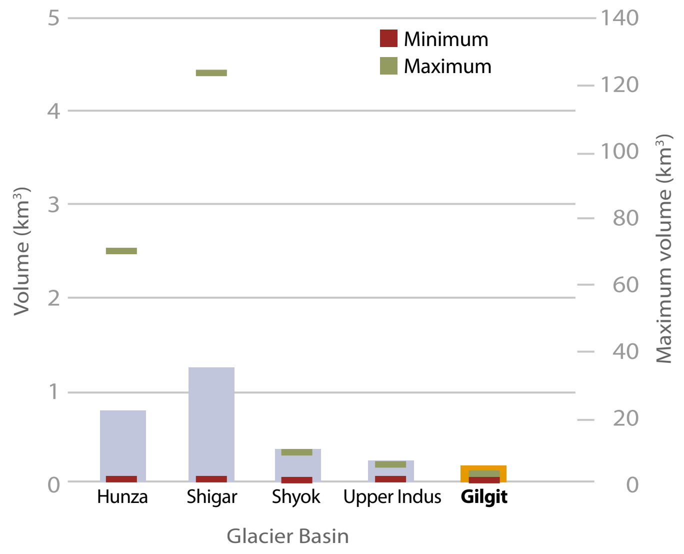


Hinarche Glacier (Bagrot valley, Gilgit Basin).


Hinarche Glacier (Gilgit Basin).


Hinarche Glacier (Gilgit Basin).


Hinarche Glacier (Gilgit Basin).

Conclusions

Conclusions and future prospectives

In this glacier inventory, we described the fresh-water resource nested in the Central Karakorum National Park (CKNP, an extensive protected area of about 10000 km² in Northern Pakistan, in the main glaciated region of the Central Karakorum). In particular, we reported the total number of glaciers (608 ice bodies) and their features in 2001 and 2010, listing location, type, size, surface conditions (i.e. debris occurrence and extent, if any), geometry, and ice volume. In addition, we analyzed in more detail the five basins included in the CKNP area and found that they reflect the overall conditions regarding glacier distribution per size class, terminus elevation, length, and thickness. The widest basin (for number of ice bodies, glacier extent and ice volume) is the Shigar basin, where the largest glaciers are present (among which Baltoro Glacier), and the smallest one is the Gilgit basin. Finally, the highest number of debris-covered glaciers is found in the Shyok basin (62 glaciers). Comparing glacier areas in 2001 and 2010, sorted according to 2001 size classes, the Hunza glacierized area is characterized by the maximum shrinkage albeit not particularly intense (i.e. -0.76 km²), and the Upper Indus by the maximum increase (i.e. +0.52 km²). Generally, the glaciers found to be affected by higher variations belong to the 10-20 km² size class. However, the analysis of area changes during 2001–2010 reveals a general stability, evidence of the anomalous behavior of glaciers in the Karakorum in contrast to the worldwide shrinkage of mountain glaciers. In Minora et al. (2016), the Karakorum Anomaly was analyzed in view of the ongoing climate change. A slight increase in late summer average snow covered area during 2001–2010 was observed from MODIS snow data. At the same time, the available weather stations revealed an increase of snowfall events and a decrease of mean summer air temperatures since 1980, which would translate into more persistent snow cover during the melt season. These results support an enhanced glacier preservation in the ablation areas due to a long-lasting snow cover, and stronger accumulation at higher altitudes, pushing towards positive net balances. Nevertheless, linking these observations to the analysis of glacier area changes is not unambiguous, since there is a delay in the glacier area response to climate change depending on glacier size, with usually longer response times (even several decades) for larger glaciers (Bolch et al., 2012). The data source used in this inventory is Landsat imagery with a resolution of 15-30 m. The availability of data with higher resolution (e.g. Pleiades with 0.5 m of resolution, SPOT with 2.5 m, IKONOS with 1-4 m, QuickBird with 0.65 m, WorldView-2 with 0.50 m) will allow to get very small variations in glacier area.

Comparison with the other glacier inventories

We compared our glacier outlines against the Randolph Glacier Inventory, version 5.0 (RGI, Arendt et al., 2015), another region-wide inventory. To make the comparison consistent, we selected only the glacier polygons which were mapped in both inventories. We chose to compare the outlines of our inventory from 2001 because they are closer in time to the RGI inventory. The comparison was made for the entire glacier area and for the accumulation area only, because minor changes over time are expected to occur in the accumulation area. An elevation of 5200 m a.s.l. was used as the equilibrium line altitude (ELA). Table 1 shows the differences in area between the RGI inventory and our mapping results. The relative area difference is not large with respect to the total glacier surface, but shows a tendency to higher values below the ELA. Our inventory tends to underestimate the glacier area considering both the whole surface and the accumulation zones. This might derive from different strategies of mapping the upper glacier limits in the different inventories. In particular, we used a slope criterion to exclude all the headwalls steeper than 60° from the upper glacier limit, while the RGI includes steep headwalls of the accumulation basins in the glacier outlines, thus leading to larger glacier areas, as also reported by Nuimura et al. (2015). In addition, the presence of seasonal snow cover and rock outcrops within glacier areas were considered in the source data of the RGI. These different approaches can partly explain the lower overall glacier area found in our inventory, compared to the RGI 5. Indeed, if we analyze the Biafo Glacier, in our inventory it is 438.11 km² wide, while the RGI reports an area of 559.81 km². This remarkable difference is probably due to the inclusion of rock outcrops into the glacier area (Fig. 1).

	our inventory (km²)	RGI 5.0 (km²)	Difference (km²)	Difference (%)
total area	3658.8	4565.1	-906.3	-24.8%
above ELA	1053.0	1223.0	-170.0	-16.1%

Table 1: Summary of glaciers in the CKNP glacier inventory (year 2001) and the RGI 5.0. The areas are compared with respect to the CKNP 2001 inventory (see "Difference" values). Only glacier polygons mapped in both inventories are shown.

Nuimura et al. (2015) presented a new glacier inventory (the GAMDAM glacier inventory, GGI) where they report a significantly lower glacier area compared to RGI 4.0 (a previous version of RGI 5.0) in the Karakorum region (-13%), and significantly larger compared e.g. to the ICIMOD inventory (+22%, Bajracharya and Shrestha, 2011). Unfortunately, we are not able to make a direct comparison with the GGI, as the outlines are not available for download, and we cannot extract the glacier areas within the CKNP borders (which correspond to 1/3rd of the whole Karakorum glaciers, according to ICIMOD). We can only observe that our inventory is smaller than the RGI just like the GGI (Table 1).

Fig. 1: Comparison between the Biafo Glacier outlines developed by RGI 5.0 (upper figure) and in our inventory (lower figure).

References

Arendt A., Bliss A., Bolch T., Cogley J.G., Gardner A.S., Hagen J.O., Hock R., Huss M., Kaser G., Kienholz C., Pfeffer W.T., Moholdt G., Paul F., Radić V., Andreassen L., Bajracharya S., Barrand N., Beedle M., Berthier E., Bhambri R., Brown I., Burgess E., Burgess D., Cawkwell F., Chinn T., Copland L., Davies B., De Angelis H., Dolgova E., Filbert K., Forester R., Fountain A., Frey H., Giffen B., Glasser N., Gurney S., Hagg W., Hall D., Haritashya U.K., Hartmann G., Helm C., Herreid S., Howat I., Kapustin G., Khromova T., König M., Kohler J., Kriegel D., Kutuzov S., Lavrentiev I., LeBris R., Lund J., Manley W., Mayer C., Miles E.S., Li X., Menounos B., Mercer A., Mölg N., Mool P., Nosenko G., Negrete A., Nuth C., Pettersson R., Racoviteanu A., Ranzi R., Rastner P., Rau F., Raup B., Rich J., Rott H., Schneider C., Seliverstov Y., Sharp M., Sigurðsson O., Stokes C., Wheate R., Winsvold S., Wolken G., Wyatt F. and Zheltyhina N. (2014) - Randolph Glacier Inventory – *A Dataset of Global Glacier Outlines: Version 4.0. Global Land Ice Measurements from Space, Boulder Colorado, USA. Digital Media.*

Arendt, A., A. Bliss, T. Bolch, J.G. Cogley, A.S. Gardner, J.-O. Hagen, R. Hock, M. Huss, G. Kaser, C. Kienholz, W.T. Pfeffer, G. Moholdt, F. Paul, V. Radić, L. Andreassen, S. Bajracharya, N.E. Barrand, M. Beedle, E. Berthier, R. Bhambri, I. Brown, E. Burgess, D. Burgess, F. Cawkwell, T. Chinn, L. Copland, B. Davies, H. De Angelis, E. Dolgova, L. Earl, K. Filbert, R. Forester, A.G. Fountain, H. Frey, B. Giffen, N. Glasser, W.Q. Guo, S. Gurney, W. Hagg, D. Hall, U.K. Haritashya, G. Hartmann, C. Helm, S. Herreid, I. Howat, G. Kapustin, T. Khromova, M. König, J. Kohler, D. Kriegel, S. Kutuzov, I. Lavrentiev, R. LeBris, S.Y. Liu, J. Lund, W. Manley, R. Marti, C. Mayer, E.S. Miles, X. Li, B. Menounos, A. Mercer, N. Mölg, P. Mool, G. Nosenko, A. Negrete, T. Nuimura, C. Nuth, R. Pettersson, A. Racoviteanu, R. Ranzi, P. Rastner, F. Rau, B. Raup, J. Rich, H. Rott, A. Sakai, C. Schneider, Y. Seliverstov, M. Sharp, O. Sigurðsson, C. Stokes, R.G. Way, R. Wheate, S. Winsvold, G. Wolken, F. Wyatt, N. Zheltyhina, 2015, Randolph Glacier Inventory – A Dataset of Global Glacier Outlines: Version 5.0. Global Land Ice Measurements from Space, Boulder Colorado, USA. Digital Media.

Bajracharya S.R. and Shrestha B. (eds) (2011) - *The status of glaciers in the Hindu Kush-Himalayan region*. Kathmandu: ICIMOD.

Barrand N. and Murray T. (2006) - *Multivariate controls on the incidence of glacier surging in the Karakoram Himalaya*. Arct. Antarct. Alp. Res., 38, 489-498.

Barsi J.A., Barker J.L. and Schott J.R. (2003) - *An Atmospheric Correction Parameter Calculator for a Single Thermal Band Earth-Sensing Instrument*. IGARSS03, 21-25 July 2003. DOI:10.1109/IGARSS.2003.1294665

Barsi J.A., Schott J.R., Palluconi F.D. and Hook S.J. (2005) - *Validation of a Web-Based Atmospheric Correction Tool for Single Thermal Band Instruments*. Earth Observing Systems X, Proc. SPIE Vol. 5882, August 2005. DOI:10.1117/12.619990

Baumann S. and Winkler S. (2010) – *Parameterization of glacier inventory data from Jotunheimen /Norway in comparison to the European Alps and the Southern Alps of New Zealand*. Erdkunde, vol 64 (2), 155-177.

Belò M., Mayer C., Smiraglia C. and Tamburini A. (2008) - *The recent evolution of Liligo Glacier, Karakorum, Pakistan, and its present quiescent phase*. Annals of Glaciology, 48(1), 171-176.

Bhambri R. and Bolch T. (2009) - *Glacier mapping: a review with special reference to the Indian Himalayas*. Prog. Phys. Geog., 33, 672–704. DOI:10.1177/0309133309348112

Bocchiola D. and Diolaiuti G.A. (2013) - *Recent (1980-2009) evidence of climate change in the upper Karakoram, Pakistan*. Theor. Appl. Climatol. DOI:10.1007/s00704-012-0803-y

Bolch T., Kulkarni A., Kääb A., Huggel C., Paul F., Cogley J.G., Frey H., Kargel J.S., Fujita K., Scheel M., Bajracharya S. and Stoffel M. (2012) - *The state and fate of Himalayan glaciers*. Science, 336, 310-314.

Bookhagen B. and Burbank D.W. (2010) - *Towards a complete Himalayan hydrologic budget: the spatiotemporal distribution of snow melt and rainfall and their impact on river discharge*. J. Geophys. Res., 115, F03019, DOI:10.1029/2009jf001426

Brown D.G., Lusch D.P. and Duda K.A. (1998) - *Supervised classification of types of glciated landscapes using digital elevation data*. Geomorphology, 21, 233-250. DOI:10.1016/S0169-555X(97)00063-9

CGIAR-CSI, Consortium for Spatial Information (2012) - http://www.cgiar-csi.org, last access: 20 February 2014.

Citterio M., Diolaiuti G.A., Smiraglia C., D'agata C., Carnielli T., Stella G. and Siletto G.B. (2007) - *The fluctuations of Italian glaciers during the last century: a contribution to knowledge about Alpine glacier changes*. Geogr. Ann., 89 A (3), 167-184.

Cogley J.G. (2011) - *Present and future states of Himalaya and Karakoram glaciers*. Annals of Glaciology, 52(59), 69-73.

Coll C., Galve J.M., Sánchez J.M. and Caselles V. (2010) - *Validation of Landsat-7/ETM+ Thermal-Band Calibration and Atmospheric Correction With Ground-Based Measurements*. IEEE Transactions on Geoscience and Remote Sensing, *48 (1), 547-555*. DOI:10.1109/TGRS.2009.2024934

Collier E., Maussion F., Nicholson L.I., Mölg T., Immerzeel W.W. and Bush A.B.G. (2015) - *Impact of debris cover on glacier ablation and atmosphere-glacier feedbacks in the Karakoram*. The Cryosphere, 9(4), 1617-1632.

Copland L., Sharp M.J. and Dowdeswell J.A. (2003) - *The distribution and flow characteristics of surge-type glaciers in the Canadian High Arctic*. Ann. Glaciol., 36, 73-81.

Copland L., Sylvestre T., Bishop M.P., Shroder J.F., Seoung Y.B., Owen L.A., Bush A. and Kamp U. (2011) - *Expanded and Recently Increased Glacier Surging in the Karakoram*. Institute of Arctic and Alpine Reasearch (INSTAAR), University of Colorado, available at: http://www.bioone.org/DOI/full/10.1657/1938-4246-43.4.503.

Cuffey K.M. and Paterson W.S.B. (2010) - *The Physics of Glaciers*. 4th Edn., ISBN: 9780123694614, Pergamon Press, Oxford, UK.

Deline P. (2005) - *Change in surface debris cover on Mont Blanc massif glaciers after the "Little Ice Age" termination*. Holocene, 15 (2), 302–309.

Diolaiuti G.A., Pecci M. and Smiraglia C. (2003) - *Liligo Glacier, Karakoram, Pakistan: a reconstruction of the recent history of a surge-type glacier*. Annals of Glaciology, 36(1), 168-172.

Diolaiuti G.A., D'Agata C., Meazza A., Zanutta A. and Smiraglia C. (2009) - *Recent (1975-2003) changes in the Miage debris-covered glacier tongue (Mont Blanc, Italy) from analysis of aerial photos and maps*. Geogr. Fis. Dinam. Quat., 32, 117-127.

Driedger C.L. and Kennard P.M. (1986) - *Glacier volume estimation on Cascade Volcanoes: an analysis and comparison with other methods*. Annals of Glaciology, 8, 59-64.

Falorni G., Teles V., Vivoni E.R., Bras R.L. and Amaratunga K.S. (2005) - *Analysis and characterization of the vertical accuracy of digital elevation models from the Shuttle Radar Topography Mission*. Journal Of Geophysical Research, 110 F2. DOI:10.1029/2003JF000113

Fowler H.J. and Archer D.R. (2006) - *Conflicting signals of climatic change in the Upper Indus basin*. J. Climate, 19, 4276-4293.

Frey H., Machguth H., Huss M., Huggel C., Bajracharya S., Bolch T., Kulkarni A., Linsbauer A., Salzmann N. and Stoffel M. (2014) - *Estimating the volume of glaciers in the Himalayan–Karakoram region using different methods*. The Cryosphere, 8, 2313–2333. DOI:10.5194/tc-8-2313-2014

Fujita K. and Sakai A. (2014) - *Modelling runoff from a Himalayan debris-covered glacier*. Hydrology and Earth System Sciences, 18(7), 2679-2694. DOI:10.5194/hess-18-2679-2014 014

Fyffe C., Reid T.D., Brock B.W., Kirkbride M.P., Diolaiuti G., Smiraglia C. and Diotri F. (2014) - *A distributed energy-balance melt model of an alpine debris-covered glacier*. Journal of Glaciology, 60, 221, 587–602. DOI:10.3189/2014JoG13J148

Gardelle J., Berthier E. and Arnaud Y. (2012) - *Slight mass gain of Karakoram glaciers in the early 10 twenty-first century*. Nat. Geosci. Letters, 5, 322-325. DOI:10.1038/NGEO1450

Gardelle J., Berthier E., Arnaud Y. and Kääb A. (2013) - *Region-wide mass balances over the Pamir-Karakoram-Hiimalaya during 1999-2011*. The Cryosphere, 7, 1263-1286.

Gardner A.S., Moholdt G., Cogley J.G., Wouters B., Arendt A.A., Wahr J., Berthier E., Hock R., Pfeffer W.T., Kaser G., Ligtenberg S.R.M., Bolch T., Sharp M.J., Hagen J.O., Van Den Broeke M.R. and Paul F. (2013) - *A Reconciled Estimate of Glacier Contributions to Sea Level Rise: 2003 to 2009*. Science, 852-857.

Haeberli W. (1985) - *Global land-ice monitoring: present status and future perspectives*. United States Department of Energy, Glaciers, Ice sheets and Sea level: Effect of a CO2 – Induced Climate Change. Report DOE/EV 60235-I. National Academy Press, Seattle, WA, pp. 216-231.

Haeberli W. and Hoelzle M. (1995) - *Application of inventory data for estimating characteristics of and regional climate-change effects on mountain glaciers: a pilot study with the European Alps*. Annals of Glaciology, 21, 206-212.

Hagg W. and Braun L. (2005) - *The influence of glacier retreat on water yield from high mountain areas: comparison of Alps and central Asia*. In De Jong, C., R. Ranzi and D. Collins, eds. Climate and hydrology in mountain areas. Chicester, Wiley & Sons, 263–275.

Hewitt K. (2005) - *The Karakoram Anomaly? Glacier expansion and the "elevation effect", Karakoram Himalaya*. Mt. Res. Dev., 25, 332-340.

Hewitt K. (2007) - *Tributary glacier surges: an exceptional concentration at Panmah Glacier, Karakoram, Himalaya*. J. Glaciol., 53, 181-188. DOI:10.3189/172756507782202829

Hewitt K. (2011) - *Glacier Change, Concentration, and Elevation Effects in the Karakoram Himalaya, Upper Indus Basin*. Mt. Res. Dev., 31(3), 188-200, DOI: http://dx.DOI.org/10.1659/MRD-JOURNAL-D-11-00020.1

Hewitt K. (2014) - *Glaciers of the Karakoram Himalaya. Glacial Environments, Processes, Hazards and Resources*. Springer, Dordrecht, pp. 363.

Hoelzle M., Haeberli W., Dischl M. and Peschke W. (2003) - *Secular glacier mass balances derived from cumulative glacier length changes*. Global and Planetary Change, 36(4), 295-306.

Hoelzle M., Haeberli H., Dischl M. and Peschke W. (2003) - *Secular glacier mass balances derived from cumulative glacier length changes*. Global Planetary Change, 36, 295-306.

Kääb A., Paul F., Maisch M., Hoelzle M. and Haeberli W. (2002) - *The new remote sensing derived Swiss glacier inventory: II. First results*. Ann. Glaciol., 34, 362-366.

Kirkbride M.P. (2011) - *Debris-covered glaciers*. In Encyclopedia of Snow, Ice and Glaciers (pp. 180-182). Springer Netherlands.

Konovalov V.G. (1997) - *The hydrological regime of Pamir–Alai glaciers*. Z. Gletscherkd. Glazialgeol., 33(2), 125–131.

Landsat7 Handbook - http://landsathandbook.gsfc.nasa.gov/, http://lpdaac.usgs.gov, last access: 13 April 2014.

Marussi A. (1964) - *Geophysics of the Karakorum*. Vol. I, Brill Archive - Leide, 243 pp.

Mattson L.E., Gardner J.S. and Young G.J. (1993) - *Ablation on debris covered glaciers: an example from the Rakhiot Glacier, Punjab, Himalaya*. Snow and Glacier Hydrology, Proc. Kathmandu Symp. November 1992, edited by: Young, G. J., IAHS Publ. no. 218, IAHS Publishing, Wallingford, 289-296.

Mayer C., Lambrecht A., Mihalcea C., Belò M., Diolaiuti G.A., Smiraglia C. and Bashir F. (2010) - *Analysis of Glacial Meltwater in Bagrot Valley, Karakoram*. Mountain Research and Development, 30(2), 169-177.

Mihalcea C., Mayer C., Diolaiuti G.A., D'agata C., Smiraglia C., Lambrecht A., Vuillermoz E. and Tartari G. (2008a) - *Spatial distribution of debris thickness and melting from remote-sensing and meteorological data, at debris-covered Baltoro glacier, Karakoram, Pakistan*. Ann. Glaciol., 48, 49-57.

Mihalcea C., Brock B.W., Diolaiuti G., D'Agata C., Citterio M., Kirkbride M.P., Cutler M.E.J. and Smiraglia C. (2008b) - *Using ASTER satellite and ground-based surface temperature measurements to derive supraglacial debris cover and thickness patterns on Miage Glacier (Mont Blanc Massif, Italy)*. Cold Regions Science and Technology, 52, 341–354. DOI:10.1016/j.coldregions.2007.03.004

Mihalcea C., Mayer C., Diolaiuti G.A., Lambrecht A., Smiraglia C. and Tartari G. (2006) - *Ice ablation and meteorological conditions on the debris covered area of Baltoro Glacier (Karakoram, Pakistan)*. Ann. Glaciol., 43, 292-300.

Minora U., Bocchiola D., D'Agata C., Maragno D., Mayer C., Lambrecht A., Mosconi B., Vuillermoz E., Senese A., Compostella C., Smiraglia C. and Diolaiuti G. (2013) - *2001–2010 glacier changes in the Central Karakoram National Park: a contribution to evaluate the magnitude and rate of the "Karakoram anomaly"*. The Cryosphere Discuss., 7, 2891–2941. DOI:10.5194/tcd-7-2891-2013

Minora U.F., Senese A., Bocchiola D., Soncini A., D'Agata C., Ambrosini R., Mayer C., Lambrecht A., Vuillermoz E., Smiraglia C. and Diolaiuti G. (2015) - *A simple model to evaluate ice melt over the ablation area of glaciers in the Central Karakoram National Park, Pakistan.* Annals of Glaciology, 56(70), 202-216. DOI:10.3189/2015AoG70A206

Minora U., Bocchiola D., D'Agata C., Maragno D., Mayer C., Lambrecht A., Vuillermoz E., Senese A., Compostella C., Smiraglia C. and Diolaiuti G. (2016) - *Glacier area stability in the Central Karakoram National Park (Pakistan) in 2001–2010: the "Karakoram Anomaly" in the spotlight.* Progress in Physical Geography. DOI:10.1177/0309133316643926

Nakawo M. and Young G.J. (1981) - *Field experiments to determine the effect of a debris layer on ablation of glacier ice.* Ann. Glaciol., 2, 85–91.

Nakawo M. and Takahashi S. (1982) - *A simplified model for estimating glacier ablation under a debris layer.* IAHS Publ. 138 (Symposium at Exeter 1982 – Hydrological Aspects of Alpine and High Mountain Areas), 137–145. DOI:10.3189/172756481794352432

Nakawo M. and Rana B. (1999) - *Estimate of ablation rate of glacier ice under a supraglacial debris layer.* Geogr. Ann., 81A(4), 695–701.

Nicholson L. and Benn D.I. (2006) - *Calculating ice melt beneath a debris layer using meteorological data.* Journal of Glaciology, 52, 178.

Nuimura T., Sakai A., Taniguchi K., Nagai H., Lamsal D., Tsutaki S., Kozawa A., Hoshina Y., Takenaka S., Omiya S., Tsunematsu K., Tshering P. and Fujita K. (2015) - *The GAMDAM glacier inventory: a quality-controlled inventory of Asian glaciers.* The Cryosphere, 9, 849-864.

O'Gorman L. (1996) - *Subpixel precision of straight-edged shapes for registration and measurement.* IEEE Transactions on Pattern Analysis and Machine Intelligence 18: 746-751, DOI:10.1109/34.506796.

Østrem G. (1959) - *Ice melting under a thin layer of moraine, and the existence of ice cores in moraine ridges.* Geogr. Ann., 41(4), 228-230.

Paul F., Huggel C. and Kääb A. (2004) - *Combining satellite multispectral data and a digital elevation model for mapping debris-covered-glaciers.* Remote Sens. Environ., 89 (4), 510-518. DOI: 10.1016/j.rse.2003.11.007

Paul F., Barry R.G., Cogley J.G., Frey H., Haeberli W., Ohmura A., Ommanney C.S.L., Raup B., Rivera A. and Zemp M. (2009) - *Recommendations for the compilation of glacier inventory data from digital sources.* Ann. Glaciol., 50 (53).

Paul F., Barrand N.E., Baumann S., Berthier E., Bolch T., Casey K., Frey H., Joshi S.P., Konovalov V., Le Bris R., Mölg N., Nosenko G., Nuth C., Pope A., Racoviteanu A., Rastner P., Raup B., Scharrer K., Steffen S. and Windswold S. (2013) - *On the accuracy of glacier outlines derived from remote-sensing data.* Ann. Glaciol., 54 (63).

Paul F. (2015) - *Revealing glacier flow and surge dynamics from animated satellite image sequences: examples from the Karakoram.* The Cryosphere, 9(6), 2201-2214.

Pellicciotti F., Brock B.W., Strasser U., Burlando P., Funk M. and Corripio J.G. (2005) - *An enhanced temperature-index glacier melt model including shortwave radiation balance: development and testing for Haut Glacier d'Arolla, Switzerland.* J. Glaciol., *51, 573–587.* DOI:10.3189/172756505781829124

Quincey D.J., Braun M., Glasser N.F., Bishop M.P., Hewitt K. and Luckman A. (2011) - *Karakoram glacier surge dynamics.* Geophys. Res. Lett., 38, L18504. DOI: 10.1029/2011GL049004
Raina V.K. and Srivastava D. (2008) - *Glacier atlas of India.* Bangalore: Geological Society of India, 316 pp.

Rankl M., Kienholz C. and Braun M. (2014) - *Glacier changes in the Karakoram region mapped by multimission satellite imagery.* The Cryosphere, 8, 977-989.

Reid T.D. and Brock B.W. (2010) - *An energy balance model for debris-covered glaciers including heat conduction through the debris layer.* Journal of Glaciology, 56, 199.

Richards J.A. (1999) - *Remote Sensing Digital Image Analysis,* Springer-Verlag, Berlin, p. 240. DOI:10.1007/978-3-662-03978-6

Sakai A., Takeuchi N., Fujita K. and Nakawo M. (2000) - *Role of supraglacial ponds in the ablation process of a debris-covered glacier in the Nepal Himalayas.* IAHS PUBLICATION, 119-132.

Shekhar M.S., Chand H., Kumar S., Srinivasan K. and Ganju A. (2010) - *Climate-change studies in the western Himalaya.* Annals of Glaciology, 51(54).

Shukla A., Arora M.K. and Gupta R.P. (2010) - *Synergistic approach for mapping debris-covered glaciers using optical–thermal remote sensing data with inputs from geomorphometric parameters.* Remote Sens. Environ., 114 (7), 1378-1387.

Soncini A., Bocchiola D., Confortola G., Bianchi A., Rosso R., Mayer C., Lambrecht A., Palazzi E., Smiraglia C., Diolaiuti G. (2015) - *Future hydrological regimes in the upper Indus basin: a case study from a high altitude glacierized catchment,* J. Hydrometeorology, 16(1), 306-326.

Tangborn W. and Rana B. (2000) - *Mass balance and runoff of the partially debris-covered Langtang Glacier, Nepal.* IAHS PUBLICATION, 99-108.

Taschner S. and Ranzi R. (2002) - *Comparing the Opportunities of LANSAT-TM and ASTER Data for Monitoring a Debris Covered Glacier in the Italian Alps within GLIMS Project.* International Geoscience and Remote Sensing Symposium (IGARSS), 2, 1044–1046. DOI:10.1109/IGARSS.2002.1025770

Vögtle T. and Schilling K.J. (1999) - *Digitizing maps,* in: GIS for Environmental Monitoring, edited by: Bähr H.P. and Vögtle T., Schweizerbart, Stuttgart, Germany, 201-216.

Zhang Y., Fujita K., Liu S.Y., Liu Q. and Nuimura T. (2011) - *Distribution of debris thickness and its effect on ice melt at Hailuogou glacier, southeastern Tibetan Plateau, using in situ surveys and ASTER imagery.* Journal of Glaciology, 57(206), 1147-1157. DOI:10.3189/002214311798843331

Glacier data

		Coordinates (utm 43N - WGS 84 datum)																
Catchment	ID Code	Longitude	Latitude	2001 Minimum elevation (m a.s.l.)	2001 Maximum elevation (m a.s.l.)	2001 Maximum length (km)	2001 Slope (°)	2001 Area (km^2)	2001 Perimeter (km)	2010 Area (km^2)	2010 Perimeter (km)	2001 Glacier thickness (m)	2001 Ice volume (km^3)	2001 Debris cover (km^2)	2010 Debris cover (km^2)	Debris-Covered or Debris-Free glacier	Glacier Type	Glacier name
Hunza Basin																		
Hunza basin	1	445579.8	3990779.9	4700	5590	1.81	26.2	0.90	6.57	0.90	6.57	26.8	0.02	0.020	0.060	DF	glacier	
Hunza basin	2	446692.8	3990186.6	4190	5620	3.09	24.8	1.98	7.94	1.98	7.94	36.4	0.07	0.070	0.290	DF	glacier	
Hunza basin	3	447765.5	4003458.2	2730	5590	4.47	32.6	2.83	10.10	2.83	10.10	30.4	0.09	2.640	1.910	DC	glacier	
Hunza basin	4	448118.9	3991054.7	4110	5170	2.04	27.5	1.29	7.35	1.29	7.35	28.6	0.04	0.010	0.340	DF	glacier	
Hunza basin	5	448337.9	4001589.6	4930	5370	0.45	44.4	0.05	1.03	0.05	1.03	9.7	0.00	0.000	0.000	DF	glacieret	
Hunza basin	6	451481.2	3999090.3	3260	7270	9.77	22.3	8.93	39.47	8.94	39.47	43.1	0.39	1.970	1.930	DC	glacier	Bira
Hunza basin	7	449081.9	4001210.7	5030	5520	0.50	44.4	0.05	1.27	0.05	1.27	10.7	0.00	0.000	0.000	DF	glacieret	
Hunza basin	8	449366.8	4000286.4	4830	5080	0.40	32.0	0.03	0.87	0.03	0.87	7.8	0.00	0.000	0.000	DF	glacieret	
Hunza basin	9	449233.7	4002363.9	4650	5860	1.15	46.5	0.52	4.01	0.52	4.01	19.6	0.01	0.000	0.000	DF	glacier	
Hunza basin	10	449762.6	3997134.2	4740	5740	1.56	32.7	0.58	5.51	0.58	5.51	23.6	0.01	0.050	0.070	DC	glacier	
Hunza basin	11	449512.0	4001047.0	5030	5950	0.86	46.9	0.42	3.70	0.42	3.70	16.5	0.01	0.000	0.000	DF	glacier	
Hunza basin	12	449986.7	3999893.6	4850	5330	0.49	44.4	0.05	1.09	0.05	1.11	10.5	0.00	0.000	0.000	DF	glacieret	
Hunza basin	13	450531.5	4000644.6	5680	6430	0.67	48.2	0.24	2.37	0.24	2.37	14.0	0.00	0.000	0.000	DF	glacier	
Hunza basin	14	447196.1	3993877.5	3380	6180	8.40	18.4	6.61	27.75	6.61	27.75	51.8	0.34	4.190	4.300	DC	glacier	Kunti
Hunza basin	15	452050.4	3994705.9	4250	5470	1.50	39.1	0.58	5.27	0.58	5.27	22.6	0.01	0.020	0.030	DF	glacier	
Hunza basin	16	450755.5	4004624.9	2730	6110	6.65	26.9	7.22	21.38	7.22	21.38	36.1	0.26	1.720	1.630	DC	glacier	Masot
Hunza basin	17	453559.1	4004711.5	3060	5640	5.32	25.9	4.58	12.23	4.58	12.23	37.5	0.17	0.320	0.350	DF	glacier	Ghulmet
Hunza basin	18	452644.8	3992002.7	3200	7600	10.37	23.0	14.74	53.61	14.73	53.61	41.9	0.62	3.870	4.500	DC	glacier	Surjin
Hunza basin	19	454713.6	3989870.7	4400	4710	0.72	23.3	0.08	1.65	0.08	1.65	12.7	0.00	0.000	0.000	DF	glacieret	
Hunza basin	20	455530.2	3992926.5	4260	5460	2.69	24.0	1.01	6.34	1.01	6.34	34.7	0.04	0.090	0.170	DF	glacier	
Hunza basin	21	455504.6	4004407.9	2400	5540	9.32	18.6	7.73	26.59	7.74	26.59	51.3	0.40	1.980	1.690	DC	glacier	Pisan
Hunza basin	22	455670.1	3991025.7	4260	4770	0.83	31.6	0.22	2.22	0.22	2.22	14.7	0.00	0.000	0.000	DF	glacier	
Hunza basin	23	458487.1	4004067.1	3900	4630	1.62	24.3	0.71	3.94	0.71	3.94	25.0	0.02	0.000	0.070	DF	glacier	
Hunza basin	24	458325.1	4004786.3	3720	4570	1.85	24.7	0.79	4.53	0.79	4.53	27.4	0.02	0.050	0.310	DF	glacier	
Hunza basin	25	467124.6	4000864.6	2470	6610	16.65	14.0	42.61	92.55	42.62	92.55	67.8	2.89	4.760	8.370	DF	glacier	Minapin
Hunza basin	26	464335.4	4009354.7	3830	4020	0.47	22.0	0.07	1.14	0.07	1.14	8.5	0.00	0.000	0.000	DF	glacieret	
Hunza basin	27	464595.3	4007100.5	4350	4970	1.53	22.1	0.39	5.11	0.39	5.11	24.1	0.01	0.010	0.160	DF	glacier	
Hunza basin	28	464973.4	4007861.6	4930	5260	0.38	41.0	0.07	1.69	0.07	1.69	8.1	0.00	0.000	0.000	DF	glacieret	
Hunza basin	29	465298.2	4006651.7	4500	5030	1.03	27.2	0.37	4.75	0.37	4.75	17.4	0.01	0.010	0.170	DF	glacier	
Hunza basin	30	465763.0	4005848.2	4510	4680	0.36	25.3	0.04	1.06	0.03	0.85	6.7	0.00	0.000	0.000	DF	glacieret	
Hunza basin	31	465831.2	4009918.3	3680	4380	1.16	31.1	0.21	2.60	0.21	2.60	19.2	0.00	0.000	0.000	DF	glacier	

		Coordinates (utm 43N - WGS 84 datum)																
Catchment	ID Code	Longitude	Latitude	2001 Minimum elevation (m a.s.l.)	2001 Maximum elevation (m a.s.l.)	2001 Maximum length (km)	2001 Slope (°)	2001 Area (km²)	2001 Perimeter (km)	2010 Area (km²)	2010 Perimeter (km)	2001 Glacier thickness (m)	2001 Ice volume (km³)	2001 Debris cover (km²)	2010 Debris cover (km²)	Debris-Covered or Debris-Free glacier	Glacier Type	Glacier name
Hunza basin	32	465776.8	4008280.7	4830	5430	1.13	28.0	0.64	4.17	0.64	4.17	18.8	0.01	0.010	0.010	DF	glacier	
Hunza basin	33	466264.3	4006378.7	4580	5090	1.33	21.0	0.33	3.56	0.32	3.49	21.5	0.01	0.000	0.000	DF	glacier	
Hunza basin	34	466562.5	4005378.1	4310	4780	0.83	29.5	0.29	2.59	0.29	2.59	14.6	0.00	0.000	0.110	DF	glacier	
Hunza basin	35	466403.0	4008865.8	4590	4860	0.36	36.9	0.04	1.05	0.04	1.05	7.4	0.00	0.000	0.000	DF	glacieret	
Hunza basin	36	466257.8	4007220.8	4770	5400	0.84	36.9	0.13	2.48	0.13	2.48	15.3	0.00	0.000	0.000	DF	glacier	
Hunza basin	37	467025.5	4008140.3	4140	4690	0.71	37.8	0.12	2.70	0.12	2.70	13.4	0.00	0.000	0.070	DF	glacier	
Hunza basin	38	466803.7	4003530.1	4280	4710	0.69	31.9	0.10	1.98	0.08	1.43	12.6	0.00	0.000	0.060	DF	glacier	
Hunza basin	39	466794.8	4006289.9	4790	5200	0.63	33.1	0.14	1.72	0.13	1.65	11.7	0.00	0.000	0.000	DF	glacier	
Hunza basin	40	466799.8	4008891.8	4320	4670	0.45	37.9	0.06	1.17	0.06	1.17	9.1	0.00	0.000	0.030	DF	glacieret	
Hunza basin	41	467321.4	4003996.8	4610	4760	0.46	18.1	0.07	1.33	0.07	1.33	8.3	0.00	0.000	0.000	DF	glacieret	
Hunza basin	42	467197.2	4006542.6	4980	5240	0.41	32.4	0.07	1.11	0.07	1.11	8.0	0.00	0.000	0.000	DF	glacieret	
Hunza basin	43	467446.1	4009762.1	4080	4320	0.34	35.2	0.03	0.87	0.03	0.87	6.9	0.00	0.000	0.000	DF	glacieret	
Hunza basin	44	467490.7	4004366.5	4270	5180	1.86	26.1	1.16	9.25	1.16	9.25	27.3	0.03	0.000	0.000	DF	glacier	
Hunza basin	45	468524.8	4007219.2	3870	4330	0.95	25.8	0.20	2.39	0.20	2.39	16.2	0.00	0.000	0.090	DF	glacier	
Hunza basin	46	468701.9	4006316.2	4430	4720	0.42	34.6	0.05	1.15	0.05	1.15	8.3	0.00	0.000	0.000	DF	glacieret	
Hunza basin	47	468157.4	4007455.7	3870	4390	0.94	29.0	0.22	2.20	0.22	2.20	16.2	0.00	0.000	0.080	DF	glacier	
Hunza basin	48	468710.1	4004500.2	4770	5150	0.37	45.8	0.07	1.20	0.07	1.20	8.4	0.00	0.000	0.000	DF	glacieret	
Hunza basin	49	468730.6	4004068.0	4940	5100	0.28	29.7	0.04	0.91	0.04	0.91	5.5	0.00	0.000	0.000	DF	glacieret	
Hunza basin	50	469029.6	4004381.4	4780	5100	0.37	40.9	0.06	1.07	0.06	1.07	7.9	0.00	0.000	0.000	DF	glacieret	
Hunza basin	51	468788.8	4003729.3	4700	5090	0.51	37.4	0.10	1.72	0.10	1.72	10.1	0.00	0.000	0.000	DF	glacier	
Hunza basin	52	471223.5	4005924.0	4410	4980	2.03	15.7	0.70	4.54	0.70	4.54	31.3	0.02	0.020	0.030	DF	glacier	
Hunza basin	53	472264.8	4006381.3	4390	5450	2.95	19.8	1.88	10.60	1.88	10.60	39.1	0.07	0.060	0.150	DF	glacier	
Hunza basin	54	472869.8	4007464.1	4390	4850	1.02	24.3	0.22	2.43	0.22	2.43	17.2	0.00	0.000	0.000	DF	glacier	
Hunza basin	55	473114.4	4007235.3	4710	4910	0.33	31.2	0.03	0.80	0.03	0.80	6.5	0.00	0.000	0.000	DF	glacieret	
Hunza basin	56	472833.1	4003049.6	3190	5650	7.94	17.2	15.10	43.56	14.73	42.51	55.3	0.84	0.400	1.040	DF	glacier	Silkiang
Hunza basin	57	473059.5	4002440.5	4770	5660	1.10	39.0	0.14	2.43	0.14	2.43	18.8	0.00	0.000	0.000	DF	glacier	
Hunza basin	58	473253.2	4002851.4	5390	5450	0.38	9.0	0.06	1.15	0.06	1.15	6.9	0.00	0.000	0.000	DF	glacieret	
Hunza basin	59	473188.2	4007102.9	4720	4980	0.44	30.6	0.08	1.28	0.08	1.29	8.4	0.00	0.000	0.000	DF	glacieret	
Hunza basin	60	473591.3	4006307.9	4730	5390	1.40	25.2	0.43	3.71	0.43	3.71	22.3	0.01	0.000	0.000	DF	glacier	
Hunza basin	61	473975.4	4004859.5	5020	5450	0.76	29.5	0.15	2.70	0.15	2.70	13.6	0.00	0.000	0.000	DF	glacier	
Hunza basin	62	473740.4	4007118.8	4340	5070	1.18	31.7	0.28	3.42	0.28	3.42	19.5	0.01	0.020	0.050	DF	glacier	
Hunza basin	63	474372.9	4001760.2	4000	5430	2.48	30.0	0.48	6.03	0.48	6.03	30.6	0.01	0.120	0.140	DC	glacier	
Hunza basin	64	474548.5	4002719.3	4670	4910	0.52	24.8	0.07	1.19	0.07	1.19	9.5	0.00	0.020	0.020	DC	glacieret	

Catchment	ID Code	Longitude	Latitude	2001 Minimum elevation (m a.s.l.)	2001 Maximum elevation (m a.s.l.)	2001 Maximum length (km)	2001 Slope (°)	2001 Area (km²)	2001 Perimeter (km)	2010 Area (km²)	2010 Perimeter (km)	2001 Glacier thickness (m)	2001 Ice volume (km³)	2001 Debris cover (km²)	2010 Debris cover (km²)	Debris-Covered or Debris-Free glacier	Glacier Type	Glacier name
		Coordinates (utm 43N - WGS 84 datum)																
Hunza basin	65	474697.1	4004878.6	3860	5040	2.20	28.2	1.09	11.16	1.09	11.16	29.7	0.03	0.080	0.420	DF	glacier	
Hunza basin	66	476669.0	3996230.9	4970	5260	0.44	33.4	0.10	1.23	0.10	1.23	8.6	0.00	0.000	0.000	DF	glacier	
Hunza basin	67	476929.4	3995674.2	4860	5170	0.29	46.9	0.09	1.24	0.09	1.24	6.9	0.00	0.000	0.000	DF	glacieret	
Hunza basin	68	477422.3	3997083.8	3930	4690	1.11	34.4	0.27	2.53	0.27	2.53	18.7	0.01	0.000	0.070	DF	glacier	
Hunza basin	69	479515.5	3992543.1	2250	6850	24.11	10.8	55.43	168.10	55.43	168.10	87.3	4.84	9.680	11.450	DF	glacier	Bualtar/Hoper
Hunza basin	70	480529.5	3999861.8	4390	5550	1.48	38.1	0.40	4.44	0.40	4.44	22.5	0.01	0.080	0.070	DC	glacier	
Hunza basin	71	480285.7	4001345.2	4460	5260	1.12	35.5	0.39	2.82	0.39	2.82	18.9	0.01	0.040	0.000	DF	glacier	
Hunza basin	72	480600.3	4000478.3	5350	5480	0.25	27.5	0.02	0.68	0.02	0.68	4.9	0.00	0.000	0.000	DF	glacieret	
Hunza basin	73	480850.3	3999397.4	5230	5520	0.72	21.9	0.16	1.72	0.16	1.72	12.6	0.00	0.000	0.000	DF	glacier	
Hunza basin	74	481418.7	3998420.2	4970	5390	0.98	23.2	0.18	2.20	0.18	2.20	16.6	0.00	0.000	0.000	DF	glacier	
Hunza basin	75	481153.2	4001180.4	4180	5250	2.12	26.8	0.85	7.20	0.85	7.20	29.5	0.03	0.050	0.180	DF	glacier	
Hunza basin	76	481190.3	4000403.0	4630	5430	1.07	36.8	0.15	2.41	0.15	2.41	18.3	0.00	0.000	0.000	DF	glacier	
Hunza basin	77	482153.7	3998661.4	4860	5210	0.52	33.9	0.06	1.19	0.06	1.19	10.0	0.00	0.000	0.000	DF	glacieret	
Hunza basin	78	482257.5	3996701.7	3660	5370	3.85	23.9	2.01	16.81	2.01	16.81	40.3	0.08	0.600	0.790	DC	glacier	
Hunza basin	79	482416.0	3999683.8	3870	5160	4.44	16.2	1.75	10.22	1.75	10.22	52.5	0.09	0.470	0.680	DC	glacier	
Hunza basin	80	483247.0	3995678.1	4460	5500	1.62	32.7	0.37	5.68	0.37	5.68	24.2	0.01	0.000	0.000	DF	glacier	
Hunza basin	81	483041.8	3991068.6	2800	6830	25.17	9.1	82.45	165.11	82.15	165.17	103.5	8.54	15.950	18.820	DC	glacier	Barpu
Hunza basin	82	489054.9	3986972.1	5590	7010	3.34	23.0	4.44	9.96	4.44	9.96	39.0	0.17	0.000	0.000	DF	glacier	
Hunza basin	83	490079.9	3985619.3	5240	7370	4.65	24.6	5.10	12.20	5.10	12.20	39.3	0.20	0.000	0.000	DF	glacier	
Hunza basin	84	490275.4	4003314.0	4650	4830	0.50	19.8	0.09	1.27	0.09	1.27	9.0	0.00	0.000	0.070	DF	glacieret	
Hunza basin	85	492928.9	3998395.1	4010	5580	3.16	26.4	0.96	7.73	0.94	7.71	35.4	0.03	0.660	0.390	DC	glacier	
Hunza basin	86	492926.4	3994195.6	3790	5230	3.67	21.4	2.50	8.66	2.50	8.66	42.0	0.10	0.430	1.010	DF	glacier	
Hunza basin	87	493845.2	4000574.6	4360	5360	1.80	29.1	0.58	4.29	0.65	4.93	26.2	0.02	0.160	0.190	DC	glacier	
Hunza basin	88	494041.0	3994986.3	4760	6140	1.86	36.6	0.57	4.76	0.57	4.76	25.3	0.01	0.010	0.000	DF	glacier	
Hunza basin	89	497440.7	3997139.9	3530	6260	8.16	18.5	4.83	25.81	4.85	26.07	51.6	0.25	1.650	1.950	DC	glacier	Yangutz Har
Hunza basin	90	495303.8	4000905.5	3480	4720	2.69	24.7	0.95	5.84	0.95	5.84	34.4	0.03	0.480	0.620	DC	glacier	
Hunza basin	91	496878.9	4015892.0	5040	5460	1.09	21.1	0.24	2.70	0.24	2.70	18.2	0.00	0.000	0.000	DF	glacier	
Hunza basin	92	496984.9	4016608.5	5000	5700	1.10	32.5	0.19	2.47	0.20	2.62	18.5	0.00	6.530	9.310	DC	glacier	
Hunza basin	93	502439.5	3992317.4	3850	6120	10.76	11.9	15.92	52.48	15.78	51.27	79.3	1.26	8.110	10.940	DC	glacier	Garumbar
Hunza basin	94	497119.7	4011872.2	3410	7340	23.00	9.7	45.69	148.61	45.52	148.32	97.2	4.44	0.010	0.030	DF	glacier	Trivor
Hunza basin	95	503868.8	4009337.3	4770	6110	2.31	30.1	1.24	6.41	1.24	6.41	29.7	0.04	0.060	0.070	DF	glacier	
Hunza basin	96	505371.9	4007814.2	4830	5770	2.35	21.8	2.05	6.61	2.05	6.61	33.0	0.07	0.480	0.370	DC	glacier	
Hunza basin	97	505025.6	3998044.1	3860	5430	2.51	32.0	1.23	6.07	1.23	6.07	29.7	0.04	0.000	0.000	DF	glacier	

Catchment	ID Code	Coordinates (utm 43N - WGS 84 datum) Longitude	Latitude	2001 Minimum elevation (m a.s.l.)	2001 Maximum elevation (m a.s.l.)	2001 Maximum length (km)	2001 Slope (°)	2001 Area (km^2)	2001 Perimeter (km)	2010 Area (km^2)	2010 Perimeter (km)	2001 Glacier thickness (m)	2001 Ice volume (km^3)	2001 Debris cover (km^2)	2010 Debris cover (km^2)	Debris-Covered or Debris-Free glacier	Glacier Type	Glacier name
Hunza basin	98	505589.7	4010548.7	5650	6490	1.30	32.9	0.55	4.27	0.55	4.27	20.9	0.01	0.000	0.000	DF	glacier	
Hunza basin	99	506727.6	4014498.5	6350	7500	2.36	26.0	3.63	9.51	3.63	9.51	31.6	0.11	0.000	0.000	DF	glacier	
Hunza basin	100	506739.7	4006987.1	4600	5670	3.44	17.3	2.23	8.36	2.23	8.36	44.7	0.10	0.300	0.460	DF	glacier	
Hunza basin	101	507136.0	4011839.9	5330	6370	0.76	53.8	0.39	2.49	0.39	2.49	16.2	0.01	0.000	0.000	DF	glacier	
Hunza basin	102	508893.7	4006023.0	4580	6120	2.94	27.6	1.35	10.99	1.35	10.99	33.7	0.05	0.270	0.220	DC	glacier	
Hunza basin	103	513360.2	4014478.5	4760	5420	2.58	14.3	1.18	6.27	1.18	6.27	38.3	0.05	0.030	0.130	DF	glacier	
Hunza basin	104	513801.3	4003484.3	4100	6730	4.89	28.3	3.06	15.63	3.07	15.63	34.6	0.11	1.460	1.210	DC	glacier	
Hunza basin	105	516353.8	4003114.4	4770	6340	2.16	36.0	0.54	4.97	0.54	4.97	26.8	0.01	0.020	0.010	DF	glacier	
Hunza basin	106	516615.6	4002813.4	5380	6260	0.94	43.1	0.26	2.55	0.26	2.55	17.2	0.00	0.000	0.000	DF	glacier	
Hunza basin	107	517570.0	4002272.9	4730	6260	1.83	39.9	0.59	4.08	0.59	4.08	24.4	0.01	0.000	0.010	DF	glacier	
Hunza basin	108	517035.3	3992744.5	4050	5100	3.26	17.9	1.61	8.25	1.61	8.25	42.8	0.07	0.000	0.360	DF	glacier	
Hunza basin	109	517317.9	4005894.2	6320	7590	2.48	27.1	2.00	6.01	2.00	6.01	31.9	0.06	0.000	0.000	DF	glacier	
Hunza basin	110	520264.8	4002145.6	4540	4790	0.75	18.4	0.15	1.75	0.15	1.77	13.0	0.00	0.000	0.070	DF	glacier	
Hunza basin	111	537991.2	3989808.8	3060	7480	51.16	4.9	369.06	1063.85	369.09	1063.84	190.18	70.19	96.100	134.440	DC	glacier	Hispar
Hunza basin	112	524101.5	3999935.9	4200	6140	5.68	18.9	4.93	24.00	4.99	24.70	50.6	0.25	0.910	1.150	DC	glacier	
Hunza basin	113	524279.7	3998706.3	4430	5760	3.26	22.2	1.48	9.30	1.48	9.30	39.3	0.06	0.310	0.390	DC	glacier	
Hunza basin	114	525195.7	3997390.3	4860	5690	1.50	29.0	0.52	3.46	0.52	3.46	23.3	0.01	0.100	0.080	DC	glacier	
Hunza basin	115	526683.9	3998003.5	4700	5150	0.67	33.9	0.13	1.75	0.13	1.75	12.4	0.00	0.000	0.000	DF	glacier	
Hunza basin	116	526854.7	3998573.8	4590	4960	0.61	31.2	0.10	1.50	0.10	1.50	11.3	0.00	0.000	0.010	DF	glacieret	
Hunza basin	117	530920.8	4001599.0	4860	5880	2.27	24.2	0.85	5.52	0.85	5.52	31.5	0.03	0.030	0.040	DF	glacier	
Hunza basin	118	531181.5	3994319.3	4560	5780	2.90	22.8	1.21	8.52	1.21	8.52	36.8	0.04	0.250	0.590	DF	glacier	
Hunza basin	119	532478.2	3994922.8	4640	5640	2.53	21.6	1.47	6.16	1.47	6.16	34.7	0.05	0.010	0.740	DF	glacier	
Hunza basin	120	532913.8	3993455.7	4660	5050	1.10	19.5	0.23	2.60	0.23	2.60	18.4	0.00	0.030	0.170	DF	glacier	
Hunza basin	121	533861.4	3995824.3	4370	6030	5.75	16.1	3.98	17.50	4.04	17.90	59.0	0.23	0.200	0.910	DF	glacier	
Hunza basin	122	538078.9	3994567.4	4620	5270	1.91	18.8	0.60	5.06	0.61	5.06	29.1	0.02	0.010	0.160	DF	glacier	
Hunza basin	123	539164.4	3992702.5	4570	5610	3.91	14.9	2.14	11.33	2.14	11.33	50.8	0.11	0.000	0.080	DF	glacier	
Shigar Basin																		
Shigar basin	124	519839.4	3969777.1	2760	6810	45.59	5.1	264.97	858.89	263.40	843.59	185.0	49.02	47.590	77.680	DF	glacier	Chogo Lungma
Shigar basin	125	498069.8	3979638.3	5260	6780	2.90	27.7	1.66	7.43	1.66	7.43	33.6	0.06	0.000	0.000	DF	glacier	
Shigar basin	126	503625.2	3985809.6	4390	5460	2.20	25.9	1.38	11.51	1.38	11.51	30.4	0.04	0.050	0.270	DF	glacier	
Shigar basin	127	502953.3	3985534.0	4900	5200	0.65	24.8	0.07	1.51	0.07	1.51	11.6	0.00	0.000	0.010	DF	glacieret	

Catchment	ID Code	Coordinates (utm 43N - WGS 84 datum)		2001 Minimum elevation (m a.s.l.)	2001 Maximum elevation (m a.s.l.)	2001 Maximum length (km)	2001 Slope (°)	2001 Area (km²)	2001 Perimeter (km)	2010 Area (km²)	2010 Perimeter (km)	2001 Glacier thickness (m)	2001 Ice volume (km³)	2001 Debris cover (km²)	2010 Debris cover (km²)	Debris-Covered or Debris-Free glacier	Glacier Type	Glacier name
		Longitude	Latitude															
Shigar basin	128	503437.6	3984754.9	4720	5020	0.63	25.5	0.10	1.70	0.10	1.70	11.3	0.00	0.010	0.060	DF	glacier	
Shigar basin	129	504273.7	3986634.1	4660	5340	1.00	34.2	0.39	3.09	0.39	3.09	17.3	0.01	0.000	0.000	DF	glacier	
Shigar basin	130	510004.4	3984598.3	4100	6090	6.94	16.0	9.45	50.71	9.44	50.71	59.4	0.56	0.670	1.510	DF	glacier	Sgari-Byen
Shigar basin	131	511439.4	3960612.7	3450	5810	10.50	12.7	25.96	90.06	25.96	90.06	74.7	1.94	5.410	8.200	DF	glacier	Remeduk
Shigar basin	132	514598.6	3968790.1	3920	5560	3.52	25.0	1.40	8.89	1.38	8.62	38.8	0.05	0.020	0.100	DF	glacier	
Shigar basin	133	513147.3	3972991.7	3740	5320	3.60	23.7	2.86	12.64	2.85	12.64	39.2	0.11	0.090	0.710	DF	glacier	
Shigar basin	134	513197.2	3967765.5	4560	5560	1.36	36.3	0.62	7.66	0.62	7.66	21.5	0.01	0.000	0.020	DF	glacier	
Shigar basin	135	513698.4	3980307.7	4360	5060	1.22	29.8	0.43	3.03	0.43	3.03	20.0	0.01	0.010	0.090	DF	glacier	
Shigar basin	136	513296.2	3971627.1	4140	5340	2.81	23.1	1.36	10.53	1.36	10.53	36.0	0.05	0.000	0.440	DF	glacier	
Shigar basin	137	514019.0	3967591.0	4140	4910	1.31	30.4	0.36	3.88	0.36	3.88	21.1	0.01	0.000	0.000	DF	glacier	
Shigar basin	138	514821.1	3980967.0	4900	5470	1.10	27.4	0.27	2.67	0.27	2.67	18.4	0.00	0.010	0.010	DF	glacier	
Shigar basin	139	516486.8	3982919.5	3890	5620	9.82	10.0	20.58	73.29	20.57	73.29	94.4	1.94	2.120	4.700	DF	glacier	Bolocho
Shigar basin	140	516673.9	3961383.8	4840	5180	0.75	24.4	0.12	1.75	0.12	1.75	13.2	0.00	0.000	0.000	DF	glacier	
Shigar basin	141	517116.2	3962070.8	4690	5250	1.11	26.8	0.18	2.50	0.18	2.50	18.5	0.00	0.000	0.020	DF	glacier	
Shigar basin	142	517452.8	3977469.1	3730	5590	6.93	15.0	7.59	42.15	7.59	42.15	63.2	0.48	0.690	1.280	DF	glacier	
Shigar basin	143	516270.7	3963610.2	4380	5170	2.31	18.9	0.86	7.10	0.86	7.10	33.6	0.03	0.070	0.210	DF	glacier	
Shigar basin	144	517696.5	3963020.3	4430	5220	2.14	20.3	0.57	4.91	0.57	4.91	31.4	0.02	0.050	0.020	DF	glacier	
Shigar basin	145	516785.3	3961750.4	4660	5220	1.29	23.5	0.23	3.05	0.23	3.05	20.9	0.00	0.000	0.000	DF	glacier	
Shigar basin	146	516719.8	3958809.8	3860	5530	6.00	15.6	10.63	32.97	10.62	32.97	61.1	0.65	0.820	1.610	DF	glacier	W. Niamul
Shigar basin	147	518245.5	3965414.6	4000	4740	2.65	15.6	1.51	8.89	1.51	8.89	38.5	0.06	0.180	0.810	DF	glacier	
Shigar basin	148	517956.8	3963429.9	4610	5020	1.38	16.5	0.36	3.22	0.36	3.22	22.5	0.01	0.010	0.010	DF	glacier	
Shigar basin	149	519432.1	3965898.6	4340	4660	0.78	22.3	0.14	1.82	0.14	1.82	13.6	0.00	0.000	0.000	DF	glacier	
Shigar basin	150	519771.2	3965278.2	4910	4990	0.33	13.6	0.05	0.90	0.05	0.90	6.0	0.00	0.000	0.000	DF	glacieret	
Shigar basin	151	520050.4	3959932.5	4550	4780	0.95	13.6	0.17	2.16	0.17	2.16	16.2	0.00	0.000	0.000	DF	glacier	
Shigar basin	152	520261.5	3965521.0	4420	4660	0.38	32.3	0.05	0.97	0.05	0.97	7.4	0.00	0.000	0.000	DF	glacieret	
Shigar basin	153	519551.5	3958588.4	3800	5330	5.88	14.6	6.15	28.60	6.16	28.60	62.0	0.38	1.240	2.540	DF	glacier	
Shigar basin	154	520140.8	3964937.5	4210	4890	1.37	26.4	0.25	3.14	0.25	3.14	21.9	0.01	0.000	0.000	DF	glacier	
Shigar basin	155	520531.6	3975601.0	4420	5860	2.53	29.6	0.71	6.96	0.71	6.96	31.0	0.02	0.050	0.060	DF	glacier	
Shigar basin	156	521680.6	3985734.1	3730	5920	10.63	11.6	36.79	194.85	36.65	194.03	81.1	2.98	5.530	10.810	DF	glacier	Kero Lnunga
Shigar basin	157	521363.5	3988427.7	4240	5450	2.81	23.3	1.68	11.16	1.68	11.16	35.9	0.06	0.100	0.180	DF	glacier	
Shigar basin	158	525104.7	3973625.8	3320	5710	6.96	19.0	10.79	53.14	10.79	53.14	50.4	0.54	1.420	2.800	DF	glacier	Niaro
Shigar basin	159	522468.1	3988214.8	4400	5590	2.55	25.0	1.23	9.73	1.23	9.73	33.3	0.04	0.040	0.130	DF	glacier	
Shigar basin	160	523618.0	3980681.1	3770	5250	3.98	20.4	1.34	11.95	1.34	11.95	44.4	0.06	0.230	0.530	DF	glacier	

		Coordinates (utm 43N - WGS 84 datum)																
Catchment	ID Code	Longitude	Latitude	2001 Minimum elevation (m a.s.l.)	2001 Maximum elevation (m a.s.l.)	2001 Maximum length (km)	2001 Slope (°)	2001 Area (km²)	2001 Perimeter (km)	2010 Area (km²)	2010 Perimeter (km)	2001 Glacier thickness (m)	2001 Ice volume (km³)	2001 Debris cover (km²)	2010 Debris cover (km²)	Debris-Covered or Debris-Free glacier	Glacier Type	Glacier name
Shigar basin	161	522947.6	3972647.5	4650	5110	0.82	29.3	0.11	1.93	0.10	1.86	14.5	0.00	0.030	0.030	DF	glacier	
Shigar basin	162	522897.8	3978910.7	4330	5170	1.94	23.4	0.51	4.21	0.51	4.21	28.6	0.01	0.000	0.030	DF	glacier	
Shigar basin	163	524018.2	3957778.1	4470	4720	0.58	23.3	0.19	1.73	0.19	1.73	10.4	0.00	0.000	0.020	DF	glacier	
Shigar basin	164	523474.0	3977952.4	3760	5470	5.32	17.8	2.99	15.75	3.00	15.75	53.5	0.16	0.250	1.080	DF	glacier	
Shigar basin	165	524236.6	3971942.7	4880	5340	0.64	35.7	0.10	1.56	0.10	1.56	12.1	0.00	0.000	0.000	DF	glacier	
Shigar basin	166	525212.2	3963113.1	4860	5120	0.82	17.6	0.20	2.27	0.20	2.27	14.1	0.00	0.000	0.000	DF	glacier	
Shigar basin	167	525263.0	3956866.2	4060	4330	5.50	2.8	6.74	22.26	7.05	23.62	90.1	0.61	0.380	0.790	DF	glacier	
Shigar basin	168	524752.9	3962220.9	4300	5510	2.22	28.6	0.79	5.72	0.79	5.72	29.7	0.02	0.120	0.050	DC	glacier	
Shigar basin	169	525839.6	3958999.2	4390	4960	1.83	17.3	0.74	4.85	0.74	4.85	28.4	0.02	0.020	0.130	DF	glacier	
Shigar basin	170	525647.4	3962926.6	3600	5570	4.42	24.0	2.53	15.17	2.53	15.17	40.2	0.10	0.410	0.860	DF	glacier	
Shigar basin	171	526989.4	3984284.3	4440	5240	1.42	29.4	0.64	4.02	0.64	4.02	22.3	0.01	0.060	0.430	DF	glacier	
Shigar basin	172	527355.5	3960457.0	4260	5650	3.21	23.4	3.34	15.78	3.34	15.79	38.1	0.13	0.140	0.200	DF	glacier	
Shigar basin	173	526933.4	3973117.0	4160	5000	2.30	20.1	0.49	5.06	0.49	5.06	33.1	0.02	0.000	0.100	DF	glacier	
Shigar basin	174	527697.0	3963860.2	4800	5110	0.39	38.5	0.07	1.03	0.07	1.03	8.0	0.00	0.000	0.000	DF	glacieret	
Shigar basin	175	528304.1	3959506.0	4390	5430	2.32	24.1	0.71	6.33	0.71	6.33	31.9	0.02	0.000	0.040	DF	glacier	
Shigar basin	176	528549.7	3958515.5	4400	4990	1.09	28.4	0.20	2.70	0.20	2.70	18.3	0.00	0.000	0.000	DF	glacier	
Shigar basin	177	528275.7	3985274.3	4580	5140	1.78	17.5	0.85	5.15	0.85	5.15	27.8	0.02	0.010	0.050	DF	glacier	
Shigar basin	178	528201.9	3957317.1	4310	4590	1.08	14.5	0.32	2.84	0.32	2.84	18.2	0.01	0.000	0.080	DF	glacier	
Shigar basin	179	528690.5	3956707.1	4250	4510	1.25	11.7	0.59	3.43	0.59	3.43	21.0	0.01	0.000	0.000	DF	glacier	
Shigar basin	180	528474.0	3965598.6	3910	5030	2.39	25.1	0.87	6.09	0.87	6.09	32.1	0.03	0.070	0.350	DF	glacier	
Shigar basin	181	528122.3	3962302.6	2740	5650	8.84	18.2	8.86	44.68	8.87	44.68	52.4	0.46	1.740	2.140	DF	glacier	Tppur
Shigar basin	182	530529.1	3960469.2	3610	5560	5.14	20.8	2.81	15.97	2.81	15.97	46.2	0.13	0.480	0.920	DF	glacier	
Shigar basin	183	529672.4	3984173.1	4650	5220	1.21	25.2	0.55	4.77	0.55	4.77	19.8	0.01	0.090	0.320	DF	glacier	
Shigar basin	184	530480.2	3961261.4	4570	4850	0.54	27.4	0.14	1.49	0.14	1.49	9.9	0.00	0.000	0.000	DF	glacier	
Shigar basin	185	531797.9	3966217.3	4250	4600	0.61	29.8	0.10	1.52	0.10	1.49	11.2	0.00	0.010	0.010	DF	glacieret	
Shigar basin	186	531978.7	3978801.2	4010	5380	3.09	23.9	2.37	13.30	2.38	13.30	37.1	0.09	0.120	0.230	DF	glacier	
Shigar basin	187	532350.5	3966668.9	3940	4300	0.56	32.7	0.13	1.46	0.13	1.46	10.6	0.00	0.050	0.030	DC	glacier	
Shigar basin	188	533097.3	3965734.3	3360	5010	3.70	24.0	1.76	12.79	1.76	12.79	40.2	0.07	0.310	0.400	DF	glacier	
Shigar basin	189	532631.2	3947566.4	3760	5170	2.39	30.5	1.56	7.79	1.56	7.79	29.9	0.05	1.110	0.850	DC	glacier	
Shigar basin	190	533871.5	3975268.2	4180	4910	1.42	27.2	0.47	3.68	0.47	3.68	22.4	0.01	0.010	0.030	DF	glacier	
Shigar basin	191	534327.1	3945710.1	4380	5010	1.07	30.5	0.24	2.41	0.24	2.41	18.0	0.00	0.090	0.110	DC	glacier	
Shigar basin	192	534060.0	3944682.9	4570	4950	0.71	28.2	0.19	2.59	0.19	2.59	12.7	0.00	0.010	0.040	DF	glacier	
Shigar basin	193	533734.4	3946367.7	4080	5010	1.67	29.1	0.65	3.90	0.65	3.90	25.0	0.02	0.050	0.310	DF	glacier	

		Coordinates (utm 43N - WGS 84 datum)																
Catchment	ID Code	Longitude	Latitude	2001 Minimum elevation (m a.s.l.)	2001 Maximum elevation (m a.s.l.)	2001 Maximum length (km)	2001 Slope (°)	2001 Area (km^2)	2001 Perimeter (km)	2010 Area (km^2)	2010 Perimeter (km)	2001 Glacier thickness (m)	2001 Ice volume (km^3)	2001 Debris cover (km^2)	2010 Debris cover (km^2)	Debris-Covered or Debris-Free glacier	Glacier Type	Glacier name
Shigar basin	194	534423.3	3944380.0	4540	4840	1.05	15.9	0.35	2.64	0.35	2.64	17.7	0.01	0.000	0.010	DF	glacier	
Shigar basin	195	534568.0	3966013.6	3870	4730	2.14	21.9	0.67	4.87	0.67	4.87	31.0	0.02	0.000	0.080	DF	glacier	
Shigar basin	196	533523.2	3977044.6	3560	5330	6.31	15.7	3.06	19.16	3.04	19.03	60.6	0.19	1.140	1.460	DC	glacier	
Shigar basin	197	534927.4	3944096.5	4490	4850	0.70	27.2	0.12	1.62	0.12	1.62	12.5	0.00	0.040	0.030	DC	glacier	
Shigar basin	198	535196.7	3943324.2	4340	4930	1.27	24.9	0.32	3.12	0.32	3.12	20.6	0.01	0.140	0.130	DC	glacier	
Shigar basin	199	536092.4	3943238.2	4190	4860	1.15	30.2	0.32	2.88	0.32	2.88	19.1	0.01	0.030	0.060	DF	glacier	
Shigar basin	200	536972.2	3943212.8	3850	5070	1.93	32.3	0.59	4.52	0.59	4.52	26.7	0.02	0.260	0.170	DC	glacier	
Shigar basin	201	536506.0	3978985.5	4460	4840	0.76	26.6	0.16	1.81	0.16	1.81	13.4	0.00	0.000	0.000	DF	glacier	
Shigar basin	202	530671.5	3981786.3	3610	5980	12.14	11.0	32.86	133.51	32.86	133.51	85.4	2.81	5.470	10.400	DF	glacier	Hucho Alchori
Shigar basin	203	536274.5	3980471.3	3920	5240	3.59	20.2	1.94	9.30	1.94	9.30	42.9	0.08	0.170	0.370	DF	glacier	
Shigar basin	204	538219.7	3982753.2	4120	5240	2.47	24.4	1.40	6.93	1.40	6.93	33.0	0.05	0.010	0.050	DF	glacier	
Shigar basin	205	537715.4	3943415.9	3910	4530	0.79	38.1	0.18	2.26	0.18	2.26	14.6	0.00	0.120	0.070	DC	glacier	
Shigar basin	206	537786.2	3981910.0	4240	5290	2.09	26.7	0.93	5.33	0.93	5.33	29.3	0.03	0.010	0.050	DF	glacier	
Shigar basin	207	538743.0	3984025.8	4410	5440	2.74	20.6	1.42	7.77	1.42	7.77	36.9	0.05	0.010	0.050	DF	glacier	
Shigar basin	208	538897.4	3942267.7	4050	5290	1.84	34.0	1.29	7.60	1.26	7.49	25.7	0.03	0.120	0.250	DF	glacier	
Shigar basin	209	540712.2	3940192.9	4020	5480	3.40	23.2	2.34	13.80	2.35	13.80	39.0	0.09	0.270	0.300	DF	glacier	
Shigar basin	210	539356.1	3941401.6	3810	5120	2.06	32.5	1.59	5.65	1.59	5.65	27.5	0.04	0.350	0.290	DF	glacier	
Shigar basin	211	540623.6	3958728.9	4610	4930	0.57	29.3	0.11	1.70	0.11	1.70	10.5	0.00	0.000	0.000	DF	glacier	
Shigar basin	212	541435.9	3955816.4	4580	4690	0.40	15.4	0.08	1.10	0.08	1.10	7.2	0.00	0.000	0.000	DF	glacieret	
Shigar basin	213	541497.5	3959315.2	3860	5160	3.64	19.7	2.07	10.63	2.07	10.63	43.7	0.09	0.190	0.580	DF	glacier	
Shigar basin	214	541853.8	3956101.7	4590	4990	1.28	17.4	0.45	3.20	0.45	3.20	21.0	0.01	0.000	0.080	DF	glacier	
Shigar basin	215	543604.3	3965379.2	3880	6070	5.96	20.2	7.63	28.24	7.63	28.24	47.5	0.36	0.110	0.810	DF	glacier	
Shigar basin	216	542584.0	3985429.8	4130	5550	3.74	20.8	4.52	14.81	4.52	14.81	43.0	0.19	0.020	0.120	DF	glacier	
Shigar basin	217	543009.5	3961505.0	4850	5690	1.57	28.1	0.45	5.65	0.45	5.65	24.1	0.01	0.000	0.120	DF	glacier	
Shigar basin	218	542369.4	3963474.8	4110	6260	2.90	36.6	0.81	7.05	0.81	7.05	27.5	0.02	0.190	0.110	DC	glacier	
Shigar basin	219	543000.4	3969522.9	4690	5030	1.11	17.0	0.61	3.63	0.61	3.63	18.6	0.01	0.000	0.060	DF	glacier	
Shigar basin	220	542642.2	3962725.5	4760	6160	1.98	35.3	0.63	5.08	0.63	5.08	26.3	0.02	0.000	0.000	DF	glacier	
Shigar basin	221	543828.4	3969774.7	4270	5290	3.34	17.0	2.21	9.43	2.21	9.43	44.2	0.10	0.010	0.260	DF	glacier	
Shigar basin	222	542269.4	3964854.9	3840	6220	4.19	29.6	1.94	10.87	1.94	10.87	33.1	0.06	0.120	0.170	DF	glacier	
Shigar basin	223	543478.4	3956653.9	4190	5450	1.85	34.3	0.86	6.16	0.86	6.16	25.7	0.02	0.040	0.050	DF	glacier	
Shigar basin	224	543598.0	3979243.9	4670	5750	1.97	28.7	0.83	9.54	0.83	9.54	27.8	0.02	0.020	0.020	DF	glacier	
Shigar basin	225	543180.5	3960564.6	4300	5690	3.44	22.0	1.94	14.98	1.94	14.98	40.4	0.08	0.040	0.070	DF	glacier	
Shigar basin	226	544209.0	3958005.4	3870	5700	4.56	21.9	4.40	19.36	4.39	19.09	44.0	0.19	0.300	0.400	DF	glacier	

		Coordinates (utm 43N - WGS 84 datum)																
Catchment	ID Code	Longitude	Latitude	2001 Minimum elevation (m a.s.l.)	2001 Maximum elevation (m a.s.l.)	2001 Maximum length (km)	2001 Slope (°)	2001 Area (km^2)	2001 Perimeter (km)	2010 Area (km^2)	2010 Perimeter (km)	2001 Glacier thickness (m)	2001 Ice volume (km^3)	2001 Debris cover (km^2)	2010 Debris cover (km^2)	Debris-Covered or Debris-Free glacier	Glacier Type	Glacier name
Shigar basin	227	544395.9	3973340.4	4170	5310	4.01	15.9	2.73	12.65	2.73	12.65	50.3	0.14	0.210	0.390	DF	glacier	
Shigar basin	228	543988.7	3970888.1	4510	5330	1.87	23.7	0.74	4.72	0.74	4.72	27.8	0.02	0.000	0.050	DF	glacier	
Shigar basin	229	545491.2	3980045.1	4960	5420	0.63	36.1	0.16	2.27	0.16	2.27	12.0	0.00	0.000	0.000	DF	glacier	
Shigar basin	230	547767.1	3980613.4	4380	5330	1.27	36.8	0.29	3.35	0.29	3.35	20.6	0.01	0.000	0.010	DF	glacier	
Shigar basin	231	547000.3	3959686.5	4160	5580	4.99	15.9	5.68	28.84	5.68	28.84	55.7	0.32	0.580	1.110	DF	glacier	
Shigar basin	232	547739.4	3961420.9	4300	5130	2.08	21.8	1.59	8.52	1.57	8.31	30.4	0.05	0.000	0.080	DF	glacier	
Shigar basin	233	549568.1	3957678.0	4650	5020	1.03	19.8	0.48	3.05	0.48	3.05	17.3	0.01	0.010	0.010	DF	glacier	
Shigar basin	234	550315.7	3960082.3	4520	4770	0.95	14.7	0.19	2.50	0.19	2.50	16.2	0.00	0.000	0.000	DF	glacier	
Shigar basin	235	540698.8	3977392.4	3260	5980	16.10	9.6	47.69	153.26	47.69	153.26	98.3	4.69	19.080	20.740	DC	glacier	Solu
Shigar basin	236	550788.8	3960052.1	4530	4950	1.57	15.0	0.42	3.80	0.42	3.80	25.3	0.01	0.000	0.000	DF	glacier	
Shigar basin	237	553703.9	3968935.5	4350	4860	0.59	40.8	0.16	2.22	0.16	2.22	11.8	0.00	0.010	0.010	DF	glacier	
Shigar basin	238	552365.6	3965151.3	3540	6050	12.09	11.7	61.64	211.94	61.45	211.69	80.5	4.96	15.700	23.540	DC	glacier	Sosbun
Shigar basin	239	554801.1	3945006.2	4840	5230	0.53	36.3	0.08	1.33	0.08	1.33	10.3	0.00	0.010	0.000	DF	glacieret	
Shigar basin	240	555340.8	3968717.2	4430	5570	2.20	27.4	1.16	8.19	1.16	8.19	29.9	0.03	0.070	0.030	DF	glacier	
Shigar basin	241	555764.0	3967839.6	4470	5400	2.00	24.9	0.71	6.62	0.71	6.62	28.9	0.02	0.080	0.080	DF	glacier	
Shigar basin	242	556572.7	3944471.4	4460	5590	2.95	21.0	2.31	10.72	2.32	10.72	38.3	0.09	0.220	0.120	DF	glacier	
Shigar basin	243	556588.0	3966774.6	4110	5650	3.18	25.8	1.38	9.94	1.38	9.94	35.9	0.05	0.290	0.140	DC	glacier	
Shigar basin	244	557959.3	3962638.2	4560	5150	1.87	17.5	0.53	4.48	0.53	4.48	28.9	0.02	0.010	0.000	DF	glacier	
Shigar basin	245	557889.6	3945718.5	4440	5450	2.16	25.1	0.71	5.80	0.71	5.80	30.3	0.02	0.240	0.220	DC	glacier	
Shigar basin	246	561045.9	3961949.0	4070	5690	6.88	13.2	5.30	18.86	5.23	18.43	71.4	0.38	0.140	0.400	DF	glacier	
Shigar basin	247	558886.4	3945616.3	5100	5400	0.55	28.6	0.08	1.63	0.08	1.63	10.1	0.00	0.000	0.000	DF	glacieret	
Shigar basin	248	559964.8	3944926.3	4760	5670	2.73	18.4	1.59	9.54	1.59	9.54	37.9	0.06	0.080	0.120	DF	glacier	
Shigar basin	249	559095.5	3940075.9	4170	5850	3.69	24.5	1.40	11.07	1.40	11.07	39.5	0.06	0.150	0.190	DC	glacier	
Shigar basin	250	558968.8	3946873.1	4650	5370	1.08	33.7	0.15	2.48	0.15	2.48	18.3	0.00	0.050	0.010	DC	glacier	
Shigar basin	251	559488.3	3945855.4	4990	5400	0.95	23.3	0.38	3.01	0.38	3.01	16.2	0.01	0.000	0.000	DF	glacier	
Shigar basin	252	558608.4	3963984.3	4380	5460	4.26	14.2	2.94	14.68	2.94	14.68	54.3	0.16	0.000	0.280	DF	glacier	
Shigar basin	253	559396.3	3946878.8	4690	5380	1.15	31.0	0.23	3.16	0.23	3.16	19.1	0.00	0.020	0.040	DF	glacier	
Shigar basin	254	561356.3	3940296.1	3760	5870	5.97	19.5	4.24	18.74	4.24	18.74	49.1	0.21	0.150	0.200	DF	glacier	
Shigar basin	255	560064.5	3967954.0	4960	5470	0.47	47.3	0.13	1.42	0.13	1.42	10.5	0.00	0.000	0.000	DF	glacier	
Shigar basin	256	560184.4	3947332.3	4750	5450	1.32	27.9	0.41	3.71	0.41	3.71	21.2	0.01	0.010	0.010	DF	glacier	
Shigar basin	257	560244.4	3948723.0	4360	5260	2.23	22.0	0.51	6.43	0.51	6.43	31.8	0.02	0.250	0.180	DC	glacier	
Shigar basin	258	561203.1	3960408.3	4840	5770	1.38	34.0	0.45	6.75	0.45	6.75	21.8	0.01	0.000	0.000	DF	glacier	
Shigar basin	259	560244.8	3942846.7	3880	5850	8.85	12.5	9.57	32.64	9.57	32.64	75.3	0.72	0.940	1.160	DF	glacier	

Catchment	ID Code	Coordinates (utm 43N - WGS 84 datum)		2001 Minimum elevation (m a.s.l.)	2001 Maximum elevation (m a.s.l.)	2001 Maximum length (km)	2001 Slope (°)	2001 Area (km²)	2001 Perimeter (km)	2010 Area (km²)	2010 Perimeter (km)	2001 Glacier thickness (m)	2001 Ice volume (km³)	2001 Debris cover (km²)	2010 Debris cover (km²)	Debris-Covered or Debris-Free glacier	Glacier Type	Glacier name
		Longitude	Latitude															
Shigar basin	260	561049.5	3959516.6	4490	5330	2.57	18.1	1.41	6.37	1.41	6.37	36.5	0.05	0.340	0.350	DC	glacier	
Shigar basin	261	562092.0	3960921.5	5270	5790	0.81	32.7	0.29	2.16	0.29	2.16	14.5	0.00	0.000	0.000	DF	glacier	
Shigar basin	262	562153.5	3945242.6	4720	5100	0.90	22.9	0.18	2.17	0.18	2.17	15.4	0.00	0.000	0.000	DF	glacier	
Shigar basin	263	561935.1	3958964.8	4730	5350	1.26	26.2	0.46	3.39	0.46	3.39	20.5	0.01	0.050	0.050	DF	glacier	
Shigar basin	264	563218.8	3960351.2	5510	5830	0.94	18.8	0.31	2.70	0.31	2.70	16.0	0.00	0.000	0.000	DF	glacier	
Shigar basin	265	562857.1	3944131.7	4610	5280	1.50	24.1	0.52	4.20	0.52	4.20	23.6	0.01	0.000	0.000	DF	glacier	
Shigar basin	266	563910.9	3942174.1	3520	5760	7.30	17.1	8.76	33.48	8.77	33.48	55.8	0.49	0.700	1.780	DF	glacier	
Shigar basin	267	563197.2	3965417.2	4840	5290	0.59	37.3	0.12	1.91	0.12	1.91	11.4	0.00	0.000	0.000	DF	glacier	
Shigar basin	268	563483.0	3943782.4	4470	4970	1.28	21.3	0.41	3.06	0.41	3.06	20.9	0.01	0.020	0.050	DF	glacier	
Shigar basin	269	563795.0	3966227.4	4570	4820	1.21	11.7	0.24	2.62	0.24	2.62	20.4	0.00	0.000	0.030	DF	glacier	
Shigar basin	270	564435.2	3940317.3	4850	5320	1.53	17.1	0.29	3.49	0.29	3.49	24.5	0.01	0.000	0.000	DF	glacier	
Shigar basin	271	564853.9	3939709.4	4780	5190	1.44	15.9	0.22	3.15	0.22	3.15	23.4	0.01	0.000	0.000	DF	glacier	
Shigar basin	272	566357.9	3939218.7	4540	5710	3.61	18.0	2.04	13.78	2.04	13.78	45.3	0.09	0.010	0.020	DF	glacier	
Shigar basin	273	568080.8	3942527.9	3930	5670	4.28	22.1	3.88	14.00	4.42	17.36	43.5	0.17	0.240	0.200	DF	glacier	
Shigar basin	274	573405.6	3962616.6	3040	6700	63.71	3.3	438.11	906.77	439.51	909.08	285.4	125.05	59.490	78.750	DF	glacier	Biafo
Shigar basin	275	567947.8	3956051.2	4490	6220	3.96	23.6	3.68	19.15	3.68	19.15	40.9	0.15	0.060	0.050	DF	glacier	
Shigar basin	276	568964.7	3954117.3	4420	5670	2.94	23.0	1.41	14.08	1.41	14.08	36.9	0.05	0.230	0.210	DC	glacier	
Shigar basin	277	568423.8	3960747.8	4420	5420	2.80	19.7	1.19	7.18	1.19	7.18	37.9	0.05	0.010	0.020	DF	glacier	
Shigar basin	278	567194.4	3941408.1	4450	5630	3.01	21.4	1.18	8.59	1.16	8.32	38.4	0.05	0.000	0.030	DF	glacier	
Shigar basin	279	570533.0	3955755.2	3820	5720	5.80	18.1	4.75	20.00	5.13	22.25	52.6	0.25	0.240	0.600	DF	glacier	
Shigar basin	280	570758.0	3936825.8	4630	5600	2.22	23.6	0.99	6.01	0.99	6.01	31.2	0.03	0.020	0.020	DF	glacier	
Shigar basin	281	571152.5	3938279.3	3640	5610	7.96	13.9	10.69	42.60	10.70	42.60	68.1	0.73	2.450	3.140	DC	glacier	
Shigar basin	282	570656.7	3954884.0	4990	5320	0.38	41.0	0.06	1.15	0.06	1.15	8.1	0.00	0.000	0.000	DF	glacieret	
Shigar basin	283	571338.2	3937523.5	4700	5520	1.84	24.0	0.56	4.63	0.56	4.63	27.4	0.02	0.010	0.010	DF	glacier	
Shigar basin	284	571431.0	3969872.7	4740	5310	1.58	19.8	0.59	4.00	0.59	4.00	24.9	0.01	0.010	0.010	DF	glacier	
Shigar basin	285	572193.2	3937514.4	4720	5430	1.33	28.1	0.31	3.01	0.31	3.01	21.3	0.01	0.020	0.020	DF	glacier	
Shigar basin	286	572506.0	3970145.5	4570	5360	2.08	20.8	1.39	7.86	1.41	8.60	30.6	0.04	0.020	0.110	DF	glacier	
Shigar basin	287	573519.3	3938478.8	4470	5520	2.61	21.9	3.21	15.30	3.22	15.30	35.2	0.11	0.030	0.170	DF	glacier	
Shigar basin	288	573889.5	3955394.2	3850	5500	4.47	20.3	2.03	13.07	2.04	13.07	47.3	0.10	0.430	0.490	DF	glacier	
Shigar basin	289	573232.5	3974888.5	5110	6540	1.05	53.7	0.30	2.66	0.30	2.66	19.0	0.01	0.000	0.000	DF	glacier	
Shigar basin	290	572861.1	3975768.2	5740	6950	0.95	51.9	0.56	4.52	0.56	4.52	18.1	0.01	0.000	0.000	DF	glacier	
Shigar basin	291	573591.0	3975189.9	5400	5980	0.59	44.5	0.13	1.49	0.13	1.49	12.2	0.00	0.000	0.000	DF	glacier	
Shigar basin	292	574284.9	3940047.1	4700	5270	1.94	16.4	0.73	5.23	0.73	5.23	30.0	0.02	0.010	0.010	DF	glacier	

Catchment	ID Code	Coordinates (utm 43N - WGS 84 datum) Longitude	Latitude	2001 Minimum elevation (m a.s.l.)	2001 Maximum elevation (m a.s.l.)	2001 Maximum length (km)	2001 Slope (°)	2001 Area (km²)	2001 Perimeter (km)	2010 Area (km²)	2010 Perimeter (km)	2001 Glacier thickness (m)	2001 Ice volume (km³)	2001 Debris cover (km²)	2010 Debris cover (km²)	Debris-Covered or Debris-Free glacier	Glacier Type	Glacier name
Shigar basin	293	574159.6	3936817.3	4620	5150	1.24	23.1	0.36	3.16	0.36	3.16	20.3	0.01	0.000	0.000	DF	glacier	
Shigar basin	294	573630.5	3942841.3	4330	5590	3.22	21.4	1.80	7.78	1.80	7.78	39.8	0.07	0.030	0.400	DF	glacier	
Shigar basin	295	574404.7	3975762.0	5680	6870	0.89	53.2	0.49	3.77	0.49	3.77	17.6	0.01	0.000	0.000	DF	glacier	
Shigar basin	296	573348.1	3941253.3	4830	5510	1.68	22.0	0.58	4.44	0.58	4.44	25.9	0.02	0.020	0.000	DF	glacier	
Shigar basin	297	573780.0	3969519.3	4460	5650	3.24	20.2	1.85	8.37	1.86	8.37	40.9	0.08	0.240	0.200	DC	glacier	
Shigar basin	298	574718.7	3954113.1	4560	5190	1.50	22.8	0.48	3.47	0.48	3.47	23.6	0.01	0.050	0.040	DF	glacier	
Shigar basin	299	574944.7	3936183.7	4620	5250	1.42	23.9	0.29	3.19	0.29	3.19	22.6	0.01	0.000	0.000	DF	glacier	
Shigar basin	300	575992.8	3954143.0	4160	4850	1.61	23.2	0.55	3.60	0.55	3.60	24.9	0.01	0.100	0.170	DF	glacier	
Shigar basin	301	577054.2	3953988.2	4290	4960	1.23	28.6	0.26	2.79	0.26	2.79	20.1	0.01	0.120	0.110	DC	glacier	
Shigar basin	302	577066.4	3933478.6	4290	5710	3.37	22.8	1.50	10.52	1.50	10.52	39.3	0.06	0.090	0.110	DF	glacier	
Shigar basin	303	576312.1	3935884.8	4320	5830	5.68	14.9	6.02	20.16	6.01	20.16	60.6	0.36	0.220	0.510	DF	glacier	
Shigar basin	304	577487.1	3963599.2	4850	5680	0.83	45.0	0.14	1.98	0.14	1.98	15.9	0.00	0.000	0.000	DF	glacier	
Shigar basin	305	577713.8	3939617.3	4570	5540	1.30	36.7	0.52	3.55	0.52	3.55	20.9	0.01	0.030	0.050	DF	glacier	
Shigar basin	306	577564.6	3938221.5	4990	5530	0.81	33.7	0.22	2.10	0.22	2.10	14.6	0.00	0.010	0.010	DF	glacier	
Shigar basin	307	577768.0	3963095.2	5320	5690	0.57	33.0	0.13	1.46	0.12	1.40	10.8	0.00	0.000	0.000	DF	glacier	
Shigar basin	308	578047.8	3940056.0	5280	5500	0.31	35.4	0.05	0.93	0.05	0.93	6.3	0.00	0.000	0.000	DF	glacieret	
Shigar basin	309	577417.8	3965649.3	4310	6020	3.80	24.2	3.11	16.58	3.07	16.43	39.9	0.12	0.140	0.110	DF	glacier	
Shigar basin	310	578476.3	3940189.3	5420	5600	0.42	23.2	0.06	1.06	0.06	1.06	7.7	0.00	0.000	0.000	DF	glacieret	
Shigar basin	311	578835.7	3937280.0	4490	5380	2.23	21.8	0.88	5.79	0.89	5.89	31.9	0.03	0.050	0.080	DF	glacier	
Shigar basin	312	578667.5	3939174.9	4890	5460	1.13	26.8	0.32	3.00	0.32	3.00	18.8	0.01	0.000	0.010	DF	glacier	
Shigar basin	313	578790.8	3938458.5	4690	5260	1.56	20.1	0.42	3.89	0.42	3.89	24.6	0.01	0.010	0.010	DF	glacier	
Shigar basin	314	579277.8	3965192.5	5040	5690	1.06	31.5	0.21	2.37	0.21	2.37	18.0	0.00	0.000	0.000	DF	glacier	
Shigar basin	315	580487.8	3960983.5	4850	5710	1.10	38.0	0.48	3.13	0.48	3.13	18.7	0.01	0.010	0.020	DF	glacier	
Shigar basin	316	580892.8	3972726.9	4690	5640	2.11	24.2	0.74	5.49	0.74	5.49	30.1	0.02	0.000	0.010	DF	glacier	
Shigar basin	317	581177.7	3969303.7	4770	5640	2.14	22.1	0.63	5.30	0.63	5.30	30.9	0.02	0.040	0.040	DF	glacier	
Shigar basin	318	581502.3	3935449.7	4910	5540	0.96	33.3	0.28	2.36	0.27	2.27	16.7	0.00	0.000	0.010	DF	glacier	
Shigar basin	319	581495.8	3933347.2	4150	6200	11.16	10.4	18.75	59.99	18.77	60.22	90.6	1.70	1.620	2.450	DF	glacier	Stokpa Lungma-Gans
Shigar basin	320	582374.9	3980152.5	4630	5640	3.16	17.7	2.35	12.50	2.44	13.36	42.1	0.10	0.220	0.130	DF	glacier	
Shigar basin	321	582409.5	3937435.7	4440	6010	2.08	37.0	0.68	5.67	0.68	5.67	26.1	0.02	0.270	0.220	DC	glacier	
Shigar basin	322	582422.8	3968828.0	4880	5230	0.99	19.5	0.23	2.32	0.23	2.32	16.7	0.00	0.010	0.000	DF	glacier	
Shigar basin	323	582874.7	3969360.7	5040	5750	1.02	34.8	0.27	2.87	0.27	2.87	17.6	0.00	0.010	0.000	DF	glacier	
Shigar basin	324	584447.2	3932186.3	4210	5490	4.27	16.7	3.28	14.96	3.29	15.15	50.8	0.17	0.710	0.470	DC	glacier	
Shigar basin	325	584043.8	3971392.2	4030	5730	3.85	23.8	1.65	8.99	1.65	8.99	40.5	0.07	0.160	0.190	DF	glacier	

		Coordinates (utm 43N - WGS 84 datum)																
Catchment	ID Code	Longitude	Latitude	2001 Minimum elevation (m a.s.l.)	2001 Maximum elevation (m a.s.l.)	2001 Maximum length (km)	2001 Slope (°)	2001 Area (km^2)	2001 Perimeter (km)	2010 Area (km^2)	2010 Perimeter (km)	2001 Glacier thickness (m)	2001 Ice volume (km^3)	2001 Debris cover (km^2)	2010 Debris cover (km^2)	Debris-Covered or Debris-Free glacier	Glacier Type	Glacier name
Shigar basin	326	582880.5	3938538.3	4420	6040	2.89	29.3	1.22	7.80	1.22	7.80	33.5	0.04	0.090	0.130	DF	glacier	
Shigar basin	327	583809.9	3958104.6	4640	5490	2.13	21.8	0.89	5.92	0.89	5.92	30.9	0.03	0.000	0.010	DF	glacier	
Shigar basin	328	583563.0	3969591.1	4870	5260	0.57	34.4	0.11	1.64	0.11	1.64	10.9	0.00	0.000	0.000	DF	glacier	
Shigar basin	329	584199.4	3970690.8	4580	5570	1.82	28.5	0.80	5.45	0.80	5.45	26.5	0.02	0.000	0.000	DF	glacier	
Shigar basin	330	583640.5	3924662.8	4670	5320	1.44	24.3	0.57	3.95	0.57	3.95	22.8	0.01	0.240	0.260	DC	glacier	
Shigar basin	331	583632.7	3959198.0	3920	5850	5.52	19.3	5.37	34.48	5.40	34.73	49.6	0.27	0.610	0.780	DF	glacier	
Shigar basin	332	583521.8	3926588.1	4320	5340	2.74	20.4	0.89	7.85	0.89	7.85	37.0	0.03	0.310	0.270	DC	glacier	
Shigar basin	333	584057.3	3941771.4	4350	5270	2.21	22.6	0.67	5.73	0.67	5.73	31.4	0.02	0.200	0.180	DC	glacier	
Shigar basin	334	584104.9	3962110.8	4670	5280	1.80	18.7	0.96	6.96	0.96	6.96	27.8	0.03	0.010	0.010	DF	glacier	
Shigar basin	335	586772.6	3935420.5	4080	6030	10.19	10.8	13.23	53.81	13.25	54.02	87.1	1.15	2.400	3.190	DF	glacier	Mang Lungma-Gans
Shigar basin	336	584184.2	3940842.1	4780	5300	0.95	28.7	0.27	2.68	0.27	2.68	16.3	0.00	0.020	0.020	DF	glacier	
Shigar basin	337	584630.0	3924734.6	5100	5390	0.92	17.5	0.20	2.35	0.20	2.35	15.7	0.00	0.000	0.000	DF	glacier	
Shigar basin	338	584822.4	3957207.4	4000	6000	3.65	28.7	2.09	12.28	2.09	12.28	34.1	0.07	0.220	0.220	DF	glacier	
Shigar basin	339	584201.6	3940108.5	4560	5460	2.32	21.2	0.79	6.44	0.79	6.44	32.9	0.03	0.130	0.070	DF	glacier	
Shigar basin	340	585316.4	3924118.2	4720	5640	2.24	22.3	1.26	7.45	1.26	7.45	31.8	0.04	0.060	0.070	DF	glacier	
Shigar basin	341	586946.1	3925816.1	4160	5500	3.68	20.0	4.45	17.67	4.45	17.67	43.5	0.19	0.500	0.940	DF	glacier	
Shigar basin	342	586154.9	3977707.0	4540	5560	3.96	14.4	6.28	19.90	6.34	20.52	51.7	0.32	0.140	0.050	DF	glacier	
Shigar basin	343	587636.4	3939019.8	4950	5380	0.60	35.6	0.11	1.54	0.11	1.40	11.5	0.00	0.010	0.010	DF	glacier	
Shigar basin	344	587835.3	3938081.9	4920	5430	0.87	30.4	0.23	2.28	0.23	2.28	15.3	0.00	0.020	0.020	DF	glacier	
Shigar basin	345	587965.2	3941720.9	4170	5530	3.54	21.0	0.98	7.75	0.98	7.75	41.8	0.04	0.190	0.320	DF	glacier	
Shigar basin	346	591605.6	3927043.7	3910	5760	10.05	10.4	26.74	105.26	26.73	105.26	90.4	2.42	2.870	4.230	DF	glacier	
Shigar basin	347	588523.9	3934595.5	4770	5340	0.98	30.2	0.27	3.01	0.27	3.01	16.8	0.00	0.000	0.000	DF	glacier	
Shigar basin	348	588378.0	3935980.8	4410	5660	2.10	30.8	0.62	5.24	0.62	5.24	28.2	0.02	0.030	0.040	DF	glacier	
Shigar basin	349	588679.0	3986474.2	4720	6100	2.79	26.3	1.60	8.10	1.60	8.10	34.0	0.05	0.150	0.180	DF	glacier	
Shigar basin	350	588468.8	3932010.8	4950	5670	1.17	31.6	0.37	3.44	0.37	3.44	19.4	0.01	0.010	0.010	DF	glacier	
Shigar basin	351	589777.2	3933581.4	3970	5670	3.46	26.2	1.68	10.94	1.64	10.41	37.1	0.06	0.250	0.410	DF	glacier	
Shigar basin	352	589000.0	3977378.4	4800	5260	1.18	21.3	0.29	2.82	0.29	2.82	19.5	0.01	0.000	0.010	DF	glacier	
Shigar basin	353	589193.2	3937506.7	4610	5370	2.70	15.7	0.87	6.16	0.87	6.16	39.0	0.03	0.020	0.060	DF	glacier	
Shigar basin	354	589408.4	3940714.4	5040	5490	0.52	40.9	0.13	1.60	0.13	1.60	10.6	0.00	0.000	0.000	DF	glacier	
Shigar basin	355	589791.4	3938786.6	4570	5110	1.81	16.6	0.64	4.15	0.64	4.15	28.3	0.02	0.190	0.210	DC	glacier	
Shigar basin	356	590370.1	3983379.9	4400	5920	3.26	25.0	1.07	9.45	1.07	9.45	36.9	0.04	0.300	0.230	DC	glacier	
Shigar basin	357	586260.5	3967457.4	3590	6420	27.58	5.9	264.22	730.70	263.08	732.69	160.4	42.37	48.540	54.400	DC	glacier	Panmah
Shigar basin	358	589150.8	3936781.8	4090	5480	2.82	26.2	1.39	9.03	1.39	9.03	34.2	0.05	0.260	0.290	DF	glacier	

Catchment	ID Code	Coordinates (utm 43N - WGS 84 datum)		2001 Minimum elevation (m a.s.l.)	2001 Maximum elevation (m a.s.l.)	2001 Maximum length (km)	2001 Slope (°)	2001 Area (km^2)	2001 Perimeter (km)	2010 Area (km^2)	2010 Perimeter (km)	2001 Glacier thickness (m)	2001 Ice volume (km^3)	2001 Debris cover (km^2)	2010 Debris cover (km^2)	Debris-Covered or Debris-Free glacier	Glacier Type	Glacier name
		Longitude	Latitude															
Shigar basin	359	590922.0	3970770.6	4500	5480	1.93	26.9	0.59	5.65	0.61	5.97	27.8	0.02	0.030	0.070	DF	glacier	
Shigar basin	360	592218.9	3984767.6	4480	5730	3.01	22.6	1.45	7.73	1.45	7.73	37.6	0.05	0.180	0.140	DF	glacier	
Shigar basin	361	592306.1	3970301.9	4270	5610	3.43	21.3	1.89	10.15	1.85	9.63	40.9	0.08	0.070	0.150	DF	glacier	
Shigar basin	362	593008.9	3960229.7	4640	5780	2.41	25.3	0.56	6.56	0.56	6.56	32.2	0.02	0.040	0.070	DF	glacier	
Shigar basin	363	593092.2	3984312.4	4890	5320	1.71	14.1	0.61	4.12	0.61	4.12	27.4	0.02	0.000	0.000	DF	glacier	
Shigar basin	364	592887.1	3950605.4	4970	5450	0.53	42.2	0.22	1.97	0.22	1.97	10.9	0.00	0.000	0.000	DF	glacier	
Shigar basin	365	594684.5	3951602.7	4080	6560	6.84	19.9	7.48	36.11	7.48	36.11	48.0	0.36	0.600	1.610	DF	glacier	Choricho
Shigar basin	366	593323.4	3929549.1	4600	5430	1.81	24.6	0.46	4.66	0.46	4.66	27.0	0.01	0.020	0.040	DF	glacier	
Shigar basin	367	594764.9	3963427.3	4610	6070	7.33	11.3	10.90	36.16	11.71	40.07	78.8	0.86	0.250	0.110	DF	glacier	Feriole
Shigar basin	368	596374.5	3966327.0	4320	5900	7.78	11.5	11.78	32.23	13.46	37.99	79.2	0.93	0.240	0.660	DF	glacier	Shingchukpi
Shigar basin	369	593659.0	3954359.2	5270	5510	0.59	22.1	0.29	2.02	0.29	2.02	10.5	0.00	0.000	0.000	DF	glacier	
Shigar basin	370	593823.5	3950750.1	4605	5650	2.44	23.2	1.56	7.36	1.56	7.36	33.3	0.05	0.020	0.260	DF	glacier	
Shigar basin	371	594146.6	3961201.6	4650	5800	3.21	19.7	2.08	13.58	2.08	13.58	41.0	0.09	0.080	0.200	DF	glacier	
Shigar basin	372	592255.1	3932098.2	4215	5610	4.05	19.0	2.89	15.09	2.90	15.09	46.5	0.13	0.170	0.400	DF	glacier	
Shigar basin	373	594013.7	3933545.8	4210	5750	2.86	28.3	1.75	9.77	1.77	10.03	33.0	0.06	0.200	0.470	DF	glacier	
Shigar basin	374	595124.2	3935550.1	4030	5760	2.44	35.3	1.04	7.03	1.04	7.03	28.3	0.03	0.180	0.210	DC	glacier	
Shigar basin	375	595795.3	3935949.1	3980	5730	3.33	27.7	0.92	7.51	0.92	7.51	35.2	0.03	0.400	0.310	DC	glacier	
Shigar basin	376	594813.3	3959490.5	4230	5920	6.74	14.1	4.72	19.58	4.76	20.10	67.3	0.32	0.230	0.300	DF	glacier	
Shigar basin	377	597372.8	3934297.8	4280	5230	2.56	20.4	0.88	6.88	0.88	6.88	35.5	0.03	0.350	0.260	DC	glacier	
Shigar basin	378	596371.3	3950846.8	4810	5550	1.43	27.4	0.34	3.38	0.34	3.38	22.5	0.01	0.100	0.050	DC	glacier	
Shigar basin	379	596461.9	3932491.1	3910	5730	4.27	23.1	1.74	11.37	1.74	11.37	41.8	0.07	0.190	0.240	DF	glacier	
Shigar basin	380	593830.1	3956613.2	4000	5860	7.20	14.5	6.00	30.62	6.01	30.62	65.4	0.39	1.110	1.780	DC	glacier	Borum
Shigar basin	381	597175.3	3951329.2	3900	6470	5.82	23.8	4.67	31.87	4.67	31.87	40.5	0.19	0.880	0.840	DC	glacier	
Shigar basin	382	596276.5	3931403.2	3900	5810	6.17	17.2	3.64	20.03	3.64	20.03	55.4	0.20	1.960	1.660	DC	glacier	
Shigar basin	383	599089.8	3953283.6	5480	6270	0.98	38.9	0.18	2.48	0.18	2.48	17.3	0.00	0.000	0.000	DF	glacier	
Shigar basin	384	599311.0	3930421.8	4320	5720	2.41	30.2	0.55	6.10	0.55	6.10	30.2	0.02	0.070	0.060	DF	glacier	
Shigar basin	385	600655.9	3952558.7	5640	6530	0.87	45.7	0.18	2.71	0.18	2.71	16.5	0.00	0.000	0.000	DF	glacier	
Shigar basin	386	600810.6	3953536.9	5510	6170	0.89	36.6	0.59	3.91	0.60	3.91	15.9	0.01	0.000	0.000	DF	glacier	
Shigar basin	387	601505.6	3952120.7	4470	6060	2.09	37.3	0.36	5.19	0.36	5.19	26.1	0.01	0.030	0.060	DF	glacier	
Shigar basin	388	601690.9	3953332.8	5470	6200	0.73	45.0	0.13	1.74	0.13	1.74	14.5	0.00	0.000	0.000	DF	glacier	
Shigar basin	389	601604.4	3925906.1	5190	5630	0.80	28.8	0.16	2.03	0.16	2.03	14.1	0.00	0.000	0.000	DF	glacier	
Shigar basin	390	602877.7	3933151.5	4620	6130	3.00	26.7	1.92	12.38	1.92	12.38	34.6	0.07	0.210	0.240	DC	glacier	
Shigar basin	391	602385.1	3941431.9	4210	5800	5.05	17.5	3.65	20.27	3.66	20.27	52.6	0.19	0.820	0.760	DC	glacier	

Catchment	ID Code	Coordinates (utm 43N - WGS 84 datum)		2001 Minimum elevation (m a.s.l.)	2001 Maximum elevation (m a.s.l.)	2001 Maximum length (km)	2001 Slope (°)	2001 Area (km²)	2001 Perimeter (km)	2010 Area (km²)	2010 Perimeter (km)	2001 Glacier thickness (m)	2001 Ice volume (km³)	2001 Debris cover (km²)	2010 Debris cover (km²)	Debris-Covered or Debris-Free glacier	Glacier Type	Glacier name
		Longitude	Latitude															
Shigar basin	392	604462.2	3940813.4	4610	5900	5.76	12.6	3.56	18.32	3.61	18.77	67.0	0.24	1.040	0.910	DC	glacier	
Shigar basin	393	603063.2	3932381.4	5760	6220	0.76	31.2	0.16	2.43	0.16	2.43	13.7	0.00	0.000	0.000	DF	glacier	
Shigar basin	394	602990.6	3929845.0	5250	5860	0.82	36.6	0.51	5.59	0.51	5.59	15.0	0.01	0.000	0.000	DF	glacier	
Shigar basin	395	604659.2	3937380.7	4540	5970	6.55	12.3	4.39	24.45	4.56	25.62	71.7	0.31	1.420	1.490	DC	glacier	
Shigar basin	396	603476.7	3929532.9	5200	5900	1.07	33.2	0.91	5.35	0.91	5.35	18.1	0.02	0.000	0.000	DF	glacier	
Shigar basin	397	603194.0	3942329.2	4170	6630	3.73	33.4	1.56	11.46	1.56	11.46	29.7	0.05	0.400	0.390	DC	glacier	
Shigar basin	398	603724.6	3931109.2	4390	5180	4.60	9.7	1.31	12.24	1.31	12.24	64.2	0.08	0.350	0.290	DC	glacier	
Shigar basin	399	606431.4	3925489.4	4115	6145	10.63	10.8	23.27	85.48	23.29	85.59	87.3	2.03	4.810	3.890	DC	glacier	
Shigar basin	400	606273.3	3942339.3	4370	5400	4.05	14.3	1.88	10.52	1.92	10.82	52.7	0.10	0.890	0.830	DC	glacier	
Shigar basin	401	606446.1	3947125.2	3840	4820	2.77	19.5	0.63	6.31	0.63	6.31	37.7	0.02	0.510	0.480	DC	glacier	
Shigar basin	402	606156.0	3926652.0	5260	5990	0.90	39.0	0.21	2.65	0.21	2.65	16.3	0.00	0.000	0.000	DF	glacier	
Shigar basin	403	612098.2	3949494.8	4290	6010	3.17	28.5	1.06	10.30	1.05	10.10	34.3	0.04	0.320	0.290	DC	glacier	
Shigar basin	404	613126.1	3946704.9	4660	6230	2.48	32.3	0.77	6.55	0.77	6.55	29.4	0.02	0.090	0.110	DC	glacier	
Shigar basin	405	625975.3	3956004.0	3380	7900	58.68	4.4	604.23	1479.38	602.11	1481.68	213.2	128.79	164.000	161.450	DC	glacier	Baltoro
Shigar basin	406	612890.5	3944516.8	4750	6050	3.42	20.8	1.27	9.21	1.27	9.21	41.4	0.05	0.180	0.180	DC	glacier	
Shigar basin	407	617251.6	3943683.6	5540	6980	2.23	32.9	2.23	7.08	2.22	7.08	28.2	0.06	0.000	0.000	DF	glacier	
Shigar basin	408	620841.7	3960142.7	4640	5660	3.03	18.6	0.82	7.66	0.83	7.78	40.4	0.03	0.240	0.160	DC	glacier	
Shigar basin	409	623510.3	3959862.7	4290	5620	5.18	14.4	4.01	23.35	4.01	23.35	59.7	0.24	0.900	0.730	DC	glacier	
Shigar basin	410	630924.1	3960408.2	4620	5910	4.57	15.8	1.88	10.94	1.88	10.94	53.9	0.10	0.100	0.110	DC	glacier	
Shigar basin	411	631990.3	3960023.5	4590	5710	2.72	22.4	0.69	6.37	0.69	6.37	35.8	0.02	0.170	0.150	DC	glacier	
Shigar basin	412	632698.6	3959388.9	4810	5660	1.87	24.4	0.51	5.16	0.51	5.16	27.7	0.01	0.180	0.140	DC	glacier	
Shigar basin	413	634008.3	3958830.7	4550	5770	3.06	21.7	1.26	9.61	1.26	9.61	38.5	0.05	0.290	0.240	DC	glacier	
Shigar basin	414	634204.0	3963078.4	5160	5960	1.24	32.8	0.48	3.69	0.48	3.69	20.2	0.01	0.000	0.000	DF	glacier	
Shigar basin	415	634645.8	3962738.4	5060	5820	1.13	33.9	0.35	3.40	0.35	3.40	18.9	0.01	0.010	0.000	DF	glacier	
Shigar basin	416	635181.9	3959007.8	4640	5680	1.71	31.3	0.43	4.02	0.43	4.02	25.1	0.01	0.110	0.050	DC	glacier	
Shigar basin	417	636194.1	3948447.9	5080	5530	1.71	14.7	0.70	5.00	0.70	5.00	27.3	0.02	0.000	0.000	DF	glacier	
Shyok Basin																		
Shyok basin	418	638290.2	3934990.7	4400	6180	7.550	13.3	14.910	55.630	14.910	55.630	71.3	1.06	3.520	3.100	DC	glacier	
Shyok basin	419	639688.6	3928900.6	4780	6330	4.800	17.9	2.740	14.950	2.740	14.950	51.0	0.14	1.390	1.190	DC	glacier	
Shyok basin	420	638612.7	3930441.5	4790	6060	3.040	22.7	1.520	7.820	1.550	8.230	37.7	0.06	0.210	0.140	DC	glacier	
Shyok basin	421	637628.3	3930408.4	4867	5731	2.290	20.7	0.540	5.010	0.540	5.010	32.8	0.02	0.120	0.080	DC	glacier	
Shyok basin	422	636789.8	3929364.3	4754	5157	0.930	23.4	0.110	2.190	0.110	2.190	15.9	0.00	0.100	0.080	DC	glacier	

		Coordinates (utm 43N - WGS 84 datum)																
Catchment	ID Code	Longitude	Latitude	2001 Minimum elevation (m a.s.l.)	2001 Maximum elevation (m a.s.l.)	2001 Maximum length (km)	2001 Slope (°)	2001 Area (km²)	2001 Perimeter (km)	2010 Area (km²)	2010 Perimeter (km)	2001 Glacier thickness (m)	2001 Ice volume (km³)	2001 Debris cover (km²)	2010 Debris cover (km²)	Debris-Covered or Debris-Free glacier	Glacier Type	Glacier name
Shyok basin	423	636147.8	3929952.4	4764	5422	1.910	19.0	0.370	4.510	0.370	4.510	29.1	0.01	0.260	0.220	DC	glacier	
Shyok basin	424	636016.4	3931471.6	4860	5770	1.810	26.7	0.600	4.580	0.600	4.580	26.7	0.02	0.130	0.050	DC	glacier	
Shyok basin	425	636426.2	3921776.7	3440	6300	18.620	8.7	66.500	213.540	66.040	211.010	107.8	7.17	22.400	21.650	DC	glacier	Chogolisa
Shyok basin	426	632042.5	3946358.2	5030	5640	2.080	16.3	1.590	8.400	1.590	8.400	31.7	0.05	0.020	0.000	DF	glacier	
Shyok basin	427	631144.3	3923528.5	4460	6060	5.080	17.5	4.160	13.580	4.160	13.580	52.6	0.22	1.080	0.940	DC	glacier	
Shyok basin	428	630655.4	3941587.9	4920	6170	1.430	41.2	0.610	3.490	0.610	3.490	21.9	0.01	0.000	0.000	DF	glacier	
Shyok basin	429	630699.0	3921714.2	4710	6330	3.250	26.5	3.270	9.820	3.270	9.820	36.7	0.12	0.490	0.300	DC	glacier	
Shyok basin	430	630344.6	3933995.2	4830	5610	0.930	40.0	0.340	4.220	0.340	4.220	16.8	0.01	0.130	0.010	DC	glacier	
Shyok basin	431	630002.5	3936356.9	4890	5290	1.070	20.5	0.270	2.680	0.270	2.680	17.9	0.00	0.150	0.070	DC	glacier	
Shyok basin	432	629521.1	3935231.3	4530	5060	1.780	16.6	0.470	3.900	0.470	3.900	27.9	0.01	0.290	0.140	DC	glacier	
Shyok basin	433	629303.7	3923505.2	5120	5430	0.970	17.7	0.240	2.220	0.240	2.220	16.4	0.00	0.070	0.000	DC	glacier	
Shyok basin	434	628545.1	3937090.6	4310	5720	4.280	18.2	3.570	21.290	3.620	21.850	48.6	0.17	0.950	0.640	DC	glacier	
Shyok basin	435	628433.3	3924105.4	5050	5470	1.260	18.4	0.420	3.140	0.420	3.140	20.7	0.01	0.080	0.000	DC	glacier	
Shyok basin	436	626774.8	3943115.9	4750	5500	2.000	20.6	1.040	6.900	1.040	6.900	29.8	0.03	0.210	0.120	DF	glacier	
Shyok basin	437	624044.9	3936191.0	4130	4960	1.570	27.9	0.490	3.590	0.490	3.590	24.1	0.01	0.130	0.070	DC	glacier	
Shyok basin	438	627400.8	3940702.8	3440	6620	19.130	9.4	57.810	171.850	57.820	171.850	99.8	5.77	13.390	12.600	DC	glacier	Ghandogoro La
Shyok basin	439	623247.2	3936819.0	4140	5460	2.770	25.5	1.320	7.660	1.320	7.660	34.4	0.05	0.270	0.140	DF	glacier	
Shyok basin	440	622902.7	3934288.5	4270	5100	2.180	20.8	0.550	4.960	0.550	4.960	31.6	0.02	0.440	0.220	DC	glacier	
Shyok basin	441	622582.8	3935444.1	4630	5110	1.040	24.8	0.240	2.550	0.240	2.550	17.5	0.00	0.070	0.000	DC	glacier	
Shyok basin	442	621805.3	3936292.0	4670	5290	1.090	29.6	0.260	2.560	0.260	2.560	18.3	0.00	0.090	0.030	DC	glacier	
Shyok basin	443	621130.2	3937347.6	4340	5310	2.390	22.1	0.840	5.160	0.840	5.160	33.3	0.03	0.130	0.050	DF	glacier	
Shyok basin	444	619907.8	3920998.3	3780	5160	2.470	29.2	1.310	6.100	1.310	6.100	30.9	0.04	0.540	0.340	DC	glacier	
Shyok basin	445	620002.2	3937977.7	4130	5330	3.110	21.1	1.580	9.010	1.580	9.010	39.3	0.06	0.250	0.140	DF	glacier	
Shyok basin	446	617699.7	3909384.9	4200	5520	6.760	11.0	4.070	20.740	4.070	20.740	77.2	0.31	1.350	0.970	DC	glacier	
Shyok basin	447	619193.5	3938235.8	4780	5410	1.370	24.7	0.300	3.030	0.300	3.030	21.9	0.01	0.020	0.010	DF	glacier	
Shyok basin	448	618416.5	3913774.6	4070	5770	5.180	18.2	5.050	22.650	5.060	22.650	52.5	0.27	2.290	1.800	DC	glacier	
Shyok basin	449	619049.0	3908530.7	4980	5380	1.140	19.3	0.720	4.450	0.720	4.450	18.9	0.01	0.310	0.040	DC	glacier	
Shyok basin	450	618711.6	3926095.5	4360	4920	1.530	20.1	0.270	3.250	0.270	3.250	24.2	0.01	0.220	0.110	DC	glacier	
Shyok basin	451	618122.0	3921807.0	4040	5330	1.970	33.2	0.750	4.800	0.750	4.800	26.7	0.02	0.530	0.470	DC	glacier	
Shyok basin	452	617675.0	3926007.1	4200	4910	2.030	19.3	0.470	4.690	0.470	4.690	30.4	0.01	0.320	0.180	DC	glacier	
Shyok basin	453	617369.1	3908333.3	5070	5420	0.810	23.4	0.290	2.450	0.290	2.450	14.1	0.00	0.000	0.000	DF	glacier	
Shyok basin	454	617923.3	3911708.5	4730	5210	1.450	18.3	0.600	3.420	0.600	3.420	23.3	0.01	0.090	0.010	DF	glacier	
Shyok basin	455	617226.6	3921443.1	4090	5130	2.340	24.0	0.960	5.610	0.970	5.610	32.1	0.03	0.390	0.310	DC	glacier	

Catchment	ID Code	Coordinates (utm 43N - WGS 84 datum)		2001 Minimum elevation (m a.s.l.)	2001 Maximum elevation (m a.s.l.)	2001 Maximum length (km)	2001 Slope (°)	2001 Area (km²)	2001 Perimeter (km)	2010 Area (km²)	2010 Perimeter (km)	2001 Glacier thickness (m)	2001 Ice volume (km³)	2001 Debris cover (km²)	2010 Debris cover (km²)	Debris-Covered or Debris-Free glacier	Glacier Type	Glacier name
		Longitude	Latitude															
Shyok basin	456	616639.9	3926023.8	4040	4920	2.060	23.1	0.630	4.760	0.630	4.760	29.8	0.02	0.420	0.220	DC	glacier	
Shyok basin	457	616164.7	3923306.6	3920	6070	8.450	14.3	9.360	38.020	9.350	37.980	66.4	0.62	2.110	1.920	DC	glacier	
Shyok basin	458	616490.3	3921364.8	4580	5160	1.700	18.8	0.390	3.860	0.390	3.860	26.5	0.01	0.150	0.050	DC	glacier	
Shyok basin	459	615148.3	3908764.9	4220	5460	3.260	20.8	2.570	15.290	2.570	15.290	40.4	0.10	1.430	0.840	DC	glacier	
Shyok basin	460	616822.6	3914332.8	4730	5360	1.280	26.2	0.380	2.890	0.380	2.890	20.7	0.01	0.130	0.040	DC	glacier	
Shyok basin	461	616192.4	3922031.0	4450	5260	1.870	23.4	0.380	3.970	0.380	3.970	27.8	0.01	0.200	0.080	DC	glacier	
Shyok basin	462	615779.4	3931151.4	4790	5190	0.760	27.8	0.160	1.970	0.160	1.970	13.5	0.00	0.020	0.000	DF	glacier	
Shyok basin	463	615895.6	3913471.4	4760	5400	1.230	27.5	0.320	2.910	0.320	2.910	20.1	0.01	0.100	0.030	DC	glacier	
Shyok basin	464	614327.3	3913163.0	3900	5680	6.630	15.0	9.360	34.910	9.360	34.910	63.1	0.59	4.160	2.880	DC	glacier	
Shyok basin	465	617707.0	3938501.6	3490	7760	15.930	15.0	26.580	89.770	26.630	90.140	63.2	1.68	10.440	9.450	DC	glacier	Masherbrum
Shyok basin	466	615068.7	3910640.0	4500	5500	2.910	19.0	1.270	11.000	1.270	11.000	39.2	0.05	0.640	0.270	DC	glacier	
Shyok basin	467	614943.6	3926282.9	4180	4870	2.000	19.0	0.760	4.610	0.760	4.610	30.1	0.02	0.260	0.080	DC	glacier	
Shyok basin	468	614844.5	3921429.4	4270	5310	2.660	21.4	1.400	9.330	1.400	9.330	35.9	0.05	0.490	0.250	DC	glacier	
Shyok basin	469	615675.7	3932568.5	4140	5600	5.080	16.0	2.680	13.090	2.890	14.380	55.7	0.15	0.840	0.260	DC	glacier	
Shyok basin	470	614221.1	3916757.8	4720	5030	0.880	19.4	0.170	2.140	0.170	2.140	15.1	0.00	0.000	0.000	DF	glacier	
Shyok basin	471	614273.3	3922888.8	4710	5440	0.890	39.4	0.350	2.790	0.350	2.790	16.2	0.01	0.150	0.110	DC	glacier	
Shyok basin	472	613966.2	3932116.6	4900	5410	1.580	17.9	0.360	3.720	0.360	3.720	25.1	0.01	0.090	0.020	DC	glacier	
Shyok basin	473	613344.7	3932300.8	4900	5650	1.940	21.1	0.550	4.570	0.550	4.570	29.0	0.02	0.060	0.020	DC	glacier	
Shyok basin	474	613592.0	3921487.2	5460	5860	0.630	32.4	0.120	1.590	0.120	1.590	11.7	0.00	0.000	0.000	DF	glacier	
Shyok basin	475	612835.2	3921324.2	5410	5710	0.450	33.7	0.110	1.720	0.110	1.650	8.8	0.00	0.000	0.000	DF	glacier	
Shyok basin	476	612903.0	3933848.8	4690	5640	3.630	14.7	1.400	11.740	1.420	12.110	48.7	0.07	0.310	0.180	DC	glacier	
Shyok basin	477	612902.5	3914212.5	5140	5760	0.650	43.6	0.130	1.790	0.130	1.790	13.1	0.00	0.000	0.000	DF	glacier	
Shyok basin	478	612150.1	3912635.9	4700	5530	3.350	13.9	1.730	7.880	1.730	7.880	46.8	0.08	0.120	0.060	DF	glacier	
Shyok basin	479	613525.8	3910487.2	4460	5430	3.230	16.7	1.980	13.000	1.980	13.000	43.5	0.09	0.680	0.420	DC	glacier	
Shyok basin	480	613879.2	3918890.0	4060	5810	7.580	13.0	17.350	64.360	17.520	65.330	72.8	1.26	3.390	2.900	DC	glacier	
Shyok basin	481	611616.6	3910933.3	4720	5350	2.280	15.4	1.430	8.000	1.430	8.000	34.4	0.05	0.430	0.060	DC	glacier	
Shyok basin	482	611516.0	3913214.5	4820	5510	2.360	16.3	0.680	5.270	0.680	5.270	35.0	0.02	0.090	0.020	DC	glacier	
Shyok basin	483	611093.6	3915284.5	5310	5880	0.680	40.0	0.120	1.750	0.120	1.750	13.2	0.00	0.000	0.000	DF	glacier	
Shyok basin	484	610969.1	3915558.7	4950	5580	0.640	44.5	0.110	1.650	0.110	1.650	13.1	0.00	0.000	0.000	DF	glacier	
Shyok basin	485	611040.7	3913907.6	4840	5570	1.980	20.2	0.580	6.740	0.580	6.740	29.6	0.02	0.110	0.030	DC	glacier	
Shyok basin	486	610584.3	3911357.5	4740	5360	1.260	26.2	0.640	5.550	0.640	5.550	20.5	0.01	0.160	0.030	DC	glacier	
Shyok basin	487	606589.5	3932205.6	3630	6280	17.910	8.4	43.220	168.810	43.240	168.740	111.8	4.83	15.510	13.830	DC	glacier	Aling
Shyok basin	488	609345.1	3911675.5	5030	5230	0.500	21.8	0.090	1.360	0.090	1.360	9.0	0.00	0.000	0.000	DF	glacieret	

Catchment	ID Code	Coordinates (utm 43N - WGS 84 datum)		2001 Minimum elevation (m a.s.l.)	2001 Maximum elevation (m a.s.l.)	2001 Maximum length (km)	2001 Slope (°)	2001 Area (km^2)	2001 Perimeter (km)	2010 Area (km^2)	2010 Perimeter (km)	2001 Glacier thickness (m)	2001 Ice volume (km^3)	2001 Debris cover (km^2)	2010 Debris cover (km^2)	Debris-Covered or Debris-Free glacier	Glacier Type	Glacier name
		Longitude	Latitude															
Shyok basin	489	609479.3	3915555.9	4800	5280	1.030	25.0	0.300	4.390	0.300	4.390	17.4	0.01	0.070	0.010	DF	glacier	
Shyok basin	490	607359.5	3923615.1	4130	5940	7.680	13.3	6.080	26.780	6.150	27.260	71.4	0.43	2.470	2.240	DC	glacier	
Shyok basin	491	608346.4	3916585.2	4820	5440	1.720	19.8	0.720	7.870	0.720	7.870	26.7	0.02	0.050	0.000	DF	glacier	
Shyok basin	492	608392.8	3929333.6	5120	5700	0.910	32.5	0.170	2.360	0.170	2.360	15.9	0.00	0.000	0.000	DF	glacier	
Shyok basin	493	607770.4	3915856.0	4680	5360	2.260	16.7	0.680	5.480	0.680	5.480	33.7	0.02	0.420	0.260	DC	glacier	
Shyok basin	494	608298.5	3917852.9	4770	5460	2.100	18.2	1.260	6.620	1.260	6.620	31.5	0.04	0.200	0.050	DF	glacier	
Shyok basin	495	608390.4	3921735.6	4270	5370	5.640	11.0	4.160	16.820	4.160	16.820	70.5	0.29	1.430	1.240	DC	glacier	
Shyok basin	496	607286.5	3916812.9	4730	5280	1.280	23.3	0.620	4.730	0.620	4.730	20.8	0.01	0.150	0.020	DF	glacier	
Shyok basin	497	603669.6	3924281.7	5140	5650	0.760	33.9	0.180	2.200	0.180	2.200	13.8	0.00	0.000	0.000	DF	glacier	
Shyok basin	498	602514.2	3923554.8	4550	5370	2.170	20.7	0.800	5.730	0.810	5.870	31.6	0.03	0.180	0.110	DC	glacier	
Shyok basin	499	601473.2	3924435.4	4600	4820	0.760	16.1	0.120	1.850	0.130	1.990	13.2	0.00	0.040	0.000	DC	glacier	
Shyok basin	500	601404.5	3925044.8	4730	5130	1.120	19.7	0.220	3.000	0.220	3.000	18.6	0.00	0.010	0.000	DF	glacier	
Shyok basin	501	599355.9	3924474.4	4880	5140	0.640	22.1	0.140	1.790	0.140	1.790	11.3	0.00	0.000	0.000	DF	glacier	
Shyok basin	502	598654.0	3924974.7	4840	5310	1.200	21.4	0.520	3.410	0.520	3.410	19.7	0.01	0.000	0.000	DF	glacier	
Shyok basin	503	598764.8	3924272.2	4810	5190	0.750	26.9	0.180	2.030	0.180	2.030	13.3	0.00	0.000	0.000	DF	glacier	
Shyok basin	504	597867.7	3927727.9	4130	5660	3.530	23.4	1.820	8.590	1.820	8.590	39.3	0.07	0.740	0.250	DC	glacier	
Shyok basin	505	596469.3	3927980.9	4580	5210	1.910	18.3	0.630	4.490	0.680	4.840	29.2	0.02	0.210	0.050	DC	glacier	
Shyok basin	506	595004.6	3928771.6	4220	5600	3.960	19.2	5.580	16.430	5.580	16.430	45.8	0.26	0.460	0.360	DF	glacier	
Shyok basin	507	594184.6	3925870.2	4040	4690	1.200	28.4	0.330	2.990	0.330	2.990	19.7	0.01	0.150	0.040	DC	glacier	
Shyok basin	508	594209.5	3925052.9	4310	5410	1.500	36.3	0.490	4.190	0.490	4.190	22.8	0.01	0.030	0.020	DF	glacier	
Shyok basin	509	592978.9	3924577.4	5170	5540	0.670	28.9	0.180	1.780	0.180	1.780	12.1	0.00	0.000	0.000	DF	glacier	
Shyok basin	510	592183.1	3924449.3	4610	5130	1.080	25.7	0.220	2.460	0.220	2.460	18.1	0.00	0.050	0.040	DF	glacier	
Shyok basin	511	590868.0	3923331.0	4070	5120	2.400	23.6	0.960	6.200	0.960	6.200	32.8	0.03	0.840	0.660	DC	glacier	
Upper Indus Basin																		
Upper Indus basin	512	528365.7	3953539.1	4190	5430	4.37	15.8	2.35	10.17	2.35	10.17	52.7	0.124	0.240	0.310	DF	glacier	
Upper Indus basin	513	527718.6	3953024.8	4460	4970	1.80	15.8	0.67	4.30	0.67	4.30	28.3	0.019	0.000	0.010	DF	glacier	
Upper Indus basin	514	525911.4	3954006.3	4070	5020	2.73	19.2	2.37	7.83	2.37	7.83	37.5	0.089	0.950	1.220	DC	glacier	
Upper Indus basin	515	522340.7	3955654.4	3970	5100	3.00	20.6	3.49	16.04	3.49	16.04	38.9	0.136	1.160	1.440	DC	glacier	

		Coordinates (utm 43N - WGS 84 datum)																
Catchment	ID Code	Longitude	Latitude	2001 Minimum elevation (m a.s.l.)	2001 Maximum elevation (m a.s.l.)	2001 Maximum length (km)	2001 Slope (°)	2001 Area (km²)	2001 Perimeter (km)	2010 Area (km²)	2010 Perimeter (km)	2001 Glacier thickness (m)	2001 Ice volume (km³)	2001 Debris cover (km²)	2010 Debris cover (km²)	Debris-Covered or Debris-Free glacier	Glacier Type	Glacier name
Upper Indus basin	516	518696.7	3957220.3	4350	5300	2.70	19.4	1.42	6.54	1.42	6.54	37.2	0.053	0.030	0.020	DF	glacier	
Upper Indus basin	517	510746.4	3953611.4	4020	5270	4.32	16.1	4.88	12.97	4.88	12.97	51.9	0.253	0.840	1.810	DF	glacier	
Upper Indus basin	518	509867.8	3954519.7	4160	4790	1.50	22.8	0.56	3.75	0.56	3.75	23.6	0.013	0.010	0.140	DF	glacier	
Upper Indus basin	519	508180.2	3953032.4	4040	5180	2.20	27.4	1.60	8.60	1.60	8.60	29.9	0.048	0.090	0.390	DF	glacier	
Upper Indus basin	520	507118.1	3963000.9	3500	5800	10.32	12.6	16.17	63.38	16.16	63.38	75.3	1.217	3.740	4.650	DC	glacier	Gorophа
Upper Indus basin	521	505198.3	3964003.7	4110	5100	1.87	27.9	0.60	5.53	0.60	5.53	27.1	0.016	0.050	0.100	DF	glacier	
Upper Indus basin	522	504377.6	3963422.9	4560	4770	0.55	20.9	0.09	1.35	0.09	1.35	9.8	0.001	0.000	0.000	DF	glacieret	
Upper Indus basin	523	502014.5	3961163.9	2810	7330	18.82	13.5	57.72	178.67	57.53	177.54	70.1	4.046	11.580	13.740	DC	glacier	Kothia Lungma
Upper Indus basin	524	503398.9	3963855.9	4390	5150	1.26	31.1	0.39	4.21	0.39	4.21	20.5	0.008	0.010	0.030	DF	glacier	
Upper Indus basin	525	502694.7	3966688.0	4790	5480	1.04	33.6	0.13	2.65	0.13	2.65	17.8	0.002	0.000	0.000	DF	glacier	
Upper Indus basin	526	502146.5	3967053.3	4470	5090	0.89	34.9	0.15	2.20	0.15	2.20	15.8	0.002	0.000	0.000	DF	glacier	
Upper Indus basin	527	502109.3	3964737.4	4270	5040	1.12	34.5	0.16	2.97	0.15	2.94	18.8	0.003	0.000	0.030	DF	glacier	
Upper Indus basin	528	502047.4	3963612.8	4330	4620	0.69	22.8	0.09	1.47	0.09	1.47	12.2	0.001	0.080	0.020	DC	glacieret	
Upper Indus basin	529	500484.2	3958021.0	4500	4780	0.62	24.3	0.10	1.72	0.10	1.72	11.1	0.001	0.000	0.000	DF	glacier	
Upper Indus basin	530	500056.8	3958682.6	4030	5250	2.19	29.1	0.51	5.10	0.51	5.10	29.3	0.015	0.000	0.050	DF	glacier	
Upper Indus basin	531	499589.1	3958942.5	3920	5390	3.30	24.0	1.60	7.96	1.60	7.96	37.9	0.061	0.030	0.090	DF	glacier	
Upper Indus basin	532	497475.3	3956370.9	3890	5630	4.36	21.8	5.05	20.51	5.05	20.51	44.2	0.223	0.280	0.630	DF	glacier	
Upper Indus basin	533	498326.3	3953773.1	4490	4940	0.80	29.4	0.12	1.75	0.12	1.75	14.2	0.002	0.000	0.000	DF	glacier	

		Coordinates (utm 43N - WGS 84 datum)																
Catchment	ID Code	Longitude	Latitude	2001 Minimum elevation (m a.s.l.)	2001 Maximum elevation (m a.s.l.)	2001 Maximum length (km)	2001 Slope (°)	2001 Area (km^2)	2001 Perimeter (km)	2010 Area (km^2)	2010 Perimeter (km)	2001 Glacier thickness (m)	2001 Ice volume (km^3)	2001 Debris cover (km^2)	2010 Debris cover (km^2)	Debris-Covered or Debris-Free glacier	Glacier Type	Glacier name
Upper Indus basin	534	497258.3	3969030.3	5190	6570	2.08	33.6	1.10	7.39	1.10	7.39	27.3	0.030	0.000	0.000	DF	glacier	
Upper Indus basin	535	494072.3	3968109.9	4860	6810	5.31	20.2	6.91	23.09	6.91	23.09	47.5	0.328	0.000	0.010	DF	glacier	
Upper Indus basin	536	494410.3	3957781.1	4210	5520	3.18	22.4	2.13	16.91	2.13	16.91	38.7	0.083	0.180	0.700	DF	glacier	
Upper Indus basin	537	495467.0	3974680.0	4590	5050	0.83	29.0	0.33	3.64	0.33	3.64	14.6	0.005	0.010	0.040	DF	glacier	
Upper Indus basin	538	496047.7	3956206.8	4800	5560	1.54	26.3	1.00	7.98	1.00	7.98	23.9	0.024	0.000	0.080	DF	glacier	
Upper Indus basin	539	495534.1	3973097.5	3840	4680	1.34	32.1	0.28	2.95	0.28	2.95	21.4	0.006	0.170	0.060	DC	glacier	
Upper Indus basin	540	494145.5	3956905.5	4510	5030	0.88	30.6	0.26	2.20	0.26	2.20	15.4	0.004	0.010	0.070	DF	glacier	
Upper Indus basin	541	494024.7	3961086.2	4580	5210	1.25	26.7	0.33	5.79	0.33	5.79	20.3	0.007	0.040	0.030	DF	glacier	
Upper Indus basin	542	493968.0	3959761.0	4290	4780	0.67	36.2	0.06	1.47	0.06	1.47	12.6	0.001	0.000	0.000	DF	glacieret	
Upper Indus basin	543	494159.7	3960481.1	4350	5290	1.40	33.9	0.23	4.01	0.23	4.01	22.0	0.005	0.010	0.040	DF	glacier	
Upper Indus basin	544	492825.8	3962115.0	4410	5640	1.88	33.2	0.38	6.15	0.38	6.15	26.2	0.010	0.010	0.000	DF	glacier	
Upper Indus basin	545	492348.0	3960904.9	4400	5430	1.58	33.1	0.26	4.13	0.27	4.21	23.8	0.006	0.030	0.020	DF	glacier	
Upper Indus basin	546	492341.7	3978185.5	4650	5800	3.21	19.7	2.07	13.58	2.08	13.58	41.0	0.085	0.790	0.450	DC	glacier	
Upper Indus basin	547	490662.3	3961101.0	3600	6420	5.82	25.9	5.74	25.74	5.74	25.74	37.5	0.215	0.240	0.210	DF	glacier	
Upper Indus basin	548	493594.1	3971945.4	2590	5050	8.18	16.7	16.64	46.59	17.33	47.11	56.8	0.946	10.610	9.470	DC	glacier	Mani
Upper Indus basin	549	485785.0	3963398.3	3570	6990	8.29	22.4	5.93	39.04	5.92	39.07	42.9	0.255	1.580	1.570	DC	glacier	Ishakapal
Upper Indus basin	550	490017.3	3961102.7	4600	5300	1.34	27.6	0.41	4.08	0.41	4.08	21.5	0.009	0.000	0.000	DF	glacier	
Upper Indus basin	551	490641.7	3980599.6	4650	5800	3.21	19.7	2.07	13.58	2.08	13.58	41.0	0.085	3.080	3.160	DC	glacier	Baskai

		Coordinates (utm 43N - WGS 84 datum)																
Catchment	ID Code	Longitude	Latitude	2001 Minimum elevation (m a.s.l.)	2001 Maximum elevation (m a.s.l.)	2001 Maximum length (km)	2001 Slope (°)	2001 Area (km²)	2001 Perimeter (km)	2010 Area (km²)	2010 Perimeter (km)	2001 Glacier thickness (m)	2001 Ice volume (km³)	2001 Debris cover (km²)	2010 Debris cover (km²)	Debris-Covered or Debris-Free glacier	Glacier Type	Glacier name
Upper Indus basin	552	486420.3	3965287.9	4070	5860	3.90	24.7	2.55	12.92	2.55	12.92	39.2	0.100	0.470	0.530	DC	glacier	
Upper Indus basin	553	486670.8	3966423.3	4890	5410	0.94	29.0	0.22	3.25	0.22	3.25	16.2	0.004	0.000	0.000	DF	glacier	
Upper Indus basin	554	487023.3	3979303.3	4650	5800	3.21	19.7	2.07	13.58	2.08	13.58	41.0	0.085	0.000	0.000	DF	glacier	
Upper Indus basin	555	481274.1	3984071.5	2870	6480	9.77	20.3	14.79	52.46	14.79	52.46	47.2	0.699	5.080	5.380	DC	glacier	Phuparsh
Upper Indus basin	556	486164.9	3966851.2	4720	5110	1.14	18.9	0.24	3.51	0.24	3.51	19.0	0.005	0.000	0.000	DF	glacier	
Upper Indus basin	557	486025.5	3968296.9	3940	5580	4.01	22.2	1.55	9.82	1.55	9.82	43.2	0.067	0.090	0.430	DF	glacier	
Upper Indus basin	558	485672.5	3978731.1	4650	5800	3.21	19.7	2.07	13.58	2.08	13.58	41.0	0.085	0.090	0.080	DF	glacier	
Upper Indus basin	559	484742.4	3967411.4	4820	5340	1.29	22.0	0.38	3.59	0.38	3.59	21.0	0.008	0.000	0.000	DF	glacier	
Upper Indus basin	560	484707.0	3966478.5	4860	5190	0.82	21.9	0.27	3.60	0.27	3.60	14.2	0.004	0.000	0.000	DF	glacier	
Upper Indus basin	561	483907.4	3965709.2	4880	4930	0.35	8.1	0.04	0.95	0.04	0.95	6.5	0.000	0.000	0.000	DF	glacieret	
Upper Indus basin	562	482340.9	3987517.7	3430	6530	4.95	32.1	5.01	23.81	5.01	23.81	30.8	0.155	0.330	0.370	DF	glacier	
Upper Indus basin	563	477799.5	3986215.0	4650	5800	3.21	19.7	2.07	13.58	2.08	13.58	41.0	0.085	0.010	0.440	DF	glacier	Darchan
Upper Indus basin	564	476044.3	3987106.0	4320	5290	1.80	28.3	2.52	12.91	2.52	12.91	26.4	0.066	0.000	0.220	DF	glacier	
Upper Indus basin	565	471861.2	3982970.4	4430	4740	0.91	18.8	0.29	2.32	0.28	2.26	15.5	0.005	0.000	0.000	DF	glacier	
Upper Indus basin	566	470209.6	3981683.0	4120	5110	1.97	26.7	0.87	8.20	0.87	8.20	28.2	0.025	0.070	0.490	DF	glacier	
Upper Indus basin	567	470480.2	3980411.4	3740	5240	3.65	22.3	1.98	13.73	1.98	13.73	40.9	0.081	0.200	0.740	DF	glacier	
Upper Indus basin	568	467931.7	3977686.2	3980	4940	2.39	21.9	1.02	6.04	1.02	6.04	33.3	0.034	0.800	0.760	DC	glacier	
Upper Indus basin	569	468835.5	3978903.8	4090	5670	3.77	22.7	2.40	16.68	2.40	16.68	40.8	0.098	0.130	0.420	DF	glacier	

		Coordinates (utm 43N - WGS 84 datum)																
Catchment	ID Code	Longitude	Latitude	2001 Minimum elevation (m a.s.l.)	2001 Maximum elevation (m a.s.l.)	2001 Maximum length (km)	2001 Slope (°)	2001 Area (km²)	2001 Perimeter (km)	2010 Area (km²)	2010 Perimeter (km)	2001 Glacier thickness (m)	2001 Ice volume (km³)	2001 Debris cover (km²)	2010 Debris cover (km²)	Debris-Covered or Debris-Free glacier	Glacier Type	Glacier name
Upper Indus basin	570	467755.2	3974803.1	4650	5800	3.21	19.7	2.07	13.58	2.08	13.58	41.0	0.085	0.010	0.060	DF	glacier	
Upper Indus basin	571	467591.8	3978541.0	5020	5690	0.62	47.2	0.15	2.68	0.15	2.68	13.1	0.002	0.000	0.000	DF	glacier	
Upper Indus basin	572	467066.4	3977552.7	4710	4890	0.55	18.1	0.09	1.49	0.08	1.46	9.8	0.001	0.000	0.040	DF	glacieret	
Gilgit Basin																		
Gilgit basin	573	469245.4	3987677.3	2980	6790	15.74	13.6	28.46	108.51	28.46	108.51	69.6	1.98	9.950	10.800	DC	glacier	Salili
Gilgit basin	574	472479.3	3985686.0	3990	4740	1.92	21.3	1.01	5.62	1.01	5.62	28.8	0.03	0.000	0.000	DF	glacier	
Gilgit basin	575	472725.8	3987808.7	4310	4640	0.89	20.3	0.19	2.30	0.19	2.30	15.2	0.00	0.000	0.000	DF	glacier	
Gilgit basin	576	472852.4	3988456.5	4620	4800	0.34	27.9	0.04	0.90	0.04	0.90	6.5	0.00	0.000	0.000	DF	glacieret	
Gilgit basin	577	472916.5	3986690.8	4180	4620	1.08	22.2	0.37	3.22	0.37	3.22	18.0	0.01	0.000	0.000	DF	glacier	
Gilgit basin	578	471709.7	3984343.6	4170	4870	1.36	27.2	0.59	4.64	0.59	4.64	21.7	0.01	0.000	0.000	DF	glacier	
Gilgit basin	579	470732.5	3982959.1	4050	4450	0.55	36.0	0.13	1.44	0.13	1.44	10.7	0.00	0.030	0.060	DF	glacier	
Gilgit basin	580	470065.6	3982925.1	3980	4390	0.74	29.0	0.09	1.62	0.09	1.62	13.2	0.00	0.080	0.080	DC	glacieret	
Gilgit basin	581	469801.4	3983158.2	3780	4420	1.63	21.4	0.47	3.61	0.47	3.61	25.4	0.01	0.050	0.310	DF	glacier	
Gilgit basin	582	469392.6	3983378.1	3850	4730	1.84	25.6	0.56	4.17	0.56	4.17	27.2	0.02	0.090	0.310	DF	glacier	
Gilgit basin	583	465336.8	3980876.8	3260	6100	7.74	20.1	8.46	24.24	8.46	24.24	47.5	0.40	3.210	2.660	DC	glacier	
Gilgit basin	584	467879.1	3983561.6	4300	4460	0.71	12.7	0.10	2.10	0.10	2.10	12.4	0.00	0.000	0.000	DF	glacier	
Gilgit basin	585	467947.9	3981813.2	4200	5020	0.77	46.8	0.09	1.72	0.09	1.72	15.3	0.00	0.080	0.010	DC	glacieret	
Gilgit basin	586	467560.1	3998160.5	4780	6260	1.94	37.3	1.20	6.62	1.20	6.62	25.5	0.03	0.000	0.000	DF	glacier	
Gilgit basin	587	466041.4	3998596.3	4410	5860	2.07	35.0	1.74	8.31	1.74	8.31	26.8	0.05	0.000	0.110	DF	glacier	
Gilgit basin	588	466450.0	3975000.7	4530	5150	0.84	36.4	0.15	1.98	0.15	1.98	15.2	0.00	0.020	0.100	DF	glacier	
Gilgit basin	589	466114.7	3974837.5	4460	5070	0.84	36.0	0.11	1.85	0.11	1.85	15.2	0.00	0.000	0.000	DF	glacier	
Gilgit basin	590	465494.2	3977469.5	4100	5090	2.54	21.3	0.82	5.86	0.82	5.86	34.9	0.03	0.580	0.680	DC	glacier	
Gilgit basin	591	465973.7	3975648.6	4190	4530	0.80	23.0	0.18	2.08	0.18	2.08	13.9	0.00	0.000	0.180	DF	glacier	
Gilgit basin	592	465553.5	3979719.4	4900	5420	0.61	40.4	0.06	1.53	0.06	1.53	12.1	0.00	0.000	0.000	DF	glacieret	
Gilgit basin	593	464445.6	3977104.8	3730	5630	3.90	26.0	1.29	8.76	1.29	8.76	37.4	0.05	0.870	0.530	DC	glacier	
Gilgit basin	594	465732.1	3981779.7	4160	4750	1.18	26.6	0.20	3.56	0.20	3.56	19.4	0.00	0.000	0.000	DF	glacier	
Gilgit basin	595	464892.4	3998509.5	4120	5070	1.37	34.7	0.35	3.37	0.33	3.09	21.7	0.01	0.020	0.100	DF	glacier	
Gilgit basin	596	464378.6	3979779.7	4150	4720	1.39	22.3	0.37	3.16	0.37	3.16	22.3	0.01	0.350	0.330	DC	glacier	
Gilgit basin	597	464120.2	3981195.0	4210	4810	1.70	19.4	0.73	4.43	0.73	4.43	26.5	0.02	0.080	0.320	DF	glacier	
Gilgit basin	598	463618.1	3999561.9	4230	4860	0.70	42.0	0.12	1.86	0.13	1.95	13.7	0.00	0.000	0.030	DF	glacier	

		Coordinates (utm 43N - WGS 84 datum)																
Catchment	ID Code	Longitude	Latitude	2001 Minimum elevation (m a.s.l.)	2001 Maximum elevation (m a.s.l.)	2001 Maximum length (km)	2001 Slope (°)	2001 Area (km^2)	2001 Perimeter (km)	2010 Area (km^2)	2010 Perimeter (km)	2001 Glacier thickness (m)	2001 Ice volume (km^3)	2001 Debris cover (km^2)	2010 Debris cover (km^2)	Debris-Covered or Debris-Free glacier	Glacier Type	Glacier name
Gilgit basin	599	464090.9	3999512.7	4220	5490	1.85	34.5	0.51	5.71	0.51	5.71	25.7	0.01	0.000	0.000	DF	glacier	
Gilgit basin	600	460617.1	4000288.9	4450	5820	2.15	32.5	1.40	10.80	1.40	10.80	28.0	0.04	0.000	0.000	DF	glacier	
Gilgit basin	601	460096.3	3995034.4	3450	5910	2.88	40.5	1.01	7.57	1.01	7.57	25.2	0.03	0.070	0.110	DF	glacier	
Gilgit basin	602	459189.3	4000104.3	5370	6010	0.96	33.7	0.23	2.19	0.23	2.19	16.7	0.00	0.000	0.000	DF	glacier	
Gilgit basin	603	458545.6	3993666.6	4580	4990	0.49	39.9	0.09	1.86	0.09	1.86	10.0	0.00	0.000	0.080	DF	glacieret	
Gilgit basin	604	457502.1	3993416.2	3790	5770	3.13	32.3	1.77	9.93	1.77	9.93	30.6	0.05	0.230	0.510	DF	glacier	
Gilgit basin	605	457948.3	3994128.4	4670	5590	0.88	46.3	0.13	2.10	0.13	2.10	16.7	0.00	0.000	0.000	DF	glacier	
Gilgit basin	606	464904.3	3995819.0	2500	7680	17.88	16.2	29.95	97.21	29.95	97.21	58.8	1.76	6.020	7.400	DC	glacier	Hinarche
Gilgit basin	607	455724.6	3989592.8	4460	4980	1.13	24.7	0.57	5.88	0.57	5.88	18.8	0.01	0.000	0.230	DF	glacier	
Gilgit basin	608	455146.9	3989029.6	4540	4890	0.44	38.5	0.08	1.49	0.08	1.49	9.0	0.00	0.000	0.000	DF	glacieret	

Glacial lakes and potentially dangerous glacial lakes

Inventory of Glacial Lakes and potentially GLOF phenomena

In the recent years, the Scientific Community has been paying more and more attention on the occurrence of risk and hazard phenomena in glacier and glaciated areas (e.g. Cenderelli and Wohl, 2003; Harrison et al., 2006; Bajracharya et al., 2007; Bolch et al., 2008; Fujita et al., 2008). Among these events, the most important, and also largely diffuse in the Hindukush, Karakoram, Himalaya (HKH) range, are the Glacial Lakes Outburst Floods (GLOFs, Roohi et al., 2005; Richardson, 2010). In fact, with the onset of twenty first century both the intensity and frequency of natural hazards like flash floods and GLOFs have increased many folds in the HKH region (PARC et al., 2015). Such prevailing situation demanded a thorough investigation of both occurrence and current status of the glacial lakes in the CKNP area as well. Taking advantage from the results of the project "Updating GLOF lake inventory of Northern Pakistan", which is a component of the "Pakistan program on Reducing Risks and Vulnerabilities from GLOF in Northern Pakistan" (this latter supported through the Pakistan GLOF project and developed by the Pakistan Agricultural Research Council, PARC, in close cooperation with the Pakistan Meteorological Department, PMD), we listed and analyzed glacial lakes and potentially GLOF phenomena in the CKNP area and in each one of the park catchments. The main objective of this chapter is to establish an inventory and digital database of glacial lakes in the CKNP region. The inventory is based on remote sensing data of 2013, extracted from the data base of glacial lakes and potentially GLOF events developed by PARC and PMD.

Glacial Lake Inventory criteria

For the inventory of glacial lakes, the lakes associated with perennial snow and ice, originated from glaciers, and in some cases the isolated lakes found in the mountains and valleys far away from the glaciers are considered (in agreement with the criteria applied by PARC and PMD in their inventory for the Northern Pakistan).

We followed the classification applied by PARC and PMD in their glacial lake inventory, more precisely: i) Glacial Erosion lakes are the water bodies formed in a depression after the glacier has retreated. ii) Cirque and iii) Trough Valley lakes are two specific type of glacial erosion and they are generally stable lakes. These lakes might be isolated and far away from the present glaciated area. iv) Supraglacial lakes may develop in any position of the glacier surface but the extension of the lake is less than half the diameter of the Valley glacier. Shifting, merging, and draining of the lakes characterize Supraglacial lakes. The merging of lakes results in expansion of the lake area and storage of a huge volume of water with a high level of potential energy. The tendency of a glacial lake towards merging and expanding indicates the danger level of the GLOF. Moraine Dammed lakes derive from the retreating process of a glacier, in fact glacial ice tends to melt in the lowest part of the glacier surrounded by lateral moraine and end moraines, thus originating v) Lateral Moraine lakes and vi) End Moraine Dammed lakes. As a result, many supraglacial ponds are formed on the glacier tongue. These ponds sometimes enlarge to become a large lake by interconnecting with each other and have a tendency to deepen further. A Moraine Dammed lake is thus born. If one follows the lifespan of an individual glacier, it is found that the Moraine Dammed glacial lakes build up and disappear with a lapse of time. The lake is filled with melt water and rainwater from the drainage area behind the lake and starts flowing from the outlet of the lake even in the winter season when there is minimum flow. There are two kinds of moraine: an ice-cored moraine and an ice-free moraine. Before the ice body of the glacier completely melts away, glacier ice exists in the moraine and beneath the lake bottom. The ice bodies cored in the moraine and beneath the lake are sometimes called dead ice or fossil ice. As glacier ice continues to melt, the lake becomes deeper and wider. Finally, when ice contained in the moraines and beneath the lake completely melts away, the container of lake water consists of only the bedrock and the moraines. vii) Blocking lakes are formed through glacier and other factors, including the main glacier blocking the branch valley, the glacier branch blocking the main valley, and the lakes through snow avalanche, collapse and debris flow blockade. In addition, another kind of glacial lake is represented by Ice-dammed lake. It is produced on the side(s) of a glacier, when an advancing glacier happens to block a tributary/tributaries pouring into a main glacier valley. As such, an Ice core-dammed lake is usually small in size and does not come into contact with glacier ice. This type of lake is less susceptible to GLOF than a Moraine dammed lake. A glacial lake is formed and maintained only up to a certain stage of glacier fluctuation. In the CKNP, no ice-dammed glacier is found.

GLOF definition and criteria applied to identify Potentially Dangerous Glacial Lakes (PDGLs)

Periodic or occasional release of large amounts of stored water in a catastrophic outburst flood is generally referred to as a jokulhlaup (Iceland), a debacle (French), an aluvión (South America), or a Glacial Lake Outburst Flood (Himalaya and Asia). A jokulhlaup is an outburst which may be associated with volcanic activity, a debacle is an outburst but from a pro-glacial lake, an aluvión is a catastrophic flood of liquid mud, irrespective of its cause, generally transporting large boulders, and a GLOF is a catastrophic discharge of water under pressure from a glacier. GLOF events are severe geo-morphological hazards and their floodwaters can destroy all human structures located on their path. Over the last several decades, there are many outburst flood events occurred in the HKH region and in Pakistan and they had resulted in devastating socio-economical and environmental impacts. The records of past GLOF events in the Himalayas show that once every three to ten years, a GLOF has occurred with varying degrees of impacts and effects.

GLOFs create conditions for two very different types of flooding: a) upstream flooding, as a result of impoundment, and b) downstream flooding as a result of dam failure. The threat to life from upstream flooding is minimal because the water level behind the dam rises relatively slowly, although property damage can be substantial as the basin of the natural impoundment fills. It is usually possible to estimate accurately the extent and rate of upstream flooding from landslide dams. Such estimates require knowledge of the height of the dam crest, rates of stream flow into the dam lake, rates of seepage through or beneath the dam, and information on the topography upstream from the dam (Mool et al., 2001).

The criteria for identifying the potentially dangerous glacial lakes (PDGLs) are based on geo-morphological, geo-technical characteristics and records of past processes and events of the lake. For classifying a lake to be potentially dangerous, the physical conditions of the lake and its surroundings as discussed by Mool et al. (2001), Bajracharya et al. (2007), ICIMOD (2011) and PARC et al. (2015) were considered. These conditions include: i) a group of closely spaced Supraglacial lakes at glacier tongues, in fact in the case they will merge forming larger lakes these may become potentially dangerous, ii) the conditions of the damming material in moraine dammed lakes, iii) the nature of the mother glaciers (i.e. presence of large mother glacier near the lake, debris cover at glacier snout area and steep gradient at snout), iv) presence of crevasses, ponds at the glacier tongue, collapses of glacier masses at the tongue and ice blocks draining to lake, and v) physical conditions of the surrounding area like potential rockfall, mass movements, hanging glacier, snow avalanche site around the lake which can fall into the lake suddenly.

The potentially dangerous lakes are generally at the lower part of the ablation area of the glacier near to the and moraine, and the mother glacier should be sufficiently large to create a potentially dangerous lake environment.

Catastrophic Floods in the Pakistan and in the CKNP area

The history of GLOF and its hazards are as old as the glacial history of northern Pakistan. Although, GLOFs have occurred in various parts of the Hindu Kush-Himalayan region in the past, known both from the living memories of local people and from incidentally documented evidence; precise location, frequency, and actual scale of their effects are not adequately known or documented (PARC et al., 2015). More than 90 outbursts from impoundments behind glacial ice dams have been identified in HKH region. The largest and most destructive were 17 on the upper Indus River and 10 on the Yarkand (Hewitt and Liu, 2010). Thirty-five destructive outburst floods were recorded in the Karakorum region in the past two hundred years. There is also a history of outburst floods from Karakoram glaciers involving much larger impoundments by short-lived, unstable ice dams that blocked tributaries of the upper Indus River, causing outburst floods of exceptional size (Hewitt, 2010).

The Bagrot valley in Gilgit-Baltistan is highly vulnerable to flooding related to glacial lake outbursts or snow-ice/heavy rains, which occur almost every year. Bagrot valley (about 40 km from Gilgit) is considered at high risk of GLOF and flash floods. It covers an area of about 446 km^2 and is inhabited by approximately 14700 people in 10 villages. It is characterized by a strong altitude variability, ranging from 1500 m a.s.l. up to 7788 m a.s.l. at the summit of the Rakaposhi. The agriculture land here stretches over 13 km^2 area while the pastureland and forest lie over 70 km^2 and 62 km^2 areas, respectively. Local agriculture relies on irrigation for growing crops. In Bagrot valley, the main valley glaciers are Hinarchi, Burche, Gutumi, and Yune while several smaller cirque type glaciers exist in the higher reaches (Mayer et al., 2010). The snow and glaciated cover generally over 116 km^2 area in the north and northeastern parts of the valley drain into Bagrot River flowing down to join Gilgit River in the Southwest. Hinarchi Glacier is a medium size valley glacier with a strong vertical gradient in the accumulation zone and extensive debris cover on its tongue had caused flooding several times in the past resulting in heavy damage of natural forest and agriculture land of Bulchi and Chira villages.

Results

Glacial Lakes

In the CKNP area 202 glacial lakes are located thus corresponding to about 7% on the total of 3044 glacial lakes listed for the HKH region. The park lakes feature a cumulative extent of 3.56 km^2 (about 2.6% of the total glacial lake area in the HKH).

As regards lake distribution (considering the catchments as we already have done for glaciers), this gives a different picture with respect to the one obtained for the Upper Indus Basin (see the diagrams in Figs. 1A and B and Figs. 2A and 2B where HKH and CKNP are compared). Infact, in the CKNP area we found glacial lakes prevailing in the Shigar basin (54% of the total number and 59% of the cumulative lake area, see Tab. 1 and Figs. 1 and 2) followed by the

Hunza basin, where about 28% of total lake number is located and they cover about 31% of the whole lake area. In the Upper Indus basin only 1 glacial lake was found but it covers the same area (cumulative value, 0.04 km²) of the five lakes identified in the Gilgit basin. The Figures 3 and 4 show the spatial distribution of the glacial lakes in the CKNP (as raster base we used the glacier distribution map and elevation belts, respectively).

Basin	Number (Value)	Number (% with respect to the CKNP total)	Area (km²)	Area (% with respect to the CKNP total)	Area (km²) of the largest lake of the basin
Hunza	57	28.22	1.12	31.37	0.26
Shigar	109	53.96	2.12	59.48	0.17
Shyok	30	14.85	0.25	6.94	0.03
Upper Indus	1	0.50	0.04	0.99	0.04
Gilgit	5	2.48	0.04	1.21	0.02
CKNP total	**202**	**100.00**	**3.56**	**100.00**	**-**

Table 1: Summary of glacial lakes inventory in various basins of CKNP.

A supraglacial lake alt the surface of the Hinarche Glacier (Bagrot valley, Gilgit Basin).

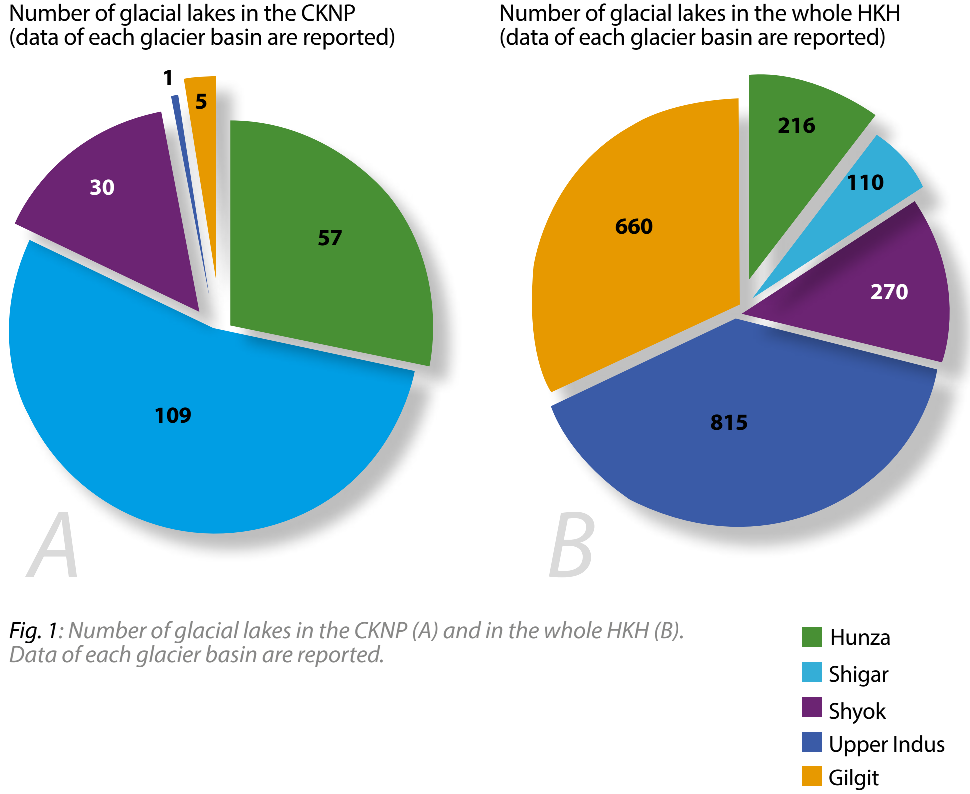

Fig. 1: Number of glacial lakes in the CKNP (A) and in the whole HKH (B). Data of each glacier basin are reported.

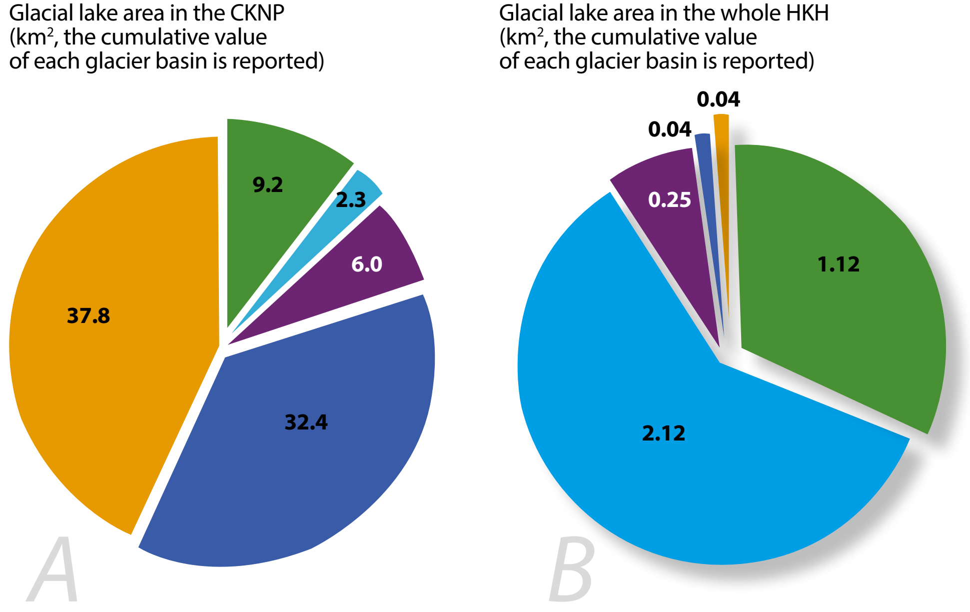

Fig.2: Cumulative glacial lake area in the CKNP (a) and in the whole HKH (b). Values of each glacier basin are reported.

Bagrot valley (Gilgit Basin)

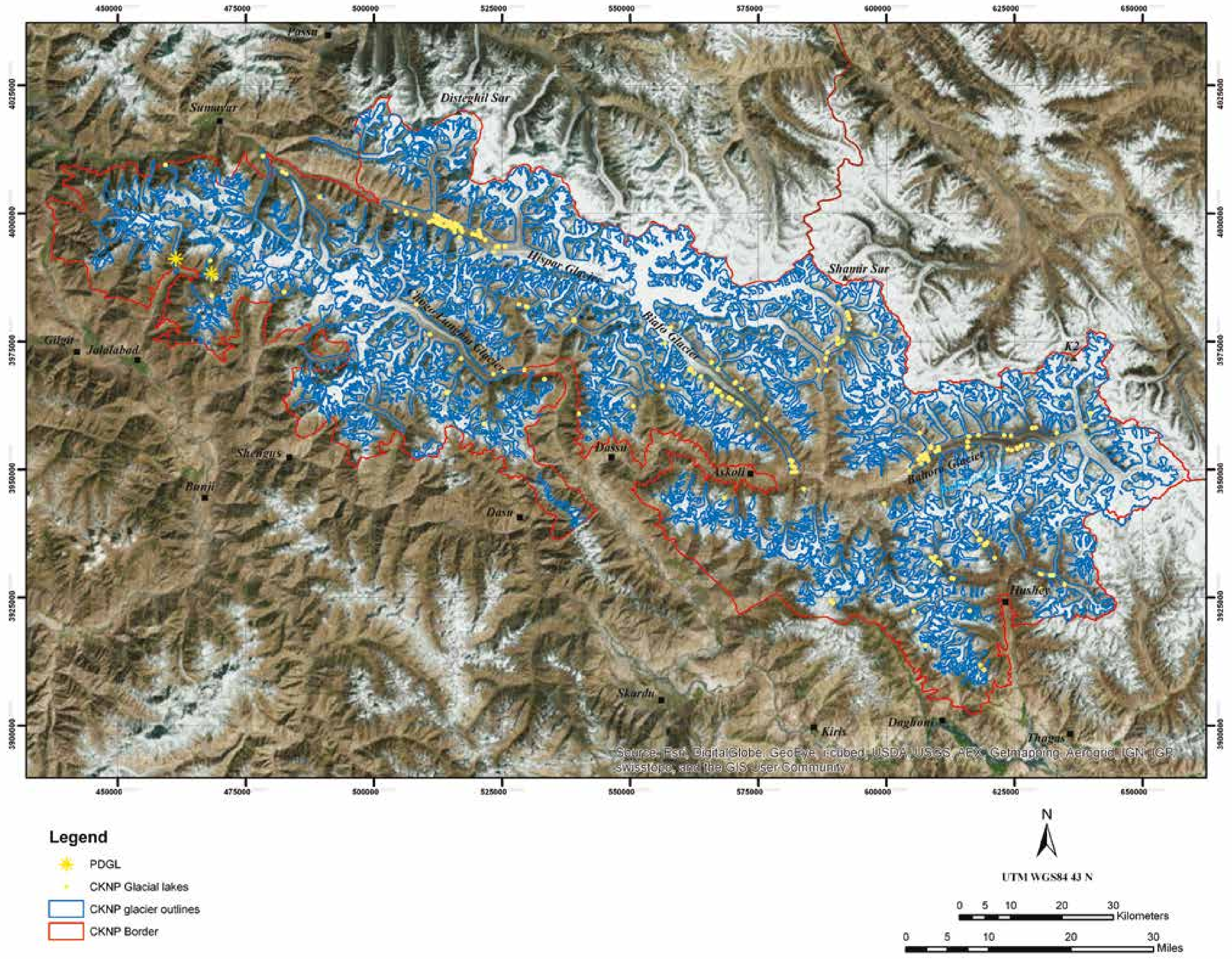

Fig. 3: Map showing the position of glacial lakes in the CKNP. With the yellow asterisks the two PDGLs are marked. The used raster base is the glacier distribution map.

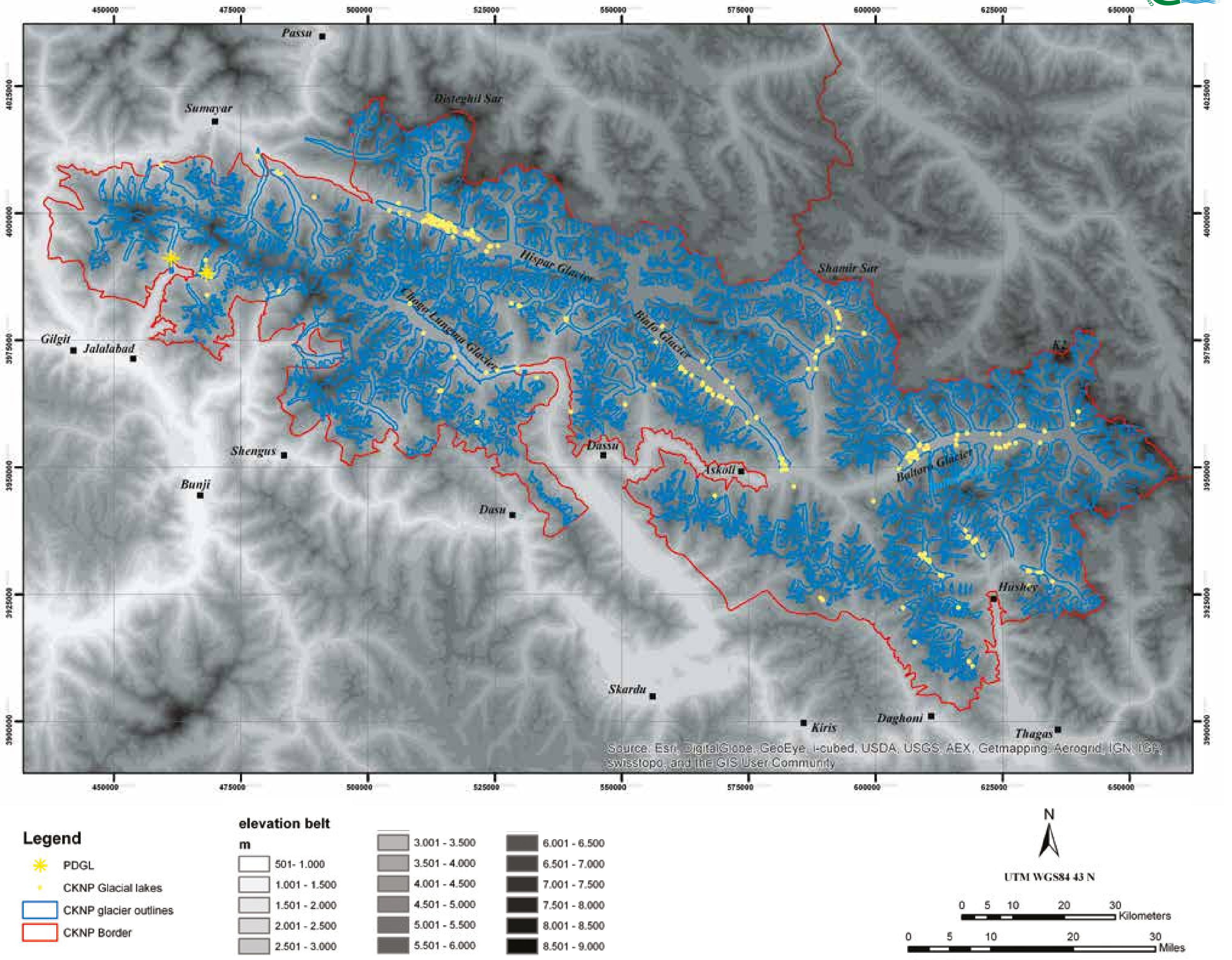

Fig. 4: Map showing the position of glacial lakes in the CKNP. With the yellow asterisks the two PDGLs are marked. The elevation belts are used as raster base.

The lake type is also considered (Tab. 2). As above reported the glacial water bodies are classified into Erosion, Cirque, Trough Valley, Supraglacial, Moraine Dammed (Lateral Moraine and End Moraine Dammed lakes), and Blocked lakes. In the CKNP the supraglacial lakes prevail, they represent the 69.31% of the total number and they cover 2.04 km^2, then blocked type lakes are abundant being 20.30% of the total number. Only 13 lakes are end moraine dammed type, 6.44% of the total.
Again the type distribution for CKNP gives a different picture with respect to the HKH general conditions. In fact, in the greater HKH region erosion lakes prevails (857 water bodies, 28.2% of the total number), followed by the end moraine dammed lakes (791 water bodies, 26% of the whole number).

Basin	Number (Value)	Number (% with respect to the CKNP total)	Area (km^2)	Area (% with respect to the CKNP total)	Area (km^2) of the largest lake per each type
Glacial Erosion	2	0.99%	0.01	0.40%	0.01
Cirque	1	0.50%	0.06	1.76%	0.06
Trough Valley	2	0.99%	0.02	0.46%	0.01
Supraglacial	140	69.31%	2.04	57.21%	0.26
Lateral Moraine	3	1.49%	0.05	1.51%	0.02
End Moraine Dammed	13	6.44%	0.22	6.12%	0.06
Blocked	41	20.30%	1.16	32.55%	0.17
CKNP total	**202**	**100.00**	**3.56**	**100.00**	**-**

Table 2: Summary of glacial lakes by various types in the CKNP.

As in most cases, major lakes are more susceptible of GLOF hazards than smaller ones, we analyzed lakes with a surface area greater than 0.02 km^2. The CKNP hosts 37 major lakes, corresponding to the 18.32% of the glacial lakes. Most part of these glaciers (64.86%) feature an area between 0.02-0.05 km^2. Overall 17 major lakes belong to Supraglacial type, 16 to Blocked type, 2 to End Moraine Dammed type and only 1 to Lateral Moraine type and Cirque type.

Basin	Number (Value)	Number (% with respect to the CKNP total)	Area (km^2)	Area (% with respect to the CKNP total)
Hunza	11	5.45%	0.79	0.39%
Shigar	24	11.88%	1.23	0.61%
Shyok	1	0.50%	0.03	0.01%
Upper Indus	1	0.50%	0.04	0.02%
Gilgit	0	0.00%	0.00	0.00%
CKNP total	**37**	**18.32%**	**2.08**	**58.41%**

Table 3: Summary of the Major lakes in the CKNP.

Potentially Dangerous Glacial Lakes and GLOFs in the CKNP area

The Inventory of glacial lakes of HKH listed 36 glacial lakes classified as potentially dangerous in Upper Indus basin of Pakistan. About 8 such lakes lie in Gilgit followed by 6 in Indus and 5 in Shyok basin. In the CKNP only 2 PDGLs are found, both of them lie in the Gilgit catchment and are identified as supraglacial lake type (Tab. 4 and Figs. 3 and 4).

Basin	Number of PDGLs in the CKNP (Value)	Number of PDGLs in the HKH
Hunza	0	3
Shigar	0	0
Shyok	0	5
Upper Indus	0	6
Gilgit	2	8

Table 4: Detail of potential dangerous glacial lakes in the CKNP and in the HKH. Only the basins common to CKNP and HKH are considered.

The potential hazardous supraglacial lakes identified in the Gilgit basin have caused frequent flooding events in the recent past. In fact, the ephemeral lake developed at the surface of the Hinarchi glacier possesses history of multiple breaching in the Bagrot valley of Gilgit basin. Also the other supraglacial lake in the Gilgit basin is growing rapidly due to melting of the associated glacier (i.e. Gargo glacier) in the Bagrot valley thus posing threat of outburst flood hazard for downstream communities. .
The integration of satellite remote sensing coupled with GIS techniques proved useful for listing, mapping and analyzing of glacial lakes and potential dangerous glacial lakes in the glaciated region of CKNP. The information reported in this study would provide base for future monitoring of glacial lakes and GLOFs and for planning and prioritizing disaster mitigation efforts in the park. In fact, even if the PDGLs identified in the park territory are only 2, they are located in a high vulnerable and fragile area and the recent history suggests us to survey over time these water bodies to avoid losses of human lives and destructions of villages and communities. Moreover, many other supraglacial lakes identified in the park area could develop into conditions of PDGLs thus suggesting to prosecute the lake monitoring and to develop early strategies for risk mitigations and disaster management.

References

Bajracharya S.R., Mool P.K. and Shrestha B.R. (2007) - *Impact of climate change on Himalayan glaciers and glacial lakes: Case studies on GLOF and associated hazards in Nepal and Bhutan*. ICIMOD, Nepal.

Bolch T., Buchroithner M.F., Peters J., Baessler M. and Bajracharya S. (2008) - *Identification of glacier motion and potentially dangerous glacial lakes in the Mt. Everest region/Nepal using spaceborne imagery*. Natural Hazards and Earth System Sciences, 8(6), 1329-1340.

Cenderelli D.A. and Wohl E.E. (2003) - *Flow hydraulics and geomorphic effects of glacial-lake outburst floods in the Mount Everest region, Nepal*. Earth Surface Processes and Landforms, 28(4), 385-407.

Fujita K., Suzuki R., Nuimura T. and Sakai A. (2008) - *Performance of ASTER and SRTM DEMs, and their potential for assessing glacial lakes in the Lunana region, Bhutan Himalaya*. Journal of Glaciology, 54(185), 220-228.

Hewitt K. (2010) - *Understanding glacier changes*. China Dialogue, 1 February 2010 www.chinadialogue.net.

Harrison S., Glasser N., Winchester V., Haresign E., Warren C. and Jansson K. (2006) - *A glacial lake outburst flood associated with recent mountain glacier retreat, Patagonian Andes*. The Holocene, 16(4), 611-620.

Hewitt K. and Liu J. (2010) - *Ice-Dammed Lakes and Outburst Floods, Karakoram Himalaya: Historical Perspectives on Emerging Threats*. Physical Geography, 31(6): 528-551.

ICIMOD (2011) - *Glacial lakes and glacial lake outburst floods in Nepal*. Kathmandu: ICIMOD.

Mayer C., A. Lambrecht, C. Mihalcea, M. Belò, G. Diolaiuti, C. Smiraglia and F. Bashir (2010) - *Analysis of glacial meltwater in Bagrot Valley, Karakoram, based on short term ablation and debris cover observations on Hinarche Glacier*. Mountain Research and Development, 30,2, 169-177.

Mool P.K., Bajracharya S.R. and Joshi S.P. (2001) - *Inventory of Glaciers, Glacial Lakes, and Glacial Lake Outburst Flood Monitoring and Early Warning System in the Hindu Kush-Himalayan Region, Nepal*. ICIMOD in cooperation with UNEP/RRC-AP, ISBN 92 9115 331 1, Published by ICIMOD, Kathmandu, Nepal.

Pakistan Agricultural Research Council (PARC), Pakistan Meteorological Department (PMD), Ministry of Climate Change, UNDP and Adaptation Fund (AF) (2015) - *Updating GLOF lake inventory of Northern Pakistan & establishment of community based early warning system in Bagrot and Bindogol Valleys* (For Pakistan GLOF Project). Final Technical Report, 130 pp. available online at http://www.glof.pk/images/Publications/PDF/Khalil/Final_Glacial_Lake%20_Inventory_Pakistan.pdf

Raj K.B.G. (2010) - *Remote sensing based hazard assessment of glacial lakes: a case study in Zanskar basin, Jammu and Kashmir, India*. Geomatics, Natural Hazards and Risk, 1:4: 339-347.

Richardson S.D. (2010) - *Remote sensing approaches for early warning of GLOF hazards in the Hindu Kush-Himalayan region*. Final report-ver 1.2, United Nations International Strategy for Disaster Reduction (UN/ISDR).

Roohi R., P. Mool, A. Ashraf, S. Bajracharya, S.A. Hussain and R. Naz (2005) - *Inventory of Glaciers, Glacial lakes the Identification of Potential Glacial lake Outburst Floods Affected by Global Warming in the Mountains of Himalayan Region*. Pakistan, ICIMOD, Nepal and PARC, Pakistan

Glacial lake data

	CKNP-Glacial lake ID	Longitude	Latitude	Area (km²)	Elevation (m a.s.l.)	Type
Hunza Basin						
Hunza	6	75.221	36.107	0.01	3956	Supraglacial
Hunza	7	75.213	36.109	0.01	3941	Supraglacial
Hunza	8	75.186	36.103	0.01	3999	Blocked
Hunza	9	75.175	36.112	0.01	3799	Supraglacial
Hunza	10	75.189	36.115	0.01	3841	Supraglacial
Hunza	11	75.188	36.119	0.02	3822	Supraglacial
Hunza	12	75.181	36.125	0.01	3812	Supraglacial
Hunza	13	75.180	36.123	0.01	3796	Supraglacial
Hunza	14	75.192	36.113	0.00	3852	Supraglacial
Hunza	15	75.284	36.086	0.01	4128	Supraglacial
Hunza	16	75.175	36.123	0.00	3786	Supraglacial
Hunza	17	75.175	36.120	0.00	3790	Supraglacial
Hunza	18	75.170	36.119	0.00	3766	Supraglacial
Hunza	19	75.267	36.086	0.01	4104	Supraglacial
Hunza	20	75.170	36.122	0.00	3783	Supraglacial
Hunza	21	75.166	36.125	0.00	3761	Supraglacial
Hunza	22	75.163	36.122	0.02	3747	Supraglacial
Hunza	23	75.164	36.124	0.00	3763	Supraglacial
Hunza	24	75.169	36.125	0.00	3772	Supraglacial
Hunza	25	75.270	36.086	0.01	4116	Supraglacial
Hunza	26	75.241	36.098	0.01	4017	Supraglacial
Hunza	27	75.175	36.127	0.00	3795	Supraglacial
Hunza	28	75.265	36.085	0.01	4101	Supraglacial
Hunza	29	75.161	36.126	0.00	3748	Supraglacial
Hunza	30	75.165	36.130	0.03	3755	Supraglacial
Hunza	31	75.161	36.129	0.01	3756	Supraglacial
Hunza	32	75.153	36.122	0.01	3734	Supraglacial
Hunza	33	75.144	36.125	0.01	3714	Supraglacial
Hunza	34	75.139	36.126	0.14	3699	Supraglacial
Hunza	35	75.145	36.131	0.13	3698	Supraglacial

Catchment	CKNP-Glacial lake ID	Longitude	Latitude	Area (km²)	Elevation (m a.s.l.)	Type
Hunza	36	75.156	36.132	0.05	3718	Supraglacial
Hunza	37	75.147	36.134	0.00	3710	Supraglacial
Hunza	38	75.145	36.135	0.01	3712	Supraglacial
Hunza	39	75.136	36.129	0.01	3688	Supraglacial
Hunza	40	75.134	36.132	0.00	3674	Supraglacial
Hunza	41	75.131	36.131	0.00	3662	Supraglacial
Hunza	42	75.126	36.132	0.01	3650	Supraglacial
Hunza	43	75.140	36.135	0.02	3686	Supraglacial
Hunza	44	75.136	36.137	0.26	3666	Supraglacial
Hunza	45	75.139	36.140	0.01	3713	Supraglacial
Hunza	46	75.132	36.143	0.01	3692	Supraglacial
Hunza	47	75.120	36.129	0.01	3647	Supraglacial
Hunza	48	75.089	36.143	0.01	3509	Supraglacial
Hunza	49	75.071	36.144	0.01	3443	Supraglacial
Hunza	50	75.070	36.146	0.02	3418	Supraglacial
Hunza	51	75.067	36.163	0.02	3442	Blocked
Hunza	52	75.047	36.150	0.01	3339	Supraglacial
Hunza	53	74.883	36.174	0.06	4608	Cirque
Hunza	54	74.809	36.214	0.01	2967	Supraglacial
Hunza	55	74.801	36.219	0.01	2927	Supraglacial
Hunza	56	74.759	36.246	0.00	2434	Supraglacial
Hunza	57	74.547	36.229	0.01	2548	Supraglacial
Shigar Basin						
Shigar	58	75.368	35.852	0.01	3423	Glacial Erosion
Shigar	59	75.238	35.774	0.02	4212	Blocked
Shigar	60	75.156	35.829	0.02	4188	Blocked
Shigar	61	75.160	35.830	0.00	4103	Supraglacial
Shigar	62	75.325	35.869	0.06	2773	End Moraine Dammed
Shigar	63	75.282	35.866	0.02	3001	Lateral Moraine
Shigar	64	75.258	35.862	0.02	3103	Supraglacial
Shigar	65	75.188	35.889	0.02	3426	Blocked

Catchment	CKNP-Glacial lake ID	Longitude	Latitude	Area (km²)	Elevation (m a.s.l.)	Type
Shigar	66	75.121	35.932	0.01	3729	Blocked
Shigar	67	75.092	35.985	0.01	3965	Trough Valley
Shigar	68	75.314	35.984	0.01	3878	Blocked
Shigar	69	75.329	35.980	0.01	3889	Supraglacial
Shigar	70	75.332	35.979	0.01	3899	Supraglacial
Shigar	71	75.432	35.958	0.02	3567	Supraglacial
Shigar	72	75.433	35.954	0.01	3561	Supraglacial
Shigar	73	75.443	35.791	0.02	3807	End Moraine Dammed
Shigar	74	75.561	35.804	0.02	4087	Lateral Moraine
Shigar	75	75.624	35.840	0.02	4213	End Moraine Dammed
Shigar	76	75.901	35.686	0.01	3087	Supraglacial
Shigar	77	75.908	35.686	0.02	3034	Supraglacial
Shigar	78	75.911	35.687	0.01	3046	Lateral Moraine
Shigar	79	75.907	35.694	0.01	3138	Supraglacial
Shigar	80	75.901	35.697	0.01	3175	Supraglacial
Shigar	81	75.902	35.706	0.01	3209	Supraglacial
Shigar	82	75.897	35.707	0.01	3227	Supraglacial
Shigar	83	75.847	35.779	0.01	3653	Blocked
Shigar	84	75.827	35.770	0.05	3672	Supraglacial
Shigar	85	75.785	35.809	0.01	3914	Blocked
Shigar	86	75.773	35.815	0.02	3968	Blocked
Shigar	87	75.792	35.805	0.01	3897	Blocked
Shigar	88	75.795	35.833	0.01	3953	Supraglacial
Shigar	89	75.768	35.818	0.02	3933	Blocked
Shigar	90	75.765	35.818	0.01	3960	Blocked
Shigar	91	75.752	35.821	0.02	4009	Blocked
Shigar	92	75.747	35.830	0.02	4004	Supraglacial
Shigar	93	75.742	35.829	0.01	4004	Blocked
Shigar	94	75.739	35.829	0.04	4004	Blocked
Shigar	95	75.780	35.844	0.01	3979	Supraglacial
Shigar	96	75.740	35.833	0.00	4015	Supraglacial

Catchment	CKNP-Glacial lake ID	Longitude	Latitude	Area (km²)	Elevation (m a.s.l.)	Type
Shigar	97	75.730	35.838	0.06	4006	Blocked
Shigar	98	75.730	35.842	0.03	3979	Supraglacial
Shigar	99	75.707	35.855	0.03	4121	Blocked
Shigar	100	75.692	35.861	0.01	4154	Blocked
Shigar	101	75.685	35.867	0.00	4154	Supraglacial
Shigar	102	75.685	35.868	0.00	4151	Supraglacial
Shigar	103	75.683	35.870	0.00	4162	Supraglacial
Shigar	104	75.682	35.867	0.01	4171	Blocked
Shigar	105	75.643	35.942	0.01	4463	Blocked
Shigar	106	75.682	35.869	0.00	4157	Blocked
Shigar	107	75.629	35.915	0.02	4430	Blocked
Shigar	108	75.730	35.880	0.01	4118	Blocked
Shigar	109	75.744	35.868	0.02	4094	Supraglacial
Shigar	110	75.782	35.845	0.02	3966	Blocked
Shigar	111	76.007	35.982	0.01	4365	Supraglacial
Shigar	112	76.024	35.966	0.01	4328	Blocked
Shigar	113	76.027	35.960	0.00	4304	Blocked
Shigar	114	76.030	35.954	0.10	4268	Blocked
Shigar	115	76.083	35.927	0.01	4754	Glacial Erosion
Shigar	116	76.026	35.937	0.09	4175	Supraglacial
Shigar	117	76.003	35.921	0.01	4146	Blocked
Shigar	118	76.003	35.916	0.00	4116	Supraglacial
Shigar	119	76.002	35.915	0.00	4114	Supraglacial
Shigar	120	76.015	35.916	0.01	4135	Supraglacial
Shigar	121	76.005	35.912	0.00	4117	Supraglacial
Shigar	122	76.003	35.911	0.00	4108	Supraglacial
Shigar	123	75.980	35.897	0.01	3989	Supraglacial
Shigar	124	75.976	35.885	0.01	3949	Supraglacial
Shigar	125	75.978	35.864	0.01	3868	Supraglacial
Shigar	126	75.960	35.865	0.01	3842	Supraglacial
Shigar	127	76.178	35.752	0.02	4052	Blocked

Catchment	CKNP-Glacial lake ID	Longitude	Latitude	Area (km²)	Elevation (m a.s.l.)	Type
Shigar	128	76.202	35.728	0.02	3738	Supraglacial
Shigar	129	76.217	35.727	0.02	3820	Supraglacial
Shigar	130	76.219	35.722	0.01	3815	Supraglacial
Shigar	131	76.212	35.719	0.01	3786	Supraglacial
Shigar	132	76.201	35.726	0.01	3768	Supraglacial
Shigar	133	76.191	35.716	0.01	3734	Supraglacial
Shigar	134	76.190	35.714	0.01	3713	Supraglacial
Shigar	135	76.194	35.709	0.01	3702	Supraglacial
Shigar	136	76.196	35.704	0.01	3714	Supraglacial
Shigar	137	76.186	35.706	0.01	3698	Supraglacial
Shigar	138	76.181	35.712	0.01	3707	Supraglacial
Shigar	139	76.179	35.713	0.03	3701	Supraglacial
Shigar	140	76.180	35.713	0.03	3687	Supraglacial
Shigar	141	76.181	35.709	0.01	3695	Supraglacial
Shigar	142	76.180	35.708	0.02	3693	Supraglacial
Shigar	143	76.174	35.706	0.01	3688	Supraglacial
Shigar	144	76.181	35.698	0.01	3656	Supraglacial
Shigar	145	76.155	35.687	0.01	3402	Supraglacial
Shigar	146	76.548	35.783	0.01	5059	Blocked
Shigar	147	76.535	35.760	0.01	4663	Supraglacial
Shigar	148	76.473	35.749	0.02	4444	Supraglacial
Shigar	149	76.464	35.729	0.03	4430	Supraglacial
Shigar	150	76.429	35.759	0.06	4299	Blocked
Shigar	151	76.421	35.759	0.05	4306	Blocked
Shigar	152	76.410	35.729	0.11	4178	Blocked
Shigar	153	76.397	35.727	0.01	4242	Supraglacial
Shigar	154	76.389	35.723	0.02	4207	Blocked
Shigar	155	76.387	35.724	0.01	4204	Supraglacial
Shigar	156	76.376	35.720	0.17	4154	Blocked
Shigar	157	76.367	35.722	0.10	4144	Blocked
Shigar	158	76.375	35.746	0.02	4226	Supraglacial

Catchment	CKNP-Glacial lake ID	Longitude	Latitude	Area (km²)	Elevation (m a.s.l.)	Type
Shigar	159	76.360	35.747	0.01	4193	Supraglacial
Shigar	160	76.305	35.747	0.02	4081	Supraglacial
Shigar	161	76.284	35.745	0.01	4018	Supraglacial
Shigar	162	76.281	35.736	0.02	4012	Supraglacial
Shigar	163	76.281	35.727	0.02	3987	Blocked
Shigar	164	76.100	35.629	0.01	4384	End Moraine Dammed
Shigar	165	75.927	35.656	0.01	4478	End Moraine Dammed
Shigar	166	75.755	35.641	0.01	4611	End Moraine Dammed
Shyok Basin						
Shyok	167	75.987	35.455	0.01	4385	Trough Valley
Shyok	168	75.983	35.458	0.01	4452	End Moraine Dammed
Shyok	169	76.161	35.439	0.00	4304	Supraglacial
Shyok	170	76.185	35.378	0.01	4850	End Moraine Dammed
Shyok	171	76.302	35.343	0.03	4716	End Moraine Dammed
Shyok	172	76.310	35.334	0.01	4714	End Moraine Dammed
Shyok	173	76.281	35.439	0.01	4512	End Moraine Dammed
Shyok	174	76.246	35.496	0.01	3906	Supraglacial
Shyok	175	76.243	35.496	0.01	3930	Supraglacial
Shyok	176	76.219	35.520	0.01	4173	Supraglacial
Shyok	177	76.218	35.523	0.00	4196	Supraglacial
Shyok	178	76.214	35.524	0.01	4204	Supraglacial
Shyok	179	76.205	35.528	0.00	4305	Blocked
Shyok	180	76.199	35.533	0.00	4374	Supraglacial
Shyok	181	76.209	35.534	0.01	4295	Supraglacial
Shyok	182	76.336	35.531	0.00	3772	Supraglacial
Shyok	183	76.315	35.554	0.00	4124	Supraglacial
Shyok	184	76.315	35.555	0.01	4120	Supraglacial
Shyok	185	76.317	35.554	0.00	4099	Supraglacial
Shyok	186	76.316	35.556	0.00	4124	Supraglacial
Shyok	187	76.320	35.558	0.02	4099	Blocked

Catchment	CKNP-Glacial lake ID	Longitude	Latitude	Area (km^2)	Elevation (m a.s.l.)	Type
Shyok	188	76.303	35.562	0.00	4200	Supraglacial
Shyok	189	76.306	35.564	0.01	4206	Supraglacial
Shyok	190	76.298	35.575	0.00	4265	Supraglacial
Shyok	191	76.433	35.502	0.02	3581	Supraglacial
Shyok	192	76.436	35.501	0.01	3599	Supraglacial
Shyok	193	76.455	35.499	0.01	3745	Supraglacial
Shyok	194	76.461	35.499	0.01	3775	Supraglacial
Shyok	195	76.485	35.483	0.01	4142	Supraglacial
Shyok	196	76.435	35.475	0.01	4405	End Moraine Dammed
Upper Indus Basin						
Upper Indus	197	74.806	36.006	0.04	3300	Blocked
Gilgit Basin						
Gilgit	198	74.571	36.064	0.00	2842	Supraglacial
Gilgit	199	74.645	36.061	0.00	3628	Supraglacial
Gilgit	200	74.647	36.039	0.02	3323	Supraglacial
Gilgit	201	74.657	36.031	0.00	3394	Supraglacial
Gilgit	202	74.649	35.999	0.02	4281	End Moraine Dammed

Authors


Claudio
Smiraglia


Guglielmina Adele
Diolaiuti


Antonella
Senese


Davide
Fugazza


Carlo
D'Agata


Davide
Maragno


Umberto
Minora


Andrea
Soncini


Roberto Sergio
Azzoni


Riaz
Ul-Hassan


Elisa
Vuillermoz

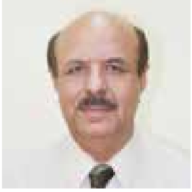
Mohammed
Asif Khan


Adnan
Shafiq Rana


Ghulam
Rasul

CENTRAL KARAKURAM NATIONAL PARK

CKNP